UNIVERSITY OF SOUTHERN QUEENSLAND

Faculty of Engineering and Surveying

DEVELOPMENT AND CALIBRATION OF BIO-KINETIC MODELS FOR ORGANIC CARBON AND NITROGEN BIODEGRADATION IN AN AEROBIC ACTIVATED SLUDGE SYSTEM

A Dissertation submitted by

Muhammad Azizul Hoque

B.Sc. (Eng.) & M.Sc. (Eng.) (BUET)

For the award of

Doctor of Philosophy

2010

Dedicated to my mother, my wife, our daughter

and

to the spirit of my father who dreamed first…

Abstract

Substrate removal mechanisms in a mixed culture of an activated sludge system are still a mystery that researchers have been trying to unravel by proposing and developing models to interpret the observed experimental data. Activated Sludge Model Number 1 (ASM1) was first introduced to better understand the biochemical mechanisms during carbon and nitrogen oxidation and was based on the assumption that the external substrate is consumed only for biomass growth. This model ignored the formation of intracellular polymers (storage products) in the biomass cell, though several researchers observed the phenomenon of storage of carbon sources and the significant role it played in the carbon removal process. As a consequence, the Activated Sludge Model Number 3 (ASM3) was formulated assuming that all the easily biodegradable substrate is first stored internally during the feast phase before being used for growth during famine conditions. However, experimental observations proved that both storage and growth occur simultaneously during the feast phase. Consequently, the simultaneous storage and growth (SSAG) model was developed as an extension to ASM3 specifically to gain an in-depth understanding of the carbon oxidation process.

While considerable investigation has been focused on model calibration using respirometric measurements of the oxygen uptake rate (OUR) during the aerobic biodegradation of substrate, model-based interpretation of titrimetric measurements has been limited. In biological systems, the oxygen consumption and corresponding pH changes occur simultaneously and can be easily monitored using respirometric and titrimetric experimental observations respectively. Attempts were, therefore, made to calibrate ASM1 using titrimetric measurements. During the subsequent successful development, consideration was given to the pH effects of carbon uptake, ammonia uptake for growth, CO_2 production from carbon metabolism and the non-linear carbon dioxide transfer rate (CTR) due to stripping. While respirometry was successfully used to calibrate every proposed new model, the interpretation of titrimetric measurements, however, was always based on ASM1, using calibration substrates such as acetate and ammonium. The SSAG model, developed in the year 2005, proposed an improved kinetic expression for the degradation of storage products under famine conditions. It was successfully calibrated using on-line

respirometric measurements and validated using off-line storage products measurements with acetate used as a calibration substrate. However it failed to explain the titrimetric behavior of the substrate biodegradation process. While in most cases the above models were calibrated using simple synthetic substrates, the application of these models for complex substrates was not investigated.

Therefore, in this dissertation, the biodegradation kinetics for different substrates like acetate (simple carbon source), sodium dodecyl sulfate (relatively complex carbon source), ammonium (simple nitrogen source), urea (relatively complex nitrogen source) and glutamic acid (combination of carbon and nitrogen) were investigated. A titrimetric respirometer, established in the Water-waste laboratory in the Faculty of Engineering and Surveying, University of Southern Queensland, Australia, was used to conduct batch experiments in order to monitor substrate biodegradation process in an aerobic activated sludge system. Both the dissolved oxygen and the pH control data were logged with the Labview software package. A spreadsheet program was used to calculate the oxygen uptake rate and the proton production/consumption rate from the raw measurements.

During batch experiments, the biodegradation of all five test substrates showed unique respirometric and titrimetric behaviors indicating that each of these compounds is biodegraded using distinctive mechanisms with the involvement and coordination of different bacterial populations. The pattern of OURs were observed varying from substrate to substrate describing the characteristics of test compounds. The titrimetric profiles were also different for different substrates biodegradation reflecting the on-going biochemical reaction of respective substrate in activated sludge system. While acetate biodegradation, for example, caused proton consumption (at pH 7.8) in the liquid medium, proton production was noted under feast conditions when either sodium dodecyl sulfate or glutamic acid was used as a test substrate.

An in-depth revision of the existing activated sludge models was completed and the models were assessed using experimental observations. An improved bio-kinetic model which includes both the oxygen and proton balances for the biodegradation of each of the test substrates was then developed. In addition, the substrates

biodegradation pathway and the non-linear CO_2 transfer process were considered during the modeling. For proper model evaluation, the proposed model was calibrated using varying initial substrate concentrations and pH levels. In addition, three different calibration approaches: using respirometric measurements alone, using titrimetric measurements alone and using combined respirometric-titrimetric measurements, were applied during the study. The estimation of model parameters was undertaken using non-linear techniques utilizing the algorithms in the optimisation toolbox (MATLAB).

For the biodegradation of each test substrate, the proposed model was successfully calibrated using both the respirometric and titrimetric behaviors in the activated sludge system. The estimated model parameters showed consistent results for all three calibration approaches thereby confirming the precision of the proposed model. The parameter estimation errors (calculated for 95% confidence intervals) as well as the mean squared errors for the different calibration approaches were quite reasonable and confirmed the statistical soundness of the proposed model. In addition, the proposed model was validated using off-line measurements.

This dissertation presents an in-depth explanation of how the proposed models interpret the biodegradation processes and how the model parameters vary for different substrates in an activated sludge system. The results will be helpful in further refining current models that can contribute to the optimization of the design operation and enhanced performance of full scale wastewater treatment plants.

Certification of Dissertation

I certify that the ideas, experimental work, results, analysis, software and conclusions reported in this dissertation are entirely my own effort, except where otherwise acknowledged. I also certify that the work is original and has not been previously submitted for any other award, except where otherwise acknowledged.

Muhammad Azizul Hoque, Candidate	Date

ENDORSEMENT

Dr Vasantha Aravinthan, Principal supervisor	Date
Prof. Mark Porter, Associate supervisor	Date

Acknowledgements

I wish to express my sincere gratitude and profound indebtedness to my principal supervisor Dr Vasantha Aravinthan for her continued encouragement, supervision, contribution of new ideas and constant guidance throughout the course of this research work. I would like to thank as well Professor Mark Porter for his invaluable support as associate supervisor. Without their direction and cordial assistance, it would have been impossible to complete this research project. I also thank Associate Professor David Buttsworth for his continual encouragement and support throughout my study.

I would like to thank the Australian Government for offering me the Endeavor International Postgraduate Research Scholarship (IPRS) to undertake my PhD program. I wish to thank the Faculty of Engineering and Surveying (FoES), University of Southern Queensland (USQ), Australia for providing me with laboratory and computer facilities. In addition, I am grateful to the USQ library for support during the period of my study.

Special gratitude is extended to the Australian Centre for Sustainable Catchments (ACSC), USQ for financial support in my research work. In addition, I wish to thank the Wetalla Water Reclamation Plant (Toowoomba City Council) authority for its cooperation in collecting activated sludge samples from the plant.

I am grateful to Dean Beliveau, Chris Galligan, Nishant Pradhan, Atul Sakhiya and all the other engineering technical staff for their valuable support and cooperation during the laboratory set-up installation and the period of experimental work.

I wish to express my sincere thanks to Ruth Hilton for her assistance with my written English language expression.

I would like to express my deepest gratitude to my parents for their love, patience and encouragement. Finally, I would like to thank my wife, Irin, and our only daughter, Rumaisha, for their care and endless support throughout this study.

List of Publications

Based on the current research, a number of papers have been published in journals and peer reviewed conferences. They are presented below for reference.

Published Journal Paper

1. **Hoque, M. A.**, Aravinthan, V. and Pradhan, N. M., 2010. Calibration of biokinetic model for acetate biodegradation using combined respirometric and titrimetric measurements, Bioresource Technology 101 (5), 1426-1434.

2. Aravinthan, V. and **Hoque, M. A.**, 2010. Development and calibration of bio-kinetic model for surfactant biodegradation with combined respirometric and titrimetric measurements, Bioresource Technology (doi: 10.1016/j.biortech.2010.08.101).

3. **Hoque, M. A.**, Aravinthan, V. and Pradhan, N. M., 2009. Assessment on activated sludge models for acetate biodegradation under aerobic conditions, Water Science and Technology 60 (4), 983-994.

4. **Hoque, M. A.**, Aravinthan, V. and Pradhan, N. M., 2009. Can We Decode the Messages of Activated Sludge Through the Respirograms?, Water, Air and Soil Pollution: Focus 9 (5-6), 449-459.

5. **Hoque, M. A.**, Aravinthan, V. and Porter, M., 2008. Respirometric and Titrimetric Techniques for monitoring Aerobic Biodegradation of Surfactant, published in the special issue of Research Journal of Biotechnology, 399-405.

6. **Hoque, M. A.**, Aravinthan, V. and Pradhan, N. M., 2008. Evaluation of Simultaneous Storage and Growth Model to explain Aerobic Biodegradation of Acetate, published in the special issue of Research Journal of Biotechnology, 274-281.

Published Conference Paper

1. **Hoque, M. A.**, Aravinthan, V., Pradhan, N. M. and Sakhiya, A., 2009. Combined Titrimetric Respirometer as a Real-time Sensor to Monitor the Aerobic Biodegradation Process of Different Substrates. Proceedings of the 3rd international conference on Chemical and Bioprocess Engineering, Sabah, Malaysia, 454-460.

Paper Selected for possible Publication in Journal/Conference

1. **Hoque, M. A.** and Aravinthan, V., Modeling urea biodegradation using combined respirometric-titrimetric data in activated sludge, International Conference on Challenges in Environmental Science and Engineering (CESE), Cairns, Australia, 26 September-1 October 2010. This paper has also been selected for possible publication in the Desalination and Water Treatment journal (currently under review process).

Table of Contents

List of Figures

List of Tables

Chapter 1
Introduction

1.1 Background

The activated sludge process is widely used in wastewater treatment plants (WWTPs) to remove dissolved organic and nutrient loads from wastewater. Municipal raw wastewater from domestic, industrial and commercial sources is conveyed to a central WWTP where it undergoes a series of physical, chemical and biological treatment processes before its final disposal into the nearest waterways. Depending on the license conditions imposed by the Environmental Protection Agency (EPA), WWTPs can be designed to include different configurations of aerobic, anoxic and anaerobic processes where the different populations of microorganisms in the biomass are engineered to undergo cyclic conditions in the reactors to achieve nutrient and organic removal. This current study focuses only on the aerobic biodegradation of organic carbon and nitrogen in an activated sludge system. Figure 1.1 shows the typical presentation of aerobic process in an activated sludge system.

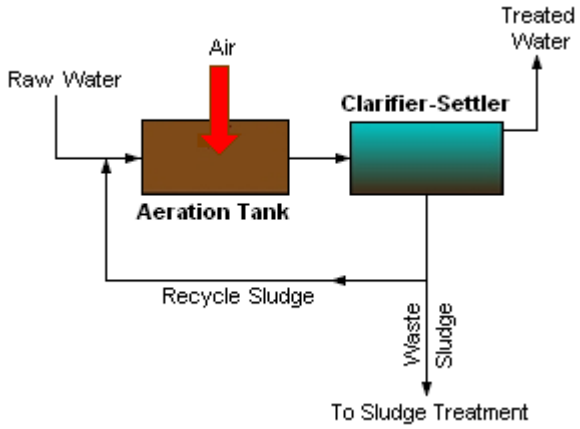

Figure 1.1: Typical presentation of aerobic process in an activated sludge system

Gernaey et al. (2002a) depicted a model diagram to explain the aerobic processes occurring in an activated sludge system using acetate as a test substrate (Figure 1.2). Substrate uptake, CO_2 production and NH_3 consumption for biomass growth are

assumed to be the main processes that influence the proton balance in the liquid phase during organic carbon degradation. This model describes in detail what happens within a bacterial cell, in the liquid phase and the gas phase under the aerobic conditions. For example, the heterotrophic biomass cell (a solid phase) consumes readily biodegradable carbon compounds, such as acetate from the liquid medium for growth. The biochemical reaction in activated sludge results in either proton (H^+) production or consumption depending on the substrate characteristics. The model prescribed by Gernaey et al. (2002a) shows that proton is extracted by the biomass from the liquid phase during the acetate uptake process (Figure 1.2). All carbon respired by the cell is transformed into CO_2 that is finally released to the liquid medium resulting in proton production in the system. CO_2 gas is produced simultaneously via stripping due to the continuous aeration process that removes dissolved CO_2 from the mixed liquor. In this model, the nitrogen incorporated in the biomass cell is taken up from the liquid as NH_3 causing proton production in the mixed liquor (Figure 1.2).

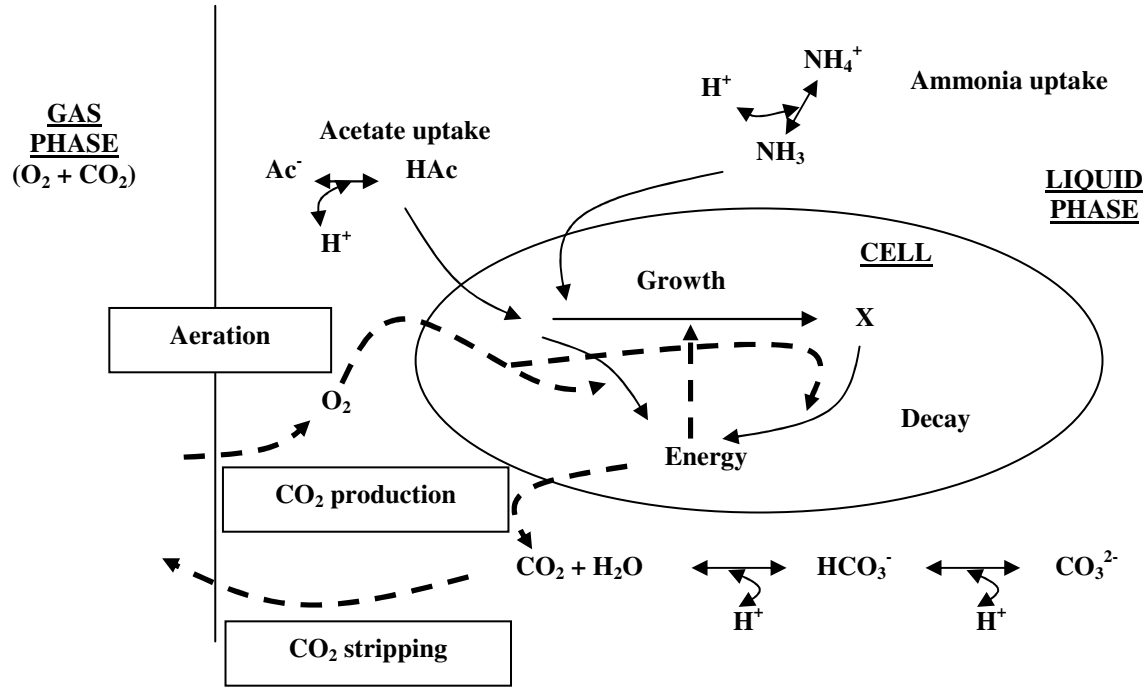

Figure 1.2: Aerobic processes involved in an activated sludge system for using acetate as a test substrate (adopted from Gernaey et al., 2002a)

Organic carbon and nitrogen removal mechanisms can be different from those described in Figure 1.2 depending on the complexity of the substrates. In general,

complex organic carbons including slowly biodegradable ones present in the wastewater are hydrolyzed to intermediate carbon compounds and finally oxidized to CO_2 (gas form) by the heterotrophic biomass. Organic nitrogen is hydrolyzed to form ammonium- nitrogen (NH_4-N). It is gone through a two-step nitrification process in presence of autotrophic microorganisms. During the first step, ammonium is oxidized to nitrite by *Nitrosomonas* species. This is followed by the conversion of nitrite to nitrate by *Nitrobacter* species. While much organic matter in wastewater can be easily biodegraded, some synthetic and complex organic compounds present in municipal wastewater are not degraded within the design period of WWTP due to their slow biodegradation rate. Proper understanding on biodegradation kinetics is, therefore, essential to upgrade the operating system of the treatment plants.

Figure 1.3 generalizes the aerobic conversion of organic carbon and nitrogen in bio-culture with different approaches to assess biodegradation rate.

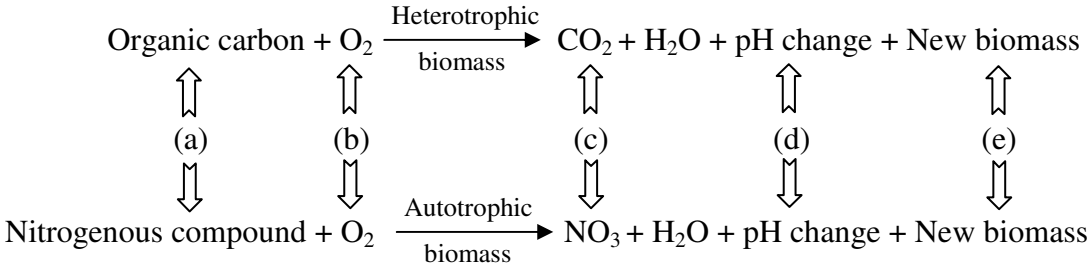

Figure 1.3: Aerobic conversion of organic carbon and nitrogen in activated sludge

As presented in Figure 1.3, the process rate can be determined using the techniques such as: (a) measuring the parent substrate concentration (in terms of COD or nitrogen) in the liquid phase; (b) measuring the oxygen consumption in the liquid phase; (c) measuring the end products such as CO_2 production in the gas phase and/or NO_3 concentration in the liquid phase; (d) monitoring the pH change in the liquid phase which virtually represents the proton production/consumption during the biodegradation period; and (e) measuring biomass concentration in the liquid phase.

Most approaches such as COD, or dissolved nitrogen measurements are based on off-line measurement techniques which are time-consuming and labor-intensive.

Besides, off-line techniques are slow to generate data thus, valuable bio-kinetic information that occurs during the biodegradation process cannot be captured. Conversely, the methods available at 'b' and 'd' (Figure 1.3), called 'respirometry' and 'titrimetry', are on-line measurement techniques that have a simple experimental setup and the capability to provide frequent recordings of data and complete bio-kinetic documentation of the system.

A detailed understanding of substrate removal kinetics is a pre-requisite for optimal design and operation of a WWTP. Researchers are trying to unravel the mystery of substrate removal mechanisms in a mixed culture of an activated sludge system by proposing and developing models that represent the experimental observations. These models assume different kinetic expressions for calibration and validation purposes. Modeling efforts are complicated by system configurations including reactor characteristics (whether it is a sequencing batch reactor or simple batch reactor) and the operating conditions of the WWTP. The biomass is usually exposed to dynamic conditions. An alternating anoxic and aerobic system can acclimatize the biomass to store the external substrate during an aerobic cycle and then to use it for biomass growth during an anoxic cycle. However, in an extended aeration system which involves a single process, this storage phenomenon may not be evident in the activated sludge. Similarly, the microorganisms operating in a sequencing batch reactor (SBR) undergo cycles of alternating anoxic and aerobic conditions, as described above, and show different microbial behavior compared to the biomass functioning in a simple batch reactor. Furthermore, the loading pattern and sludge retention time has a significant influence on sludge behavior. For example, if the feed is subjected to diurnal loading patterns, the bacteria can expect alternate feast and famine conditions resulting in the storage of substrates during feast and use in famine conditions. High sludge retention times (SRTs) and a low food to microorganism ratio as employed in most WWTPs for complete biological nutrient removal results in a low growth rate of biomass where storage becomes the dominant process (Beun et al., 2002; Sin et al., 2005). Negligible storage is observed when the mix-culture is operated at a growth rate close to its maximum substrate uptake rate (Sin et al., 2005).

Many researchers acknowledge that the substrate biodegradation process must be closely monitored, using on-line respirometric measurements (Spanjers et al., 1998; Vanrolleghem et al., 1999; Petersen, 2000; Carucci et al., 2001; Yuan and Bogaert, 2001; Beccari et al., 2002; Vanrolleghem et al., 2004; Sin et al., 2005) and titrimetry measurements (Gernaey et al., 1998; 2002b; Pratt et al., 2004; Sin and Vanrolleghem, 2007) during activated sludge model calibration. Other literature (Gernaey et al., 2001, 2002b; Sin and Vanrolleghem, 2007) supports a calibration approach with combined respirometric-titrimetric measurements for precise model calibration and validation purposes.

The International Water Association (IWA) (formerly IAWPRC, then IAWQ) task group on mathematical modeling proposed activated sludge models (ASM1, ASM2/ASM2d, ASM3) over the period of time 1982-1999 to facilitate the application of practical models to biological wastewater treatment systems. The models underwent further development, ranging from simple growth based model to more complicated models involving simultaneous storage and growth phenomena, for the better simulation of experimental observations in an activated sludge system. In most cases acetate was used as a calibration substrate. However, there is very little evidence that the recently developed models have been evaluated to determine their capacity to assess the biodegradation kinetics for other organic contaminants such as glutamic acid, urea or surfactants which are often found in wastewater.

1.2 Rationale of this study

While modeling of activated sludge is a crucial tool for understanding the substrate removal mechanism, the explanation of biodegradation behavior in the system by assessing substrate and sludge characteristics requires further investigation.

Activated Sludge Model No. 1 (ASM1) was first introduced by Henze et al. (1987) to interpret carbon and nitrogen oxidation. Though considerable attention was focused on model calibration with respirometric data such as the oxygen uptake rate (OUR) during the aerobic biodegradation of substrate (Spanjers and Vanrolleghem, 1995; Spanjers et al., 1998; Vanrolleghem et al.,1999; Carucci et al., 2001; Beccari et al., 2002; Vanrolleghem et al., 2004; Sin et al., 2005), few studies addressed model

development and calibration that indirectly measures the pH changes in aerobic systems (Gernaey et al., 2002a, 2002b; Pratt et al., 2004; Sin and Vanrolleghem, 2007). A useful model should be able to explain both the respirometric and titrimetric behaviors of the aerobic biodegradation process since dissolved oxygen and pH changes occur simultaneously in an activated sludge system. Consequently, Gernaey et al. (2002a, 2002b) extended the ASM1 model (for titrimetry) to include the pH effects of carbon uptake, ammonia uptake for growth, CO_2 production from the carbon metabolism and a constant CO_2 transfer rate (CTR) due to stripping. They calibrated this model using titrimetric and respirometric measurements. However, they assumed a constant CTR, which according to Pratt et al. (2003, 2004) may be applicable only when the system is controlled with a low CO_2 transfer coefficient at a pH higher than 8. Recently, Sin and Vanrolleghem (2007) improved the Gernaey model by considering a non-linear CTR in the liquid phase during the aerobic biodegradation process. However, the improved model was still based on ASM1 where the formation of intracellular storage products is not considered, thereby limiting the application of the model for biological treatment process.

ASM1 was extended later by the inclusion of biological phosphorus removal resulting in ASM2 and ASM2d (Henze et al., 1995, 1999). These models (ASM2 and ASM2d) are not included in this thesis since phosphorus removal is not dealt with this current study.

Gujer et al. (1999) proposed Activated Sludge Model No. 3 (ASM3) where the storage of organic polymers was first introduced. It assumed that all the substrate was stored in the biomass cell before being used for growth, but the dynamic CO_2 transfer phenomena was ignored. Pratt et al. (2004) developed a dynamic model and calibrated it using respirometric, titrimetric and off-gas CO_2 measurements where carbon storage was taken into account along with biomass growth. However the model excluded the endogenous respiration as well as the potential biomass growth on storage products during famine conditions. It was also limited because they used titration and off-gas analysis (TOGA) sensors for experimental study, where the CO_2 transfer rate was monitored using off-gas CO_2 measurements using sophisticated and expensive setup employing mass spectrometry. Meanwhile, the ASM3 model underwent further development as the experimental observations proved that both

storage and growth occur simultaneously during the feast phase (Van Aalst-van Leeuwen et al., 1997; Krishna and Van Loosdrecht, 1999; Beun et al., 2000). While the simultaneous storage and growth (SSAG) model was found to explain well the respirometric measurements for acetate biodegradation (Krishna and Van Loosdrecht, 1999; Beccari et al., 2002; Van Loosdrecht and Heijnen, 2002; Pratt et al., 2004; Sin et al., 2005), it does not provide for the titrimetric data interpretation.

Based on the discussion above, the following research problems were identified.

- Although the recently developed SSAG model was calibrated using the experimental observations of the biodegradation of readily biodegradable substrates like acetate, the applicability of its process kinetics for the biodegradation of other organic carbon compounds (such as surfactant and glutamic acid) is yet to be investigated.

- While the process kinetics involved in the SSAG model, based on respirometric measurements of acetate biodegradation, are well-calibrated, further improvement is needed. This can be achieved by introducing necessary stoichiometric components in each step of simultaneous storage and growth processes to describe the dynamics of proton balance that occurs concurrently in the system.

- Limited studies are available in the literature regarding the bio-kinetics of surfactant and glutamic acid degradation. They focus mostly on experiments using dissolved oxygen dynamics (respirometry) and fail to include any pH effect (titrimetry) thus limiting the accuracy of the estimated parameters. In addition, no model has been developed to accurately predict the pH effect on the organic carbon and organic nitrogen oxidation processes.

- The process kinetics for ammonium and urea nitrification are available in the literature where respirometric measurements are commonly used for model calibration. However, little reference is made to the titrimetric model for nitrification with due attention to the dynamic CO_2 transfer rate in the system.

1.3 Objective

The research project was undertaken for the development and calibration of activated sludge models for organic carbon and nitrogen oxidation using on-line respirometric and titrimetric measurements in the liquid phase. Acetate and surfactant were used to investigate sole carbon oxidation; while ammonium and urea were selected to observe nitrification. To determine the effect of the combined carbon and nitrogen components on the aerobic biodegradation process glutamic acid was chosen as a test substrate. A series of batch experiments was conducted for different initial substrate concentrations and pH values.

The particular objectives of this research project were:

- to monitor on-line respirometric and titrimetric measurements for the aerobic biodegradation of
    - acetate
    - surfactant
    - ammonium
    - urea and
    - glutamic acid
- to develop bio-kinetic models for test substrate biodegradation
- to calibrate the proposed model and to estimate the model parameters using:
    - respirometric measurements alone
    - titrimetric measurements alone
    - combined respirometric-titrimetric measurements
- to validate the proposed model using on-line and off-line measurements.

Finally, the estimated model parameters were compared and evaluated critically to explain the response of activated sludge to substrate oxidation process. The research outcome is expected to be helpful in further refining current models.

1.4 Scope of the research

The scope of this current research was limited to the experimental investigation of organic carbon and nitrogen biodegradation under aerobic conditions followed by the model based interpretation of both respirometric and titrimetric observations in describing biodegradation processes. The model calibration and parameter estimation were undertaken using non-linear techniques utilizing the algorithms in the optimisation toolbox (MATLAB). In addition to on-line measurements, the proposed model was validated using off-line measurements. Five different substrates, that represent sole carbon, nitrogen and a combination of carbon and nitrogen sources, were selected for experimental investigation and subsequent modeling. However, real wastewater that contains a mixture of several complex carbon and nitrogen sources was not included in this investigation. Though substrates can be biodegraded by means of aerobic, anaerobic, anoxic processes or a combination of them, the current research focuses only on aerobic processes for proposing and improving the bio-kinetic models. During the lab-scale experiments, a constant temperature and pH were maintained to monitor the biodegradation process, as it facilitated the comparison among different case studies. The experimental investigation was conducted using batch reactors in this research. The biodegradation processes were also investigated with different pH conditions for certain substrates. In practice, the temperature of the wastewater is subjected to daily and seasonal fluctuation depending on the climatic conditions of the regions concerned. Since both the autotrophic and heterotrophic biomass in activated sludge are temperature and pH sensitive, there is a scope to continue this study for different pHs and temperatures, which was not part of the current investigations.

1.5 Organization of the thesis

The thesis has been organized into eight chapters. A brief description of these chapters is given below.

The background of the study, the research questions and objectives of the current research project have been presented in **Chapter 1**.

Chapter 2 contains the literature review which focuses on the theory of respirometry and titrimetry (on-line measurement techniques that were used in the current research) for single batch reactor in monitoring substrate biodegradation under aerobic conditions. In addition, this chapter outlines the calibration and model parameter estimation protocol followed by discussion on the consecutive development of activated sludge models (ASM1, ASM3 and SSAG models) for organic carbon oxidation and nitrification.

Chapter 3 describes the materials and methods used to investigate the aerobic biodegradation of different substrates such as acetate, ammonium, surfactant, urea and glutamic acid. This chapter also includes the approaches followed for activated sludge models simulation, calibration and parameter estimation using respirometric and titrimetric on-line measurement techniques.

Modeling of acetate biodegradation is discussed in detailed under **Chapter 4**. Different activated sludge models are assessed and the results discussed initially using on-line respirometric measurements. A model is then proposed for experimental titrimetric and respirometric data interpretation using acetate as a calibration substrate. Calibration and parameter estimation results from three different calibration approaches are discussed in this chapter followed by model validation. Moreover, this chapter describes the model calibration and parameter estimation results obtained from studies using different pH values as part of the proposed model verification.

Chapter 5 introduces the modeling of surfactant (a relatively complex carbon source compared to acetate) biodegradation and describes the development of a bio-kinetic model based on the titrimetric and respirometric measurements. It includes a proposed model calibration and parameter estimation using three initial substrate concentrations and three calibration approaches. This chapter also features the application of the proposed model for different pH levels with discussion on the estimated parameters.

Modeling of nitrification process is presented in **Chapter 6** which covers the biodegradation modeling for ammonium (a nitrogen source) and for urea (a relatively

complex nitrogen compound compared to ammonium). This chapter describes the proposed model calibration and parameter estimation results obtained from titrimetric and respirometric measurements followed by model validation with off-line measurements.

Chapter 7 represents the modeling of glutamic acid biodegradation that includes model development, calibration and parameter estimation both with and without nitrification inhibition process in an activated sludge system. Combined respirometric-titrimetric measurements were used for the proposed model calibration. Nitrification inhibition is described first to explain the sole carbon oxidation followed by model calibration and discussion for combined nitrogen and carbon oxidation during glutamic acid biodegradation.

Chapter 8 details the conclusions and recommendations from the research and suggests aspects for further study.

Chapter 2
Literature Review

2.1 Introduction

The activated sludge process is one of the most widespread biological wastewater treatment processes. The biomass (bacteria) present in the sludge is engineered to remove commonly occurring contaminants in wastewater such as organics and nutrients by providing suitable conditions needed for specific microorganisms in required processes. Researchers have been working for more than two decades to demonstrate the mechanisms of different biological processes occur in a wastewater treatment plant (WWTP) by developing dynamic activated sludge models along with calibrating and validating them through several experimental observations occurring simultaneously. But the substrate removal mechanisms by microorganisms are not yet fully understood. This chapter, therefore, critically reviews the existing activated sludge models for aerobic carbon oxidation and nitrification. It further includes discussion on respirometry and titrimetry since these on-line measurement techniques were used in this current research project for investigating substrate biodegradation under aerobic conditions. In addition, the principles of model development, model processes and components as well as model calibration and limitations are outlined in this chapter.

2.2 Respirometry and Titrimetry

Respirometry is the measurement and interpretation of the respiration rate of activated sludge and is defined as the amount of oxygen per unit of volume and time that is consumed by microorganisms in a dynamic system. As the conventional BOD_5 or ultimate BOD measurements cannot provide detailed bio-kinetic information in the frame of wastewater treatment plant operation, the concept of short-term biochemical oxygen demand (BOD_{st}) was introduced through respirometric analysis (Spanjers, 1993; Vanrolleghem and Spanjers, 1994). The oxygen uptake rate (OUR) measurement technique, in which the OUR is derived from dissolved oxygen mass balance in a bio-culture, has been employed recently as

a powerful tool for assessing the bio-kinetics of a system since it is directly related to biomass growth and substrate consumption (Spanjers and Vanrolleghem, 1995; Brouwer et al., 1998; Spanjers et al., 1998; Vanrolleghem et al., 1999; Petersen et al., 2001; Gernaey et al., 2002a; Karahan-Gul et al., 2002; Hoque et al., 2009a).

Titrimetry is the measurement technique that yields information about the pH change occurring due to microbial metabolism in a bio-culture. It has recently reached a useful level of precision as it provides an indication of the status of ongoing biological reactions. The equilibrium pH of sludge is affected by several processes such as: (a) CO_2 production due to the respiration of biomass; (b) proton production /consumption during the substrate uptake (Gernaey et al., 1998; Gernaey et al., 2002a); (c) aqueous CO_2 equilibrium; and (d) CO_2 stripping (Sin and Vanrolleghem, 2007). The proton in the bio-culture, either consumed or produced, can be measured by maintaining a constant pH of the liquid medium through the addition of acid and/or base (Gernaey et al., 1997). This technique was found to be very useful to quantify the kinetics of activated sludge process (Petersen et al., 2002; Pratt et al., 2003; Sin et al., 2003).

Furthermore, combined respirometric-titrimetric measurements can be used for appropriate bio-kinetic parameter estimation (Petersen et al., 2001; Yuan and Bogaert 2001; Sin and Vanrolleghem, 2007; Hoque et al., 2010). While Petersen et al., 2001 successfully applied this approach for nitrification process; carbon source biodegradation was investigated by Gernaey et al. (2002b) who showed combined respirometric-titrimetric measurements to be more effective in improving parameter confidence intervals than estimation based on separate respirometric or titrimetric data sets. Figure 2.1 shows the schematic diagram of combined respirometric-titrimetric measurements for acetate oxidation and nitrification. Heterotrophic biomass consumes carbon (acetate) during the feast period causing acid addition in the system along with resulting OUR to reach the first peak (Figure 2.1). OUR drops after the complete removal of acetate from the system that can be confirmed through the titrimetric measurement indicating the end point of acetate degradation (Sin, 2004). The second peak in the figure indicates the nitrification process governed by autotrophic biomass where base addition takes place concurrently with a change in slope indicating the end point of the nitrification (Yuan and Bogaert 2001).

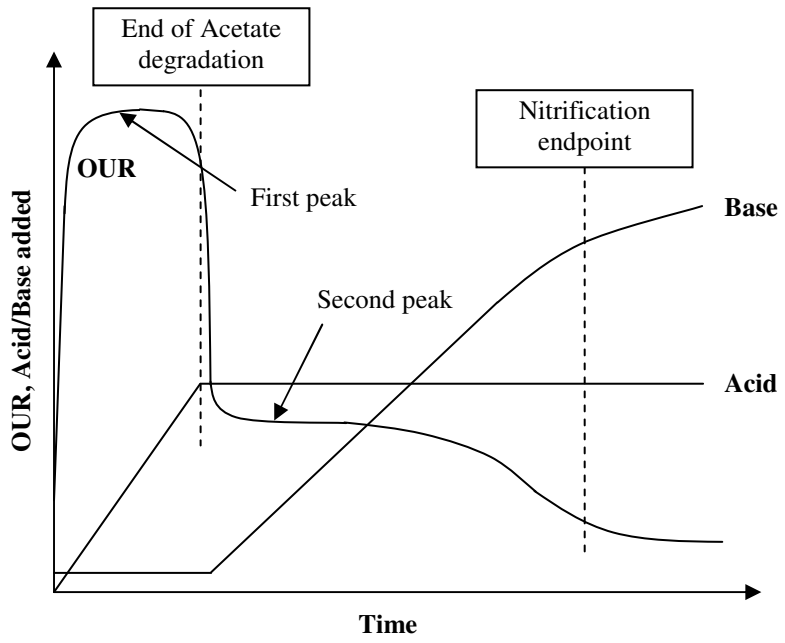

Figure 2.1: Schematic presentation of combined respirometric-titrimetric measurements for acetate oxidation and nitrification

2.2.1 Theory of respirometry for single batch reactor

The dissolved oxygen (DO) mass balance in an activated sludge filled batch reactor is determined by the oxygen supply and biological oxygen uptake process. Respiration can be sub-divided into endogenous (OUR_{end}) and exogenous (OUR_{exo}, substrate degradation induced) oxygen uptake rates. The change in DO concentration over time ($\frac{dS_o}{dt}$) can therefore be expressed as follows:

Change in DO = Input - Output

$$\frac{dS_o}{dt} = K_L a(S^*_o - S_o) - \left(OUR_{end} + OUR_{exo}\right) \qquad \text{----- (Equation 2.1)}$$

When aeration takes place in the absence of substrate, the DO concentration will reach a steady state, reflecting the equilibrium between oxygen transfer and endogenous respiration:

$$\frac{dS_o}{dt} = 0 = K_L a(S^*_o - S_{eq}) - OUR_{end} \quad \text{----- (Equation 2.2)}$$

From this, the difference between the equilibrium concentration (S_{eq}) and the saturated level (S^*_o) multiplied by the volumetric mass transfer coefficient ($K_L a$) reflects the OUR_{end}. By substituting OUR_{end} with $K_L a(S^*_o - S_{eq})$ in equation 2.1, the exogenous respiration can be determined.

$$\frac{dS_o}{dt} = K_L a(S_{eq} - S_o) - OUR_{exo} \quad \text{----- (Equation 2.3)}$$

The addition of biodegradable substrate to the mixed liquor causes the DO level to decrease due to exogenous respiration. When the substrate is oxidized completely, OUR_{exo} returns to zero. Due to continuous aeration, the DO concentration will increase until the steady state is again reached. Figure 2.2 illustrates the typical respirogram (DO profile) for the biodegradable compound in an activated sludge process.

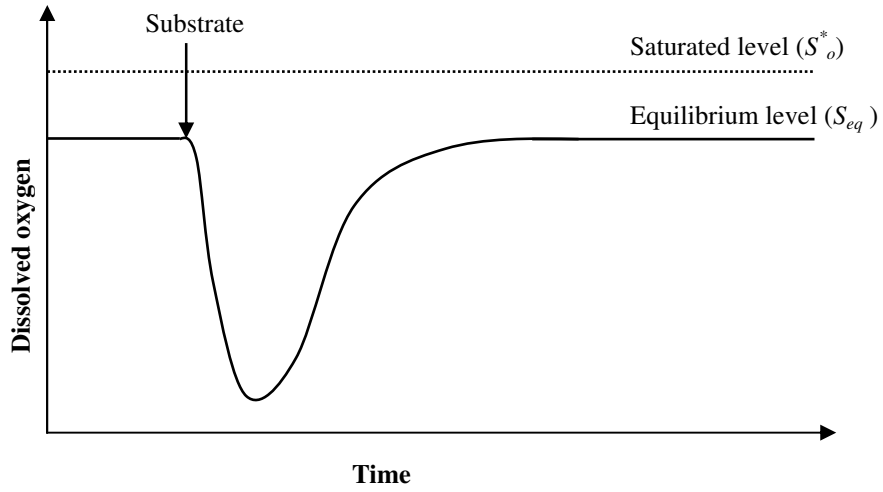

Figure 2.2: Typical respirogram for the biodegradable compound in an activated sludge process

2.2.2 Theory of Titrimetry for single batch reactor

Titrimetry is an indirect measurement of the pH effects resulting from the biomass metabolic activities. The raw titration data represents the acid/base pulse during the biological reaction which can be converted to meq/L units by using acid/base normality and flux data along with reactor volume (Gernaey et al., 1998). This can be expressed as:

$$H_{meq/L} = \frac{H_{pulse} \times Q_{flux} \times N}{V_{reactor}} \quad \text{----- (Equation 2.4)}$$

where, H_{pulse} represents the pulse number during the reaction, Q_{flux} is the acid/base flux (ml/pulse), N is the normality of the acid or base (meq/ml) and $V_{reactor}$ is the volume of the bio-reactor (L).

As well as respirometry, titrimetric data can also be used to determine the nitrogen load in wastewater using the following expression (Gernaey et al., 1997):

$$S_N = \frac{(B2 - B1) \times Q_{flux} \times N \times 7}{V_{reactor}} \quad \text{----- (Equation 2.5)}$$

where, S_N is the initial concentration of nitrogenous compound (mg N/L), *B1* represents the number of base pulses needed to adjust the pH of the sludge to the pH set point, *B2* is the cumulative base pulses corresponding to the nitrification process plus *B1* pulses, and 7 is the conversion factor (to change the unit from 'meq' to 'mg N').

2.3 Modeling of organic carbon oxidation and nitrification

2.3.1 Why modeling ?

Modeling is considered as a crucial tool for understanding the substrate removal mechanism and therefore can lead to better design and optimization of the processes in WWTPs. It has been evolving for more than two decades with attempts to give a realistic interpretation of biological substrate removal process in an activated sludge

system. Developments range from simple growth based model to more complicated models involving storage phenomena. However, the calibration step in modeling appears to be the bottleneck to the widespread use of simulating the full-scale activated sludge system (Sin and Vanrolleghem, 2007). Hence, researchers continue to investigate the substrate conversion mechanisms in an activated sludge system by proposing hypotheses for the formation of new models or improving the kinetic expression of existing models. Some recognized activated sludge models for carbon oxidation and nitrification are reviewed below.

2.3.2 Model calibration and parameter estimation protocol

Activated sludge models consist of several kinetic and stoichiometric parameters that represent the process rates involved in the system and the sludge characteristics respectively. The term "Model calibration" is used to express the adaptation of the model to fit a certain set of information obtained from the full-scale WWTP under study. While there is a wide application of activated sludge models for the optimization of operation and maintenance of WWTP, details on the model calibration procedure are rarely mentioned in the literature. In fact, it is very difficult to generalize model calibration strategies since the purpose of a model being built is very much related to how the calibration process is approached (Henze et al., 1995). Appropriate selection of models is based on the aim of the modeling (e.g. COD, nitrogen or other nutrients removal) in order to optimize the calibration efforts. Depending on the purpose of the model, modifications or extensions of the proposed models should be considered.

Parameter estimation is a process to determine the optimum values of model parameters with the aid of measured data. Figure 2.3 depicts the basics of a parameter estimation process. As it is unrealistic and time-consuming to estimate all model parameters, default values reported in previous applications should be assigned to the model parameters whenever applicable (Henze et al., 2000). A sensitivity analysis based on the aim of the modeling exercise can be conducted in order to choose the most appropriate parameters for the estimation (Weijers and Vanrolleghem, 1997; Brun et al., 2002; De Pauw et al., 2004). The application of the sensitivity analysis in the calibration protocol is expected to minimize the calibration

efforts that lead to optimize the overall calibration procedure towards the objectives of the modeling. In a non-linear parameter estimation process, an initial guess of model parameters together with the initial concentrations of the components and experimental data must be made (Petersen et al., 2003). The actual parameter estimation is then made by minimizing the objective function with certain given accuracy (Figure 2.3). The reader is referred to Dochain and Vanrolleghem (2001) for more information about different numerical techniques associated with the parameter estimation process.

After the model calibration and parameter estimation process the model is validated by using an independent data set, which was not used in the calibration. Ideally a separate measurement campaign data, performed under different operating conditions, should be used to validate the model.

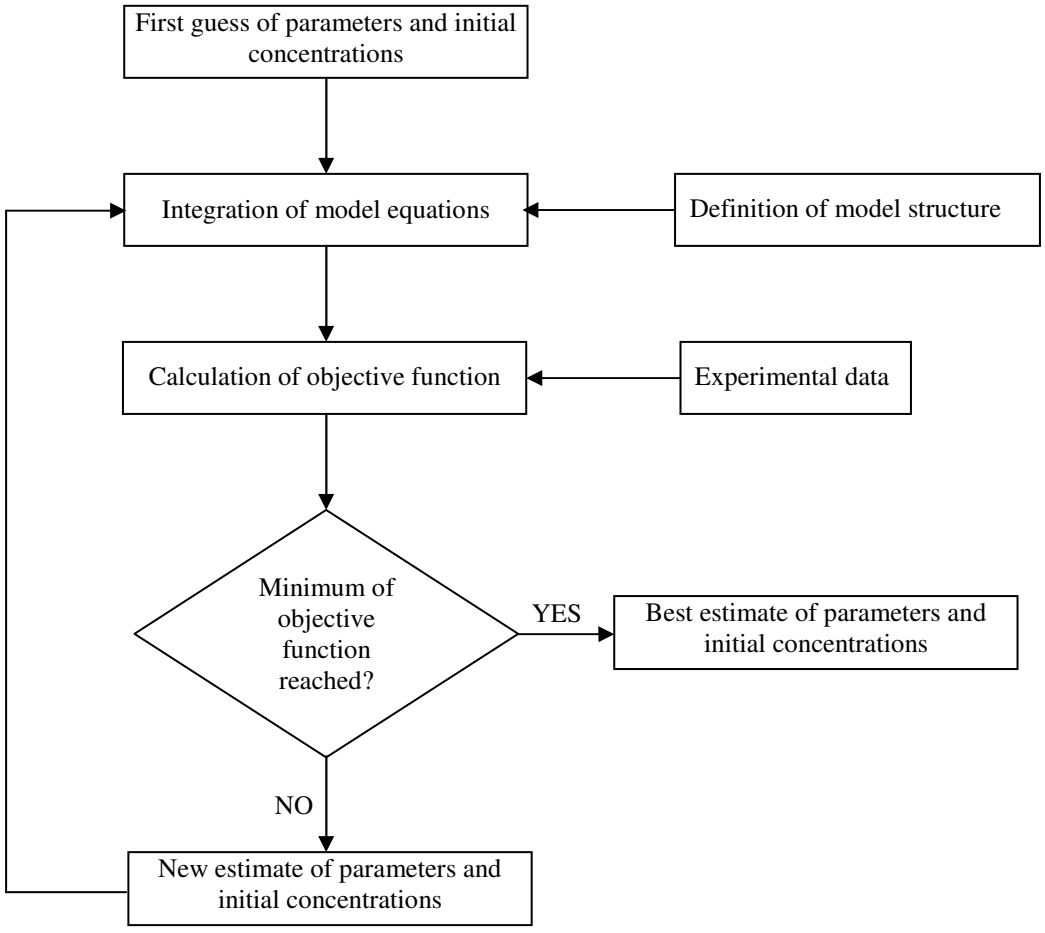

Figure 2.3: Parameter estimation procedure (adopted from Wanner et al., 1992)

2.4 Activated Sludge Model No. 1

Activated Sludge Model No. 1 (ASM1) is considered the pioneer model to describe the kinetics of micro-organisms metabolism (Henze et al., 1987).

2.4.1 Model principle

ASM1 is based on the assumption that all substrate removal is attributed solely to microbial growth. Figure 2.4 represents the model process diagram involved in ASM1. While the heterotrophic micro-organisms use COD in a cycle reaction scheme, the autotrophic micro-organisms use a reduced form of nitrogen and nitrify them in the aerobic system. Complex substrates including the decay of nitrifiers are hydrolyzed before being consumed for biomass growth. Figure 2.4 also shows the entry points of oxygen consumption that occurs during the growth of heterotrophs and nitrifiers in the system. In ASM1, both the heterotrophic and autotrophic micro-organisms are interlinked via the decay process (Figure 2.4).

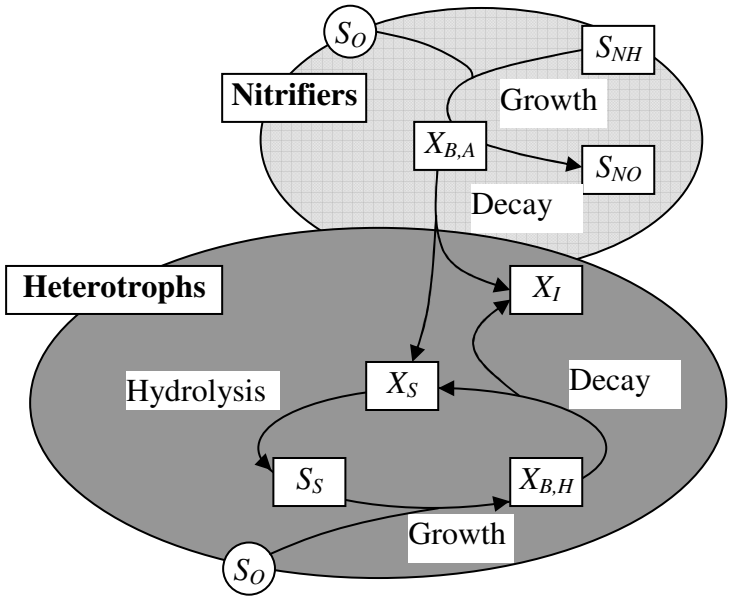

Figure 2.4: Schematic presentation of processes in ASM1 (modified from Henze et al., 2000)

2.4.2 Aerobic processes involved in ASM1

Table 2.1 shows the process kinetics and stoichiometry involved in aerobic biodegradation of substrates in ASM1. Hydrolysis is the process that breaks down the slowly biodegradable substrate (X_S) enmeshed in the sludge to produce readily biodegradable substrate (S_S).

Aerobic growth of the heterotrophic biomass takes place by the degradation of carbon source, S_S under the consumption of oxygen (S_O). On the other hand the ammonia nitrogen (S_{NH}) is oxidized to nitrate through scaling up the autotrophic biomass production in the system. All the concentration components (S_S, S_{NH} and S_O) are considered to be rate limiting for the growth process. Hence, the Monod relationships are applied to explain the growth kinetics. The alkalinity (S_{ALK}) has been affected by the nitrification (see the column for S_{ALK} in Table 2.1) in the system.

Dold (1980) introduced the "death regeneration" concept used to explain the decay of biomass in ASM1. The decay process is assumed to release slowly biodegradable substrate in the system which is recycled back to the soluble substrate to be utilized for cell growth. A parallel conversion of organic nitrogen to ammonia nitrogen takes place in the system. ASM1 considered the recycling of the substrate in the system where the magnitude of the decay coefficient is different from that of the more usually encountered rate constant (which is used for traditional endogenous respiration in ASM3). In the usual approach, the loss of one unit of biomass COD leads to the utilization of one unit of oxygen minus the COD of the inert particulate products formed. However in ASM1, the loss of one unit of biomass COD results in the ultimate formation of one unit of COD due to readily biodegradable substrate minus the COD of the inert particulate products formed. Readily biodegradable COD is used for cell synthesis where only a fraction of a unit of oxygen will be required because of the energy incorporated into the cell mass. That cell mass in turn undergoes decay before the unit of oxygen is conclusively removed. First order process rate is found to explain the conversion of biodegradable soluble organic nitrogen (S_{ND}) to ammonia nitrogen (S_{NH}). This conversion process also contributes to the change in alkalinity (see Table 2.1).

Table 2.1: Process matrix involved in ASM1 for carbon oxidation and nitrification (adopted from Henze et al., 1987)

Variables & Units → / Process ↓	S_S	X_S	$X_{B,H}$	$X_{B,A}$	X_P	S_O	S_{NO}	S_{NH}	S_{ND}	X_{ND}	S_{ALK}	Process rate
	[M(COD)L^{-3}]						[M(N)L^{-3}]				[Molar unit]	[ML^{-3}T^{-1}]
Hydrolysis	1	-1	--	--	--	--	--		--	--	--	$k_h.\left(\frac{X_S/X_{B,H}}{K_X+(X_S/X_{B,H})}\right).\left(\frac{S_O}{K_{O,H}+S_O}\right).X_{B,H}$
Aerobic growth on heterotrophs	$-\frac{1}{Y_H}$	--	1	--	-1	$-\frac{1-Y_H}{Y_H}$	--	$-i_{XB}$	--	--	$-\frac{i_{XB}}{14}$	$\mu_{mH}.\left(\frac{S_S}{K_S+S_S}\right).\left(\frac{S_O}{K_{O,H}+S_O}\right).X_{B,H}$
Aerobic growth on autotrophs	--	--	--	1	--	$-\frac{4.57-Y_A}{Y_A}$	$\frac{1}{Y_A}$	$-i_{XB}-\frac{1}{Y_A}$	--	--	$-\frac{i_{XB}}{14}-\frac{1}{7Y_A}$	$\mu_{mA}.\left(\frac{S_{NH}}{K_{NH}+S_{NH}}\right).\left(\frac{S_O}{K_{O,A}+S_O}\right).X_{B,A}$
Decay of heterotrophs	--	$(1-f_P)$	-1	--	f_P	--	--	--	--	$-i_{XB}-f_P.i_{XP}$	--	$b_H.X_{B,H}$
Decay of autotrophs	--	$(1-f_P)$	--	-1	f_P	--	--	--	--	$-i_{XB}-f_P.i_{XP}$	--	$b_A.X_{B,A}$
Ammonification	--	--	--	--	--	--	--	1	-1	--	$\frac{1}{14}$	$k_a.S_{ND}.X_{B,H}$

Soluble inert organic matter (S_I) and particulate inert organic matter (X_I) are not shown in the matrix as they are not involved in any conversion processes (Henze et al., 1987)

The kinetics and stoichiometric parameters involved in the ASM1 are presented in Table 2.1 (see Appendix A for their definition). For further details the reader is referred to the IWA (formerly IAWPRC, then IAWQ) Task group report (Henze et al., 2000). Table 2.2 shows typical parameter values related to carbon oxidation and nitrification in an activated sludge system.

Table 2.2: Typical parameter values related to carbon oxidation and nitrification at neutral pH (for ASM1) (Henze et al., 1987)

Symbol	Units	Value at 20^0C	Value at 10^0C
Stoichiometric parameters			
Y_A	g cell COD formed (g N oxidized)$^{-1}$	0.24	0.24
Y_H	g cell COD formed (g COD oxidized)$^{-1}$	0.67	0.67
f_P	dimensionless	0.08	0.08
i_{XB}	g N (g COD)$^{-1}$ in biomass	0.086	0.086
i_{XP}	g N (g COD)$^{-1}$ in endogenous mass	0.06	0.06
Kinetic parameters			
μ_{mH}	day^{-1}	6.0	3.0
K_S	g COD m^{-3}	20.0	20.0
$K_{O,H}$	g O_2 m^{-3}	0.20	0.20
K_{NO}	g NO_3-N m^{-3}	0.50	0.50
b_H	day^{-1}	0.62	0.2
k_h	g slowly biodegradable COD (g cell COD.day)$^{-1}$	3.0	1.0
K_X	g slowly biodegradable COD (g cell COD)$^{-1}$	0.03	0.01
μ_{mA}	day^{-1}	0.8	0.3
K_{NH}	g NH_3-N m^{-3}	1.0	1.0
$K_{O,A}$	g O_2 m^{-3}	0.4	0.4
k_a	m^3 .COD (g.day)$^{-1}$	0.08	0.04

2.4.3 COD and nitrogen components in ASM1

In ASM1, the total COD is divided into non-biodegradable organic matter and biodegradable matter which are further subdivided into soluble (*S*) and particulate (*X*) components.

The non-biodegradable matter includes inert soluble organic matter (S_I) and inert suspended organic matter (X_I) in the wastewater influent or produced via decay (X_P) that passes through an activated sludge system in unchanged form. The concentration of the inert component S_I is assumed to be as same as it enters in the system. The component X_I or X_P becomes enmeshed in the activated sludge and is removed from the system via the sludge wastage. The biodegradable matter includes soluble readily

biodegradable (S_S) and slowly biodegradable (X_S) substrate. The readily biodegradable substrate refers to relatively simple molecules that may directly be consumed by heterotrophic organisms and used for growth of new biomass. In contrast, enzymatic breakdown is required for the slowly biodegradable substrate prior to utilization for biomass growth. Biomass cell growth on S_S or growth on ammonia nitrogen (S_{NH}) results in heterotrophs ($X_{B,H}$) or autotrophs ($X_{B,A}$) production in mixed culture respectively; which in turn is lost via the decay process where it is converted to X_P and X_S. Figure 2.5 demonstrates the COD components involved in ASM1 and ASM3.

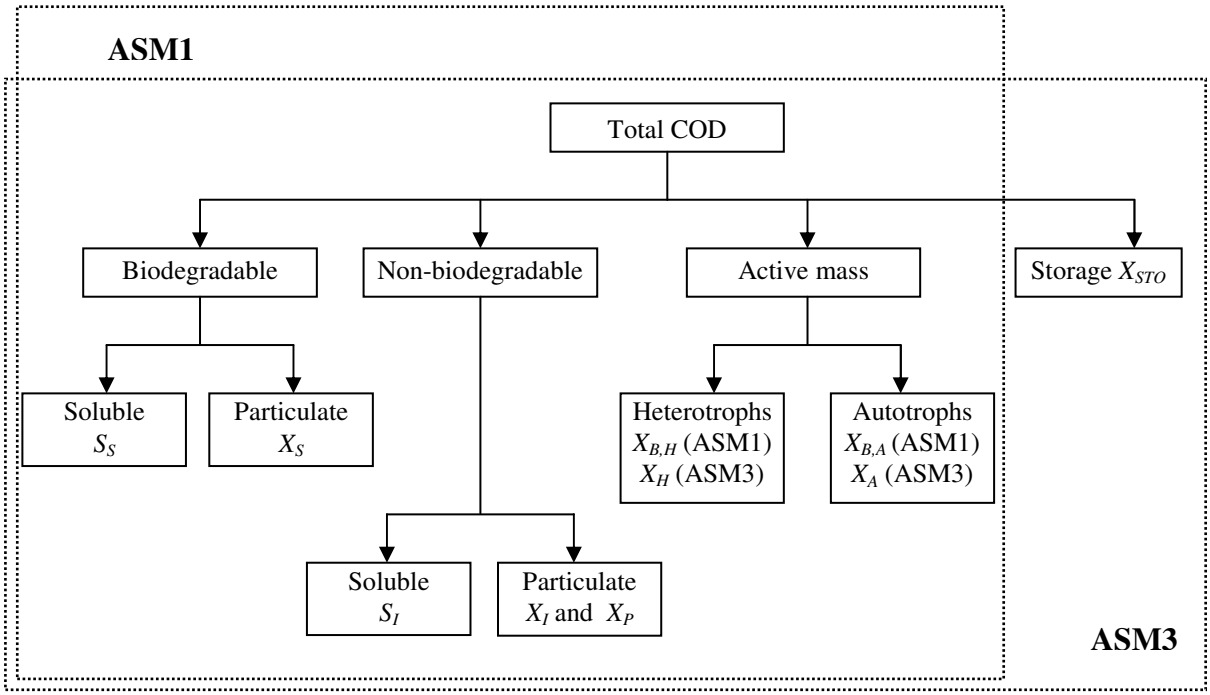

Figure 2.5: COD components in ASM1 and ASM3 (modified from Jeppsson, 1996)

Nitrogen components used in ASM1 and ASM3 are illustrated in Figure 2.6. Like COD matter, total nitrogen (Kjeldahl) is divided into non-biodegradable and biodegradable components. The soluble non-biodegradable organic nitrogen (S_{NI}) is assumed to be negligible in ASM1. On the other hand, the non-biodegradable particulate organic nitrogen is considered to be associated with non-biodegradable particulate COD (X_I or X_P). The biodegradable nitrogen includes ammonia nitrogen, (both the free compound and its salts), S_{NH}; soluble organic nitrogen, S_{ND}; and

particulate organic nitrogen X_{ND}. Ammonia nitrogen serves as the nitrogen source for synthesis of heterotrophic biomass as well as for the growth of autotrophic nitrifying bacteria. The parameter i_{XB} is used to represent the amount of nitrogen incorporated per COD unit (Figure 2.6). The particulate organic nitrogen is hydrolyzed to soluble organic nitrogen in parallel with hydrolysis of the slowly biodegradable organic matter, X_S in activated sludge system. The soluble organic nitrogen is then converted to ammonia nitrogen via ammonification. The autotrophic conversion of ammonia nitrogen to nitrate nitrogen is considered to be a single step process to keep the model simple. The reader is referred to the IWA (formerly IAWPRC, then IAWQ) Task group report (Henze et al., 2000) for more details.

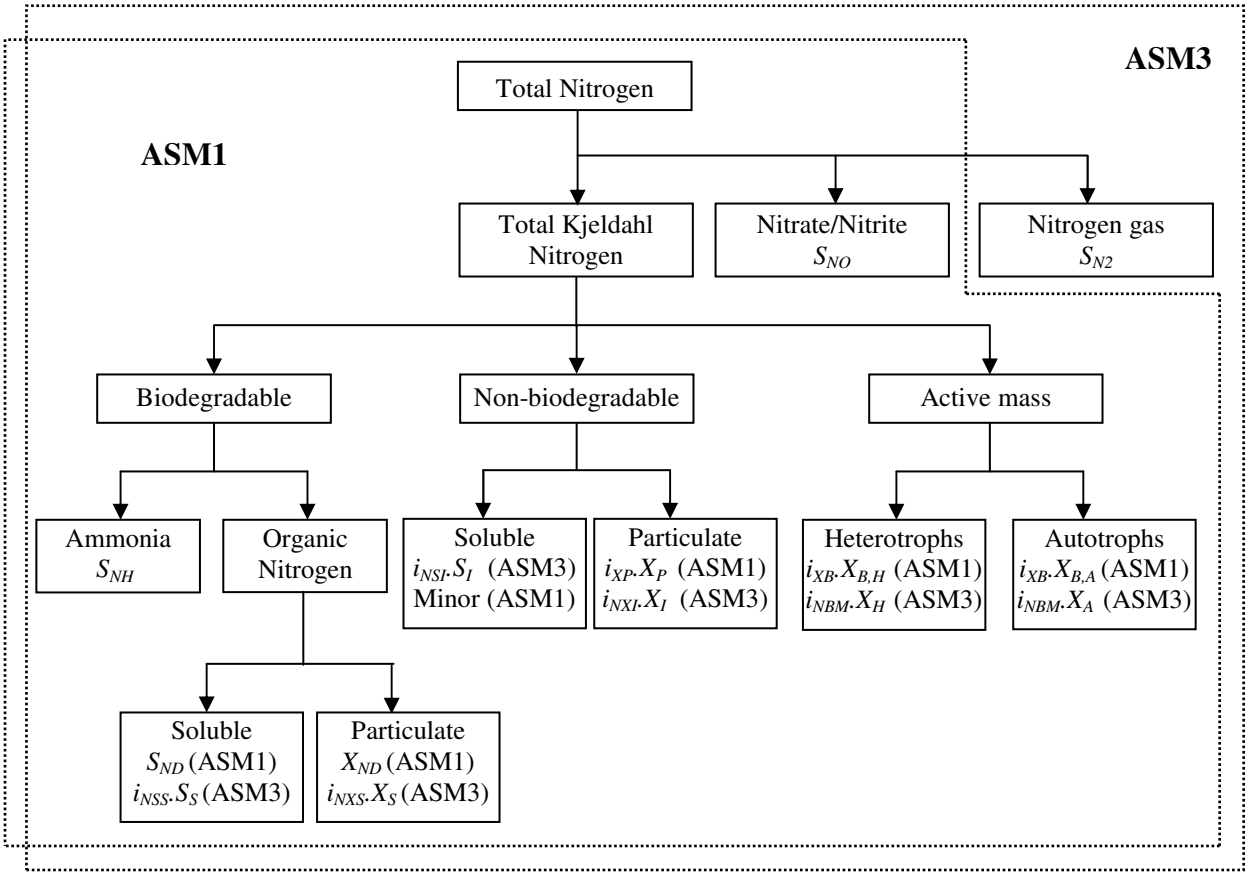

Figure 2.6: Nitrogen components in ASM1 and ASM3 (modified from Jeppsson, 1996)

2.4.4 Calibration of ASM1 under aerobic conditions

Researchers have used ASM1 to investigate substrate removal mechanisms in activated sludge using: (a) a variety of synthetic compounds and/or real wastewater; (b) different reactor configurations; and (c) various calibration approaches for model parameter estimation. An overview of the ASM1 model calibration process for aerobic biodegradation study is presented below.

Spanjers and Vanrolleghem (1995) calibrated the ASM1 model with respiration rate measurements where ammonium, acetate/ammonium mixture, raw wastewater and filtered wastewater were used as test substrates. Gernaey et al. (1997, 1998) adopted titrimetric measurements as an alternative to the oxygen consumption approach for ASM1 model calibration. A plug-flow system was used in a pilot activated sludge plant fed with synthetic wastewater. They estimated the ammonium N concentration in the activated sludge system using titrimetry and compared it to the on-line ammonium N measurements for model validation. A modified version of ASM1 was used by Brouwer et al. (1998) to investigate the identifiability of bio-kinetic parameters and biodegradable wastewater components using continuous respirometer. They calibrated the model using respiration rate measurements and estimated the wastewater fractions from modeling by comparing them with analytical data (such as nitrogen, COD and BOD_5). An aerobic batch test was performed by Carruci et al. (1999) using different proportions of wastewater. They modified ASM1 for calibration with experimental COD, ammonia, nitrate, MLVSS, pH and temperature data.

Orhon et al. (1999) reviewed the conceptual framework for the hydrolysis of slowly biodegradable substrate through activated sludge model evaluation using OUR data during model calibration. They found the saturation type surface reaction kinetics (ASM1) explains well the hydrolysis of domestic and industrial wastewater when compared with bulk reaction kinetics. They also recommended a dual hydrolysis approach for better interpretation of the hydrolysis of slowly biodegradable compounds. Schreiner et al. (1999) investigated the aerobic biodegradation kinetics of surfactants (non-ionic) using a respirometric technique. They conducted the experiments in a closed respirometer by adding alcohol ethoxylate (AEO) to the

batch reactor. They developed a model based on ASM1 and introduced a double Monod kinetic to explain the OUR in the system and estimated the model parameters for substrate and activated sludge characterization. An overview of respirometric measurement technique for calibration of ASM1 with OUR utilizing carbon-nitrogen mixture, raw wastewater, and ammonium as test substrates was developed by Vanrolleghem et al. (1999).

Gernaey et al. (2001) established a combined respirometric-titrimetric set-up with an aerated chamber and a closed respiration chamber for investigating acetate, ammonium and urea biodegradation under aerobic conditions. They applied the experimental OUR data associated with acetate and urea degradation for modified ASM1 model calibration. Moreover, they calibrated the proposed model using OUR alone, *Hp* alone and combined OUR-*Hp* measurements for ammonium nitrification showing that a combined calibration approach improved the confidence interval of estimated parameters. Okutman et al. (2001) investigated the hydrolysis kinetics for settleable substrate in domestic waste feeding in a batch reactor and estimated the kinetic parameters for OUR measurements using ASM1 as a reference model. Petersen et al. (2001) studied the theoretical identifiability of the parameters in a two-step nitrification model (ASM1) for ammonium excluding biomass growth. They used a hybrid respirometer combined with titrimetric measurements for the experiments and three different calibration approaches: using OUR data alone, *Hp* data alone and combined OUR-*Hp* data.

Benes et al. (2002) used both a static liquid respirometer and a flowing liquid type respirometer for conducting lab-based experiments to monitor acetate biodegradation in an activated sludge system. They used the ASM1 model with further modification to explain respirometric behavior during the acetate degradation process. Gernaey et al. (2002b) investigated the aerobic carbon source degradation (acetate and dextrose) using respirometric-titrimetric measurement techniques. A simplified version of ASM1 was calibrated using on-line OUR data alone, Hp data alone and with combined OUR-*Hp* data. A comparison of estimated parameters obtained from different calibration approaches was performed for model validation. A modified version of ASM1 was calibrated by Insel et al. (2002) with OUR measurements alone by adding domestic sewage to the batch reactor. They studied the sensitivity of

model parameters as well to understand their effect on respirometric profile relating to substrate biodegradation process.

Furthermore, Marsili-Libelli and Tabani (2002) assessed the experimental errors based on OUR measurements in a closed intermittent-flow device injecting ammonium as a test compound. They used a two step nitrification model (ASM1) for model calibration followed by the assessment for practical identifiability of model parameter with sensitivity analysis. Boursier et al. (2004) proposed a modified version of ASM1 for substrate (acetate, propionic and butyric acid) biodegradation including the separation of the anoxic and the aerobic sludge yields and a simplified kinetic for the hydrolysis process. They performed aerobic respirometric tests on lab-scale using an aerated reactor and a dissolved oxygen measuring chamber where the OUR data was applied for the proposed model calibration. Lopez Zavala et al. (2004) studied the kinetics for aerobic biodegradation of faeces using batch reactors equipped with on-line oxygen measurement units. A simplified version of ASM1 was calibrated with experimental OUR data and parameters were estimated for several organic loadings with sensitivity analysis. Realizing the transient phenomenon, Vanrolleghem et al. (2004) modified ASM1 by introducing a first order expression ($1\text{-}e^{-t/\tau}$) to explain the biomass behavior that was commonly observed in short-term batch experiments. The proposed model was calibrated with experimental OUR and Hp measurements obtained by feeding the reactor with acetate. The proposed model was also applied for ammonium nitrification.

Stricker and Racault (2005) applied ASM1 for characterization of pure winery effluent by calibration and validation of the model with respect to COD, DO and OUR data generated from the plant's jet-aerated tank. A sequencing batch reactor (SBR) system was used by Corominas et al. (2006) for investigating oxygen and nitrate dynamics of treated wastewater where ASM1 model was calibrated with experimental observations (DO and NO_3-N). Levstek et al. (2006) observed the nitrification-denitrification process of artificial wastewater on suspended activated sludge in a laboratory based continuous stirred tank reactor (CSTR) pilot plant where modified ASM1 was proposed and calibrated with COD and ammonia mass concentration. Furthermore, Munz et al. (2008) applied respirometric techniques for characterization of tannery wastewater and biomass in a membrane bioreactor

(MBR) using ASM1 as the reference model. They calibrated the model with experimental OUR data, whereas the biomass and COD measurements were used for model verification. Costa et al. (2009) simplified the ASM1 to explain the substrate degradation dynamics by feeding high strength wastewaters in complete mix reactor. On the other hand, Damayanti et al. (2010) used CSTR system for investigating palm oil mill effluent degradation where ASM1 model was calibrated and parameters were estimated using experimental OUR measurements.

The evaluation of activated sludge models was conducted by different researchers to investigate the model capability to explain real experimental observations. For example, Guisasola et al. (2005) assessed simplified ASM1 and ASM3 models by calibrating them with respirometric batch profiles (OUR) of the acetate biodegradation process. As another example, a porous pot membrane reactor was used by Shahriari et al. (2006) for the evaluation of bio-kinetic models (simple, intermediate, ASM1 and ASM3) to explain the soluble COD and MLVSS in the degradation process. Dizdaroglu-Risvanoglu et al. (2007) used ASM1, ASM3 and simultaneous storage and growth (SSAG) models with OUR measurements in batch reactors for tannery wastewater characterization. While in most cases the ASM1 failed to explain the experimental observations, this model was found to fit well in cases where biomass was collected from plants operated for simultaneous COD removal and nitrification. However, all the above models failed to include the physical processes occurring in the liquid phase relating to carbon dioxide transformation. Consequently, Sin and Vanrolleghem (2007) extended ASM1 to explain aerobic carbon (acetate) degradation in an activated sludge system using combined respirometric-titrimetric measurements. They introduced a non-linear carbon dioxide transfer process into the model structure and calibrated the proposed model with a practical identifiability study. A comparison of estimated parameters obtained from three different calibration methods: using OUR data alone, Hp data alone and with combined OUR-*Hp* data, was performed for model validation. However, ASM1 could not explain the tail occurring in experimental OUR observation, especially when the used biomass collected from the plants operated under alternate anoxic and aerobic conditions (Guisasola et al., 2005) that causes microorganisms to store the external substrate in the cell for growth during the

absence of external substrate in the liquid medium. Hence, ASM1 underwent further development to incorporate the storage process in the model structure.

2.4.5 Limitations of ASM1

There are a number of limitations concerning ASM1 (Henze et al., 1987). Since the intent of the current study is to investigate aerobic biodegradation process of substrate in activated sludge, only the constraints related to aerobic processes are summarized below.

- The system must operate at constant temperature since many of the parameters are functions of temperature.
- The pH is assumed to be constant and near neutral. Though the pH has an influence on many of the parameters, only limited knowledge is available to identify these possible influences. The inclusion of alkalinity in the model, however, does allow for detection of problems related to pH control.
- The changes in the nature of the organic matter within any given wastewater fractions (e.g. the readily biodegradable substrate) has not been considered. Thus, the parameters in the rate expressions have been assumed to have constant values. As a result, while concentration changes of the wastewater components can be accommodated, changes in the wastewater character cannot.
- The effects of nutrient limitations (e.g. N and P) on the removal of organic substrate and on cell growth have not been taken into account. Hence, sufficient quantities of nutrients in the system must be forced in the model.
- The parameters for nitrification are assumed to be constant and to incorporate any inhibitory effects that other wastewater constituents are likely to have.
- The heterotrophic biomass is considered to be homogeneous and does not undergo changes in species diversity over time. This assumption is inherent in the assumption of constant kinetic parameters. Therefore, any changes in substrate concentration gradients, reactor configuration, etc. on sludge settleability are not considered in modeling.
- The entrapment of particulate organic matter in the biomass is assumed to be instantaneous.

- The hydrolysis of organic matter and organic nitrogen are coupled and are considered to occur simultaneously with equal rates.
- The type of electron acceptor present does not affect the loss of biomass by decay.
- The model is not designed to deal with activated sludge systems with very high load or small sludge retention time (SRT) (<1 day).

2.5 Activated Sludge Model No. 3

The shortcomings in ASM1 suggest the model could be improved. Some of the defects addressed by Gujer et al., 1999 are listed below:

- ASM1 does not include an expression to deal with the nitrogen and alkalinity limitations of heterotrophic organisms.
- ASM1 considers biodegradable soluble and particulate organic nitrogen as model components. However, these components can not easily be measured and may in most cases unnecessarily complicate the use of ASM1.
- The ammonification kinetics can not be easily quantified in ASM1. Moreover this process is typically rather fast and therefore hardly affects model predictions.
- ASM1 differentiates inert particulate organic material based on its origin; i.e. either influent or biomass decay. In reality, however, it is impossible to differentiate these two components.
- The process of hydrolysis in ASM1 has a dominating effect upon the predictions of the oxygen consumption by heterotrophic organisms. In reality this process includes different coupled processes such as hydrolysis, lysis and storage of substrates. Thus, it is very difficult to identify the kinetic parameters for this combined process.
- Lysis combined with hydrolysis and growth is used to explain the lumped effects of endogenous respiration. This leads to further difficulties in the evaluation of kinetic parameters.
- Elevated concentrations of readily biodegradable organic substrates can lead to storage of polyhydroxyalkanoates (PHA), lipids or glycogen in the biomass cell. This is not considered in ASM1.

- ASM1 does not allow the possibility to differentiate between decay rates of nitrifiers. For a high SRT, this may lead to problems with the predictions of the maximum nitrification rates.

By assessing the shortcomings (identified above) and with due consideration of experimental evidence on the storage of organic compounds, the IWA (formerly IAWQ) Task group proposed the Activated Sludge Model No. 3 (ASM3) (Gujer et al., 1999) as a possible replacement for ASM1.

2.5.1 Model principle

ASM3 is based on the assumption that the readily biodegradable substrate (S_S) is taken up and stored in the cell as internal polymers (X_{STO}) prior to growth. The component X_{STO} is then consumed for the biomass growth in the absence of the external substrate. As a consequence a division of the storage and growth processes, which allows growth to take place on the external substrate directly is not considered. Figure 2.7 shows the model process diagram involved in ASM3 (Henze et al., 2000) where the nitrifiers and heterotrophs are clearly separated.

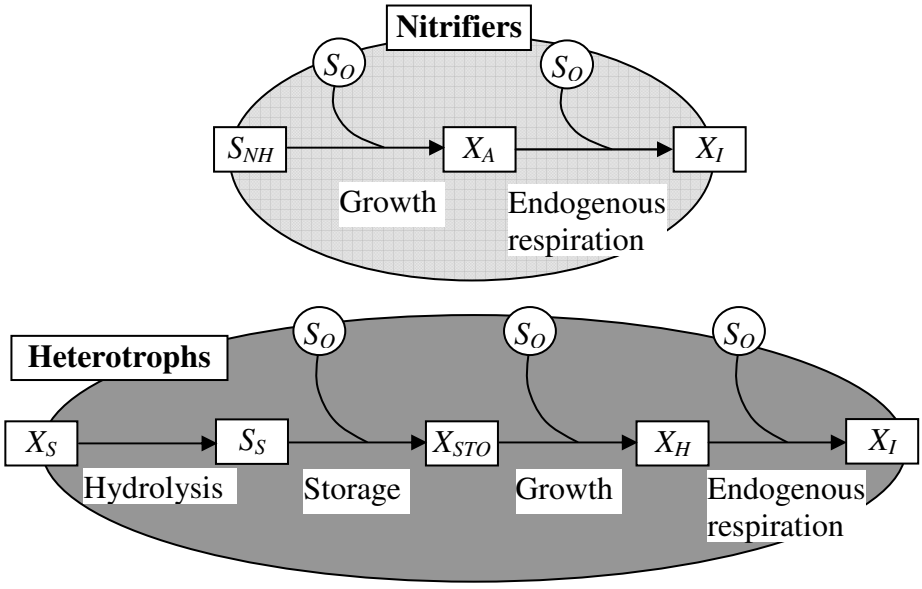

Figure 2.7: Schematic presentation of processes in ASM3 (modified from Henze et al., 2000)

The death regeneration concept prescribed in ASM1 is replaced in this model by endogenous respiration. There are many entry points for oxygen in ASM3 which is indicated in Figure 2.7.

2.5.2 Aerobic processes involved in ASM3

The process kinetics involved in ASM3 are presented in matrix form in Table 2.3. All expressions are based on switching functions (saturation terms, Monod equations, $S_S/(K_S+S_S)$) for all soluble compounds consumed. These switching functions stop all biological activities as process approaches zero concentrations, an important difference between ASM1 and ASM3. Readers are referred to Gujer at al. (1999) for a complete description of the stoichiometric components involved in ASM3.

As in ASM1, hydrolysis in this model is mainly responsible for the breakdown of slowly biodegradable substrate (X_S) to readily biodegradable substrate (S_S). Aerobic storage of substrate describes the process of storing the readily biodegradable substrate in the form of X_{STO} with the consumption of oxygen (S_O). All the readily biodegradable substrate is considered to be stored first before being used for cell growth. Afterwards, the aerobic heterotrophic growth takes place by degradation of X_{STO} with the consumption of oxygen. Aerobic growth of autotrophs represents the nitrification in an activated sludge system which is described in ASM3 as similar to ASM1.

The endogenous respiration process describes how a fraction of biomass becomes extinct to provide energy for maintenance, lysis, etc. that are presented in ASM3 using a simple first order reaction kinetics (Table 2.3). Similar to heterotrophic decay, the autotrophic biomass decay is described in ASM3 under the endogenous respiration process. In addition, the process of aerobic respiration on X_{STO} is introduced in ASM3 since the internal storage materials are observed to be used for maintenance purposes when the external substrate is depleted (Van Loosdrecht and Henze, 1999).

Table 2.4 and Table 2.5 show typical values of kinetic and stoichiometric parameters respectively for carbon oxidation and nitrification in ASM3 (Gujer et al., 1999).

Table 2.3: Kinetic rate expression ρ_j (related to carbon oxidation and nitrification) for ASM3 (Gujer et al., 1999)

j	Process	Process rate equation ρ_j, all $\rho_j \geq 0$
1	Hydrolysis	$k_H \cdot \left(\frac{X_S / X_H}{K_X + (X_S / X_H)} \right) \cdot X_H$
Heterotrophic organisms		
2	Aerobic storage of S_S	$k_{STO} \cdot \left(\frac{S_O}{K_O + S_O} \right) \cdot \left(\frac{S_S}{K_S + S_S} \right) \cdot X_H$
3	Aerobic growth of X_H	$\mu_H \cdot \left(\frac{S_O}{K_O + S_O} \right) \cdot \left(\frac{S_{NH}}{K_{NH} + S_{NH}} \right) \cdot \left(\frac{S_{HCO}}{K_{HCO} + S_{HCO}} \right) \cdot \left(\frac{X_{STO} / X_H}{K_{STO} + (X_{STO} / X_H)} \right) \cdot X_H$
4	Aerobic endog. respiration	$b_{H,O2} \cdot \left(\frac{S_O}{K_O + S_O} \right) \cdot X_H$
5	Aerobic respiration of X_{STO}	$b_{STO,O2} \cdot \left(\frac{S_O}{K_O + S_O} \right) \cdot X_{STO}$ $\quad b_{STO,O2} \geq b_{H,O2}$
Autotrophic organisms, nitrification		
6	Aerobic growth of X_A	$\mu_A \cdot \left(\frac{S_O}{K_{A,O} + S_O} \right) \cdot \left(\frac{S_{NH}}{K_{A,NH} + S_{NH}} \right) \cdot \left(\frac{S_{HCO}}{K_{A,HCO} + S_{HCO}} \right) \cdot X_A$
7	Aerobic endog. respiration	$b_{A,O2} \cdot \left(\frac{S_O}{K_{A,O} + S_O} \right) \cdot X_A$

Table 2.4: Typical values of kinetic parameters (related to carbon oxidation and nitrification) for ASM3 (Gujer et al., 1999)

Symbol	Description	Units	Value at 20^0C	Value at 10^0C
k_H	Hydrolysis rate constant	g COD X_S (g COD X_H . day)$^{-1}$	3	2
K_X	Hydrolysis saturation constant	g COD X_S (g COD X_H)$^{-1}$	1	1
Heterotrophic organisms				
k_{STO}	Storage rate constant	g COD S_S (g COD X_H . day)$^{-1}$	5	2.5
K_O	Saturation constant for S_O	g O_2 m^{-3}	0.2	0.2
K_S	Saturation constant for substrate S_S	g COD S_S m^{-3}	2	2
K_{STO}	Saturation constant for X_{STO}	g COD X_{STO} (g COD X_H)$^{-1}$	1	1
μ_H	Heterotrophic max. growth rate of X_H	day^{-1}	2	1
K_{HCO}	Saturation constant for alkalinity for X_H	mole HCO_3^- m^{-3}	0.1	0.1
$b_{H,O2}$	Aerobic endog. respiration rate of X_H	day^{-1}	0.2	0.1
$b_{STO,O2}$	Aerobic respiration rate for X_{STO}	day^{-1}	0.2	0.1
Autotrophic organisms, nitrification				
μ_A	Autotrophic max. growth rate of X_A	day^{-1}	1	0.35
$K_{A,NH}$	Ammonium substrate saturation for X_A	g N m^{-3}	1	1
$K_{A,O}$	Oxygen saturation for nitrifiers	g O_2 m^{-3}	0.5	0.5
$K_{A,HCO}$	Bicarbonate saturation for nitrifiers	mole HCO_3^- m^{-3}	0.5	0.5
$b_{A,O2}$	Aerobic endog. respiration rate of X_A	day^{-1}	0.15	0.05

Table 2.5: Typical stoichiometric and composition parameters (related to carbon oxidation and nitrification) for ASM3 (Gujer et al., 1999)

Symbol	Description	Units	Value
f_{SI}	Production of S_I in hydrolysis	g COD S_I (g COD Xs)$^{-1}$	0
$Y_{STO,O2}$	Aerobic yield of stored product per S_S	g COD X_{STO} (g COD S_S)$^{-1}$	0.85
$Y_{H,O2}$	Aerobic yield of heterotrophic biomass	g COD X_H (g COD X_{STO})$^{-1}$	0.63
Y_A	Yield of autotrophic biomass per NO_3^--N	g COD X_A (g N S_{NO})$^{-1}$	0.24
f_{XI}	Production of X_I in endog. respiration	g COD X_I (g COD X_{BM})$^{-1}$	0.2
i_{NSI}	N content of S_I	g N (g COD S_I)$^{-1}$	0.01
i_{NSS}	N content of S_S	g N (g COD S_S)$^{-1}$	0.03
i_{NXI}	N content of X_I	g N (g COD X_I)$^{-1}$	0.02
i_{NXS}	N content of X_S	g N (g COD X_S)$^{-1}$	0.04
i_{NBM}	N content of biomass, X_H, X_A	g N (g COD X_{BM})$^{-1}$	0.07

It should be noted that absolute values of these parameters are not part of ASM3; however they are suggested as a first estimate for the design of possible experiments to identify these parameters more accurately. For further details the reader is referred to the IWA Task group report (Henze et al., 2000).

2.5.3 COD and nitrogen components in ASM3

In ASM3, a new COD component X_{STO} is introduced along with the COD components described in ASM1 to represent internal polymers to be stored in biomass cell. The separation between inert suspended organic matter in the wastewater influent (X_I) and produced via the decay process (X_P) is not included in ASM3 since it is impossible in practice to differentiate these two components. Figure 2.5 illustrates a comparison of COD components in ASM3 and ASM1.

A comparison of nitrogen components used in ASM1 and ASM3 are presented in Figure 2.6. The soluble and particulate organic nitrogen components are excluded in ASM3 to avoid the complication of measuring such parameters. In addition, ASM3 model introduces a nitrogen gas component (S_{N2}) in order to allow a closed nitrogen mass balance. In ASM3, the nitrogen incorporated in S_I, S_S, X_I, X_S, and the biomass is defined as a fraction of these components. This fraction is either consumed or produced when the particular COD fraction is formed or degraded respectively.

2.5.4 Calibration of ASM3 under aerobic conditions

Information regarding ASM3 model calibration for carbon removal and nitrification using a variety of reactor configurations for experimental observations is available in the literature. The calibration and parameter estimation of ASM3 including different experimental approaches for system configurations and substrates are briefly discussed below.

Krishna and Van Loosdrecht (1999) simplified ASM3 for model evaluation by observing acetate biodegradation in a sequencing batch reactor (SBR) using acetate as the sole substrate. They found the model could not describe the difference in growth rate between the feast and the famine phase. Koch et al. (2000) assessed ASM3 with experimental COD and OUR data generated from aerobic batches and from a full-scale Swiss municipal wastewater treatment plant. They conducted model validation using ammonium, nitrite and nitrate measurements. Carucci et al. (2001) explained experimental observations (COD, PHB (polyhydroxybutyrate) and OUR measurements) with the aid of a modified ASM3 to verify the basic assumption (storage phenomena) of this model. They conducted respirometric batch tests using pure acetate, filtered and raw wastewater in an activated sludge system.

Karahan-Gul et al. (2003) modified ASM3 considering direct growth on primary substrate where both ASM3 and the modified model were assessed by calibrating them with OUR data for glucose biodegradation in an SBR system. The proposed model was validated with glucose, glycogen (storage compound) and ammonia measurements. Guisasola et al. (2005) compared the model calibration results for ASM3 and ASM1 using four different respirometric batch profiles (OUR) for acetate biodegradation. While ASM1 did not explain the experimental observations, the behavior of the sludge obtained from the WWTPs for COD removal, nitrification and denitrification was described well by ASM3. In addition, they statistically evaluated both ASM3 and ASM1 through model calibration where the sum of squared error (SSE) was found to be reasonable in case of ASM3 (Table 2.6).

Table 2.6: Assessment of ASM1 and ASM3 models using statistical tools (adopted from Guisasola et al., 2005)

Model	Parameter*	Unit	Estimated value (confidence intervals are in brackets)	SSE
ASM1	μ_H	day^{-1}	3.876 (0.003)	2.386
	Y_H	g COD X_H (g COD S_S)$^{-1}$	0.757 (0.001)	
	K_S	mg COD $(L)^{-1}$	1.789 (0.005)	
	τ	min	0.24 (0.007)	
	$X_H(0)$	mg COD X_H $(L)^{-1}$	1250	
ASM3	k_{STO}	day^{-1}	4.88 (0.009)	0.560
	Y_{STO}	g COD X_{STO} (g COD S_S)$^{-1}$	0.796 (0.006)	
	K_S	mg COD $(L)^{-1}$	0.8 (0.02)	
	μ_H	day^{-1}	28.1 (0.5)	
	$Y_{H,STO}$	g COD X_H (g COD X_{STO})$^{-1}$	0.804 (0.002)	
	τ	min	0.123 (0.005)	
	$X_H(0)$	mg COD X_H $(L)^{-1}$	1000	

*See Appendix A for parameter definition

Moussa et al. (2005) developed a model based on ASM3 components for explaining the interaction between nitrifiers, heterotrophs and predators in two laboratory-scale SBR systems operated at different sludge retention times (SRTs). They calibrated the model with respect to ammonium, nitrite, nitrate and OUR measurements for a particular SRT. The calibrated model was then validated by simulating steady state for other SRTs. Later, Iacopozzi et al. (2007) proposed an enhancement to the basic ASM3 model by introducing a two-step model for the nitrification process using a COST (European Cooperation in the field of Scientific and Technical Research) simulation benchmark configuration for wastewater treatment plants.

Shahriari et al. (2006) conducted biodegradation experiments for soluble COD and MLVSS in a porous pot membrane reactor for the evaluation of bio-kinetic models (simple, intermediate, ASM1 and ASM3). Though ASM3 was found to be good for predicting effluent soluble COD, the intermediate model was regarded as best for the prediction of MLVSS and effluent soluble COD. Dizdaroglu-Risvanoglu et al. (2007) assessed ASM3 and other activated sludge models using OUR measurements for added tannery wastewaters in batch reactors. Ni et al. (2008) modified ASM3 by using carbon removal, nitrification and denitrification to describe the simultaneous autotrophic and heterotrophic dynamic growth in an aerobic granule-based SBR fed with a fatty acid-rich wastewater. While OUR, COD and storage polymer data were

used for model calibration, the model was validated with OUR, COD, ammonium and MLVSS measurements.

On the other hand, Beccari et al. (2002) studied the removal of synthetic substrates (acetate, ethanol, glutamic acid) along with the characterization of filtered wastewater and raw wastewater using respirometric batch tests. Three different bio-kinetic models: ASM3, a simultaneous storage and growth (SSAG) model and a model combining accumulation and SSAG concept were assessed. Simulation were based on all experimentally observed data (COD, OUR, storage polymers and ammonia). While polyhydroxybutyrate (PHB) was stored when the substrate was acetate or ethanol, no appreciable formation of storage compound in the form of PHB or other polyhydroxyalkanoates (PHA) was detected when glutamic acid was used as a substrate. A low amount of PHB was also formed in tests with raw and filtered wastewater which was due to its acetate content. Besides, Beccari et al. (2002) noticed that the ammonia concentration during the experimental period remained fairly constant. Although nitrogen content of glutamic acid was in excess of that needed for active biomass formation, the excess nitrogen was not released in the medium. Though there was no experimental evidence, they explained the fact that a fraction of the removed glutamic acid might not be used for active biomass synthesis but it might be stored inside the cell in a form other than PHA or simply accumulated inside the cell. While they found ASM3 described well all of the experimental profiles used for calibration, the estimated profiles for storage compounds were strongly overestimated compared to the experimental ones under all test conditions.

2.5.5 Limitations of ASM3

Gujer et al. (1999) identified some limitations of ASM3 most of which are common to ASM1. Following are some constraints of ASM3 regarding aerobic process in an activated sludge system:

- The model was developed for the simulation of aerobic process in domestic wastewater. It was not suggested for application where industrial components dominate the wastewater.

- The development of the model was based on a temperature range of 8-23 ^{0}C. Its application outside this temperature range has not been justified.
- ASM3 was developed based on pH values from 6.5 to 7.5, which may limit the application of this model.
- An elevated concentration of nitrite cannot be handled in ASM3.
- The model is not designed for a very high wastewater load or a small sludge retention time (<1 day).
- While the structure of the model is given in ASM3, the absolute values of model parameters are not provided.

Moreover, the key limitation of ASM3 is the concept that all substrates are first converted to stored material and later assimilated to the biomass. This does not occur in reality. The development of ASM3 was based on existing knowledge and to avoid complication, extra parameters for the division of substrate between storage and growth processes were not introduced. Consequently, for better experimental data interpretation simultaneous storage and growth based phenomena was considered in the further development of activated sludge models.

2.6 Simultaneous Storage and Growth Model

Following the establishment of ASM3, researchers evaluated this model using experimental measurements and concluded that it was not suitable as storage and growth occur simultaneously during the feast phase and ASM3 is based on the assumption that only storage occurs during the feast phase (Van Aalst-van Leeuwen et al., 1997; Krishna and Van Loosdrecht, 1999; Beun et al., 2000; Van Loosdrecht and Heijnen, 2002; Pratt et al., 2004; Karahan et al., 2006). Considering real-life situations Krishna and Van Loosdrecht, 1999 proposed for the first time a simultaneous storage and growth (SSAG) model to explain organic carbon biodegradation in an activated sludge system.

2.6.1 Model principle

In a SSAG model, bacteria are considered to grow on external carbon sources while storing them as intracellular storage products during the feast period, and to use the storage products as food during famine conditions. Figure 2.8 shows the

simultaneous use of soluble readily biodegradable substrate for storage polymers formation and biomass growth. In the absence of external substrate, the bacteria depend on the accumulated storage polymers for their growth. Decay of storage products as well as biomass is illustrated in this model through respective respiration process.

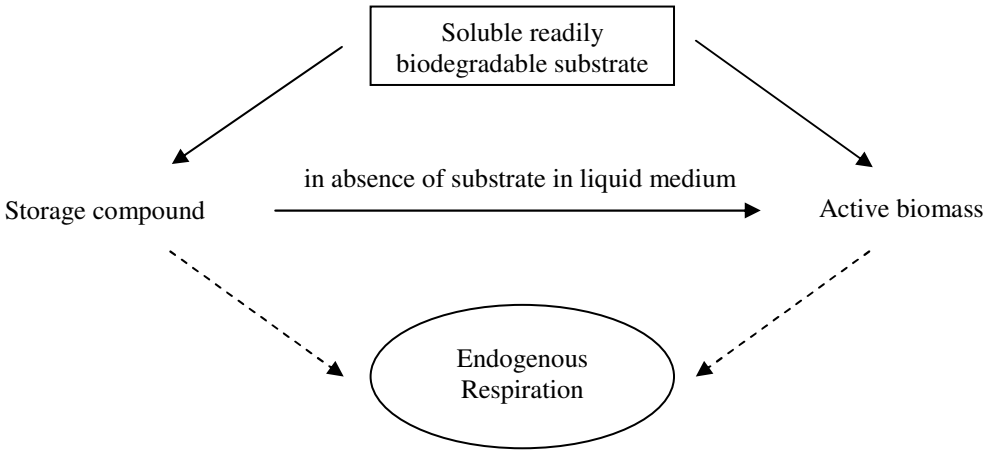

Figure 2.8: Model diagram based on the SSAG concept (modified from Krishna and Van Loosdrecht,1999)

2.6.2 Aerobic processes involved in SSAG model

The SSAG model describes the aerobic biodegradation of carbon based compound in an activated sludge system. While in ASM3 the readily biodegradable substrate (S_S) is considered to be stored first before being used for cell growth, in the SSAG model the substrate (S_S) is assumed to be consumed through a parallel path where a fraction of it is stored (X_{STO}) in the biomass cell and the remaining part is used for cell growth. It is followed by a process of aerobic growth on X_{STO} after the complete removal of S_S from the system (when there is no external carbon source available for cell growth). Endogenous respiration processes on X_{STO} and the biomass are described in the SSAG model in a similar way as in ASM3. Table 2.8 represents the kinetic expressions for different steps of aerobic process involved in the development of the SSAG model.

2.6.3 COD components in SSAG model

All COD components in SSAG model are similar to ASM3.

2.6.4 Calibration of SSAG model under aerobic conditions

The simultaneous storage and growth model has been used over the last decade for the interpretation of organic carbon removal mechanisms in an activated sludge process. The model development and calibration approaches with applied system configuration are briefly discussed in the following paragraphs.

Krishna and Van Loosdrecht (1999) attempted to evaluate the merits of ASM3 using a SBR system for acetate biodegradation. The study revealed that the difference in growth rate between feast and famine phase could not be described accurately by ASM3. They finally proposed a new model which added an extra process for growth on readily biodegradable substrate to the original ASM3. In addition, they assumed the soluble substrate inhibits the growth of heterotrophs on storage products (PHB). The proposed model was successfully calibrated and validated with experimental OUR, ammonium and PHB measurements. Dionisi et al. (2001) developed an empirical kinetic model that included substrate accumulation in the biomass cell followed by simultaneous storage and growth. They studied the substrate (acetate) removal mechanisms under transient conditions both in a SBR system and in batch tests. The model was simulated with experimental acetate, PHB, ammonia and OUR measurements followed by parameter estimation based on profiles of all available experimental variables.

Beccari et al., 2002 evaluated ASM3, the SSAG model and a model combining an accumulation and SSAG concept based on COD, OUR, PHB and ammonia measurements in a respirometric batch study. They excluded the inhibition component from the process of biomass growth on storage products that was used by Krishna and Van Loosdrecht (1999) in their SSAG model (see Table 2.8). Beccari et al. (2002) considered synthetic substrates (acetate, ethanol, glutamic acid) along with filtered wastewater and raw wastewater for the biodegradation experiments. With reference to synthetic substrates ASM3 was found to better describe the experimental data only by assuming a stored products formation much higher than the analytically

detected one, whereas the SSAG model described well the observed stored product profile only assuming a direct contribution of growth much higher that estimated from ammonia consumption. They concluded that the third model that considers accumulation and SSAG principles described well all of the experimental observations.

Karahan-Gul et al. (2003) proposed a model considering direct growth on primary substrate along with storage products formation to describe organic carbon (glucose) biodegradation in a SBR system. They calibrated the proposed model with OUR data and validated it with glucose, glycogen (storage compound) and ammonia measurements. Pratt et al. (2004) proposed a method for detailed investigation of the aerobic carbon degradation process using acetate as a test compound. They adopted the principle of simultaneous storage and growth for modeling and excluded the endogenous process in their model structure. Titration and Off-Gas Analysis (TOGA) was applied for experimental study. While the model was calibrated using accumulative oxygen consumption and hydrogen ion production data, validation was done with acetate, PHB (storage products) and ammonium concentration measurements.

After a critical evaluation of previous models, Sin et al. (2005) proposed a new mechanistic model for explaining simultaneous storage and growth processes in an activated sludge system. A hybrid respirometer was used to investigate the aerobic biodegradation of acetate in the system. They considered a metabolic model for the feast phase to demonstrate that the yield coefficients of storage (Y_{STO}), direct growth on substrate ($Y_{H,S}$) and growth on internal storage products ($Y_{H,STO}$) respectively are linked to each other through metabolism of the substrate. The literature shows the yield coefficients are dependent on the efficiency of the oxidative phosphorylation (δ) i.e. the efficiency of energy (ATP) generation in cells (Beun et al., 2000; Van Aalst-van Leeuwen et al., 1997). The efficiency of the oxidative phosphorylation (δ) is expressed in terms of mol/mol. While Beun et al. (2000) estimated the parameter, δ as 1.6 mol/mol using a slow growing activated sludge culture, Sin et al. (2005) noted higher value (2.57-2.88 mol/mol) when acetate was used as an external carbon source.

Sin et al. (2005) modified the SSAG model calibration process so that it was possible to estimate only one parameter (δ) instead of three yield coefficients. The yield coefficients were then calculated from the following relationships (equations 2.6-2.8) derived from the conversion of substrate (acetate) to PHB (polyhydroxybutyrate) and growth on PHB in bio-culture (Beun et al., 2000; Van Loosdrecht and Heijnen 2002).

$$Y_{H,S} = \frac{4 \cdot \delta - 2}{4.2 \cdot \delta + 4.32} \times \frac{4.2}{4} \quad \text{----- (Equation 2.6)}$$

$$Y_{STO} = \frac{4 \cdot \delta - 2}{4.5 \cdot \delta} \times \frac{4.5}{4} \quad \text{----- (Equation 2.7)}$$

$$Y_{H,STO} = \frac{4.5 \cdot \delta - 0.5}{4.2 \cdot \delta + 4.32} \times \frac{4.2}{4.5} \quad \text{----- (Equation 2.8)}$$

In the above equations all the yield coefficients are expressed in COD units. Furthermore, the rates of simultaneous storage and growth are reduced to the estimation of two parameters, i.e. q_{MAX} and f_{STO}. The maximum storage rate (k_{STO}) and the maximum growth rate of biomass ($\mu_{MAX,S}$) can then be calculated using equation 2.9 and equation 2.10 respectively. Table 2.7 summarises the parameters that were usually chosen by researchers for estimation during respirometric model calibration.

$$k_{STO} = f_{STO} \cdot q_{MAX} \cdot Y_{STO} \quad \text{----- (Equation 2.9)}$$

and

$$\mu_{MAX,S} = (1 - f_{STO}) \cdot q_{MAX} \cdot Y_{H,S} \quad \text{----- (Equation 2.10)}$$

In the above equations, the maximum substrate uptake rate is presented as q_{MAX} and the fraction of the substrate flux diverted to the storage products is defined by f_{STO}. Sin et al. (2005) also introduced a second order type kinetic expression in their proposed SSAG model to describe the degradation of storage products (see Table 2.8). They gave due attention to practical identifiability of the model structure as it tells which parameter combinations can be estimated under given measurement accuracy and quantity. The proposed model was successfully calibrated with OUR data, while model validation was performed measuring storage products (PHB) during acetate biodegradation study.

Karahan et al. (2006) explained starch biodegradation in a SBR system using a SSAG model. The proposed model included adsorption and hydrolysis followed by simultaneous growth and storage. The model was calibrated and validated using starch (substrate), glycogen (storage products) and OUR observations in the system. On the other hand, Dizdaroglu-Risvanoglu et al. (2007) assessed different activated sludge models including a SSAG model using OUR measurements in a batch reactor for tannery wastewater biodegradation. Karahan et al. (2008) investigated the aerobic biodegradation of acetic acid only, starch only and mixture of both in a SBR system. They proposed a SSAG model for calibration with OUR observation which was validated with storage compounds measurements. Ni et al. (2008) adopted a SSAG model for carbon removal in an aerobic granule-based SBR which was fed with a fatty acid-rich wastewater. While OUR, COD and storage polymer data were used for model calibration, the model was validated using different sets of OUR, COD, ammonium and MLVSS measurements.

Table 2.7: Parameters selected by researchers for estimation during respirometric model calibration

Model	Parameters for estimation	Source
ASM1	μ_H, Y_H, K_S and τ	Sin and Vanrolleghem, 2007
ASM3	k_{STO}, Y_{STO}, K_S, μ_H, $Y_{H,STO}$ and τ	Guisasola et al., 2005
SSAG	q_{MAX}, f_{STO}, δ, K_S, K_1, K_2 and τ	Sin et al., 2005

See Appendix A for parameter definitation

Table 2.8: Development of kinetics expression for SSAG model

Process	Kinetics expression		
	Krishna and van Loosdrecht., 1999	Beccari et al., 2002	Sin et al., 2005
1 Aerobic storage of S_S	$k_{STO}.\left(\frac{S_S}{K_S+S_S}\right).X_H$	$k_{STO}.\left(\frac{S_S}{K_S+S_S}\right).X_H$	$(1-e^{-t/\tau}).k_{STO}.\left(\frac{S_S}{K_S+S_S}\right).X_H$
2 Aerobic growth on S_S	$\mu_H.\left(\frac{S_S}{K_S+S_S}\right).X_H$	$\mu_H.\left(\frac{S_S}{K_S+S_S}\right).X_H$	$(1-e^{-t/\tau}).\mu_H.\left(\frac{S_S}{K_S+S_S}\right).X_H$
3 Aerobic growth on X_{STO}	$\mu_H.\left(\frac{X_{STO}/X_H}{K_{STO}+(X_{STO}/X_H)}\right).\left(\frac{K_S}{S_S+K_S}\right).X_H$	$\mu_H.\left(\frac{X_{STO}/X_H}{K_{STO}+(X_{STO}/X_H)}\right).X_H$	$\mu_H.\left(\frac{(X_{STO}/X_H)^2}{K_2+(X_{STO}/X_H).K_1}\right).\left(\frac{K_S}{S_S+K_S}\right).X_H$
4 Aerobic endog. respiration	$b_H.X_H$	$b_H.X_H$	$b_H.X_H$
5 Aerobic respiration of X_{STO}	$b_{STO}.X_{STO}$	$b_{STO}.X_{STO}$	$b_{STO}.X_{STO}$

Monod kinetics function for the state variables S_O and S_{NH} are excluded to keep above equations simple

2.6.5 Scope for further development of SSAG model

The recently developed SSAG model with improved kinetic expressions fits well with the experimental observation on oxygen consumption in the organic carbon removal process. However, model-based calibration using titrimetric measurements in a dynamic CO_2 transfer system has not yet been done. Acknowledging the fact that both oxygen uptake and pH change occur concurrently in an activated sludge system, Sin and Vanrolleghem (2007) introduced the dynamic CO_2 process; however their model was based on ASM1. In order to describe the titrimetric behavior of organic substrate oxidation, further development of the SSAG model is required in each step of simultaneous storage and growth processes with proper attention to CO_2 dynamics in the liquid phase. The model also needs calibration using different substrates other than acetate.

2.7 Summary

Respirometry and titrimetry are acknowledged as simple and powerful on-line measurement techniques for investigating aerobic biodegradation process. They enable high frequency collection of bio-kinetic information relating to the substrate removal process in a mixed culture. ASM1 was established to determine the substrate removal mechanism in an activated sludge system. Calibration of the model was achieved using respirometric-titrimetric techniques as well as different off-line measurements. However the model failed to explain observed experimental behavior particularly when the utilized biomass experiences alternate anoxic and aerobic environments in a WWTP. Consequently, ASM3 which recognized the importance of storage polymers in heterotrophic conversions in activated sludge process was developed. It was based on the assumption that substrates are first stored before being consumed by micro-organisms. However experimental observations indicated that storage and growth occur simultaneously during the feast phase, which is inconsistent with the assumption of ASM3. As a result, ASM3 underwent further improvement resulting in the SSAG model. Though the SSAG model was successfully calibrated using respirometric measurements with acetate as a carbon source, calibration of it using titrimetry is yet to be developed and validated for different substrates biodegradation.

Chapter 3
Materials and Methods

3.1 Introduction

This chapter contains details of the materials and methods used to investigate the aerobic biodegradation of different substrates including acetate, ammonium, surfactant, urea and glutamic acid. Experiments were performed using bench-scale laboratory reactors equipped with on-line monitoring systems. The outline of the methodology is presented in Figure 3.1. Experimental dissolved oxygen (DO) and pH change data occurring in the bio-reactor were collected by the on-line measurement system at the desired frequency and were used for bio-kinetic model calibrations. Existing models were reviewed and improved accordingly for satisfactory experimental data (respirometric and titrimetric) interpretation. Model validation is the final step of the methodology where the simulated model profiles were verified with on-line and off-line experimental measurements.

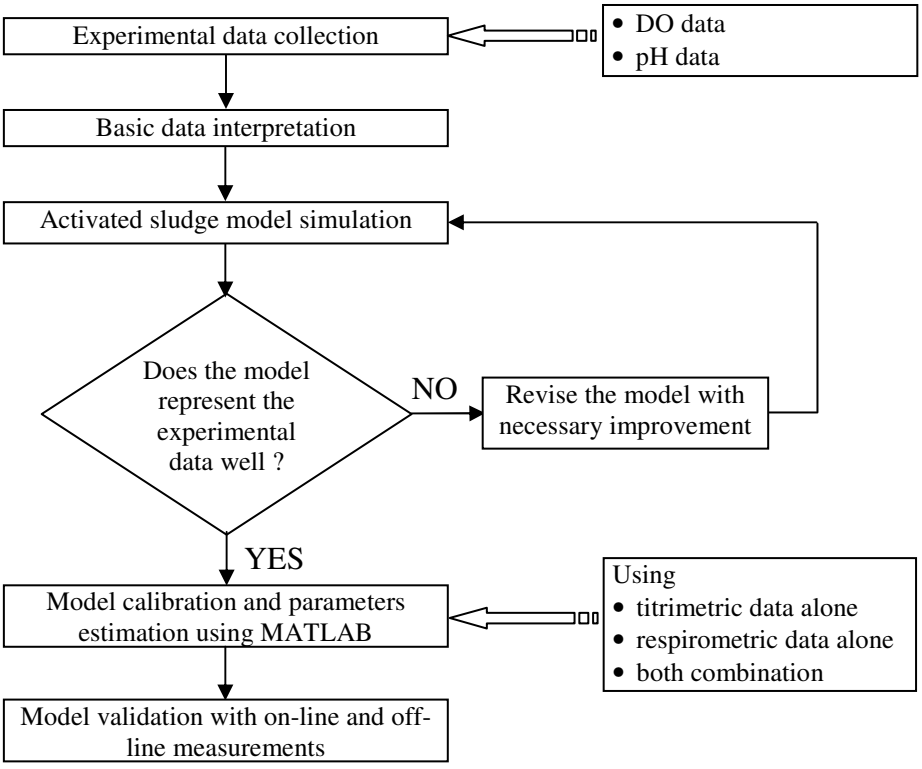

Figure 3.1: Outline of the methodology for the aerobic biodegradation study

3.2 Materials

3.2.1 Laboratory set-up

An activated sludge based titrimetric respirometer was installed in the Environmental (water) laboratory, Faculty of Engineering and Surveying, University of Southern Queensland, Australia. It enables the real time collection of data relating to the aerobic biodegradation of substrates (Figure 3.2). A batch study was conducted using a single reactor with a capacity of 3.5 liters. Compressed air was supplied continuously for proper aeration and an overhead stirrer was used to mix the contents uniformly. A titrimetric unit consisting of an Ionode pH electrode connected to a pH transmitter (TSP Mini Chem), two 3- way solenoid valves, an acid tank and a base tank, was installed to monitor and control the pH of the system during the experimental run. The acid and base were continuously pumped by a peristaltic pump to keep a constant liquid pressure in the dosage system and to maintain a constant dose rate. The data acquisition unit transmits the signals to the computer which was equipped with the Labview software package (National Instruments). In addition, the reactor was equipped with a dissolved oxygen electrode (YSI). The time response for the pH electrode was 10 seconds with the accuracy and repeatability of ±0.01. Whereas, both the accuracy and repeatability of the DO electrode was ±0.2% and the time response was found to be 16 seconds.

The Labview software monitored the dissolved oxygen as well as the temperature serial output from dissolved oxygen meter (TPS 90-D). A description of the Labview software package is presented in section 3.2.2.

During the batch experiments, both pH and DO profiles were monitored every 5 seconds. In general, pH was controlled at a set point of 7.8 ± 0.03 by the automatic addition of base (0.05 N) or acid (0.05 N) solution via two 3-way solenoid valves. The dosage system in this study was calibrated according to the procedure followed by Gernaey et al. (2002a). Temperature was controlled in the laboratory by setting the air conditioning system at 20^0C. However, the reactor temperature sometimes fluctuated between 18 and 22^0C. Therefore, a temperature correction was performed

on the experimental data to a base of 20^0C to maintain consistency. For more details, the reader is referred to the sub-section 3.4.1.

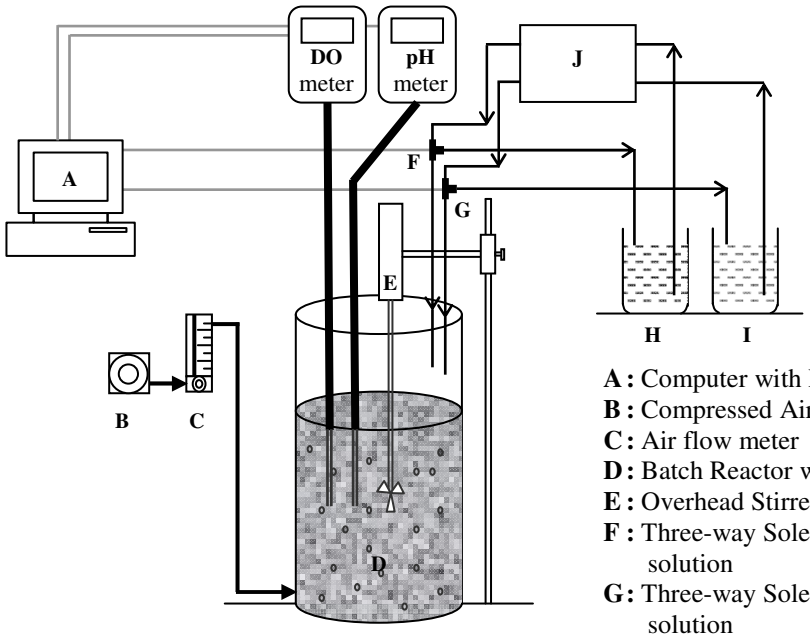

(a)

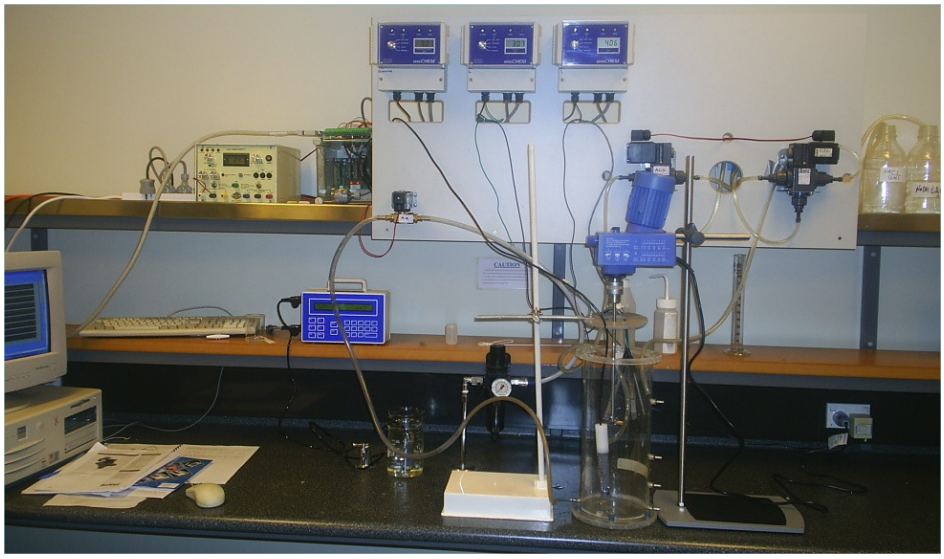

(b)

Figure 3.2: The laboratory based titrimetric respirometer (a) schematic (b) photographic overview

3.2.2 Labview software package

Labview software developed by National Instruments has a graphical programming system that is designed for data acquisition, data analysis and instrumental control. In this study, Labview software was used for monitoring and collecting the real time DO and pH data at a high frequency. The Labview package also controlled both of the 3-way solenoid valves in the titrimetric respirometer for acid and base pulsing respectively to keep the pH in the reactor constant. The 0-1 volt signals from the transmitter were logged by a PC equipped with the Labview software package and a combined A/D I/O card (National Instruments, PCI-6013). All data acquired from the experiment were recorded in a Microsoft Excel spreadsheet. The parameters on the front panel were set with the tolerance set-point limit. The real time profiles during the experimental run were also displayed on the front panel indicating experimental progress. Figure 3.3 represents the front panel of the Labview software.

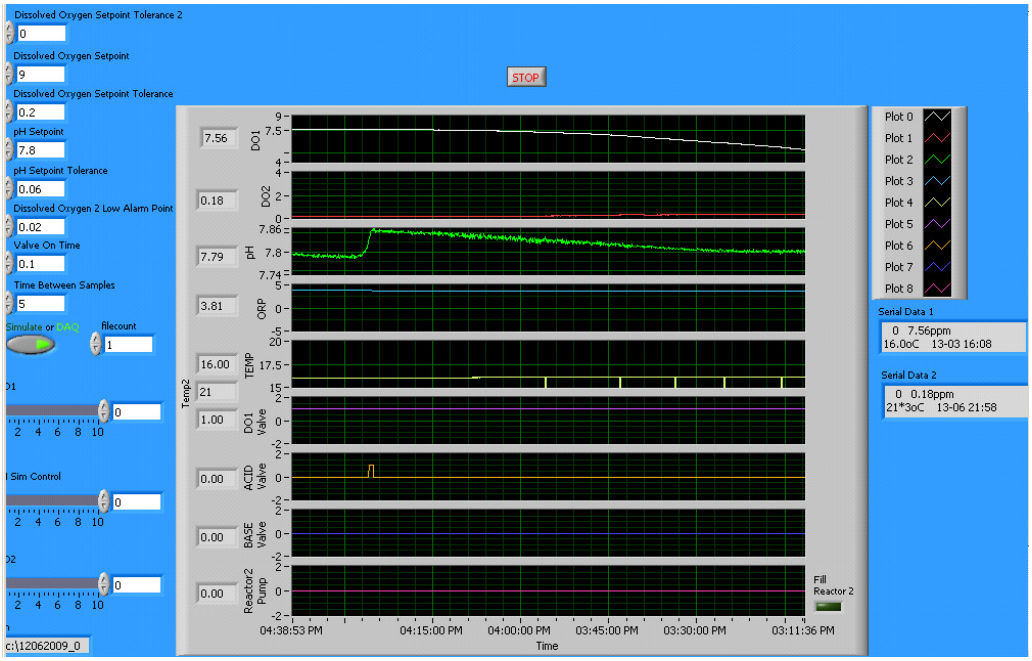

Figure 3.3: Front panel of the Labview software

3.2.3 Sludge

Activated sludge was collected from Wetalla Water Reclamation Plant (operated by Toowoomba Regional Council), Australia at different periods of time for experimental use. The sludge in the treatment facility experiences alternate aerobic and anoxic processes as the treatment plant is operated for both organic and nitrogen removal from the wastewater. After collection, the sludge was stored in a cold room at 4°C until usage for experimental purposes.

Sludge preparation included aeration for about 12 hours as mentioned by Sin and Vanrolleghem (2007) followed by regular feeding in the aerobic system with the respective test substrate until it was completely acclimatized. Sludge acclimatization refers to the adaptation capacity of the activated sludge to the respective substrate. It is noted that five different substrates such as acetate, surfactant, ammonium, urea and glutamic acid were selected as test substrates for conducting aerobic biodegradation study in an activated sludge system. The DO profiles (respirograms) resulting from the continuous assays of test substrate oxidation were studied for particular initial substrate concentration and the sludge was considered to be acclimatized when successive respirograms showed consistent profiles. Complete sludge acclimatization allowed the microorganisms to perform at their optimum capacity during the test substrate biodegradation study. While the acclimatization period for acetate, ammonium and urea substrates was 3-5 days, a longer acclimatization period was required when the sludge was fed with complex organic sources like glutamic acid (12 days) or surfactant (15 days). The volume of the sludge was found to reduce by evaporation during the sludge acclimatization process. This was adjusted by adding enzyme rich supernatant from the stored sludge for optimal sludge performance in the batch reactor.

3.2.4 Carbon and nitrogen sources

An aerobic biodegradation study was conducted in a batch reactor using the individual application of 5 different substrates as presented in Table 3.1. Since the function of microorganisms is substrate dependent, the test substrates were selected in such a way as to cover the biomass behaviour for simple as well as for complex compound biodegradation process as well as with and without nitrification inhibition

where applicable. Acetate is the simplest and most common organic carbon compound used in lab-scale based experimental work and was selected here to observe the heterotrophic biomass behaviour during the aerobic biodegradation process. On the other hand, sodium dodecyl sulfate (SDS), which is one of the common anionic surfactants used for domestic purposes, was selected for the slowly biodegradable carbon biodegradation study. Both ammonium and urea were applied to investigate the nitrification process governed by the autotrophic biomass under aerobic conditions. Glutamic acid (a common dairy diet ingredient) contains both carbon and nitrogen that usually undergo the oxidation process together. In order to assess the contribution made by heterotrophic microorganisms in the biodegradation of glutamic acid, the experimental study was extended by inhibiting the autotrophic microbial activity by the addition of allylthiourea (ATU) in the reactor (Carvalho et al., 2001). Besides, the biodegradation study for glutamic acid was conducted without nitrification inhibition to investigate the combined carbon and nitrogen oxidation in an activated sludge system where both heterotrophic and autotrophic biomass play role in the biodegradation process.

Table 3.1: Substrates added in activated sludge to investigate aerobic biodegradation

Test Substrate	Investigate	Active Biomass for oxidation	
		Heterotrophs	Autotrophs
Acetate (CH_3COOH) with ATU	Easily biodegradable carbon oxidation	√	×
Surfactant, SDS ($C_{12}H_{25}SO_4Na$) with ATU	Slowly biodegradable carbon oxidation	√	×
Ammonium (NH_4Cl)	Easily biodegradable nitrogen oxidation	×	√
Urea (NH_2CONH_2)	Slowly biodegradable nitrogen oxidation	×	√
Glutamic acid ($C_5H_9NO_4$) with ATU	Sole carbon oxidation	√	×
Glutamic acid ($C_5H_9NO_4$)	Combined Carbon & nitrogen oxidation	√	√

3.2.5 Nutrients

The nutrients and chemicals added during different substrates biodegradation studies are summarized below:

- Basic trace nutrient solutions consisting of $MgSO_4$, $CaCl_2$, $FeCl_3$ and phosphorus source (NaH_2PO_4 and Na_2HPO_4) were fed in general before dosing the test substrates to ensure that bacterial growth was not limited by their absence.
- Sufficient inorganic nitrogen (NH_4Cl) was added at the beginning of the experiment for the acetate and surfactant biodegradation studies in order to not limit the biomass growth. In addition, allylthiourea (ATU) was added to inhibit the nitrification process in the system.
- In the ammonium and urea oxidation studies, only $NaHCO_3$ was added to provide sufficient inorganic carbon, to keep the metabolic function of the autotrophic biomass normal.
- Inorganic carbon ($NaHCO_3$) was also added during the glutamic acid biodegradation study. Again, allylthiourea (ATU) was applied for nitrification inhibition so that the sole carbon oxidation could be investigated during glutamic acid biodegradation process.

3.3 Methods

3.3.1 Calibration of DO and pH meter

The DO meter (TPS 90-D) was calibrated for zero and air span where sodium sulphite was used as zero dissolved oxygen solution. The membrane of the DO probe was replaced on a regular basis by adding DO probe solution inside the electrode as prescribed by the manufacturer for proper functioning of the electrode. Zero and span calibration for the pH meter (MiniChem) was performed at pH of 4.0 and 7 respectively before running the experiments.

3.3.2 Acid and base valves calibration

Sulfuric acid (0.05 N) and sodium hydroxide (0.05 N) were used as acid and base solution respectively for the titrimetric measurements during the aerobic

biodegradation process. The calibration of acid and base valves was performed before starting the main experiments. Acid or base volume for 50 subsequent pulses was measured and the average dosage was calculated during calibration (Gernaey et al., 2002a). Table 3.2 represents the acid and base measurements for different pump rates and valve opening times. The optimum pulse rate for respective substrate oxidation studies was applied to eliminate pH noise during the biodegradation process.

Table 3.2: Acid and Base Valve Calibration

Pump rate (Regulator point)	Acid Volume*			Base Volume*		
	(0.5 Sec.)	(1.0 Sec.)	(1.5 Sec.)	(0.5 Sec.)	(1.0 Sec.)	(1.5 Sec.)
3	0.476	0.97	1.52	0.586	1.05	1.5
6	0.87	1.43	2.3	0.91	1.31	2.51
10	1.4	2.5	3.93	1.43	2.25	3.88

* Volumes are expressed as ml/pulse and valve opening time is shown in bracket

3.3.3 Endogenous respiration study

A study conducted by Sin and Vanrolleghem (2007) showed that the titrimetric measurements were mostly influenced by the physical and chemical processes instead of biological activities. The process of CO_2 stripping played a vital role in changing the pH of liquid medium under endogenous conditions. In this current study, the effect of dynamic CO_2 stripping process on pH of activated sludge was, therefore, studied under endogenous conditions. Collected sludge was left overnight (for about 12 hours) to aerate at a rate of 0.2 LPM and a room temperature of 20^0C. Titrimetric observations were then conducted at a particular pH (commonly 7.8) to investigate the CO_2 stripping behavior prior to sludge acclimatization. Continuous aeration was supplied during the endogenous respiration study to ensure oxygen unlimited conditions in the rector. Experiments for endogenous respiration were also carried out after the sludge was acclimatized with respective test substrates. Since the dynamics of CO_2 stripping are case sensitive with substrate concentration and pH, an experiment was performed before each test to determine the relevant titrimetric parameter involved in the endogenous respiration process.

3.3.4 Different substrates biodegradation studies

Five different compounds were used as test substrates in order to investigate the organic carbon and nitrogen biodegradation in an activated sludge system under aerobic condition. Test substrates have distinctive characteristics and show different biodegradation behavior depending on the complexity of the organic and nitrogen components and the nature of the active biomass in the system.

Acetate which is readily biodegradable in nature was used as a simple carbon source. Experiments with varying acetate concentration of 25, 50 and 75 mg COD/L were conducted to observe the effect of initial concentration on acetate biodegradation maintaining the pH at 7.8. In addition, the pH effect was studied maintaining two different pH levels (7 and 7.8) and a constant initial acetate concentration in activated sludge. For precise investigation, pH studies were performed for two different initial acetate concentrations (50 and 75 mg COD/L).

Anionic surfactant, SDS, was used as a complex organic carbon source with initial concentrations of 50, 75 and 100 mg COD/L being added to the activated sludge to investigate the concentration effect on the biodegradation process at pH 7.8. In addition, experiments for a constant SDS concentration of 75 mg COD/L were conducted for the pH levels of 7, 7.8 and 8.5 to examine the titrimetric behavior in an activated sludge process.

Ammonium is a simple nitrogenous compound that undergoes a nitrification process in the presence of autotrophic bacteria. Three different initial ammonium concentrations, 2.5, 6.5 and 11 mg N/L, were added to the activated sludge (at a constant pH 7.8) to observe the respirometric and titrimetric behavior during the nitrification process.

Urea was selected as a test substrate to observe the nitrification process under aerobic conditions. It has a more complex chemical composition than ammonium and needs to be hydrolyzed to ammonium which is then subjected to the nitrification process. Experiments with varying initial concentrations (5, 10 and 20 mg N/L) and a constant pH (7.8) were conducted to investigate the substrate removal mechanism in

activated sludge. Though urea consists of both carbon and nitrogen molecules, only nitrogen is oxidized by autotrophic bacteria whereas carbon is directly converted to carbon dioxide through a hydrolysis process.

The test substrate glutamic acid contains carbon and nitrogen both of which are oxidized by two different biomass species. While the organic carbon is oxidized by heterotrophic bacteria, autotrophic bacteria converts ammonium to nitrate as the final product in the bioreactor. Experiments with varying initial concentrations of glutamic acid, 50, 100 and 150 mg COD/L, were carried out to illustrate the concentration effect on the biodegradation process at a pH level of 7.8. Moreover, the bio-kinetics for sole carbon removal during glutamic acid biodegradation process was studied allowing nitrification inhibition during the batch experiments where the initial glutamic acid concentration of 100 mg COD/L and a constant pH level of 7.8 were considered.

3.3.5 Analytical techniques

A validation study for the nitrification process was carried out to measure the cation (ammonium) and the anions (nitrite and nitrate) in the liquid phase using an ion chromatography system (ICS 2000) with two different columns for cation (CS-16) and anion (AS-18) for the analytical process. Figure 3.4 is a photograph of the ion chromatography system installed in the laboratory. An off-line COD test was also performed as part of the validation experiment where the standard method was applied (APHA, 1995). In addition, sludge in the bioreactor was measured in terms of MLSS and MLVSS by following the standard methods.

Figure 3.4: Ion Chromatography System installed in the laboratory

3.4 Data analysis

3.4.1 Respirometric data interpretation

The oxygen uptake rate (OUR) is the combination of endogenous (OUR_{end}, oxygen consumption in the absence of external carbon source) and exogenous (OUR_{exo}, substrate degradation induced) oxygen uptake rates (Spanjers, 1993). It can be derived from the dissolved oxygen profile resulting from the metabolic functions of bacteria during the biodegradation process. The following expression is used to calculate the OUR_{exo} in the system (see the sub-section 2.2.1 in Chapter 2 for derivation).

$$\frac{dS_O}{dt} = K_L a(S_{eq} - S_O) - OUR_{exo} \qquad \text{----- (Equation 3.1)}$$

A moving window regression was applied for the determination of change in dissolved oxygen (DO) concentration, dS_O/dt calculation. The term S_{eq} represents the equilibrium concentration of DO in the bioreactor. A separate re-aeration process was carried out to calculate the oxygen transfer coefficient, K_La (see section 3.4.3). The difference between the equilibrium concentration (S_{eq}) and the saturated

dissolved oxygen level (S^*_O) multiplied by K_La reflects the OUR_{end} (see equation 2.2 in Chapter 2).

Dissolved oxygen data was then corrected for the reference temperature (20^0C) and pressure (1013 hPa). The DO data was interpolated for the respective temperature using the chart supplied with the DO meter (TPS 90-D) for saturated dissolved oxygen (see Table B1 in Appendix B). Colt (1984) established the following relationship between the dissolved oxygen and the pressure which was applied in this study for DO pressure correction.

$$C^* = \frac{C^* 760(P_t - p)}{(760 - p)} \qquad \text{----- (Equation 3.2)}$$

where, *C** and *C*760* stand for oxygen solubility and saturated value at 760 mm Hg respectively. *Pt* and *p* represent the barometric pressure and the vapor pressure of water in mm Hg unit accordingly. Table B2 in Appendix B represents the vapor pressure of water formulated by Colt (1984) for the respective temperature.

3.4.2 Titrimetric data interpretation

Gernaey et al. (1998) used the following expression (equation 3.3) for the titrimetric data interpretation which was used in the current study for the same purpose.

$$H_p = \frac{H_{pulse} \times Q_{flux} \times N}{V_{reactor}} \qquad \text{----- (Equation 3.3)}$$

where, H_p represents the proton concentration in meq/L, H_{pulse} is the pulse number during the reaction, Q_{flux} is the acid/base flux (ml/pulse), N refers to the normality of acid or base (meq/ml) and $V_{reactor}$ is the volume of the bio-reactor (L). A spreadsheet program was used to process the dissolved oxygen and titration raw data.

Nitrogen load in the activated sludge was also determined using the titrimetric data and applying equation 3.4 (Gernaey et al., 1997):

$$S_N = \frac{(B2 - B1) \times Q_{flux} \times N \times 7}{V_{reactor}} \quad \text{----- (Equation 3.4)}$$

where, S_N is the initial concentration of nitrogenous compound (mg N/L), *B1* represents the number of base pulses needed to adjust the pH of the sludge to the pH set-point, *B2* is the cumulative base pulses corresponding to the nitrification process plus *B1* pulses, and 7 is the conversion factor (to change the unit from 'meq' to 'mg N').

3.4.3 Oxygen transfer coefficient determination

There are several methods available to determine the oxygen transfer coefficient (K_La) liquid phase (ASCE, 1996). In this current study, the re-aeration approach was followed. The aeration of endogenously respired activated sludge was stopped for a while to deplete the DO from its equilibrium level as presented in Figure 3.5 (zone 1) to enable the calculation of the endogenous oxygen uptake rate (OUR_{end}) in the system. The sludge was then re-aerated at the same aeration rate allowing the DO profile to reach its equilibrium level. Zone 2 represents the re-aeration part of the study from which the analytical parameter corresponding to the K_La determination was estimated.

Equation 3.5 represents the mass balance of dissolved oxygen for a constant aeration in the liquid phase which was employed for K_La determination.

$$\frac{dS_O}{dt} = K_L a(S^*_O - S_O) - OUR_{exo} - OUR_{end} \quad \text{----- (Equation 3.5)}$$

In the absence of external substrate the value for OUR_{exo} (oxygen uptake under exogenous state) will be zero and the above equation can be written as:

$$\frac{dS_O}{dt} = K_L a(S^*_O - S_O) - OUR_{end} \quad \text{----- (Equation 3.6)}$$

The endogenous oxygen uptake rate can easily be calculated from equation 3.7 which is simplified from equation 3.6 where there is no aeration in the system (zone 1 in Figure 3.5)

$$OUR_{end} = -\frac{dS_O}{dt} \quad \text{----- (Equation 3.7)}$$

Equation 3.6 can be expressed in the form of the linear equation, y = mx + C using the data corresponding to the zone 2 as shown in Figure 3.5.

$$S_O = -\frac{1}{K_L a}\left(\frac{dS_O}{dt} + OUR_{end}\right) + S^*_O \quad \text{----- (Equation 3.8)}$$

The negative sign represents the negative slope where, y = S_O, m = -1/K_La, x = $dS_O/dt + OUR_{end}$ and C = S^*_O. Figure 3.6 was plotted considering the respective x and y data collected from the experiment and finally the parameter K_La, which is the inverse of the slope (m), was calculated for the particular aeration rate.

Different aeration rates were employed during the substrates biodegradation study to obtain representative respirograms from the experiments. The oxygen transfer coefficients corresponding to the aeration rates of 0.2, 0.4, 0.5 and 0.75 LPM for different trials are shown in Figure 3.7. From the experiment, a linear relationship between the aeration rate and K_La value was observed having a high coefficient of determination value ($R^2 = 0.99$).

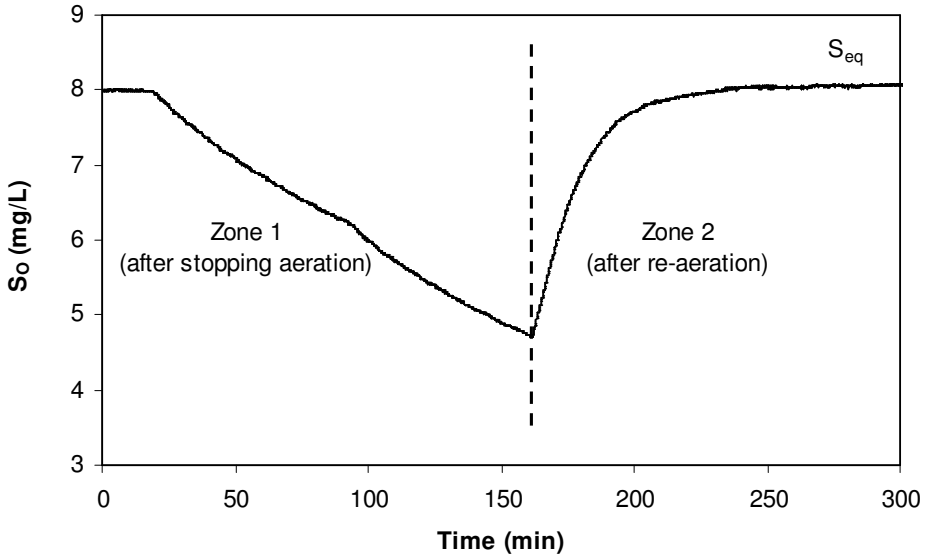

Figure 3.5: Respirogram observed during oxygen transfer coefficient determination (aeration rate = 0.2 LPM)

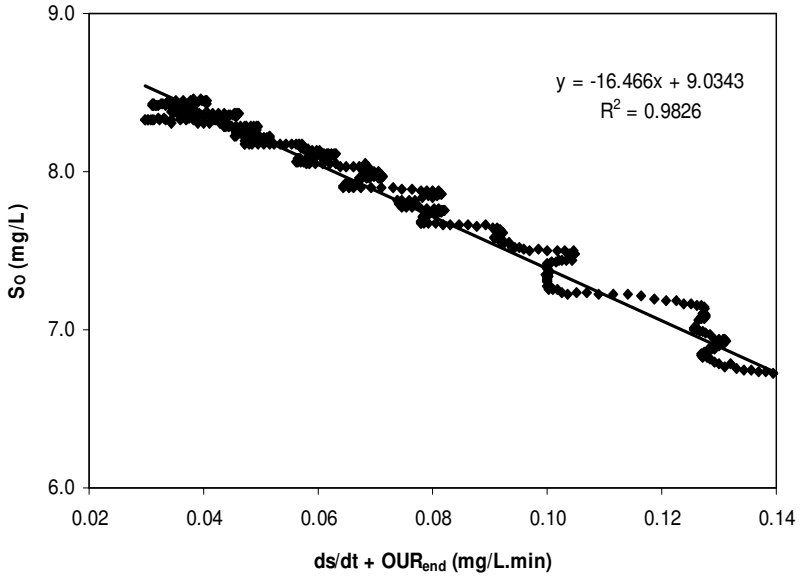

Figure 3.6: Graphical presentation of the analytical result corresponding to oxygen transfer coefficient determination (aeration rate = 0.2 LPM)

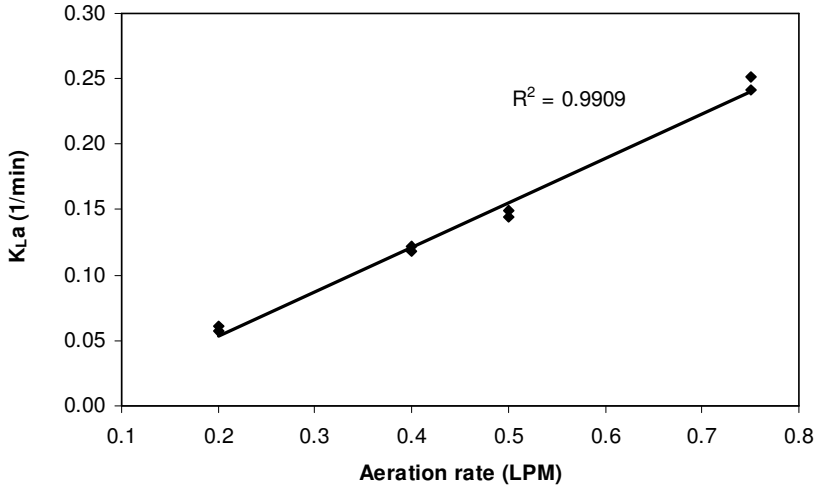

Figure 3.7: Different oxygen transfer coefficients (K_La) for respective aeration rate

3.5 Model simulation and parameters estimation

Bio-kinetic models to interpret the organic carbon and nitrogen removal mechanisms in an activated sludge system have been evolving. A model assessment study was performed by conducting simulation of existing activated sludge models followed by a calibration process with experimental OUR measurements to find the model that best represented the experimental respirometric behavior. Both MS Excel and MATLAB (R2007a) software were used for the cross verification of the simulation process. The best fit model found from the activated sludge model assessment was then improved by introducing stoichiometric parameters involved in titrimetry in each step of the biodegradation processes keeping the same process rate kinetics along with the consideration of non-linear carbon dioxide transfer rate in liquid phase.

Following a satisfactory simulation process, model calibration and parameter estimations were done following non-linear techniques employing the algorithms in the optimization toolbox included in MATLAB (R2007a). The model underwent further improvement until the simulated model profile was consistent with the experimental behavior. In calibration of the model, minimization of the mean squared error (MSE) between the model and experimental output was used as the main criterion for curve fitting. The MSE value was determined from the sum of squared errors by dividing it by the number of observations. Confidence intervals

were presented as an absolute percentage of parameter estimates (Sin et al., 2005) to justify the estimated parameters from a statistical point of view. The proposed models were calibrated using the respirometric and titrimetric measurements followed by the parameter estimation process. The results were finally compared to validate the proposed model. Figure 3.8 illustrates the steps involved in the MATLAB optimization toolbox programming corresponding to the parameter estimation process.

The key parameters that had a significant influence on the biodegradation process were estimated. Some parameters were calculated using predefined relationships with the estimated parameters and other parameters were kept fixed by assuming a reasonable literature value for them (see sections for parameter estimation strategy/approach in chapters 4, 5, 6 and 7 for the details). The initial concentrations of all state variables were also kept constant during the parameter estimation process. Non-linear parameter estimation involves the use of "initial guess values" for these parameters. The integration of model equations was performed by using 'ode45' solver in MATLAB which returns the model state variables for objective function calculation. Model error is calculated from the objective function and checked by 'lsqnonlin' MATLAB solver for the minimum value. Model parameters are estimated finally when the error reaches its minimum objective function (in this current study the termination tolerance was set to 1e-4). Otherwise, a new estimate of model parameters is generated and circulated for model equation integration through repeating the steps presented in Figure 3.8.

For each test substrate biodegradation study, the MATLAB program was developed for three different calibration approaches: using respirometric measurements alone, using titrimetric measurements alone and using combined respirometric-titrimetric measurements. The original MATLAB program for the model calibration and parameter estimation of acetate biodegradation was written by Dr Vasantha Aravinthan. This program was improved/extended in this current study to calibrate and estimate the model parameters relating to the surfactant, urea, ammonium and glutamic acid biodegradation processes. A sample MATLAB program written for glutamic acid biodegradation modeling is presented in Appendix D.

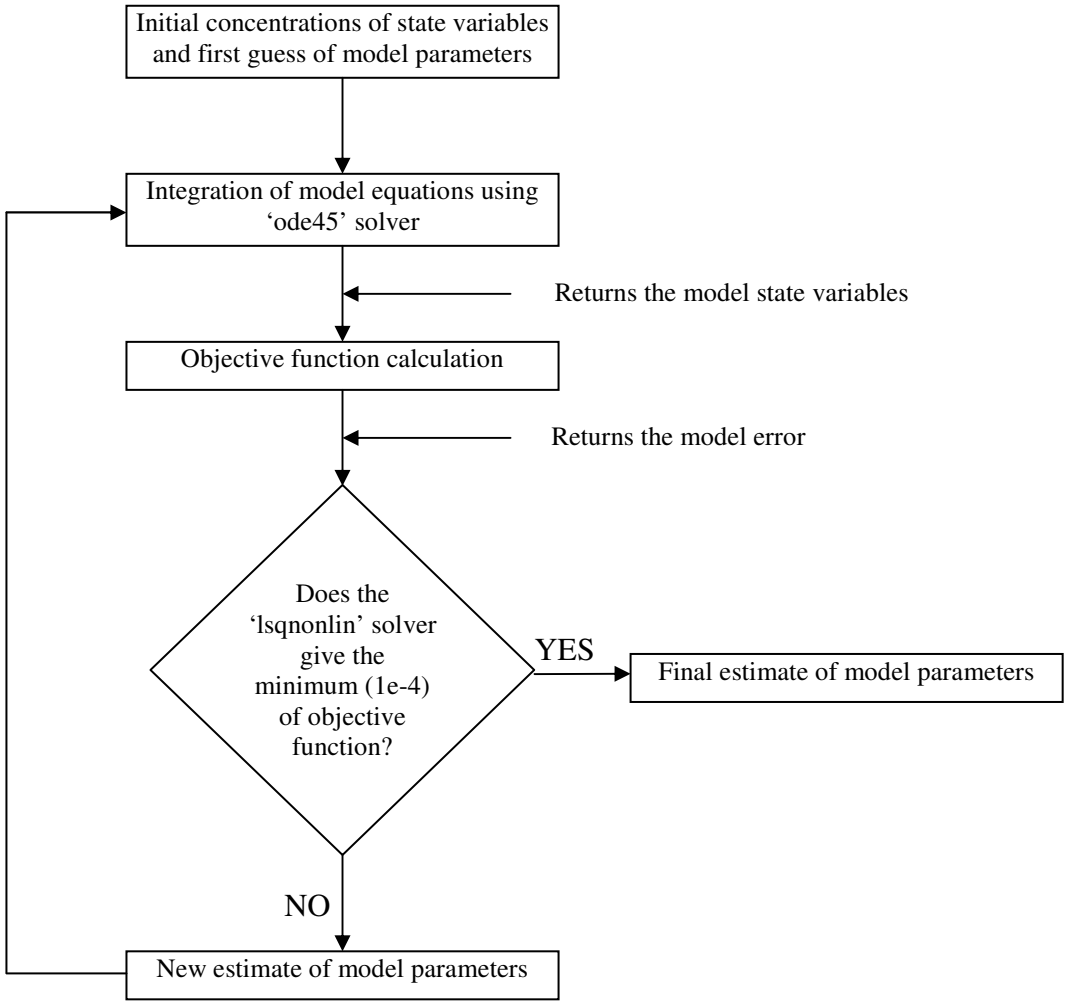

Figure 3.8: Model parameter estimation procedure using MATLAB optimization toolbox (modified from Petersen, 2000)

3.6 Summary

In this chapter, the materials and methodology used for experimental investigation of the biodegradation of different substrates were described. On-line measurements of DO and pH in the liquid phase were performed using a titrimetric respirometer to investigate organic carbon and nitrogen biodegradation under aerobic conditions. The methods used for the model development, calibration and validation were detailed and the application of MS Excel and MATLAB for the simulation, model calibration and parameter estimation were explained.

Chapter 4
Modeling of Acetate Biodegradation

4.1 Introduction

Acetate is a well known readily biodegradable compound that was selected in this study to investigate its biodegradation in an activated sludge system under aerobic conditions using combined respirometric-titrimetric measurements. This chapter focuses initially on the investigation of existing activated sludge models and their calibration with experimental measurements. Then it describes the proposed bio-kinetic model for acetate biodegradation that was calibrated successfully with both respirometric and titrimetric measurements. The model parameters were estimated from three different calibration approaches: using on-line titrimetric measurements alone, respirometric measurements alone and combined respirometric-titrimetric measurements. They were then compared to validate the proposed model. Validation was also performed using off-line measurements. The proposed model was evaluated for three different concentrations of acetate along with different pH observations. The outcome is discussed using logical and statistical approaches for appropriate evaluation of the proposed model. Finally, the Monod kinetics are presented in this chapter comparing acetate biodegradation in activated sludge with different pH levels.

4.2 Experimental observations on Acetate biodegradation

Sludge collected from Wetalla Water Reclamation Plant, Toowoomba was used for the endogenous respiration study where no external carbon sources were provided as feed in order to investigate the CO_2 stripping behavior prior to sludge acclimatization. Acid was added during the endogenous study that shows the proton consumption in the system for maintaining the pH at 7.8 ± 0.03. Figure 4.1 shows the pH and *Hp* (proton concentration) profiles during the endogenous respiration period. The proton consumption rate is higher at the beginning of the experiment as CO_2 stripping governs the whole process which decreases exponentially with time until the aqueous CO_2 reaches the equilibrium point. Sin and Vanrolleghem (2007) also

noticed the gradual reductionin the proton consumption rate as the removal rate of HCO_3 from the liquid phase decreases due to stripping. However, the proton consumption rate in the endogenous state was observed to be different when the sludge was acclimatized with substrate and left in the endogenous state overnight. The pattern was found to vary with different pH levels. The *Hp* profile was also noted different when the endogenous experiments were conducted with sludge collected from the plant at different periods of time. Hence, a separate experiment for endogenous respiration was conducted before each set of run for acetate biodegradation study, i.e. different initial substrate concentrations at different pH value, in order to apply the titrimetic measurements accordingly to estimate the proposed titrimetric model parameters (see the sub-sections 4.5.2 and 4.6.2 for the details).

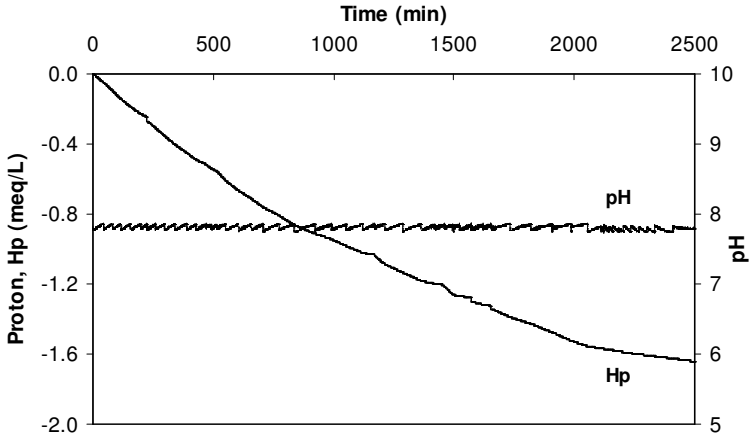

Figure 4.1: Proton consumption profile under endogenous condition (pH = 7.8)

Acetate, which is readily biodegradable in nature, was used as a simple carbon source. Experiments with varying acetate concentrations of 25, 50 and 75 mg COD/L were conducted to observe the effect of initial concentrations on acetate biodegradation. During these experiments, pH was maintained at 7.8. In addition, the pH effect was investigated for acetate pulses of 75 and 50 mg COD/L by maintaining a constant pH of 7 and 7.8 respectively in the reactor.

Figure 4.2 shows the dissolved oxygen profile with titrimetric measurements resulting from acetate (50 mg COD/L) biodegradation in the activated sludge process at pH 7.8. It can be seen that DO was reduced drastically soon after the acetate was dosed into the system and continued to decrease until all of the acetate within the liquid medium was consumed. Once the acetate was fully depleted in the liquid phase, DO started to increase gradually to reach the steady state equilibrium DO level. The biodegradation process results in acid or base addition along with oxygen consumption in the system depending on the respective carbon source used for the investigation. In this current study, acid addition was noticed during the acetate consumption period and was found to continue throughout the endogenous phase with a mild acid pulse rate in the system.

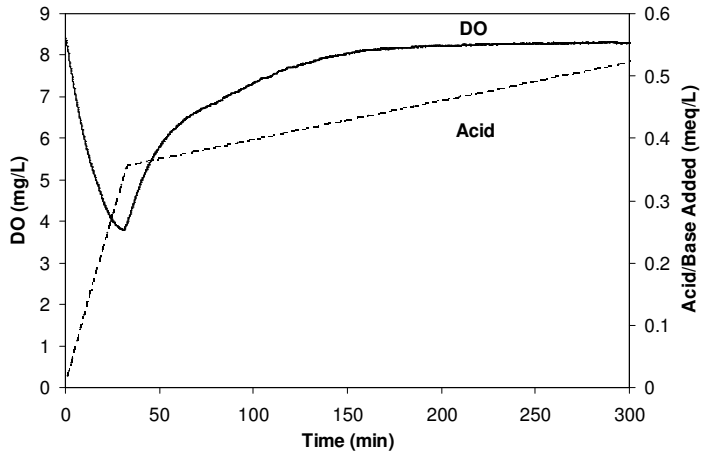

Figure 4.2: Dissolved oxygen and titrimetric measurements collected from the titrimetric respirometer for the acetate pulse of 50 mg COD/L

Figure 4.3 illustrates the OUR and titrimetric profiles for acetate pulses of 25, 50 and 75 mg COD/L at time t=0. The OUR increases to a maximum level due to the consumption of acetate under the feast period and remains the same until it is completely removed from the liquid medium for simultaneous storage and growth (Krishna and Van Loosdrecht, 1999; Beccari et al., 2002; Van Loosdrecht and Heijnen 2002; Guisasola et al., 2005; Sin et al., 2005; Karahan et al., 2008). Acetate uptake also causes acid addition to the system (Figure 4.3) as noted in previous studies (Gernaey et al., 2001, 2002a; Pratt et al., 2004; Sin and Vanrolleghem, 2007).

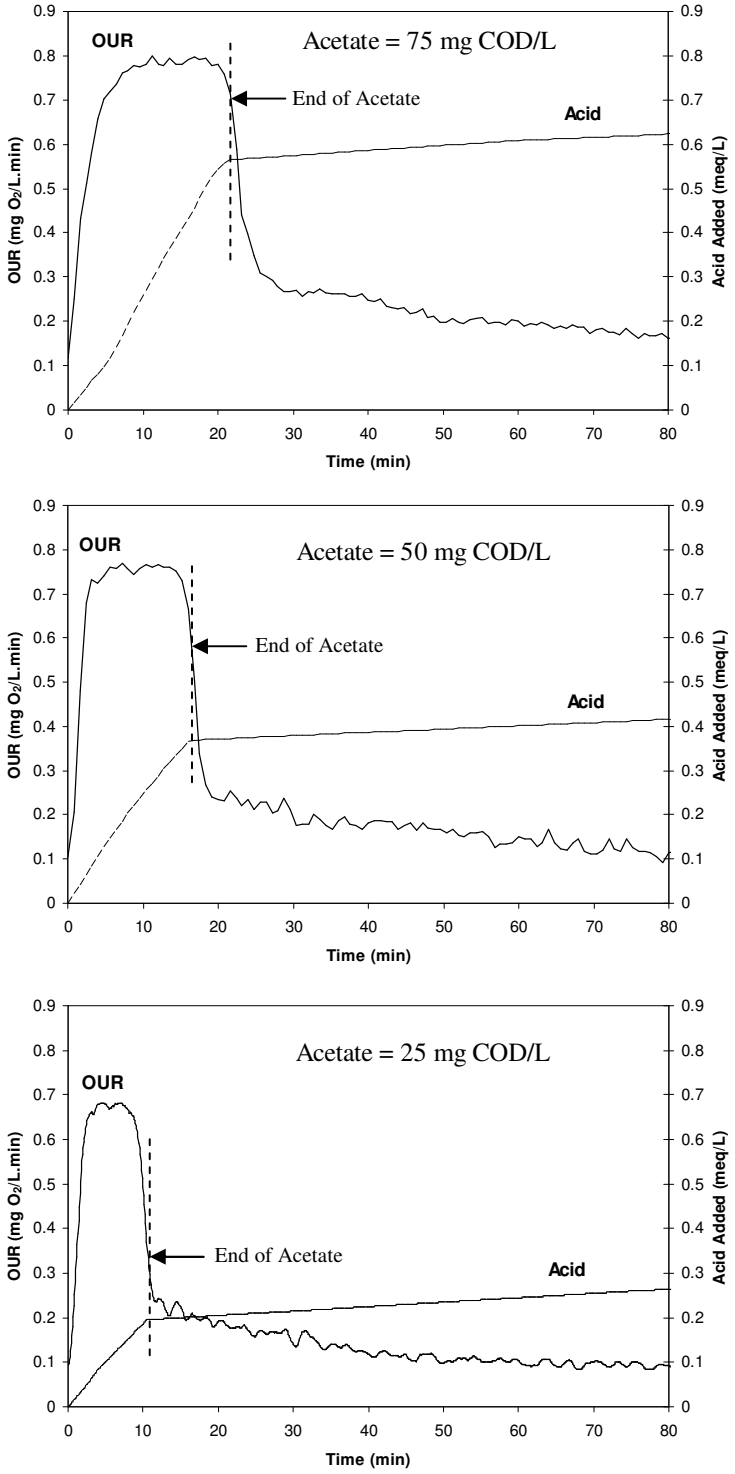

Figure 4.3: OUR with titrimetric profiles for three different acetate concentrations in an activated sludge system

Acid addition during the biodegradation process represents the proton consumption in the system which is the net result of acetate and ammonia uptake, storage formation and

the CO_2 production as described in section 4.4. Both the oxygen uptake and proton consumption rate fall at the same time after the total consumption of acetate indicating the end of acetate in the liquid phase (Sin, 2004). Figure 4.3 depicts the end point of acetate degradation showing the approximate degradation period of 22, 17.1 and 10.9 min for initial acetate concentrations of 75, 50 and 25 mg COD/L respectively.

In every case, the OUR drops from its maximum peak to a level higher than the endogenous OUR level followed by a gradual decline until it reaches the endogenous level for the consumption of previously stored products (Van Loosdrecht et al., 1997). The CO_2 stripping leads to a drop in the titrimetric profile to the background proton consumption rate that was observed before adding acetate into the reactor. It is noteworthy that three successive trials were made in each initial concentration study to ensure the reproducibility of the experimental results. The area under the OUR profiles were calculated to evaluate short-term BOD_{st} for different acetate concentrations. Figure 4.4 represents the outcomes obtained from different trials in terms of short-term BOD (BOD_{st}) and corresponding standard deviations (SDs) BOD_{st} for different initial acetate concentrations.

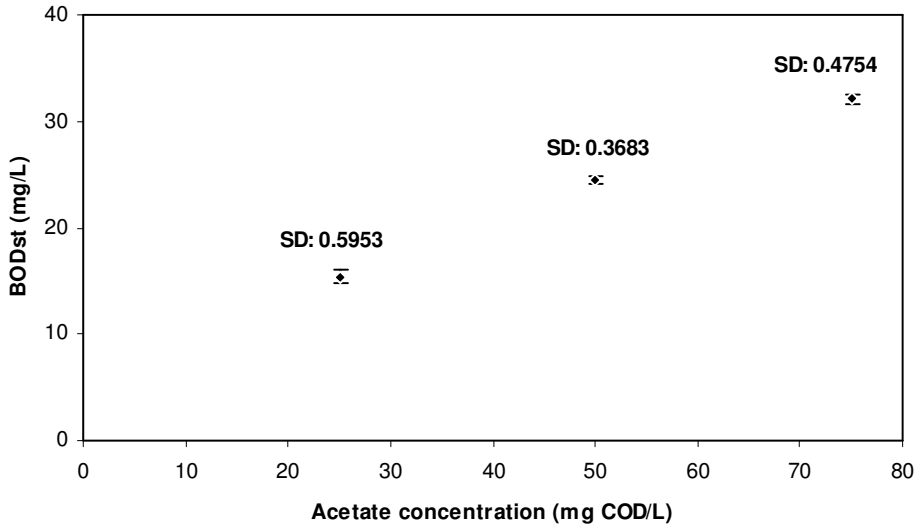

Figure 4.4: Short-term BOD obtained from different initial acetate concentration studies

4.3 Assessment of Activated sludge models

Although several models have been proposed to explain the biodegradation mechanism of readily biodegradable compounds such as acetate, as yet there is no commonly agreed model. This study was conducted to gain a complete understanding of hitherto developed biokinetic models, which are normally calibrated using OUR measurements when different carbon sources are fed in aerobic conditions. In biological systems, both dissolved oxygen and pH changes occur simultaneously and can be easily monitored using respirometric and titrimetric observations respectively. While model based interpretation of OUR has been widely undertaken, the same with titrimetric data has been limited. Therefore, different models were initially evaluated based on OUR first with a view to conducting further studies on model based interpretations using titrimetric experimental observation for different substrates. This study aims to investigate in depth the acetate removal mechanisms in an activated sludge process by calibrating four different activated sludge models using experimentally derived respirometric measurements. The models were assessed and compared using the estimated model parameters so as to get a quantitative description of the acetate biodegradation process.

4.3.1 Model calibration and parameter estimation approaches

Four different existing activated sludge models herein named Model 1, Model 2, Model 3 and Model 4 were studied based on OUR measurements. Batch experiments were conducted using a titrimetric respirometer by maintaining a constant pH of 7.8 ± 0.03. Acetate with varying concentrations of 25, 50 and 75 mg COD/L was applied during model evaluation. The parameter estimation procedure involved using non-linear least-squares optimization to minimize the sum of squared errors (SSE) between the numerical solution for the modeled output and the experimentally obtained OUR.

Model 1

The simplified ASM1 model used by Vanrolleghem et al. (2004) where it was assumed that the biomass growth was linked directly to the external substrate

consumptions is presented as Model 1. The process matrix is presented in Table 4.1. The model parameters K_S, $Y_{H,S}$, τ and combined parameter, $\mu_{MAX,S}X_H$ were estimated by using a non-linear estimation technique whereas the biomass concentration, X_H was considered constant due to the short degradation period of acetate.

Table 4.1: Stoichiometric matrix related to Model 1

Process	X_H	S_S	S_O	Kinetics
Aerobic growth on S_S	1	$-\frac{1}{Y_{H,S}}$	$-\frac{1-Y_{H,S}}{Y_{H,S}}$	$(1-e^{-t/\tau}).\mu_{MAX,S}.M_S.X_H$

Model 2

Model 2 in this study is based on a simplified ASM3 model (Gujer et al., 1999 and Guisasola et al., 2005). The basic assumption is that the readily biodegradable compound, acetate is removed only by storage and then growth occurs on the internal storage polymer (see Table 4.2 for the process matrix). With reference to parameter estimation, the model parameters k_{STO}, Y_{STO}, $\mu_{MAX,STO}$, $Y_{H,STO}$, K_S and τ were estimated.

Table 4.2: Stoichiometric matrix related to Model 2

Process	X_H	X_{STO}	S_S	S_{NH}	S_O	Kinetics
Formation of X_{STO}		1	$-\frac{1}{Y_{STO}}$		$-\frac{1-Y_{STO}}{Y_{STO}}$	$(1-e^{-t/\tau}).k_{STO}.M_S.X_H$
Aerobic growth on X_{STO}	1	$-\frac{1}{Y_{H,STO}}$		$-i_{NBM}$	$-\frac{1-Y_{H,STO}}{Y_{H,STO}}$	$\mu_{MAX,STO}.M_{X_{STO}/X_H}.X_H$
Endogenous respiration	-1			$i_{NBM}-i_{NXI}f_{XI}$	-1	$b_H.X_H$
X_{STO} respiration		-1			-1	$b_{STO}.X_{STO}$

Model 3

The simultaneous storage and growth model developed by Sin et al. (2005) for aerobic biodegradation of a carbon source is presented in this current study as Model 3. Under feast conditions, the metabolic model approach was employed. The yield coefficients of storage, direct growth on substrate and growth on internal storage products respectively were linked to each other through metabolism of the substrate. The yield coefficients were found to be correlated with the efficiency of the oxidative

phosphorylation (δ). This model eases the way to estimate only one parameter (δ), instead of three different yield coefficients (refer to Sin et al., 2005 for details of this model). Under famine conditions, a second order model was used to describe the degradation of storage products. In this model, the parameters q_{MAX}, f_{STO}, K_S, δ, K_1, K_2, and τ were estimated by following the non-linear estimation technique (process matrix is shown in Table 4.3).

Table 4.3: Stoichiometric matrix related to Model 3

Process	X_H	X_{STO}	S_S	S_{NH}	S_O	Kinetics
Formation of X_{STO}		1	$-\frac{1}{Y_{STO}}$		$-\frac{1-Y_{STO}}{Y_{STO}}$	$(1-e^{-t/\tau}).k_{STO}.M_S.X_H$
Aerobic growth on S_S	1		$-\frac{1}{Y_{H,S}}$	$-i_{NBM}$	$-\frac{1-Y_{H,S}}{Y_{H,S}}$	$(1-e^{-t/\tau}).\mu_{MAX,S}.M_S.X_H$
Aerobic growth on X_{STO}	1	$-\frac{1}{Y_{H,STO}}$		$-i_{NBM}$	$-\frac{1-Y_{H,STO}}{Y_{H,STO}}$	$\mu_{MAX,STO}\left(\frac{(X_{STO}/X_H)^2}{K_2+K_1.(X_{STO}/X_H)}\right)\left(\frac{K_S}{S_S+K_S}\right).X_H$
Endogenous respiration	-1			$i_{NBM}-i_{NXI}f_{XI}$	$-(1-f_{XI})$	$b_H.X_H$
X_{STO} respiration		-1			-1	$b_{STO}.X_{STO}$

The parameters k_{STO} and $\mu_{MAX,S}$ were calculated from the estimates of the parameters q_{MAX} and f_{STO} based on the procedure explained in Sin et al. (2005) where they assumed the parameter $\mu_{MAX,STO}$ to be the same order of magnitude as $\mu_{MAX,S}$.

Model 4

Model 4 is based on the assumption by Beccari et al. (2002) that the first step of substrate removal is always a sort of internal accumulation. The accumulation compound then can be used for growth either directly or through previous storage and subsequent use of the stored products. The process matrix is presented in Table 4.4. With regard to parameter estimation, the parameters k_{STO}, $\mu_{MAX,STO}$, $Y_{H,ACC}$, k_{ACC}, $K_{H,ACC}$, K_S and $K_{STO,ACC}$ were estimated for different substrate concentrations to fit the model with the experimental OUR data. The parameters $f_{max,acc}$ and $K_{H,STO}$ were fixed in all tests to 0.2 and 1.0 respectively as used by Beccari et al. (2002) in their model whereas, the parameter Y_{ACC} was fixed to 0.99 in all the

tests considering low energy requirement in the process. Reasonable values for the parameters $Y_{H,STO}$ and $Y_{STO,ACC}$ were assumed for different concentrations study to fit the experimental profile with the model.

Table 4.4: Stoichiometric matrix related to Model 4

Process	X_H	X_{STO}	X_{ACC}	S_S	S_{NH}	S_O	Kinetics
Accumulation of X_{ACC}		1	Y_{ACC}	-1		$-(1-Y_{ACC})$	$k_{ACC}.M_S.\left(1-\frac{X_{ACC}/X_H}{f_{\max,acc}}\right).X_H$
Storage of X_{ACC}		$Y_{STO,ACC}$	-1			$-(1-Y_{STOACC})$	$k_{STO}.\left(\frac{X_{ACC}/X_H}{K_{STO,ACC}+X_{ACC}/X_H}\right).X_H$
Aerobic growth on X_{ACC}	1		$-\frac{1}{Y_{H,ACC}}$		-0.07	$-\frac{1-Y_{H,ACC}}{Y_{H,ACC}}$	$\mu_{MAX,STO}.M_{X_{ACC}/X_H}.X_H$
Aerobic growth on X_{STO}	1	$-\frac{1}{Y_{H,STO}}$			-0.07	$-\frac{1-Y_{H,STO}}{Y_{H,STO}}$	$\mu_{MAX,STO}.M_{X_{STO}/X_H}.X_H$
Endogenous respiration	-1				0.04	-1	$b_H.X_H$
X_{STO} respiration		-1				-1	$b_{STO}.X_{STO}$

The initial concentration of biomass, $X_H(0)$ was calculated using the baseline endogenous OUR level prior to substrate addition for Models 1, 2 and 4 using the relationship OUR_{end} (0) = $b_H.X_H(0)$, whereas for Model 3 the concentration was calculated using OUR_{end} (0) = $(1-f_{XI}).b_H.X_H(0)$. The default values assigned in the ASM3 model for the parameters b_H and b_{STO} (0.2 per day), f_{XI} (0.2) and $K_{H,STO}$ (1) were assumed during the analysis. The empirical factor $(1-e^{-t/\tau})$ was added in the kinetics to describe the so-called "start-up" phase observed in the batch OURs for Models 1, 2 and 3. This was not considered by Beccari et al., 2002 (Model 4). Besides, the default values prescribed in ASM3 for the parameters i_{NBM} (0.07 g N/g COD X_H) and i_{NXI} (0.02 g N/g COD X_I) were used during ammonia profile simulation for Models 2 and 3. The column value corresponding to S_{NH} (Table 4.4) was taken from the study conducted by Beccari et al. (2002) in order to simulate the ammonia profile.

4.3.2 Results and discussions of models assessment

OUR profile

Calibration of the four different models was performed using OUR measurements resulting from varying acetate pulses (75 mg COD/L, 50 mg COD/L and 25 mg COD/L) applied in an activated sludge system. Figure 4.5 represents the experimental OUR profiles for different acetate pulses along with model calibration. Acetate is consumed during the feast period. As a result the OUR increases to a maximum level and remains constant until acetate is completely removed for aerobic growth as is described in ASM1 model (Henze et al., 1987; Gernaey et al., 2002a; Vanrolleghem et al., 2004), or for storage followed by growth with reference to ASM3 model (Gujer et al., 1999; Carucci et al., 2001; Guisasola et al., 2005), or for simultaneous storage and growth (Krishna and Van Loosdrecht, 1999; Beccari et al., 2002; Van Loosdrecht and Heijnen 2002; Sin et al., 2005) or through accumulation or sorption phenomena (Majone et al., 1999; Dionisi et al., 2001; Beccari et al., 2002). The OUR during the famine phase drops from the maximum level to a level higher than the endogenous OUR level and gradually reaches the endogenous level (Figure 4.5) which is assumed to be due to the consumption of previously stored products (Van Loosdrecht et al., 1997).

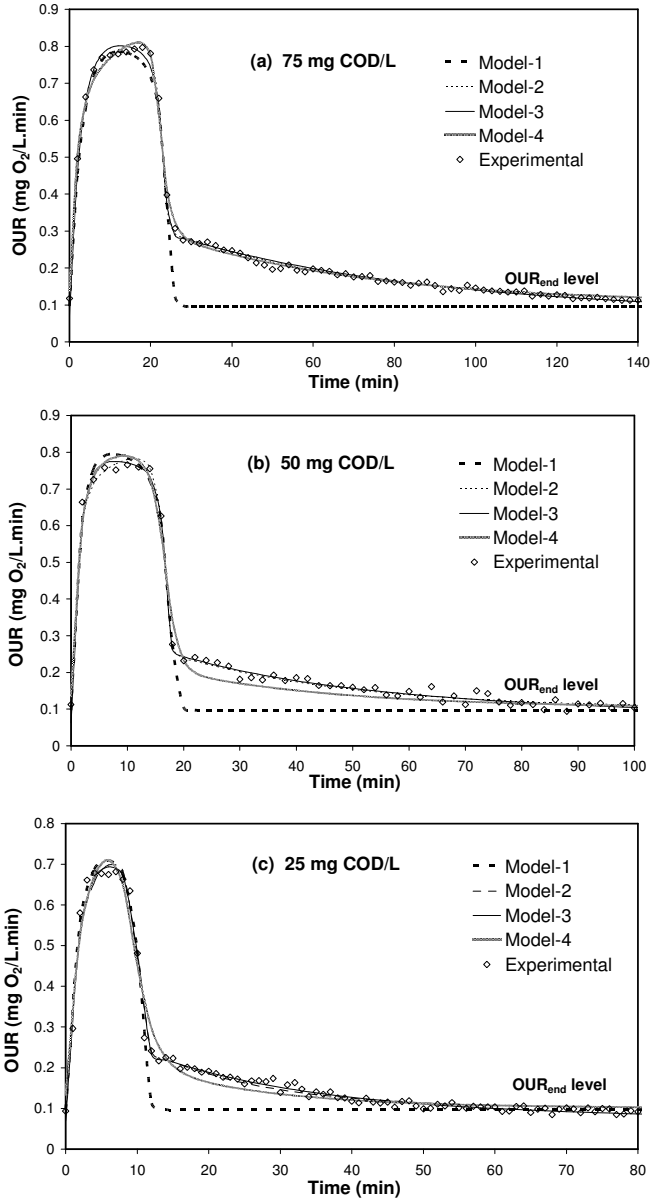

Figure 4.5: Model comparisons with experimental data (every 24th data point is presented to keep the figure clearer) for the acetate pulse of (a) 75 mg COD/L (b) 50 mg COD/L and (c) 25 mg COD/L

Parameter estimation

The parameters relating to Model 1 for all three concentrations are presented in Table 4.5. The model parameter $Y_{H,S}$ (growth yield) ranges from 0.78 to 0.81 after fitting the experimental data with the ASM1 model (Model 1), which is higher than its default value (0.67). However, a similar value (0.78) for growth yield was observed by Vanrolleghem et al. (2004) in their study. Another study conducted by Guisasola

et al. (2005) found $Y_{H,S}$ varies from 0.76 to 0.79 which is due to the storage phenomena. In the current project, the parameters K_S (1.19 to 2.3 mg COD/L) and $\mu_{MAX,S}$ (0.0036 to 0.0046 min^{-1}) were found to be within the range observed by Guisasola et al. (2005) whereas, these values found by Vanrolleghem et al. (2004) in their study to be 0.66 mg COD/L and 0.00071 min^{-1} respectively. However, it is clear from the current work that Model 1 is not suitable to describe the famine part of the experimental data due to exclusion of storage phenomena. Therefore, Model 1 will not be further discussed in this study.

Table 4.5: Parameter estimation results related to Model 1

Parameters	Acetate 75 mg COD/L (Confidence interval, %)	Acetate 50 mg COD/L (Confidence interval, %)	Acetate 25 mg COD/L (Confidence interval, %)
Parameters Estimated:			
$\mu_{MAX,S}.X_H$ (mg/L.min)	3.19 ± 0.008 (0.25)	2.76 ± 0.009 (0.33)	2.51 ± 0.013 (0.52)
K_S (mgCOD/L)	2.3 ± 0.041 (1.78)	1.83 ± 0.046 (2.51)	1.19 ± 0.033 (2.77)
$Y_{H,S}$ (mgCOD X_H/mgCOD S_S)	0.81 ± 2.6x10^{-4} (0.03)	0.79 ± 4.3x10^{-4} (0.05)	0.78 ± 4.7x10^{-4} (0.06)
τ (min)	2.89 ± 0.025 (0.87)	1.59 ± 0.022 (1.38)	1.65 ± 0.023 (1.39)
Parameters Assumed:			
b_H (1/min)	0.000139	0.000139	0.000139
Parameters Calculated:			
$\mu_{MAX,S}$ (1/min)	0.0046	0.0039	0.0036
X_H (mgCOD/L)	720	720	720
SSE	9.784	4.045	2.045

In Model 2, the estimated parameters $\mu_{MAX,STO}$ (27.9 -77.3 day^{-1}) and $Y_{H,STO}$ (0.83-0.86) show higher values than the ASM3 default one (2 day^{-1} and 0.63 respectively) as presented in Table 4.6. Such high values for both the parameters $\mu_{MAX,STO}$ (28 -64 day^{-1}) and $Y_{H,STO}$ (0.8-0.96) were also noticed by Guisasola et al. (2005) in their study where it was explained as due to the overestimation of storage production (X_{STO}) with respect to experimental one. High growth yields of 0.85 and 0.8 respectively were also observed from the studies conducted by Beccari et al. (2002) and Koch et al. (2000). The estimated model parameter Y_{STO} from this current study lies between 0.83 and 0.85, which meets the default value prescribed by ASM3 model (0.85).

Table 4.6: Parameter estimation results related to Model 2

Parameters	Acetate 75 mg COD/L (Confidence interval, %)	Acetate 50 mg COD/L (Confidence interval, %)	Acetate 25 mg COD/L (Confidence interval, %)
Parameters Estimated:			
k_{STO} (1/min)	$0.0046 \pm 7.38 \times 10^{-6}$ (0.16)	$0.00406 \pm 1.7 \times 10^{-5}$ (0.42)	$0.00376 \pm 3.5 \times 10^{-5}$ (0.93)
$\mu_{MAX,STO}$ (1/min)	$0.0194 \pm 1.6 \times 10^{-4}$ (0.83)	$0.03 \pm 6.5 \times 10^{-4}$ (2.17)	0.05365 ± 0.0015 (2.8)
K_S (mgCOD/L)	2.16 ± 0.041 (1.9)	1.43 ± 0.053 (3.7)	1.15 ± 0.063 (5.5)
$Y_{H,STO}$ (mgCOD X_H/mgCOD X_{STO})	$0.83 \pm 7.6 \times 10^{-4}$ (0.09)	0.86 ± 0.0015 (0.17)	0.85 ± 0.0022 (0.26)
Y_{STO} (mgCOD X_{STO}/mgCOD S_S)	$0.85 \pm 3.3 \times 10^{-4}$ (0.04)	$0.83 \pm 7.2 \times 10^{-4}$ (0.09)	0.83 ± 0.0012 (0.14)
τ (min)	1.88 ± 0.012 (0.64)	1.18 ± 0.025 (2.12)	1.38 ± 0.04 (2.9)
Parameters Assumed:			
b_H (1/min)	0.000139	0.000139	0.000139
b_{STO} (1/min)	0.000139	0.000139	0.000139
$K_{H,STO}$ (mgCOD X_{STO}/mgCOD X_H)	1	1	1
Parameters Calculated:			
X_H (mgCOD/L)	720	720	720
SSE	0.167	0.36	0.252

The estimated parameter f_{STO} in Model 3 shows a range of 0.51-0.65 (Table 4.7) which supports the observations made by Sin et al., 2005 (0.6-0.65). The calculated parameter k_{STO} (i.e. for the concentration 75 mg COD/L, the value is 3.7 day^{-1}) is found to be faster than the parameter $\mu_{MAX,S}$ (i.e. for the concentration 75 mg COD/L, the value is 1.6 day^{-1}) which was also observed by Sin et al. (2005) and Pratt et al. (2004). In addition, the yield coefficient, Y_{STO} is found to be higher (0.88) than the yield coefficient, $Y_{H,S}$ (0.71) which is similar to the findings by Sin et al. (2005). The parameter K_S estimated by Sin et al. (2005) is lower (0.6 -0.67 mg COD/L) than the ASM3 default value (2.0 mg COD/L), whereas the current study estimated the value to range from 1.0 to 2.29 mg COD/L. However, the estimated parameter K_2 shows a higher confidence interval for all three concentration studies. A similar problem was noticed by Sin et al. (2005) in their study and was explained by the correlation between the parameters K_1 and K_2 during the feast phase of the biodegradation process.

Table 4.7: Parameter estimation results related to Model 3

Parameters	Acetate 75 mg COD/L (Confidence interval, %)	Acetate 50 mg COD/L (Confidence interval, %)	Acetate 25 mg COD/L (Confidence interval, %)
Parameters Estimated:			
q_{MAX} (1/min)	$0.004509 \pm 1.3 \times 10^{-5}$ (0.29)	$0.00392 \pm 1.6 \times 10^{-5}$ (0.4)	$0.003703 \pm 3.7 \times 10^{-5}$ (1.0)
K_S (mgCOD/L)	2.29 ± 0.063 (2.75)	1.23 ± 0.056 (4.55)	1.0 ± 0.063 (6.3)
f_{STO} (mgCOD X_{STO}/mgCOD S_S)	0.65 ± 0.022 (3.38)	0.51 ± 0.029 (5.69)	0.56 ± 0.036 (6.43)
K_1 (mgCOD X_{STO}/mgCOD X_H)	0.065 ± 0.004 (6.15)	0.0506 ± 0.0033 (6.52)	0.024 ± 0.002 (8.3)
K_2 (mgCOD X_{STO}/mgCOD X_H)	$5.7 \times 10^{-6} \pm 1.5 \times 10^{-5}$ (263.2)	$1.7 \times 10^{-7} \pm 4.8 \times 10^{-7}$ (282.4)	$5.6 \times 10^{-7} \pm 2.0 \times 10^{-6}$ (357.1)
δ (mol/mol)	4.16 ± 0.098 (2.36)	4.36 ± 0.132 (3.03)	4.16 ± 0.144 (3.46)
τ (min)	2.78 ± 0.02 (0.72)	1.5 ± 0.024 (1.6)	1.73 ± 0.039 (2.25)
Parameters Assumed:			
b_H (1/min)	0.000139	0.000139	0.000139
b_{STO} (1/min)	0.000139	0.000139	0.000139
f_{XI} (mgCOD /mgCOD)	0.2	0.2	0.2
Parameters Calculated:			
k_{STO} (1/min)	0.002573	0.00176	0.001826
$\mu_{MAX,S}$ (1/min)	0.001118	0.001385	0.001147
$\mu_{MAX,STO}$ (1/min)	0.001118	0.001385	0.001147
$Y_{H,S}$ (mgCOD X_H/mgCOD S_S)	0.71	0.72	0.71
$Y_{H,STO}$ (mgCOD X_H/mgCOD X_{STO})	0.78	0.79	0.78
Y_{STO} (mgCOD X_{STO}/mgCOD S_S)	0.88	0.89	0.88
X_H (mgCOD/L)	900	900	900
SSE	0.167	0.312	0.222

Table 4.8 shows the estimated parameters related to Model 4. In this current study, the parameters k_{ACC}, k_{STO}, $\mu_{MAX,STO}$ and $Y_{H,ACC}$ were found to be higher than the values optimized by Beccari et al. (2002) where they concluded the values to be 0.03 h^{-1}, 1.8 h^{-1}, 0.3 h^{-1} and 0.77 respectively. The estimated value for the parameter $\mu_{MAX,STO}$ in this current study varies from 0.97 to 2.79 h^{-1} which is closer to the value (0.52 to 1.33 h^{-1}) estimated in Model 2 (Table 4.6). The range for the estimated parameter $K_{STO,ACC}$ lies between 0.32 and 0.4 whereas the study conducted by Beccari et al. (2002) showed the value equal to 0.45. The results for the estimated parameters K_S (1.67 - 2.34 mg COD/L) and $K_{H,ACC}$ (0.1 – 0.27 mg/mg) satisfy the predictions of Beccari (2 mg COD/L and 0.21 mg/mg respectively). However, in this model, the calculated confidence intervals particularly for the parameters k_{STO} and $K_{STO,ACC}$ were found to be much higher for all three concentrations which are not satisfactory from a statistical perspective.

Table 4.8: Parameter estimation results related to Model 4

Parameters	Acetate 75 mg COD/L (Confidence interval, %)	Acetate 50 mg COD/L (Confidence interval, %)	Acetate 25 mg COD/L (Confidence interval, %)
Parameters Estimated:			
k_{ACC} (mgCOD S_S/mgCOD X_H .min)	0.005459 ± 2.2x10^{-5} (0.4)	0.005113 ± 7.3x10^{-5} (1.43)	0.005184 ± 1.7x10^{-4} (3.28)
k_{STO} (1/min)	0.132 ± 0.273 (206.82)	0.13 ± 0.653 (502.31)	0.13 ± 0.653 (502.31)
$\mu_{MAX,STO}$ (1/min)	0.01614 ± 1.8x10^{-4} (1.12)	0.028353 ± 0.0015 (5.29)	0.046456 ± 0.0036 (7.75)
K_S (mgCOD/L)	1.67 ± 0.072 (4.31)	2.34 ± 0.174 (7.44)	2.19 ± 0.216 (9.86)
$K_{H,ACC}$ (mgCOD X_{ACC}/mgCOD X_H)	0.12 ± 0.0019 (1.58)	0.1 ± 0.0052 (5.2)	0.27 ± 0.02 (7.4)
$K_{STO,ACC}$ (mgCOD X_{STO}/mgCOD X_{ACC})	0.37 ± 0.775 (209.46)	0.32 ± 1.63 (509.38)	0.4 ± 2.027 (506.75)
$Y_{H,ACC}$ (mgCOD X_H/mgCOD X_{ACC})	0.84 ± 0.0015 (0.18)	0.98 ± 0.012 (1.22)	0.98 ± 0.027 (2.76)
Parameters Assumed:			
b_H (1/min)	0.000139	0.000139	0.000139
b_{STO} (1/min)	0.000139	0.000139	0.000139
$K_{H,STO}$ (mgCOD X_{STO}/mgCOD X_H)	1	1	1
Y_{ACC} (mgCOD X_{ACC}/mgCOD S_S)	0.99	0.99	0.99
$Y_{H,STO}$ (mgCOD X_H/mgCOD X_{STO})	0.75	0.81	0.8
$Y_{STO,ACC}$ (mgCOD X_{STO} /mgCOD X_{ACC})	0.85	0.7	0.71
$f_{max,acc}$ (mgCOD X_{ACC}/mgCOD X_H)	0.2	0.2	0.2
Parameters Calculated:			
X_H (mgCOD/L)	720	720	720
SSE	0.242	0.822	0.519

4.3.3 Model comparison

The parameter values relating to the four different models are presented in Table 4.5-4.8 including the parameter estimation errors calculated for 95% confidence intervals and SSE value for each concentration in order to evaluate those models statistically. For the three concentrations, the calculated SSE ranges from 2.045 to 9.784 in Model 1 which is relatively high as compared to the other three models. The lowest SSE was observed for both Model 2 and Model 3.

The successful validation of these models requires the measurement of substrate, storage products, accumulated substrate and ammonia along with OUR data. A comparison of the simulated profiles of acetate degradation, PHB (as storage products) formation and ammonium consumption for the acetate pulse of 75 mg COD/L for the three models is presented in Figure 4.6. The substrate degradation rate for Models 2, 3 and 4 were almost the same as shown in Figure 4.6. However, the simulated storage profile using Model 2 (representing ASM3) gives highest storage rate, followed by that using Model 3 (representing simultaneous storage and growth) and Model 4 (accumulation). This reinforces the fact that ASM3 overestimates the

formation of storage products as experimentally determined by Krishna and Van Loosdrecht (1999) and Beccari et al. (2002). In their experimental evaluation of storage products, Beccari et al. (2002) concluded that both Model 3 and Model 4 fitted well with the observed storage phenomenon. In this simulation, Model 4 predicted the storage formation to be lower than that of Model 3.

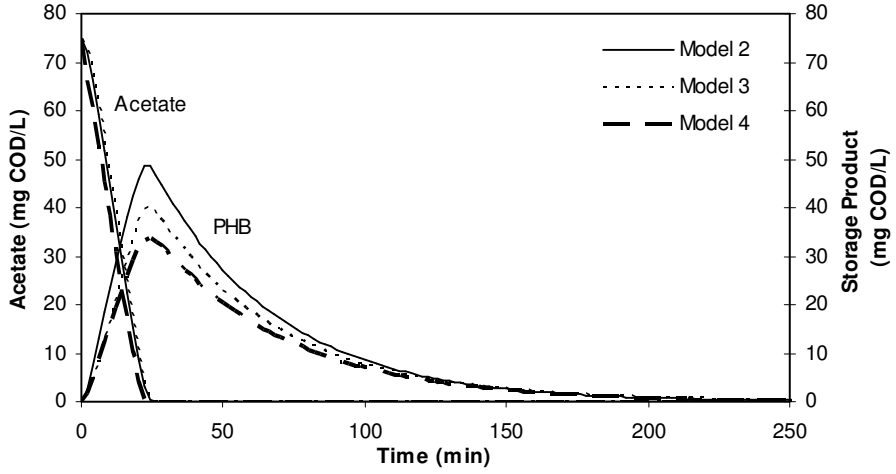

Figure 4.6: Simulated profiles (acetate and PHB) for the acetate pulse of 75 mg COD/L

Experimental measurements for COD and ammonium in the liquid phase were also conducted and the results are presented in Figure 4.7 along with the simulated acetate and ammonium profiles. Simulation of the three models shows the ammonia consumption rate to be faster for Model 4 followed by Models 3 and 2. The study conducted by Beccari et al. (2002) also showed the ammonium consumption rate for Model 4 to be higher than Model 2 but lower than Model 3. They concluded that Model 4 (accumulation followed by simultaneous storage and growth mechanism) was the best as it describes the whole experimentally observed behavior. However, the concept in Model 4 that the internal accumulation occurs as a first step is too difficult to be quantified by experimental means. In this current study, the off-line measurements of ammonium concentration were found to be very close to the profile for Model 3 (Figure 4.7) confirming the validity of this model. Based on these discussions, the simultaneous storage and growth mechanism (Model 3) as modified by Sin et al. (2005) best explains acetate biodegradation process.

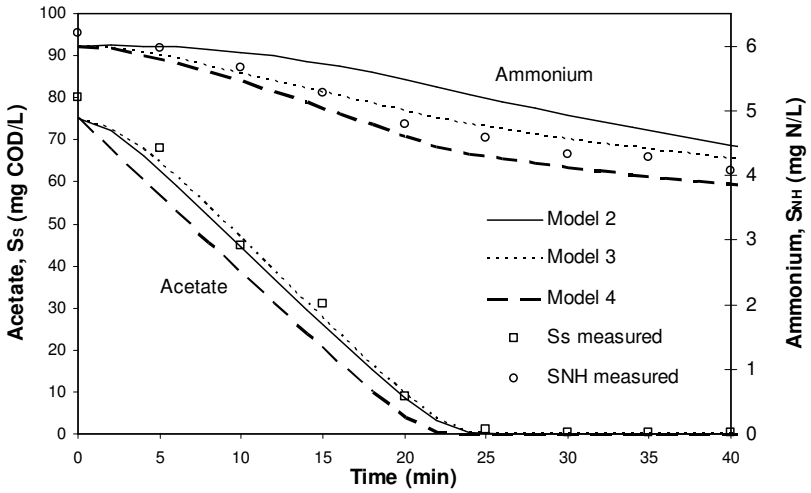

Figure 4.7: Simulated model profiles with measured data during acetate (75 mg COD/L) biodegradation

4.4 Extension of SSAG model

The assessment of activated sludge models, described in the previous section (section 4.3), revealed that the SSAG model (Model 3) explained very well the experimentally observed OUR which was also validated with off-line measurements relating to the acetate biodegradation process.

Figure 4.8 is the model diagram based on the SSAG concept. Sin et al. (2005) developed the latest version of the SSAG models that incorporated crucial change to the previously developed models based on the concept of SSAG. They particularly improved the model of substrate metabolism under feast conditions, and proposed a second-order type kinetic expression for the degradation of storage products under famine conditions using acetate as the model substrate. Researchers calibrated this model successfully using respirometric data and validated it using off-line storage products measurements as well, but it still needs model based interpretation of titrimetry. Any proposed model should be able to explain both the respirometric and titrimetric behavior of the aerobic biodegradation process since dissolved oxygen and pH changes occur simultaneously in an activated sludge system. Though Sin and Vanrolleghem (2007) improved the Gernaey model (Gernaey et al., 2002a) by considering a non-linear CTR in the liquid phase during the aerobic biodegradation

process, the model was still based on ASM1 where the formation of intracellular storage products was not considered.

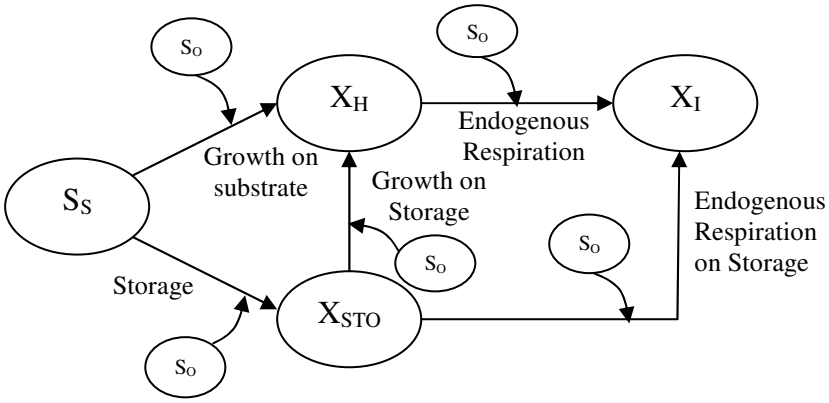

Figure 4.8: Model diagram representing the SSAG concept

Hence, in this current study the SSAG model developed by Sin et al. (2005) was improved further to enable model based calibration of both respirometric and titrimetric behavior in an activated sludge system. The proposed SSAG model introduces the stoichiometric parameters involved in titrimetry in each step of the growth and storage phases along with the consideration of non-linear carbon dioxide transfer rate in the liquid phase. The major steps during the biodegradation process include the formation of storage products, aerobic growth on substrate, aerobic growth on storage, endogenous respiration, respiration on storage products, aqueous CO_2 equilibrium and stripping of CO_2 (see Table 4.9 for process matrix). During the extension of ASM1 model, Sin and Vanrolleghem (2007) demonstrated the physical-chemical interactions of CO_2 in typical bioreactors and introduced titrimetry related stoichiometric components for both aerobic growth on substrate and endogenous respiration that were applied in our model. Additionally, our proposed model includes titrimetric components for the processes such as formation of storage products and aerobic growth on storage that were derived from the approach described by Sin and Vanrolleghem (2007). The following sub-sections describe the basic theory corresponding to the proposed titrimetric model development.

4.4.1 Formation of storage products

The formation of storage products results in the production of CO_2 during the aerobic biodegradation of an organic compound. The stoichiometry related to the formation of storage products from substrate indicates the respective CO_2 production rate that can be determined simply from the biochemical reaction involved in the biodegradation process (Sin and Vanrolleghem, 2007). The C-mol basis expression for the storage products formation approach is shown in equation 4.1 where elemental conservation and a balance of the degrees of reduction were used to determine the stoichiometric coefficient.

$$\frac{1}{Y_{SSTO}} CH_yO_z(C-mmol) + \frac{1}{4}\left(\gamma_{STO} - \frac{\gamma_S}{Y_{SSTO}}\right) O_2(mmol)$$
$$\rightarrow 1CH_pO_q(C-mmol) + \left(\frac{1}{Y_{SSTO}} - 1\right) CO_2(mmol-C) + (...)H_2O \quad \text{----- (Equation 4.1)}$$

Here, CH_yO_z and CH_pO_q represent the elemental composition of the substrate and the storage products respectively. Y_{SSTO} is the yield for storage formation on C-mol basis. The degree of reduction of the substrate and the storage products are presented as γ_S and γ_{STO} that give the value 4+y-2z and 4+p-2q respectively. Equation 4.2 is the stoichiometric expression that can be derived by converting the unit from C-mol to g COD and dividing both sides of equation 4.1 with "$8\gamma_{STO}$" where 8 gCOD is assumed as equivalent for each mol electron (Henze et al., 2000).

$$\frac{1}{Y_{STO}}(mgCOD)CH_yO_z + \left(1 - \frac{1}{Y_{STO}}\right)(mgCOD)O_2$$
$$\rightarrow 1(mgCOD)CH_pO_q + \frac{1}{8\gamma_S}\left(\frac{1}{Y_{STO}} - \frac{\gamma_S}{\gamma_{STO}}\right)(mmol)CO_2 + (...)H_2O \quad \text{----- (Equation 4.2)}$$

where, Y_{STO} refers to the growth yield (mgCOD/mgCOD) which is equal to $Y_{SSTO}.(\gamma_{STO}/\gamma_S)$. The coefficient related to CO_2 production/consumption is expressed in molar units that is more relevant to titrimetric analysis (Table 4.9).

The proton (H^+) balance during acetate biodegradation was modeled by Gernaey et al. (2002a) where H^+ consumption was observed. The biomass cell directly extracts a

proton from the liquid phase along with the dissociated weak acid during the acetate uptake process resulting in a pH change in the system. The corresponding H^+ consumption can be estimated by using the matrix as shown in Table 4.9 where the parameter "C" represents the molecular weight of acetate (64 gCOD/mol) and "m" refers to the fraction of the dissociated monoprotic acid in the liquid phase expressed as $1/(1+10^{pKa-pH})$ (See Gernaey et al., 2002a). In the SSAG model, part of the acetate is taken up for storage formation while the rest of it is consumed for simultaneous heterotrophic biomass growth. That is why H^+ consumption is assumed to take place during both stages, influenced by the respective yield coefficient (Table 4.9)

4.4.2 Aerobic growth on substrate

The production of CO_2 due to the heterotrophic biomass growth on substrate can be estimated by using the following C-mol basis expression (derived by Sin and Vanrolleghem, 2007):

$$\frac{1}{Y_{SX}} CH_yO_z(C-mmol) + \frac{1}{4}\left(\gamma_X - \frac{\gamma_S}{Y_{SX}}\right) O_2(mmol) + cNH_3(mmol-N) \quad \text{----- (Equation 4.3)}$$
$$\rightarrow 1CH_aO_bN_c(C-mmol) + \left(\frac{1}{Y_{SX}} - 1\right) CO_2(mmol-C) + (...).H_2O$$

where, $CH_aO_bN_c$ refers to the elemental composition of the biomass and γ_X represents the degree of reduction of the biomass which is calculated as 4+a-2b-3c. Equation 4.4 can be derived similarly to the previous section where the growth yield, $Y_{H,S}$ is presented in terms of gCOD basis that equals to $Y_{SX}.(\gamma_X / \gamma_S)$. The coefficient related to ammonia uptake (i_{NBM}) is expressed as gN per gCOD biomass unit basis that can be determined from the relation $14c/8\gamma_X$ (Sin, 2004).

$$\frac{1}{Y_{H,S}}(mgCOD)CH_yO_z + \left(1 - \frac{1}{Y_{H,S}}\right)(mgCOD)O_2 + i_{NBM}(mgN)NH_3 \quad \text{----- (Equation 4.4)}$$
$$\rightarrow 1(mgCOD)CH_aO_bN_c + \frac{1}{8}\left(\frac{1}{\gamma_S Y_{H,S}} - \frac{1}{\gamma_X}\right)(mmol)CO_2 + (...)H_2O$$

The proton consumption/production during aerobic growth on substrate consists of two components, i.e. H^+ consumption due to acetate uptake and H^+ production due to

ammonia assimilation for biomass growth. In Table 4.9, the parameter "p" represents the fraction of NH_4^+ in the liquid phase which is derived as $1/(1+10^{pH-pK_{NH4}})$ by Gernaey et al. (2002a).

4.4.3 Aerobic growth on storage

Equation 4.5 is the C-mol basis expression for the corresponding biological process that can be used to determine the respective CO_2 production rate.

$$\frac{1}{Y_{STOX}} CH_pO_q(C-mmol) + \frac{1}{4}\left(\gamma_X - \frac{\gamma_{STO}}{Y_{STOX}}\right) O_2(mmol) + cNH_3(mmol-N) \quad \text{----- (Equation 4.5)}$$
$$\rightarrow 1CH_aO_bN_c(C-mmol) + \left(\frac{1}{Y_{STOX}} - 1\right) CO_2(mmol-C) + (...).H_2O$$

The following expression is derived from the above equation after converting the unit from C-mol to g COD where the growth yield on storage product, $Y_{H,STO}$ is replaced with $Y_{STOX}.(\gamma_X/\gamma_{STO})$.

$$\frac{1}{Y_{H,STO}}(mgCOD)CH_pO_q + \left(1 - \frac{1}{Y_{H,STO}}\right)(mgCOD)O_2 + i_{NBM}(mgN)NH_3 \quad \text{----- (Equation 4.6)}$$
$$\rightarrow 1(mgCOD)CH_aO_bN_c + \frac{1}{8\gamma_{STO}}\left(\frac{1}{Y_{H,STO}} - \frac{\gamma_{STO}}{\gamma_X}\right)(mmol)CO_2 + (...)H_2O$$

Under the aerobic growth on storage process, it is assumed that the biomass accumulates nitrogen too within the cell along with carbon for subsequent growth purposes (see the ammonium balance in Table 4.9). This is also in agreement with the concept described by Beccari et al. (2002).

4.4.4 Endogenous respiration

The biological reaction during endogenous respiration leads to CO_2 production that can be estimated using the stoichiometric expression as mentioned in equation 4.7.

$$CH_aO_bN_c + \frac{\gamma_X}{4}O_2 \rightarrow CO_2 + \frac{a-3c}{2}H_2O + c.NH_3 \quad \text{----- (Equation 4.7)}$$

Table 4.9 presents the production of CO_2 for the respective oxygen uptake of (1-f_{XI}) gCOD (as derived by Sin and Vanrolleghem, 2007).

4.4.5 Respiration on storage products

The respiration on storage can be expressed as the following biological reaction:

$$CH_pO_q + \frac{\gamma_{STO}}{4} O_2 \rightarrow CO_2 + \frac{p}{2} H_2O \qquad \text{----- (Equation 4.8)}$$

The respective CO_2 production presented in Table 4.9 can be calculated by using equation 4.8, where the parameter γ_{STO} refers to the value 4+p-2q.

4.4.6 Aqueous CO_2 equilibrium

Sin and Vanrolleghem (2007) used the dynamic model in their study to explain the physical-chemical interactions of CO_2 in typical biological reactors. This is also applied in our model to represent the aqueous CO_2 equilibrium phase. Equation 4.9 is the simplified form of the chemical reaction related to the CO_2 equilibrium process in the liquid phase.

$$CO_2 + H_2O \Leftrightarrow HCO_3^- + H^+ \qquad \text{----- (Equation 4.9)}$$

The kinetics of the above reaction can be expressed as:

$$k_1 S_{CO_2} - k_1 10^{pk_1 - pH} S_{HCO_3}$$

where, S_{CO_2} and S_{HCO_3} are the state variables for CO_2 and HCO_3^- respectively, k_1 is the forward reaction rate constant of CO_2 equilibrium and pK_1 is the negative logarithm of CO_2 to HCO_3^- equilibrium constant (adopted from Sin and Vanrolleghem, 2007).

Table 4.9: Process matrix involved in proposed extension of SSAG model for acetate biodegradation

Process	X_H (g COD)	X_{NHacc} (g N)	X_{STO} (g COD)	S_S (g COD)	S_{HCO_3} (mol)	S_{CO_2} (mol)	S_{Hp} (mol)	S_{NH} (g N)	S_O (g O_2)	Kinetics
Formation of X_{STO}	--	--	1	$-1/Y_{STO}$	--	$\frac{1}{8\gamma_S}\left(\frac{1}{Y_{STO}}-\frac{\gamma_S}{\gamma_{STO}}\right)$	$-\frac{m}{Y_{STO}C}$	--	$-(1-Y_{STO})/Y_{STO}$	$(1-e^{-t/\tau}).k_{STO}.M_S.X_H$
S_{NH} accumulation	--	i_{NBM}	--	--	--	--	$\frac{i_{NBM}\,p}{14}$	$-i_{NBM}$	--	$(1-e^{-t/\tau}).k_{NHacc}.M_S.X_H$
Aerobic growth on S_S	1	--	--	$-1/Y_{H,S}$	--	$\frac{1}{8\gamma_S}\left(\frac{1}{Y_{H,S}}-\frac{\gamma_S}{\gamma_X}\right)$	$\frac{i_{NBM}\,p}{14}-\frac{m}{Y_{H,S}C}$	$-i_{NBM}$	$-(1-Y_{H,S})/Y_{H,S}$	$(1-e^{-t/\tau}).\mu_{MAX,S}.M_S.X_H$
Aerobic growth on X_{STO}	1	$-i_{NBM}$	$-1/Y_{H,STO}$	--	--	$\frac{1}{8\gamma_{STO}}\left(\frac{1}{Y_{H,STO}}-\frac{\gamma_{STO}}{\gamma_X}\right)$	--	--	$-(1-Y_{H,STO})/Y_{H,STO}$	$\mu_{MAX,STO}\left(\frac{(X_{STO}/X_H)^2}{K_2+K_1.(X_{STO}/X_H)}\right)\left(\frac{K_S}{S_S+K_S}\right)X_H$
Endogenous respiration	-1	--	--	--	--	$\frac{1-f_{XI}}{8\gamma_X}$	$-((i_{NBM}-f_{XI}i_{NXI})/14)\,p$	$i_{NBM}-i_{NXI}f_{XI}$	$-(1-f_{XI})$	$b_H.X_H$
X_{STO} respiration	--	--	-1	--	--	$\frac{1}{8\gamma_{STO}}$	--	--	-1	$b_{STO}.X_{STO}$
Aqueous CO_2 equilibrum	--	--	--	--	1	-1	1	--	--	$k_1 S_{CO_2}-k_1 10^{pk_1-pH} S_{HCO_3}$
CO_2 stripping	--	--	--	--	--	1	--	--	--	$K_L a_{CO_2}(S^*_{CO_2}-S_{CO_2})$

Assuming that ammonia required for the biomass growth during storage to growth process is taken from the internal source (cell accumulation) instead of the external environment

4.4.7 CO_2 stripping

This process refers to the transfer of aqueous CO_2 to the gas phase that depends on the equilibrium CO_2 concentration ($S^*_{CO_2}$) and the mass transfer coefficient of CO_2 ($K_L a_{CO_2}$). The following kinetics expression was used by Sin and Vanrolleghem (2007) to represent the CO_2 stripping process:

$$K_L a_{CO_2}(S^*_{CO_2} - S_{CO_2})$$

The Henry law can be used to determine the equilibrium CO_2 concentration (see equation 4.10).

$$S^*_{CO_2} = P_{CO_2} * K_H \qquad \text{----- (Equation 4.10)}$$

where, P_{CO_2} is the partial pressure of CO_2 (atm) and K_H is the Henry coefficient for CO_2 (mol/atm-L).

4.5 Proposed model calibration and parameter estimation

4.5.1 Parameter estimation strategy

Model calibration was performed for acetate with the initial concentrations of 25, 50 and 75 mg COD/L. The estimation of model parameters was undertaken using non-linear techniques employing the algorithms in the optimisation toolbox included in MATLAB (R2007a). Minimization of the mean squared error (MSE) between the model and experimental output was used as the main criterion for curve fitting. The titrimetric data alone was applied to estimate the model parameters. It was then followed by the parameter estimation process using respirometric data alone and then the combined respirometric-titrimetric data. The results were finally compared to validate the proposed SSAG model.

Seven model parameters such as q_{MAX}, K_S, f_{STO}, K_1, K_2, δ, and τ were estimated along with calculation of their errors (see Appendix A for the description of the parameters

and Table 4.9 for the process matrix). The maximum storage rate (k_{STO}) and the maximum growth rate of biomass ($\mu_{MAX,S}$) were calculated from the estimates of the parameters q_{MAX} and f_{STO} based on the procedure explained in Sin et al. (2005) where they assumed the parameter $\mu_{MAX,STO}$ to be the same order of magnitude as $\mu_{MAX,S}$. The yield coefficients Y_{STO}, $Y_{H,S}$ and $Y_{H,STO}$ were calculated from the estimated parameter δ (see Sin et al., 2005 for details). The initial concentration of biomass, $X_H(0)$ was calculated using the baseline endogenous OUR level prior to substrate addition using $OUR_{end}(0) = (1-f_{XI}).b_H.X_H(0)$. The default values assigned in the ASM3 model for the parameters b_H, b_{STO} (0.2 per day or 0.000139 per min) and f_{XI} (0.2) were assumed during the analysis. A similar value was assumed (0.2 per day) at the beginning of the parameter estimation process for the parameter k_{NHacc}. This was revised later for better curve fitting. The ASM3 prescribed value for the parameters i_{NXI} (0.02 gN/g COD X_I) and i_{NBM} (0.07 gN/g COD X_H) were fixed during the proposed model calibration.

Total inorganic carbon in the aqueous medium, $C_{T,init}$ and the parameter k_1 were estimated from a separate model calibration under endogenous state and were kept fixed during exogenous titrimetric data interpretation (see parameter estimation from the endogenous study under sub-section 4.5.2 for more details). Furthermore, the initial concentrations of CO_2 and HCO_3 in the reactor were calculated using their relationship with $C_{T,init}$ (Sin, 2004). During the model calibration, the value for $K_L a_{CO_2}$ was calculated as 0.052 min^{-1} from the oxygen transfer coefficient ($K_L a$) using the relationship between their diffusivity coefficients (Sperandio and Paul, 1997; Sin and Vanrolleghem, 2007), whereas the parameter pK_1 was taken as 6.39 which is the negative logarithm of the first acidity constant in the CO_2 equilibrium (Sperandio and Paul, 1997). The default values suggested by Stumm and Morgan (1996) for the parameters pK_a (4.75), pK_{NH4} (9.25) and $S^*_{CO_2}$ (0.017 mmol/L) were assumed during the parameter estimation process. In addition, the default values prescribed by Sin and Vanrolleghem (2007) for the stoichiometric coefficients, γ_S (4) and γ_X (4.2) were used for the model calibration that depends on the elemental composition of acetate ($C_2H_4O_2$) and biomass ($CH_{1.8}O_{0.5}N_{0.2}$) respectively. On the other hand, the storage products formula $CH_{1.5}O_{0.5}$ used by Van Aalst-van Leeuwen et al. (1997) was assumed here to calculate the coefficient γ_{STO} (4.5).

4.5.2 Discussion on model calibration and parameter estimation

Model calibration using respirometry alone

The proposed SSAG model was successfully calibrated with experimental OUR data for the acetate pulses of 75, 50 and 25 mg COD/L that are presented in Figure 4.9a, Figure 4.10a and Figure 4.11a correspondingly. Results from the parameter estimation shows the substrate affinity constant, K_S lies between 0.73 and 2.27 mg COD/L for the initial acetate concentration of 25 and 75 mg COD/L respectively, whereas Sin et al. (2005) estimated the value lower (0.6 -0.67 mg COD/L) than the ASM3 default value (2.0 mg COD/L). The estimated parameter f_{STO} varies from 0.56 to 0.6 (Table 4.10) which supports the observation made by Sin et al., 2005. The calculated storage uptake rate, k_{STO} is faster than the maximum growth rate, $\mu_{MAX,S}$ which is also observed by Sin et al. (2005) and Pratt et al. (2004). Besides, the Gernaey et al. (2002b) estimated the combined parameter $\mu_{MAX,S.}\ X_H(0)$ based on the model ASM1 that varies from 1.48 to 1.61 mg COD/L.min. The calculated combined parameter $\mu_{MAX,S.}X_H(0)$ in our SSAG model gives a value ranging from 0.97 to 1.12 mg COD/L.min which is a bit lower than the Gernaey study as storage formation dominates the biodegradation process here. Besides, the average yield coefficient for storage on substrate Y_{STO} is higher (0.88) than the average yield coefficient for growth on substrate $Y_{H,S}$ (0.71) which matches well with the findings by Sin et al. (2005). A Similar yield coefficient for growth on substrate ($Y_{H,S}$) that was estimated using ASM1 was noticed in the literature (Beccari et al., 2002; Gernaey et al. 2002b; Vanrolleghem et al., 2004; Sin and Vanrolleghem, 2007).

Model calibration using titrimetry alone

Based on the titrimetric measurements the model calibration for acetate concentrations of 75, 50 and 25 mg COD/L are shown in Figure 4.9b, Figure 4.10b and Figure 4.11b respectively. The parameter estimation results for the three different acetate concentrations are presented in Table 4.11 where the parameters $C_{T,init}$ and k_1 that were estimated from separation calibration process (Figure 4.12), were kept as fixed here and the seven model parameters q_{MAX}, K_S, f_{STO}, K_1, K_2, δ, and τ were estimated. The estimated parameters K_S and f_{STO} vary within the range

0.72-2.27 mg COD/L and 0.56-0.6 respectively. The confidence intervals for all the estimated parameters are reasonable except that for K_2 which is higher for every case. A similar problem was noticed by Sin et al. (2005) in their study and was explained by the correlation between the parameters K_1 and K_2 under the feast phase of the biodegradation process. Moreover, the calculated model parameters $\mu_{MAX,S}$, k_{STO}, $Y_{H,S}$ and Y_{STO} are very close to the values obtained from the other two calibration methods discussed in this subsection.

Model calibration using combined respirometric-titrimetric measurements

Figure 4.9c-4.11c represents the model profiles that fit well with the experimental OURs and *Hp* observations where the combined respirometric-titrimetic data was used for the model calibration. The parameter estimation outcome is presented in Table 4.12. In this calibration method, the estimated model parameters including K_S (0.72-2.27 mg COD/L), f_{STO} (0.56-0.6), k_{STO} (2.55-3.45 day^{-1}), $\mu_{MAX,S}$ (1.58-1.82 day^{-1}), $Y_{H,S}$ (0.71) and Y_{STO} (0.88) are found in agreement with the respective parameters that were estimated using either respirometric data alone or titrimetric data alone (see Table 4.10-4.12) validating the proposed model.

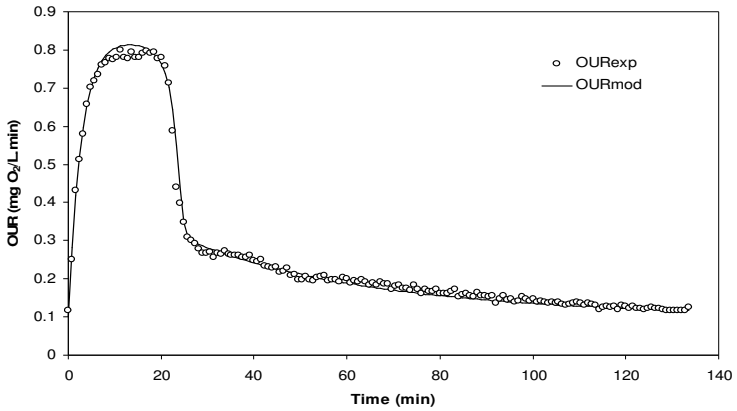

(a)

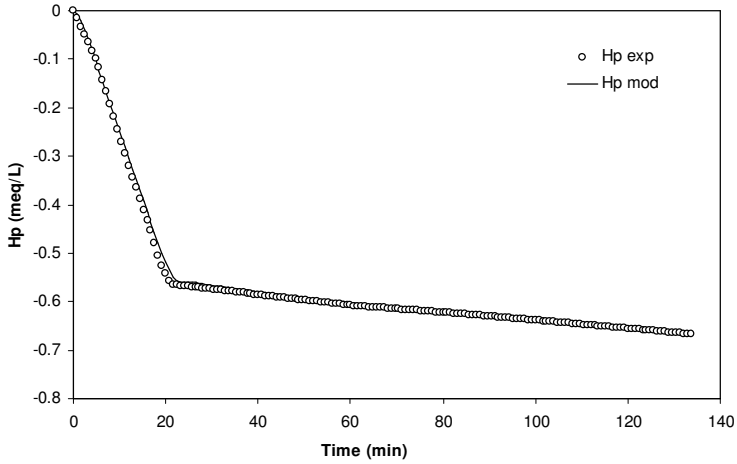

(b)

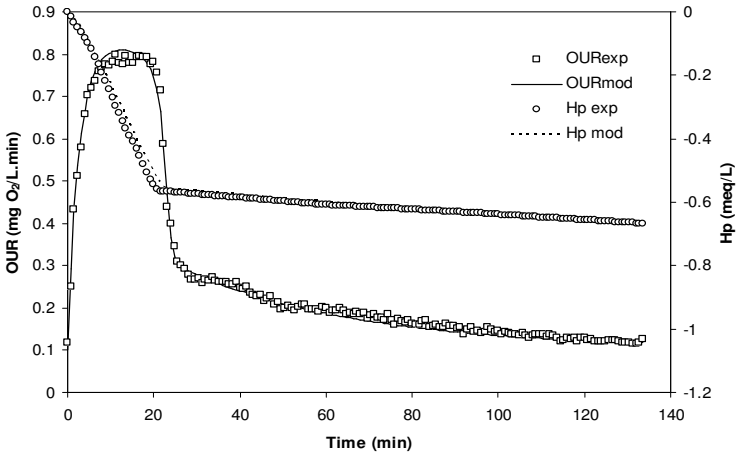

(c)

Figure 4.9: Model calibration using (a) respirometric data alone (b) titrimetric data alone and (c) combined respirometric-titrimetric data (acetate = 75 mg COD /L)

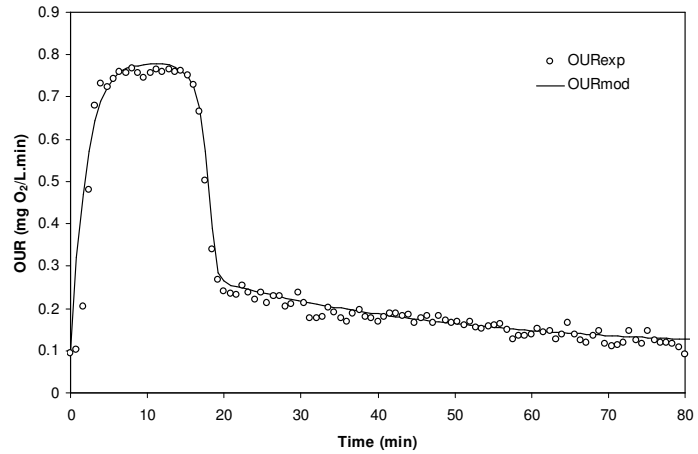

(a)

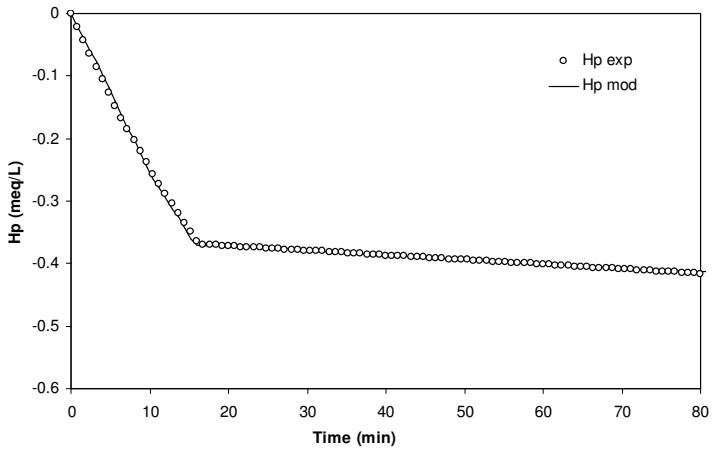

(b)

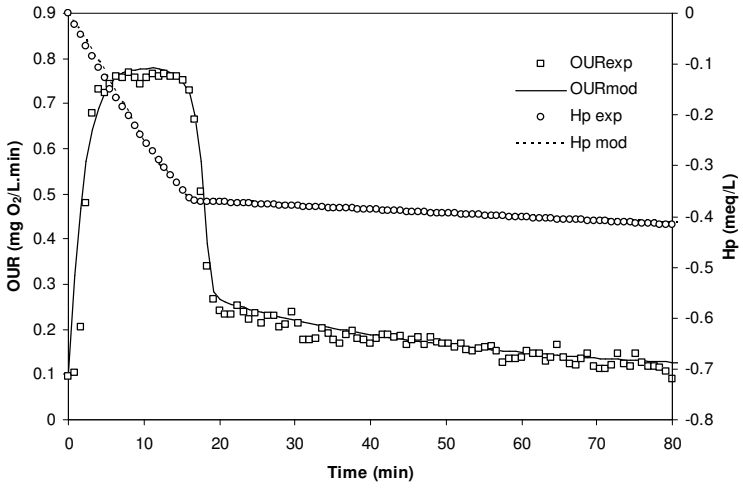

(c)

Figure 4.10: Model calibration using (a) respirometric data alone (b) titrimetric data alone and (c) combined respirometric-titrimetric data (acetate = 50 mg COD /L)

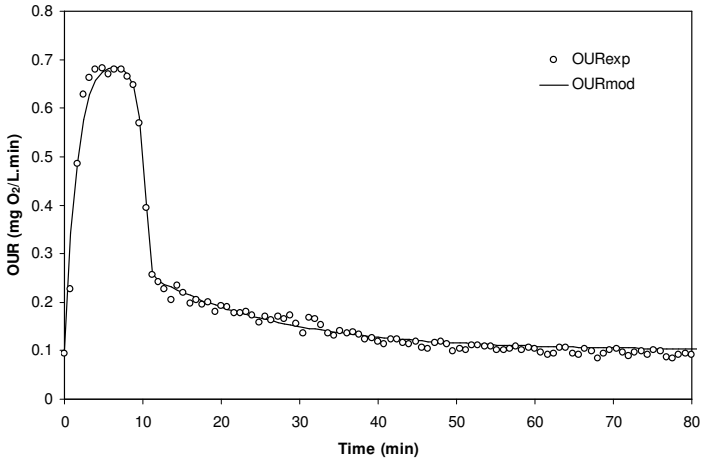

(a)

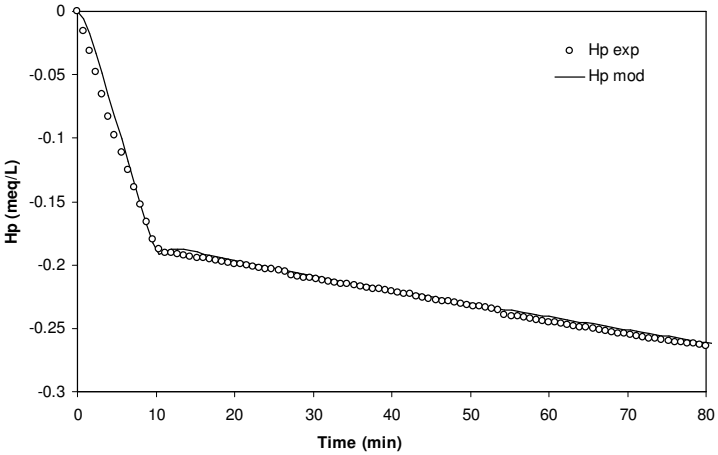

(b)

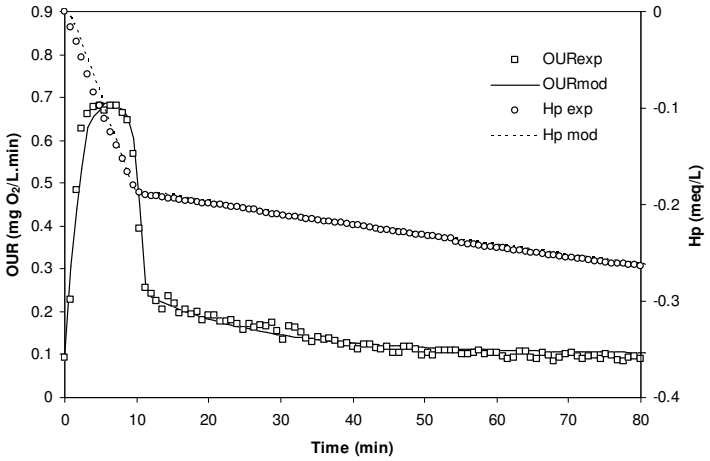

(c)

Figure 4.11: Model calibration using (a) respirometric data alone (b) titrimetric data alone and (c) combined respirometric-titrimetric data (acetate = 25 mg COD /L)

Table 4.10: Parameter estimation results using respirometric data alone for three different concentration studies (confidence intervals are shown in brackets as percentages)

Parameters	Acetate 75 mg COD/L (Confidence interval, %)	Acetate 50 mg COD/L (Confidence interval, %)	Acetate 25 mg COD/L (Confidence interval, %)
Parameters Estimated:			
q_{MAX} (1/min)	$0.0044 \pm 1.88\times10^{-5}$ (0. 43)	$0.0042 \pm 5.06\times10^{-5}$ (1.2)	$0.0035 \pm 2.85\times10^{-5}$ (0.81)
K_S (mgCOD/L)	2.27 ± 0.08 (3.52)	1.27 ± 0.131 (10.3)	0.73 ± 0.048 (6.58)
f_{STO} (mgCOD X_{STO}/mgCOD S_S)	0.6 ± 0.096 (16.00)	0.59 ± 0.049 (8.31)	0.56 ± 0.019 (3.39)
K_1 (mgCOD X_{STO}/mgCOD X_H)	0.065 ± 0.01 (15.38)	0.0506 ± 0.0063 (12.45)	0.023 ± 0.0014 (6.09)
K_2 (mgCOD X_{STO}/mgCOD X_H)	$5.0\times10^{-6} \pm 6.5\times10^{-6}$ (130.0)	$1.0\times10^{-7} \pm 1.7\times10^{-7}$ (170.0)	$2.8\times10^{-6} \pm 1.67\times10^{-6}$ (59.64)
δ (mol/mol)	4.20 ± 0.43 (10.24)	4.19 ± 0.229 (5.47)	4.11 ± 0.078 (1.9)
τ (min)	2.76 ± 0.03 (1.09)	2.5 ± 0.087 (3.48)	1.57 ± 0.035 (2.23)
Parameters Assumed:			
b_H (1/min)	0.000139	0.000139	0.000139
b_{STO} (1/min)	0.000139	0.000139	0.000139
f_{XI} (mgCOD /mgCOD)	0.2	0.2	0.2
Parameters Calculated:			
k_{STO} (1/min)	0.002325	0.002169	0.001728
$\mu_{MAX,S}$ (1/min)	0.001245	0.001228	0.001077
$\mu_{MAX,STO}$ (1/min)	0.001245	0.001228	0.001077
$Y_{H,S}$ (mgCOD X_H/mgCOD S_S)	0.71	0.71	0.70
$Y_{H,STO}$ (mgCOD X_H/mgCOD X_{STO})	0.78	0.78	0.78
Y_{STO} (mgCOD X_{STO}/mgCOD S_S)	0.88	0.88	0.88
X_H (mgCOD/L)	900	900	900
MSE[a]	2.2×10^{-4}	1.5×10^{-3}	2.84×10^{-4}

a MSE refers to the mean squared error which is calculated from sum of squared errors divided by number of observations

Table 4.11: Parameter estimation results using titrimetric data alone for three different concentration studies (confidence intervals are shown in brackets as percentages)

Parameters	Acetate 75 mg COD/L (Confidence interval, %)	Acetate 50 mg COD/L (Confidence interval, %)	Acetate 25 mg COD/L (Confidence interval, %)
Parameters Estimated:			
q_{MAX} (1/min)	$0.0045 \pm 8.10\times10^{-5}$ (1.8)	$0.0042 \pm 2.12\times10^{-4}$ (5.05)	$0.0036 \pm 3.24\times10^{-4}$ (9.0)
K_S (mgCOD/L)	2.27 ± 0.382 (16.83)	1.26 ± 0.141 (11.19)	0.72 ± 0.049 (6.8)
f_{STO} (mgCOD X_{STO}/mgCOD S_S)	0.6 ± 0.081 (13.5)	0.59 ± 0.039 (6.61)	0.56 ± 0.084 (15)
K_1 (mgCOD X_{STO}/mgCOD X_H)	0.053 ± 0.0063 (11.89)	0.051 ± 0.0129 (25.3)	0.02 ± 0.005 (25)
K_2 (mgCOD X_{STO}/mgCOD X_H)	$1.0\times10^{-8} \pm 2.51\times10^{-8}$ (251)	$1.1\times10^{-8} \pm 2.02\times10^{-8}$ (183.6)	$6.0\times10^{-8} \pm 1.9\times10^{-7}$ (316.7)
δ (mol/mol)	4.3 ± 0.55 (12.79)	4.3 ± 0.152 (3.53)	4.16 ± 0.788 (18.94)
τ (min)	2.06 ± 0.16 (7.77)	1.9 ± 0.41 (21.58)	1.95 ± 0.41 (21.03)
Parameters Assumed:			
b_H (1/min)	0.000139	0.000139	0.000139
b_{STO} (1/min)	0.000139	0.000139	0.000139
k_{NHacc} (1/min)	0.000056	0.000056	0.000056
f_{XI} (mgCOD /mgCOD)	0.2	0.2	0.2
k_1 [b] (1/min)	1.0762	1.0762	1.0762
K_La_{CO2} (1/min)	0.052	0.052	0.052
$C_{T,init}$ [b] (mmol/L)	1.8	1.8	2.25
Parameters Calculated:			
HCO_3 (mmol/L)	1.7323	1.7323	2.1654
CO_2 (mmol/L)	0.06771	0.06771	0.08463
k_{STO} (1/min)	0.0024	0.002185	0.001755
$\mu_{MAX,S}$ (1/min)	0.001265	0.001235	0.001124
$\mu_{MAX,STO}$ (1/min)	0.001265	0.001235	0.001124
$Y_{H,S}$ (mgCOD X_H/mgCOD S_S)	0.71	0.71	0.71
$Y_{H,STO}$ (mgCOD X_H/mgCOD X_{STO})	0.79	0.79	0.78
Y_{STO} (mgCOD X_{STO}/mgCOD S_S)	0.88	0.88	0.88
X_H (mgCOD/L)	900	900	900
MSE [a]	5.05×10^{-5}	6.14×10^{-5}	4.13×10^{-5}

[a] MSE refers to the mean squared error which is calculated from sum of squared errors divided by number of observations

[b] Parameters were estimated from separated calibration process using the titrimetric data under endogenous condition

Table 4.12: Parameter estimation results using combined respirometric-titrimetric data for three different concentration studies (confidence intervals are shown in brackets as percentages)

Parameters	Acetate 75 mg COD/L (Confidence interval, %)	Acetate 50 mg COD/L (Confidence interval, %)	Acetate 25 mg COD/L (Confidence interval, %)
Parameters Estimated:			
q_{MAX} (1/min)	$0.0045 \pm 3.85 \times 10^{-5}$ (0.86)	$0.0042 \pm 1.24 \times 10^{-4}$ (2.95)	$0.0036 \pm 8.03 \times 10^{-5}$ (2.23)
K_S (mgCOD/L)	2.27 ± 0.176 (7.75)	1.28 ± 0.352 (27.5)	0.72 ± 0.109 (15.14)
f_{STO} (mgCOD X_{STO}/mgCOD S_S)	0.6 ± 0.018 (3.0)	0.59 ± 0.079 (13.38)	0.56 ± 0.0199 (3.55)
K_1 (mgCOD X_{STO}/mgCOD X_H)	0.065 ± 0.0072 (11.08)	0.051 ± 0.0013 (2.55)	0.023 ± 0.004 (17.39)
K_2 (mgCOD X_{STO}/mgCOD X_H)	$4.0 \times 10^{-8} \pm 2.6 \times 10^{-8}$ (65)	$1.0 \times 10^{-8} \pm 1.02 \times 10^{-8}$ (102)	$3.97 \times 10^{-5} \pm 4.24 \times 10^{-5}$ (106.8)
δ (mol/mol)	4.3 ± 0.08 (1.86)	4.27 ± 0.332 (7.78)	4.16 ± 0.06 (1.44)
τ (min)	2.58 ± 0.07 (2.71)	2.1 ± 0.21 (10.0)	1.95 ± 0.1 (5.13)
Parameters Assumed:			
b_H (1/min)	0.000139	0.000139	0.000139
b_{STO} (1/min)	0.000139	0.000139	0.000139
k_{NHacc} (1/min)	0.000056	0.000056	0.000056
f_{XI} (mgCOD /mgCOD)	0.2	0.2	0.2
k_1[b]	1.0762	1.0762	1.0762
$K_L a_{CO2}$	0.052	0.052	0.052
$C_{T,init}$[b] (mmol/L)	1.8	1.8	2.25
Parameters Calculated:			
HCO_3 (mmol/L)	1.7326	1.7326	2.1657
CO_2 (mmol/L)	0.06740	0.06740	0.0842
k_{STO} (1/min)	0.002397	0.002177	0.001768
$\mu_{MAX,S}$ (1/min)	0.001263	0.001234	0.0011
$\mu_{MAX,STO}$ (1/min)	0.001263	0.001234	0.0011
$Y_{H,S}$ (mgCOD X_H/mgCOD S_S)	0.71	0.71	0.71
$Y_{H,STO}$ (mgCOD X_H/mgCOD X_{STO})	0.79	0.79	0.78
Y_{STO} (mgCOD X_{STO}/mgCOD S_S)	0.88	0.88	0.88
X_H (mgCOD/L)	900	900	900
MSE[a]	1.56×10^{-4}	0.0013	1.92×10^{-4}

[a] MSE refers to the mean squared error which is calculated from sum of squared errors divided by number of observations

[b] Parameters were estimated from separated calibration process using the titrimetric data under endogenous condition

Parameter estimation from endogenous study

A study of endogenous respiration for collected activated sludge was carried out prior to the commencement of the test substrate biodegradation process maintaining the pH of sludge at 7.8 ± 0.03. Three different assays such as assay 1, 2 and 3 were performed before dosing the sludge with 75, 50 and 25 mg COD/L of acetate respectively. The proposed model was calibrated using titrimetric measurements of the endogenous respiration process. Moreover, the model parameters, associated with titrimetric behavior, were estimated for all three assays which are presented in Table 4.13.

Figure 4.12 shows the representative model calibration result corresponding to assay 1. The parameter k_1 was estimated as 1.0762 min^{-1} for all assays which is similar to the value used by Sperandio and Paul (1997). However, the estimated value for total inorganic carbon in the aqueous medium, $C_{T,init}$ (2.25 mmol CO_2/L) under endogenous state (before dosing the acetate of 25 mg COD/L) was found to be higher than that for other two concentrations (1.8 mmol CO_2/L). It should be noted that the experiment for 25 mg COD/L acetate concentration was performed after finishing the run for 75 and 50 mg COD/L concentrations. As a result inorganic carbon accumulation may have taken place in the reactor resulting in a higher $C_{T,init}$ value.

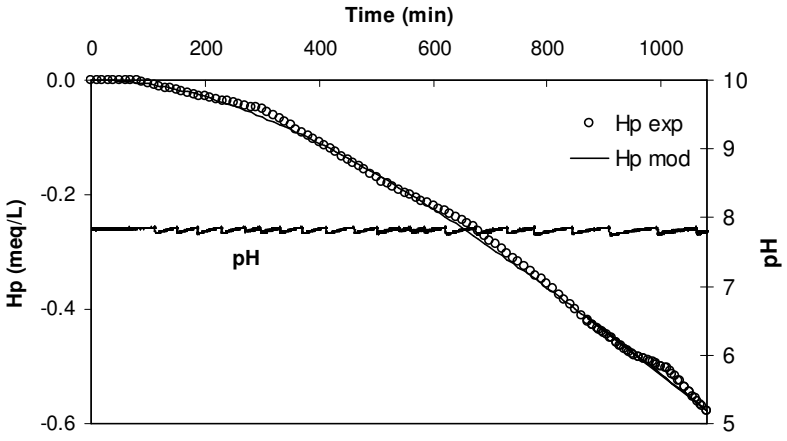

Figure 4.12: Model calibration with titrimetric measurements (at pH = 7.8) under endogenous conditions

Table 4.13: Estimated parameters under endogenous state (pH = 7.8)

Parameter	Estimated value		
	Assay 1	Assay 2	Assay 3
k_1 (min^{-1})	1.0762 ± 0.03	1.0762 ± 0.05	1.0762 ± 0.06
$C_{T,init}$ (mmol/L)	1.8 ± 0.06	1.8 ± 0.03	2.25 ± 0.05

4.5.3 Proposed model evaluation

Three different approaches for proposed SSAG model calibration: (a) titrimetric data alone, (b) respirometric data alone, and (c) combined respirometric titrimetric data, were followed in this current study with acetate pulses of 25, 50 and 75 mg COD/L. The estimated parameters are shown in tabular form (Table 4.10-4.12) along with parameter estimation errors calculated for 95% confidence intervals and mean squared error (MSE). The experimental data from titrimetry as well as respirometry were found to fit well during the model calibrations (Figure 4.9-4.11). In addition, the estimated parameters using titrimetric data alone gives almost the same values to the estimation from respirometry alone as well as from the combined approach which indicate the accuracy of the proposed model. Along with on-line measurements the proposed model was validated by following off-line methods where the acetate and ammonium in the liquid phase were monitored during the acetate oxidation period. Figure 4.13 illustrates the time profile study with model simulation that also validates the proposed SSAG model.

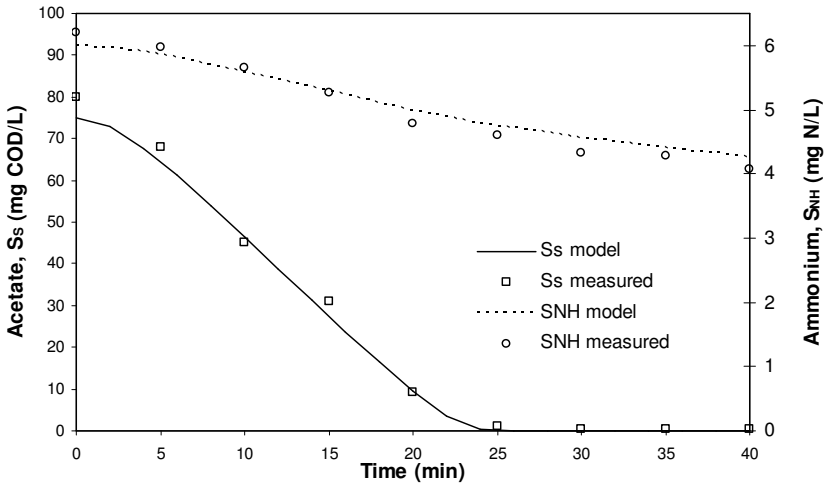

Figure 4.13: Model validation using off-line measurements for acetate (75 mg COD/L) biodegradation

The parameter k_{NHacc} was adjusted to 0.08 per day for better model calibration indicating a very slow nitrogen accumulation rate during the process. In addition, the biomass formula was assumed as $CH_{1.4}O_{0.65}N_{0.2}$ to achieve a good fit between model and experimental data during all three calibration approaches. Pratt et al. (2004) also noted that the best fit between measured and simulated data was obtained with the

assumption of a biomass formula of $CH_{1.87}O_{0.66}N_{0.17}$ during their model calibration study. However, the biomass composition should be determined experimentally where the biomass growth plays the most significant role. The degree of reduction of storage products, γ_{STO} was fixed to 4.6 for a better fit by considering the formula $CH_{1.4}O_{0.4}$. The i_{NBM} content corresponding to this biomass formula was calculated as 0.1 gN/g COD X_H, though the typical value for the nitrogen content of biomass was reported between the range 7% to 8.6% (Henze et al., 2000). Though the elemental composition of substrates, storage products and biomass are pre-requisites (in calculating the respective degree of reduction coefficient) for the titrimetric model development, the proposed SSAG model seems to explain well the acetate biodegradation by considering the dynamic CO_2 processes taking place in the biological system during the biodegradation process.

4.6 Applicability of proposed SSAG model at pH 7

The proposed SSAG model was calibrated with the respirometric and titrimetric measurements by maintaining a pH of 7.0 ± 0.03 in order to verify the applicability of the model. Two different initial concentrations of acetate, 50 and 75 mg COD/L, were used in batch experiments to investigate the aerobic biodegradation process. The compilation of experimental OUR and *Hp* profiles together shows the end of acetate degradation at approximately 30.5 and 21.2 minutes for acetate pulses of 75 and 50 mg COD/L respectively (Figure 4.14c and Figure 4.15c). Details of the model calibration and parameter estimation are discussed in the following sub-sections.

4.6.1 Parameter estimation strategy

Fresh sludge was collected to investigate the aerobic biodegradation of acetate at pH 7. Separate endogenous experiments were performed to estimate the titrimetric model parameters $C_{T,init}$ and k_1 to use them as default (fixed) value during exogenous titrimetric data interpretation (see Figure 4.16, Table 4.15, Table 4.16 and Table 4.17). As described in sub-section 4.5.1, seven model parameters q_{MAX}, K_S, f_{STO}, K_1, K_2, δ, and τ were estimated along with calculation of their confidence intervals. The parameters k_{STO}, $\mu_{MAX,S}$, $\mu_{MAX,STO}$, Y_{STO}, $Y_{H,S}$, $Y_{H,STO}$ and $X_H(0)$ were calculated following the same procedure as discussed in sub-section 4.5.1 All of the assumptions for respective parameters were kept as same as in the pH 7.8 study

including the elemental composition of different components (see sub-section 4.5.1 for details). The titrimetric data alone was applied to estimate the model parameters initially that was followed by the parameter estimation process using respirometric data alone and combined respirometric-titrimetric data. Finally the parameter estimation results were compared for the model validation.

4.6.2 Discussion on model calibration and parameter estimation

Parameter estimation for acetate biodegradation

The proposed model successfully applied for acetate biodegradation at pH 7 and the model was found to fit well with experimental respirometric-titrimetric measurements obtained from acetate dosages of 75 and 50 mg COD/L to the activated sludge (Figure 4.14 and Figure 4.15). The parameter estimation results from the three calibration approaches: using respirometric data alone, titrimetric data alone and combined respirometric-titrimetric data, are presented in Table 4.14, Table 4.15 and Table 4.16 respectively with parameter estimation errors calculated for 95% confidence intervals and MSE for each concentration study.

The estimated substrate affinity constant, K_S, lies between 0.91 and 0.92 mg COD/L using all three model calibration approaches. In addition, the estimated parameter f_{STO} ranges from 0.76 to 0.77 indicating significant storage during the biodegradation process. The calculated maximum biomass growth rate, $\mu_{MAX,S}$ ranges from 1.17 to 1.22 day^{-1} and from 1.15 to 1.19 day^{-1} for acetate concentrations of 75 and 50 mg COD/L respectively. On the other hand, the storage uptake rates calculated from both concentrations study are noteworthy (4.6-4.81 day^{-1}) when compared to the biomass in the activated sludge used for the pH 7.8 study. The average yield coefficients $Y_{H,S}$, $Y_{H,STO}$ and Y_{STO} were calculated as 0.73, 0.8 and 0.89 respectively (Table 4.14-4.16).

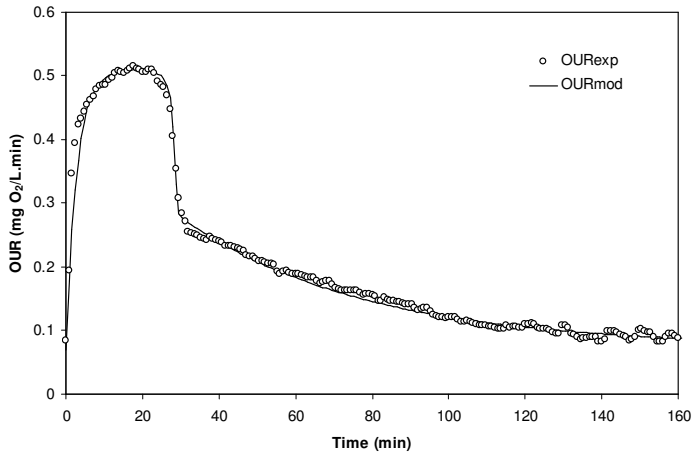

(a)

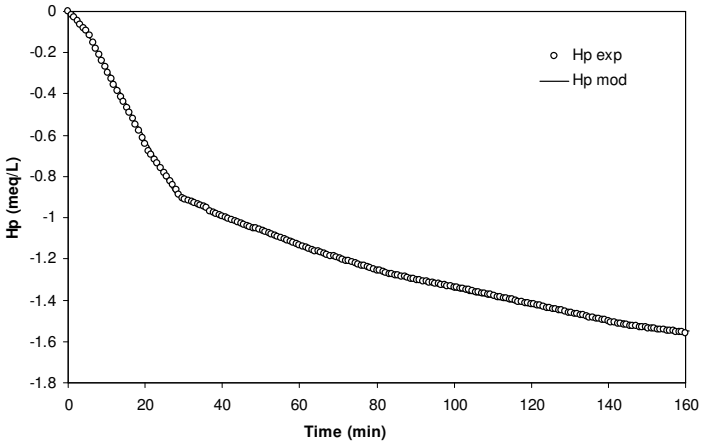

(b)

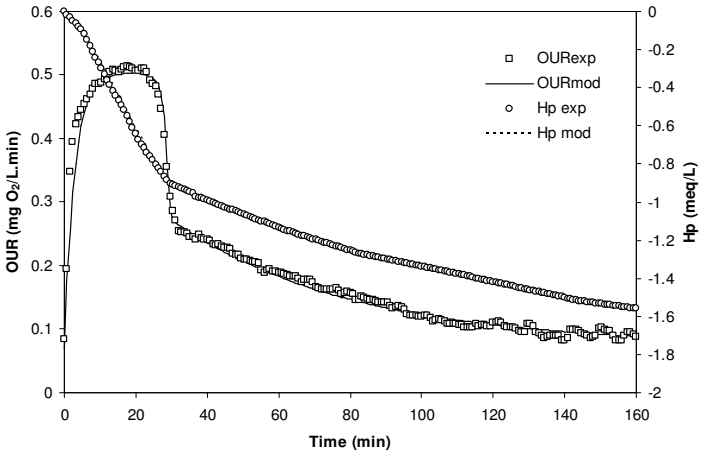

(c)

Figure 4.14: Model calibration for pH 7 using (a) respirometric data alone (b) titrimetric data alone and (c) combined respirometric-titrimetric data (acetate = 75 mg COD /L)

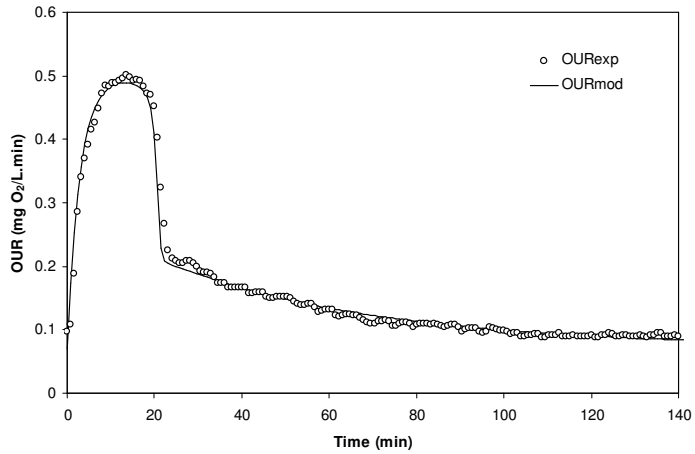

(a)

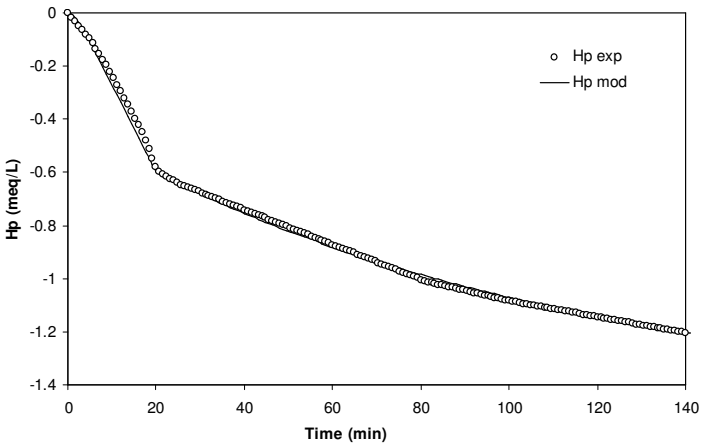

(b)

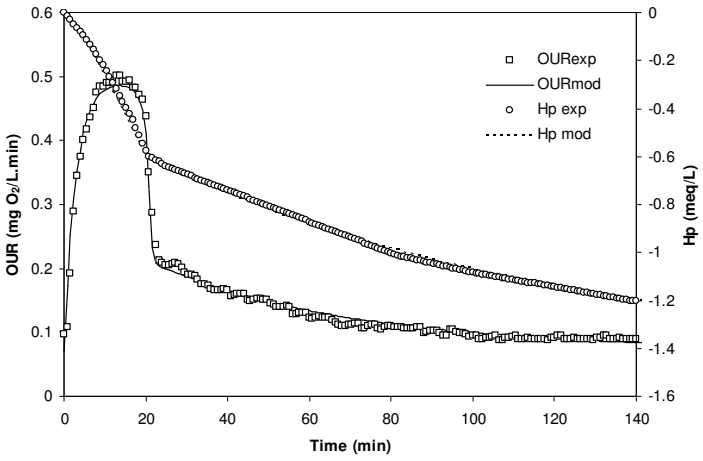

(c)

Figure 4.15: Model calibration for pH 7 using (a) respirometric data alone (b) titrimetric data alone and (c) combined respirometric-titrimetric data (acetate = 50 mg COD /L)

Table 4.14: Parameter estimation results (for pH 7) using respirometric data alone for two different concentration studies (confidence intervals are shown in brackets as percentages)

Parameters	Acetate 75 mg COD/L (Confidence interval, %)	Acetate 50 mg COD/L (Confidence interval, %)
Parameters Estimated:		
q_{MAX} (1/min)	$0.0048 \pm 1.64 \times 10^{-5}$ (0. 34)	$0.0047 \pm 3.07 \times 10^{-5}$ (0.65)
K_S (mgCOD/L)	0.92 ± 0.05 (5.43)	0.92 ± 0.061 (6.63)
f_{STO} (mgCOD X_{STO}/mgCOD S_S)	0.76 ± 0.019 (2.5)	0.76 ± 0.031 (4.08)
K_1 (mgCOD X_{STO}/mgCOD X_H)	0.05 ± 0.004 (8.0)	0.05 ± 0.0074 (14.8)
K_2 (mgCOD X_{STO}/mgCOD X_H)	$4.0 \times 10^{-5} \pm 1.8 \times 10^{-5}$ (45.0)	$4.0 \times 10^{-5} \pm 2.1 \times 10^{-5}$ (52.5)
δ (mol/mol)	4.7 ± 0.11 (2.34)	4.68 ± 0.173 (3.7)
τ (min)	2.8 ± 0.03 (1.07)	2.85 ± 0.053 (1.86)
Parameters Assumed:		
b_H (1/min)	0.000139	0.000139
b_{STO} (1/min)	0.000139	0.000139
f_{XI} (mgCOD /mgCOD)	0.2	0.2
Parameters Calculated:		
k_{STO} (1/min)	0.003311	0.003204
$\mu_{MAX,S}$ (1/min)	0.000837	0.000829
$\mu_{MAX,STO}$ (1/min)	0.000837	0.000829
$Y_{H,S}$ (mgCOD X_H/mgCOD S_S)	0.73	0.73
$Y_{H,STO}$ (mgCOD X_H/mgCOD X_{STO})	0.8	0.8
Y_{STO} (mgCOD X_{STO}/mgCOD S_S)	0.89	0.89
X_H (mgCOD/L)	630	630
MSE[a]	5.4×10^{-4}	8.16×10^{-4}

a MSE refers to the mean squared error which is calculated from sum of squared errors divided by number of observations

The similar elemental composition of biomass ($CH_{1.4}O_{0.65}N_{0.2}$) and storage products ($CH_{1.4}O_{0.4}$) as used for pH 7.8 study (see sub-section 4.5.3) were assumed here as well to achieve a good fit between model and experimental measurements. The i_{NBM} content was calculated as 0.1 gN/g COD X_H using respective biomass formula, whereas the typical value for the nitrogen content of biomass was reported between the range 7% to 8.6% (Henze et al., 2000). In addition, the degree of reduction of storage products, γ_{STO} was fixed to 4.6 for a better fit by considering the composition of respective storage products.

Table 4.15: Parameter estimation results (for pH 7) using titrimetric data alone for two different concentration studies (confidence intervals are shown in brackets as percentages)

Parameters	Acetate 75 mg COD/L (Confidence interval, %)	Acetate 50 mg COD/L (Confidence interval, %)
Parameters Estimated:		
q_{MAX} (1/min)	$0.0049 \pm 9.02 \times 10^{-5}$ (1.84)	$0.0048 \pm 3.4 \times 10^{-4}$ (7.08)
K_S (mgCOD/L)	0.91 ± 0.0379 (4.16)	0.92 ± 0.083 (9.02)
f_{STO} (mgCOD X_{STO}/mgCOD S_S)	0.76 ± 0.029 (3.82)	0.77 ± 0.051 (6.62)
K_1 (mgCOD X_{STO}/mgCOD X_H)	0.052 ± 0.0029 (5.58)	0.05 ± 0.0097 (19.4)
K_2 (mgCOD X_{STO}/mgCOD X_H)	$8.96 \times 10^{-5} \pm 8.92 \times 10^{-8}$ (99.56)	$4.0 \times 10^{-5} \pm 5.1 \times 10^{-5}$ (127.5)
δ (mol/mol)	4.7 ± 0.25 (5.32)	4.7 ± 0.563 (11.97)
τ (min)	2.8 ± 0.16 (5.71)	2.85 ± 0.48 (16.8)
Parameters Assumed:		
b_H (1/min)	0.000139	0.000139
b_{STO} (1/min)	0.000139	0.000139
k_{NHacc} (1/min)	9.25×10^{-7}	9.25×10^{-7}
f_{XI} (mgCOD /mgCOD)	0.2	0.2
k_1 [b] (1/min)	1.0762	1.0762
$K_L a_{CO2}$ (1/min)	0.052	0.052
$C_{T,init}$ [b] (mmol/L)	1.05	1.1
Parameters Calculated:		
HCO_3 (mmol/L)	0.8423	0.8824
CO_2 (mmol/L)	0.2077	0.2176
k_{STO} (1/min)	0.003343	0.00328
$\mu_{MAX,S}$ (1/min)	0.000849	0.000799
$\mu_{MAX,STO}$ (1/min)	0.000849	0.000799
$Y_{H,S}$ (mgCOD X_H/mgCOD S_S)	0.73	0.73
$Y_{H,STO}$ (mgCOD X_H/mgCOD X_{STO})	0.8	0.8
Y_{STO} (mgCOD X_{STO}/mgCOD S_S)	0.89	0.89
X_H (mgCOD/L)	630	630
MSE [a]	7.03×10^{-5}	2.38×10^{-4}

[a] MSE refers to the mean squared error which is calculated from sum of squared errors divided by number of observations

[b] Parameters were estimated from separated calibration process using the titrimetric data under endogenous condition

Table 4.16: Parameter estimation results (for pH 7) using combined respirometric-titrimetric data for two different concentration studies (confidence intervals are shown in brackets as percentages)

Parameters	Acetate 75 mg COD/L (Confidence interval, %)	Acetate 50 mg COD/L (Confidence interval, %)
Parameters Estimated:		
q_{MAX} (1/min)	$0.0048 \pm 3.7 \times 10^{-5}$ (0.77)	$0.0047 \pm 8.05 \times 10^{-5}$ (1.71)
K_S (mgCOD/L)	0.91 ± 0.063 (6.92)	0.92 ± 0.081 (8.8)
f_{STO} (mgCOD X_{STO}/mgCOD S_S)	0.77 ± 0.015 (1.95)	0.76 ± 0.02 (2.63)
K_1 (mgCOD X_{STO}/mgCOD X_H)	0.051 ± 0.0036 (7.06)	0.05 ± 0.0093 (18.6)
K_2 (mgCOD X_{STO}/mgCOD X_H)	$4.1 \times 10^{-5} \pm 2.9 \times 10^{-5}$ (70.73)	$4.0 \times 10^{-5} \pm 5.2 \times 10^{-5}$ (130)
δ (mol/mol)	4.7 ± 0.1 (2.13)	4.7 ± 0.26 (5.53)
τ (min)	2.83 ± 0.09 (3.18)	2.85 ± 0.16 (5.61)
Parameters Assumed:		
b_H (1/min)	0.000139	0.000139
b_{STO} (1/min)	0.000139	0.000139
k_{NHacc} (1/min)	9.25×10^{-7}	9.25×10^{-7}
f_{XI} (mgCOD /mgCOD)	0.2	0.2
k_1 [b]	1.0762	1.0762
$K_L a_{CO2}$	0.052	0.052
$C_{T,init}$ [b] (mmol/L)	1.05	1.1
Parameters Calculated:		
HCO_3 (mmol/L)	0.8423	0.8832
CO_2 (mmol/L)	0.2077	0.2168
k_{STO} (1/min)	0.003296	0.003192
$\mu_{MAX,S}$ (1/min)	0.000812	0.000827
$\mu_{MAX,STO}$ (1/min)	0.000812	0.000827
$Y_{H,S}$ (mgCOD X_H/mgCOD S_S)	0.73	0.73
$Y_{H,STO}$ (mgCOD X_H/mgCOD X_{STO})	0.8	0.8
Y_{STO} (mgCOD X_{STO}/mgCOD S_S)	0.89	0.89
X_H (mgCOD/L)	630	630
MSE[a]	9.25×10^{-5}	2.15×10^{-4}

[a] MSE refers to the mean squared error which is calculated from sum of squared errors divided by number of observations

[b] Parameters were estimated from separated calibration process using the titrimetric data under endogenous condition

Parameter estimation from endogenous study

The calibration result with titrimetric measurements under endogenous conditions is presented in Figure 4.16 where the sludge was maintained at a pH of 7 ± 0.03. Similar to the procedure described in sub-section 4.5.2, two assays were conducted prior to the acetate biodegradation study to estimate the titrimetric model parameters which are shown in Table 4.17 along with parameter estimation errors. Assay 1 was performed for investigating the endogenous respiration before adding acetate with the initial concentration of 75 mg COD/L, whereas assay 2 was done prior to the dosing of 50 mg COD/L acetate to the activated sludge. For all assays the parameter

k_1 was estimated as 1.0762 min^{-1} which is similar to the value used by Sperandio and Paul (1997). The total inorganic carbon in the aqueous medium, $C_{T,init}$ was estimated as 1.05 and 1.1 mmol CO_2/L for assays 1 and 2 respectively.

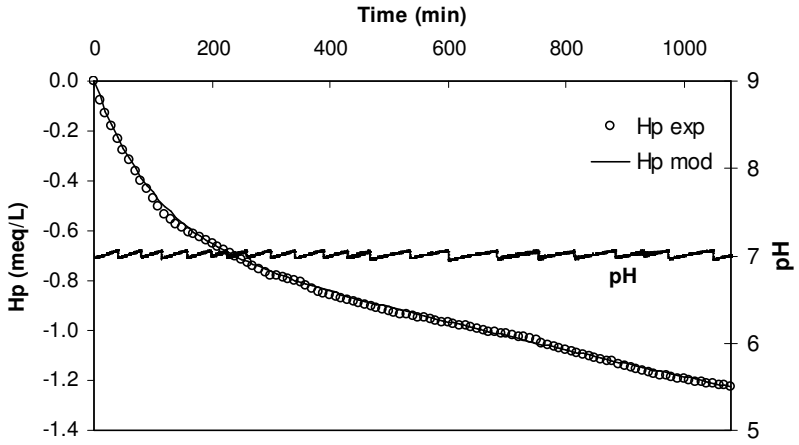

Figure 4.16: Model calibration with titrimetric measurements (at pH = 7.0) under endogenous conditions

Table 4.17: Estimated parameters under endogenous state (pH = 7)

Parameter	Estimated value	
	Assay 1	Assay 2
k_1 (min^{-1})	1.0762 ± 0.01	1.0762 ± 0.05
$C_{T,init}$ (mmol/L)	1.05 ± 0.07	1.1 ± 0.02

4.6.3 Comparison of estimated parameters between two different pH

Figure 4.17 demonstrates the relative values of five important model parameters that were estimated during the pH 7.8 and the pH 7 study with an acetate pulse of 50 mg COD/L. The average value of the parameter K_S was estimated as 1.27 and 0.92 mg COD/L for the pH 7.8 and 7 respectively. The parameter $\mu_{MAX,S}$ varies from 1.76-1.78 day^{-1} at pH 7.8 and it falls within the range 1.15-1.19 day^{-1} when the pH is maintained at 7. As a result the acetate removal was faster (t = 17.1 min) for the pH 7.8, while the acetate degradation time was approximately 21.2 min when the pH of the activated sludge was maintained at 7 (Figure 4.18). The study also reveals the

parameters that are sensitive to storage phenomena (f_{STO}, k_{STO}, δ) have higher estimated values at pH 7 compared with those for pH 7.8 indicating a significant formation of storage products in the biomass cell during the acetate biodegradation process.

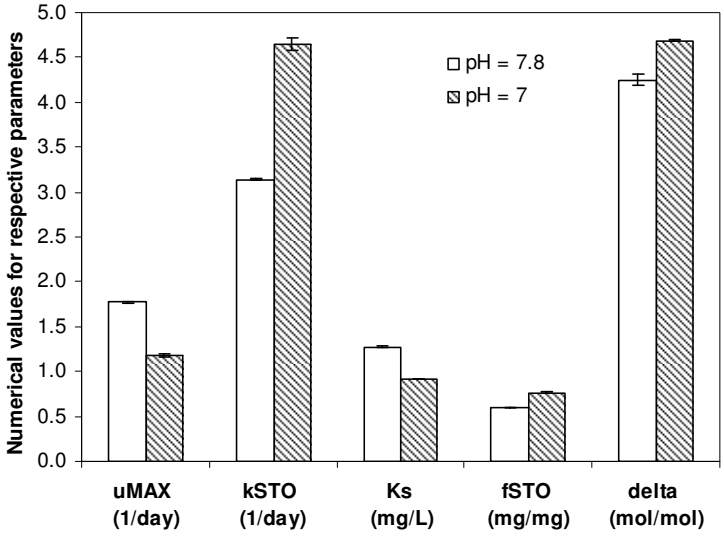

Figure 4.17: Comparison of model parameters for two different pH levels of sludge (acetate = 50 mg COD/L)

Figure 4.18 represents the specific OUR_{exo} for the pH 7.8 and the pH 7 study with acetate pulses of 50 mg COD/L to the activated sludge. The experimental observation shows the peak OUR decreases remarkably for pH 7 and the tail part becomes significant compared with pH 7.8. Guisasola et al. (2005) in their study found the peak of OUR increases with reduced tail for the increase of the percentage of the acetate used directly for growth that supports our findings (Figure 4.18). The peak of OUR at pH 7 is influenced not only by the parameter $\mu_{MAX,S}$ but is also due to increase of the parameters f_{STO} and δ that plays significant role to reduce the peak OUR that can be examined from model simulation. Based on parameters such as maximum growth rate and biodegradation period, pH 7.8 seems to be more favorable for successful biodegradation within a shorter time (Figure 4.18). As there is little evidence in the literature that pH variation impacts on acetate biodegradation and subsequent modeling, the distinctive characteristics of activated sludge collected from the plant at different periods of time for the pH 7.8 and the pH 7 study, may have contributed to variations in experimental observations and derived parameters.

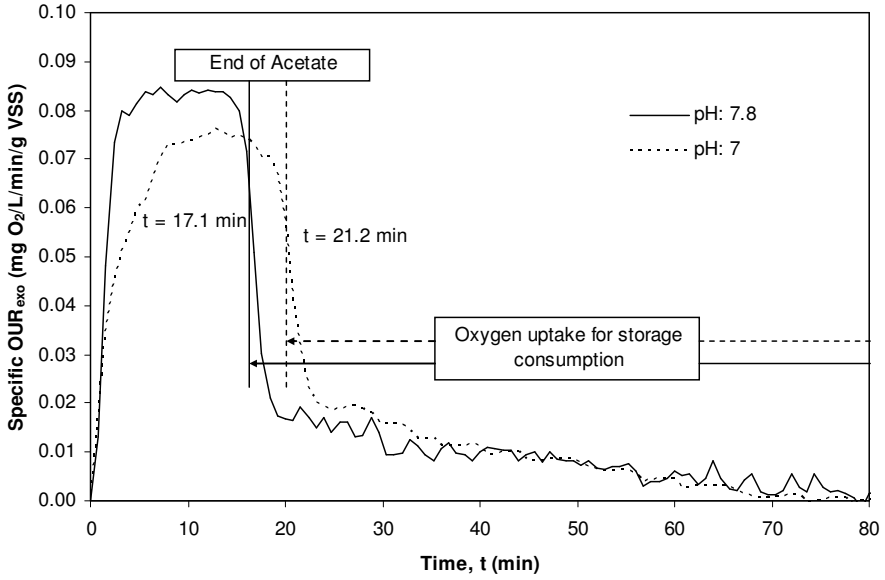

Figure 4.18: Specific OURs during acetate (50 mg COD/L) biodegradation for the pH of 7.8 and pH of 7

4.7 Monod kinetics for acetate biodegradation

Monod parameters were estimated from the aerobic biodegradation of acetate in an activated sludge system with different pH values. Monod profile was plotted for the maximum biomass growth rate using the relationship, $\mu_{MAX} = \mu_{MAX,S}.S_S/(K_S+S_S)$. Here, the biomass growth rate, μ_{MAX} is a function of the substrate concentration (S_S). Figure 4.19 represents the estimated biomass growth rate for different acetate concentrations (S_S) along with the Monod curve for the pH values of 7.8 and 7 showing the coefficient of determination (R^2) of 0.95 and 0.97 respectively. Non-linear parameter estimation technique was applied for the determination of Monod parameters. The estimated parameters K_S and $\mu_{MAX,S}$ were 0.84 mg COD/L and 1.81 day^{-1} respectively when the pH was 7.8, whereas the estimated parameters were 0.76 mg COD/L and 1.21 day^{-1} respectively when the pH was maintained at 7 (Table 4.18). While the ASM3 prescribed the default value for the parameter K_S as 2.0 mg COD/L, Sin et al. (2005) estimated the parameter ranges from 0.6 to 0.67 mg COD/L when the pH was maintained at 7.8. The result shows a higher biomass growth rate at pH 7.8 compared with that at pH 7 indicating faster acetate biodegradation in the sludge used for pH 7.8 study (Figure 4.19). However, it can not be concluded that the

biomass growth increases when the pH is slightly alkaline, as there are several parameters that may affect the process kinetics such as the sludge composition and operating system of the treatment plants from where the sludge is collected for the study (Hoque et al., 2009b). No significant research was found in the literature with respect to bio-kinetics for acetate biodegradation in activated sludge at different pH levels. Sin and Vanrolleghem (2007) calibrated the ASM1 model where the pH (7.7) was slightly lower than 7.8, resulting in a higher value for the estimated parameter $\mu_{MAX,S}$ (3.4 day^{-1}) compared with SSAG phenomena since storage was completely excluded in ASM1 model. However, the SSAG model proposed by Sin et al. (2005) gives the $\mu_{MAX,S}$ range from 0.72 to 1.3 day^{-1} for pH 7.8 which is consistent with current estimation result.

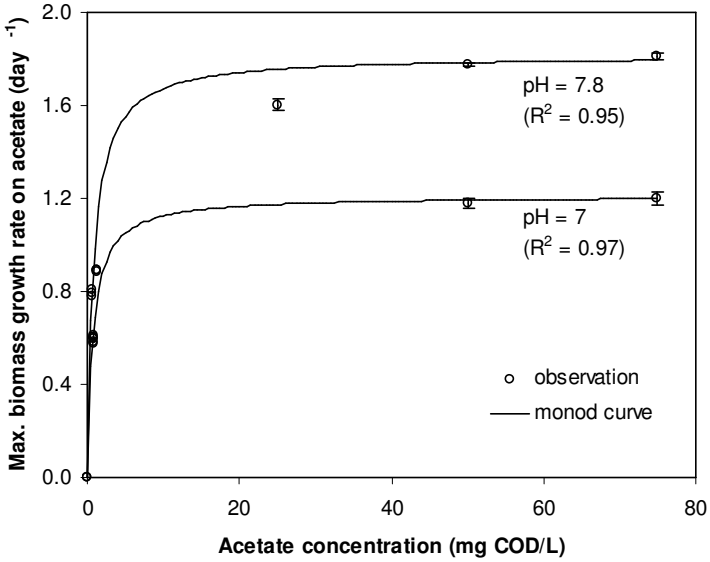

Figure 4.19: Monod profile for maximum biomass growth rate on acetate at different pH levels

Table 4.18: Estimated Monod kinetics for acetate biodegradation at different pH levels

Parameter	pH = 7.8	pH = 7
K_S (mg COD/L)	$0.84 \pm 1.27 \times 10^{-3}$	0.76 ± 0.008
$\mu_{MAX,S}$ (day^{-1})	$1.81 \pm 7.7 \times 10^{-4}$	$1.21 \pm 4 \times 10^{-4}$

4.8 Conclusions

The assessment of several activated sludge models reveals that the SSAG model represents well the experimentally derived respirometric measurements for acetate biodegradation. The SSAG model was improved by introducing stoichiometric parameters involving in titrimetry in each step of the growth and storage phases along with the inclusion of a non-linear carbon dioxide transfer rate in the liquid phase. The proposed SSAG model was successfully calibrated for different initial acetate concentrations and pH levels of the sludge. Parameter estimation using three different calibration approaches was also found to be satisfactory and show very close results that validates the proposed model. In addition, off-line measurements of COD and ammonium concentration in the liquid phase confirm the accuracy of the model. The Monod kinetics estimated from the acetate biodegradation process shows a better growth rate of biomass at pH 7.8 compared with pH 7 indicating faster acetate oxidation in an activated sludge system.

Chapter 5
Modeling of Surfactant Biodegradation

5.1 Introduction

Sodium dodecyl sulfate (SDS) is an anionic surfactant commonly used in household products such as toothpastes, shampoos, shaving foams and bubble baths (Swisher, 1987). The chemical composition of sodium dodecyl sulfate is: $C_{12}H_{25}SO_4Na$ (molecular weight: 288.38). In this current study, SDS has been selected as a slowly biodegradable organic carbon source that has a relatively more complex chemical structure than a biodegradable organic carbon such as acetate. Combined respirometric-titrimetric measurements were conducted in the laboratory using activated sludge with varying initial SDS concentrations and pH levels. This chapter focuses on a bio-kinetic model that explains the surfactant biodegradation behavior and that was calibrated successfully with both respirometric and titrimetric measurements. It further discusses the estimated parameters obtained from three different calibration approaches: on-line respirometric measurements alone, titrimetric measurements alone and combined respirometric-titrimetric measurements, and compares them for the model validation. The model was also validated using off-line measurements. The proposed model was evaluated for three different concentrations of surfactant along with different pH values. Calibration and parameter estimation results have been discussed in this chapter using logical and statistical approaches for proper evaluation of the proposed model. Monod kinetic parameters for surfactant biodegradation were also determined and compared to that for acetate biodegradation in activated sludge.

5.2 Experimental observations on surfactant biodegradation

Activated sludge was acclimatized with the anionic surfactant, SDS, for about 15 days before starting the main experimental work in order to allow the microorganisms to perform at their optimum capacity. Batch experiments with varying initial concentrations of 50, 75 and 100 mg COD/L were performed to investigate the influence of initial concentrations on the SDS biodegradation process

where pH was maintained at 7.8 ± 0.03. Furthermore, the effect of pH on SDS biodegradation was investigated by feeding a constant SDS concentration of 75 mg COD/L to the activated sludge with three different pH levels of 7, 7.8 and 8.5 during the study.

The dissolved oxygen profile for a SDS pulse of 100 mg COD/L is shown in Figure 5.1 along with the titrimetric measurements where the pH was maintained at 7.8. Observation reveals that DO was reduced drastically soon after the SDS was added into the system and continued to decrease until all the SDS was completely removed from the liquid medium. This is followed by a long tail showing a gradual increase of DO to reach a steady state equilibrium level. The titrimetric observation shows that base addition takes place during the exogenous period, representing the removal of SDS from the liquid medium through oxidation, followed by acid addition during the endogenous phase of the biodegradation process. Acid addition was also observed when a separate assay for the endogenous respiration was performed maintaining the pH at 7.8 (see section 4.2 in Chapter 4).

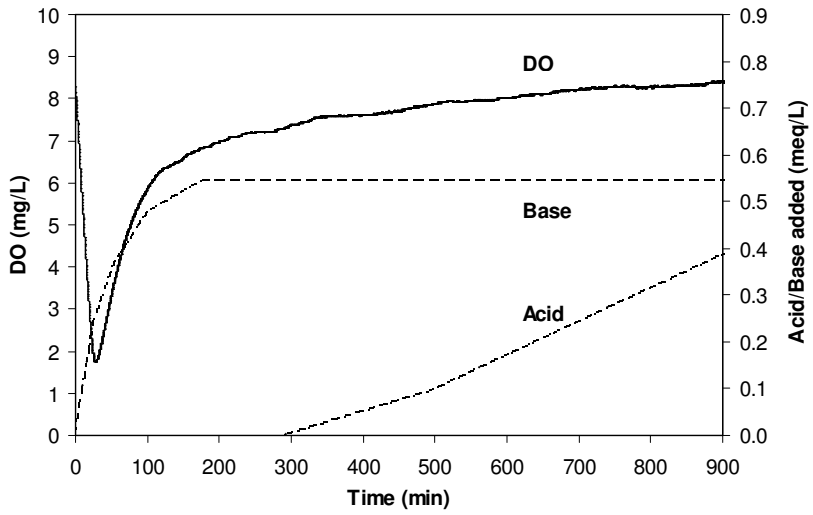

Figure 5.1: Dissolved oxygen and titrimetric measurements collected from the titrimetric respirometer for the SDS pulse of 100 mg COD/L

The OUR profiles corresponding to the SDS concentrations of 50, 75 and 100 mg COD/L at time t=0 are presented in Figure 5.2 with the titrimetric measurements. The OUR increases to a maximum level due to the consumption of SDS under the

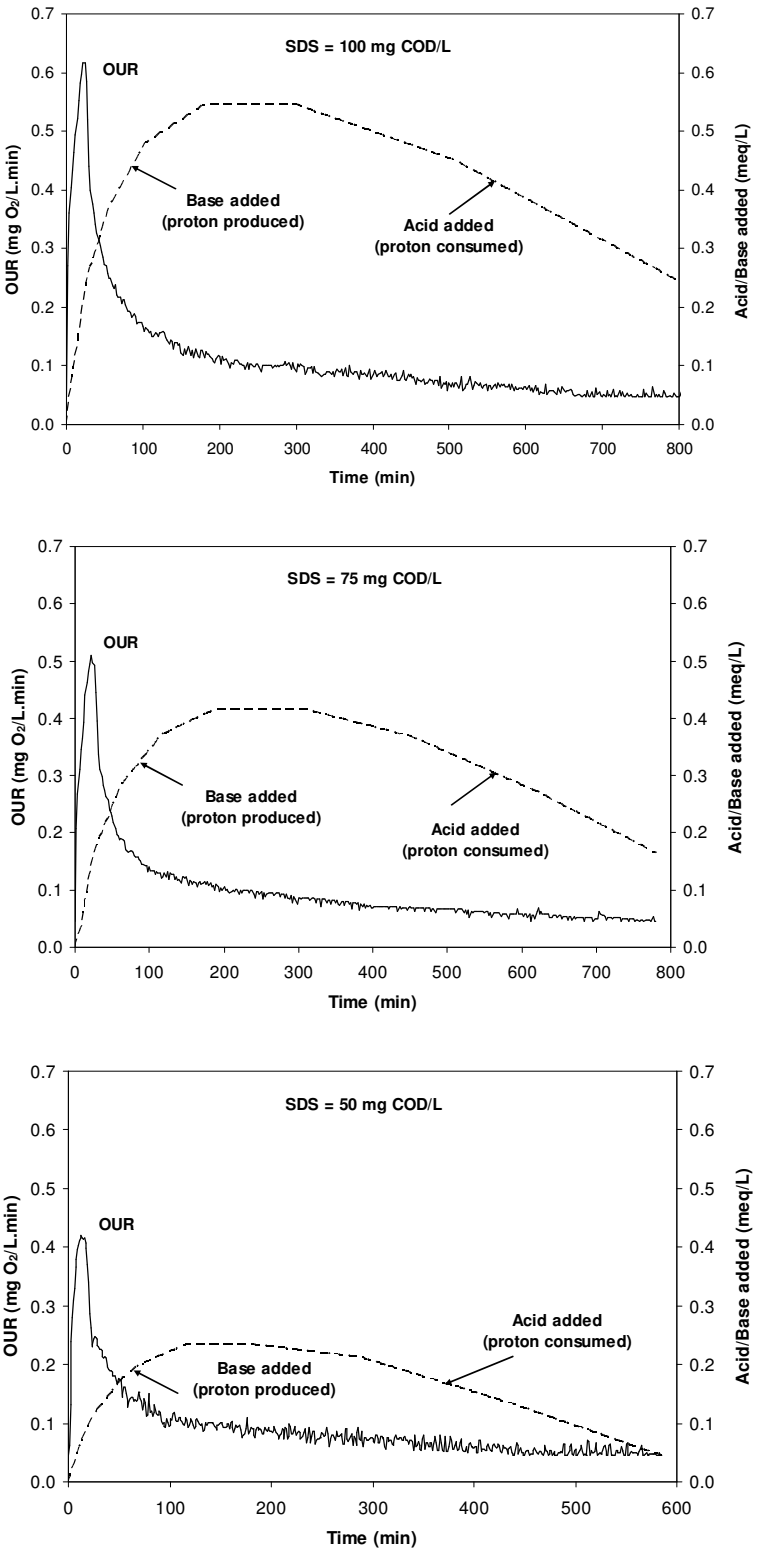

Figure 5.2: OUR with titrimetric profiles for three different SDS concentrations in an activated sludge system

feast period, then drops to a level higher than the endogenous OUR level followed by a gradual declination until it reaches the endogenous level. A similar pattern was also observed in the acetate biodegradation study, in which the consumption of previously stored products occurred, resulting in a tail in the OUR profile (Van Loosdrecht et al., 1997; Van Loosdrecht and Heijnen 2002; Guisasola et al., 2005; Sin et al., 2005). In case of SDS, the tail part of the OUR is found to be much more prominent compared to that for the acetate biodegradation study, indicating a significant influence of storage products in the overall biodegradation process. It is noteworthy that three successive trials were made in each initial concentration study to ensure the reproducibility of the experimental results. The area under the OUR profiles were calculated to evaluate short-term BOD_{st} for respective SDS concentrations. Figure 5.3 represents the outcomes obtained from different trials in terms of short-term BOD (BOD_{st}) and their corresponding standard deviations (SDs) for different initial SDS concentrations .

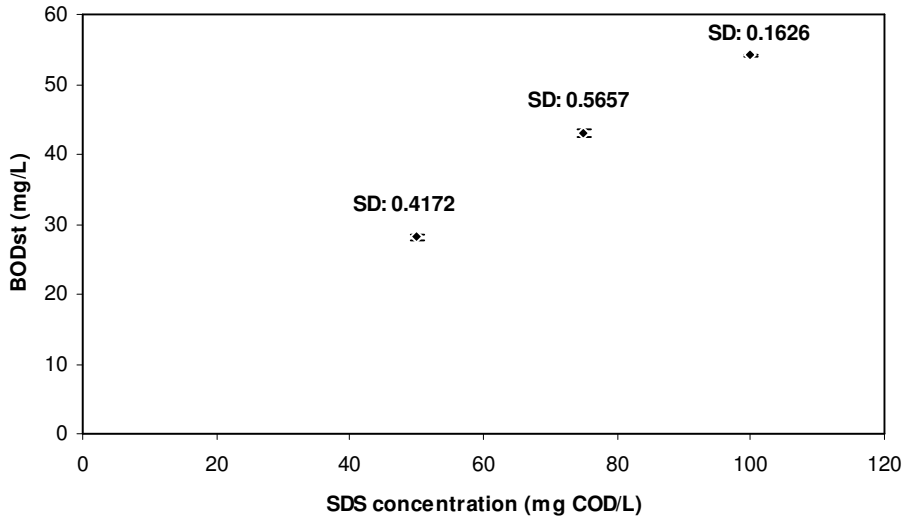

Figure 5.3: Short-term BOD obtained from different initial SDS concentration studies

In addition to oxygen consumption, SDS biodegradation results in base addition to the reactor under exogenous state where the cumulative pulses are proportionally increased with the initial concentration (Figure 5.2). Base addition in the reactor represents the proton production in the system which is the net result of SDS and ammonia uptake, endogenous respiration and the CO_2 production as described in

sub-section 5.3.2. Figure 5.2 depicts that the base addition profile has a steeper slope until the OUR reaches its maximum level. This is followed by a mild base pulse rate that represents the oxidization of respective intermediate products (see the sub-section 5.3.1 for the SDS biodegradation pathway). The CO_2 stripping leads to a drop in the titrimetric profile to the background proton consumption (acid addition) rate which was also observed before adding SDS to the reactor when pH was maintained at 7.8. However, distinctive experimental results were observed during the different pH studies conducted with a constant SDS concentration in the system. Figure 5.4 shows the *Hp* profiles for three different pH studies with a SDS concentration of 75 mg COD/L in the activated sludge. The profiles indicate that the SDS biodegradation process is pH sensitive. Though similar pattern of OUR profiles was observed for the three different pH studies, the titrimetric profile for SDS biodegradation was found to be different for different pH levels. In fact, the titrimetric profile is the net result of proton generation/consumption taking place in each step of the aerobic biodegradation processes such as hydrolysis, the formation of storage products, aerobic growth on the substrate, aerobic growth on the storage, endogenous respiration, respiration on storage products, aqueous CO_2 equilibrium and stripping of CO_2. However, the pH of the liquid medium is highly influenced by the stripping of CO_2 and aqueous CO_2 equilibrium processes that govern the net proton production in the system and cause different titrimetric profiles, even though the initial substrate concentration for different pH studies was same.

While proton production was observed throughout the exogenous and endogenous states of the SDS biodegradation process when the pH was maintained at 8.5, both base and acid additions were noticed for the pH 7 and 7.8 studies (Figure 5.4). With these pH levels proton production was observed under exogenous state and was followed by proton consumption in the liquid medium. The continuous addition of acid during the endogenous period resulted in the reduction of the proton concentration (*Hp*) in the reactor. Observation showed that the base addition ended after approximately 66 and 187 min when the pH was maintained at 7 and 7.8 respectively. The net proton production was found to be decreased significantly lower when the pH of the reactor drops from 7.8 to 7 (Figure 5.4).

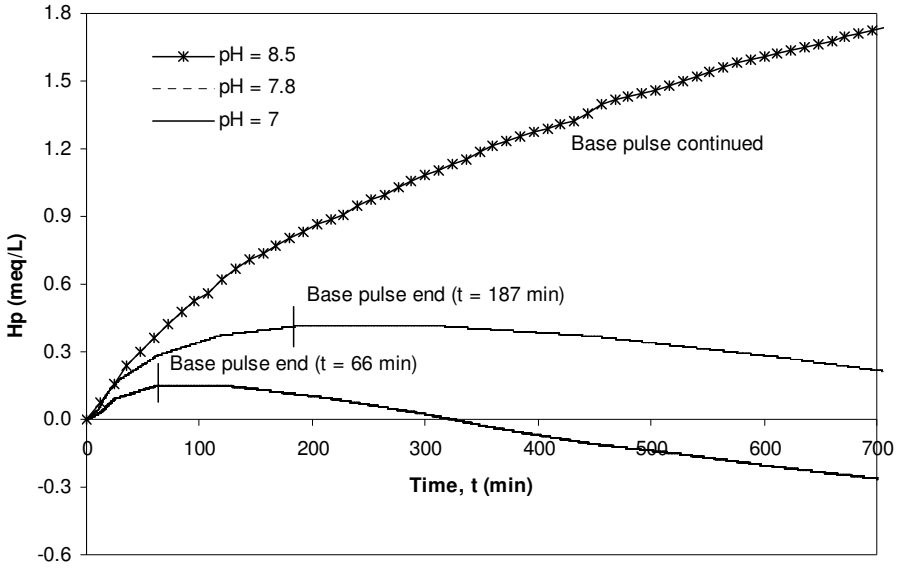

Figure 5.4: Experimental Hp profiles for different pH of activated sludge (SDS = 75 mg COD/L)

5.3 Proposed model for surfactant (SDS) biodegradation

A bio-kinetic model has been proposed in this study to describe both the respirometric and the titrimetric behavior resulting from the aerobic biodegradation of the surfactant, SDS, in an activated sludge system. An in-depth understanding of the biodegradation pathway of this substrate is essential especially for modeling the titrimetric components. The following sub-sections include discussion on the biodegradation pathway of SDS and development of the bio-kinetic model to explain the SDS biodegradation process.

5.3.1 SDS biodegradation pathway

Sodium dodecyl sulfate (SDS) has a tail of 12 carbon atoms attached to a sulfate group. The literature shows that *Pseudomonads*, an ubiquitous group of bacterial organisms, have the capacity to degrade sulfate esters of long-chain primary alcohols (Davison et al., 1992; Van Beilen et al., 1992; Kok et al., 1989). Dodecyl sulfate is hydrolyzed to alcohol (1-dodecanol) releasing inorganic sulfate by alkyl sulfatase. The liberated alcohol is then oxidized to dodecanal and lauric acid by the enzymes alcohol dehydrogenase and aldehyde dehydrogenase respectively (Figure 5.5).

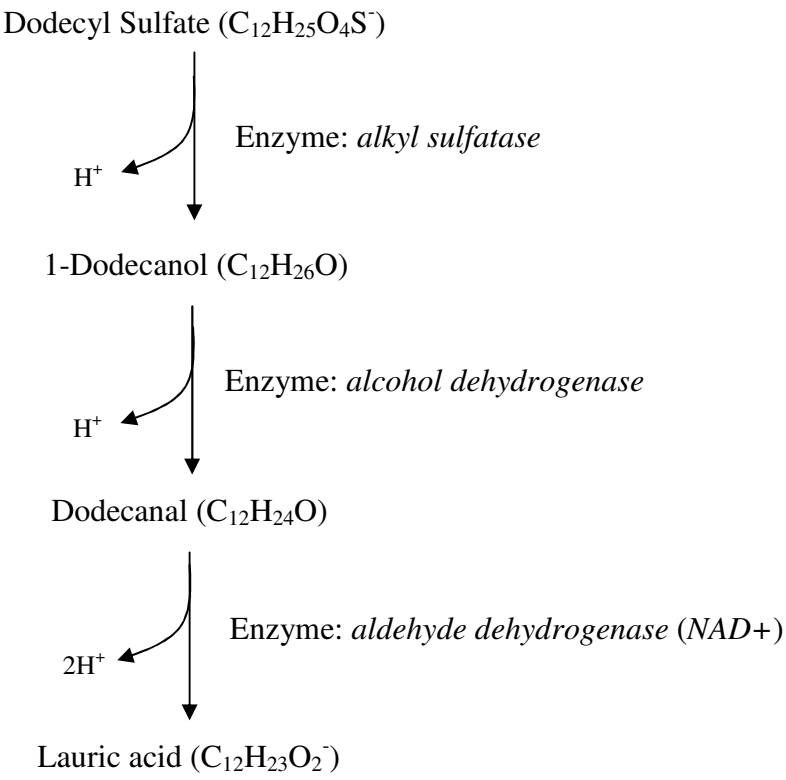

Figure 5.5: Biodegradation pathway of dodecyl sulfate (modified from Yao, 2006)

5.3.2 Model development

Figure 5.6 illustrates the proposed model diagram with processes involved during SDS biodegradation. The hydrolysis component is introduced using the extended SSAG model that was proposed for acetate biodegradation (as described in Chapter 4).

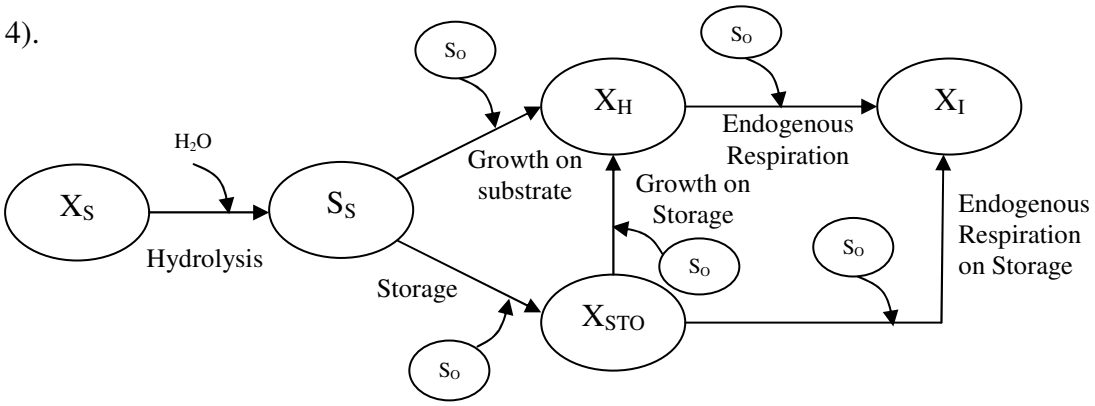

Figure 5.6: Model diagram for aerobic biodegradation of SDS

The proposed SSAG model includes the stoichiometric parameters involved in titrimetry in each step of the growth and storage phases along with consideration of the non-linear carbon dioxide transfer rate in the liquid phase. The major steps, other than hydrolysis, during the aerobic biodegradation of SDS are the formation of storage products, aerobic growth on the substrate, aerobic growth on the storage, endogenous respiration, respiration on storage products, aqueous CO_2 equilibrium and stripping of CO_2 (see Table 5.1 for the process matrix).

The conversion of sodium dodecyl sulfate to alcohol (1-dedecanol) occurs through a hydrolysis process that releases H^+ in the liquid medium (equation 5.1). The proton production during hydrolysis can be estimated by using the matrix shown in Table 5.1, where the parameter "C" represents the molecular weight of the substrate, SDS (576 gCOD/mol).

$$C_{12}H_{25}O_4SNa + H_2O \rightarrow C_{12}H_{26}O + NaSO_4 + H^+ \qquad \text{----- (Equation 5.1)}$$

The alcohol undergoes a multi-step oxidation process producing lauric acid in a liquid medium. During modeling, the course of oxidation was consolidated into one step to keep the proposed model simple. While the SDS biodegradation pathway shows proton production during the lauric acid formation, a fraction of the proton is consumed for lauroyl-CoA synthesis. The net H^+ production occurs in the liquid medium as shown in Table 5.1 considering lauric acid as a readily biodegradable compound (S_S) to be used for biomass growth. The stoichiometry related to the processes such as aerobic growth on substrate, formation of storage products from substrate and aerobic growth on storage indicates the CO_2 production rate that can be determined simply from equations 5.2, 5.3 and 5.4 respectively (see section 4.4 in Chapter 4 for the derivation).

$$\begin{aligned}&\frac{1}{Y_{H,S}}(mgCOD)CH_yO_z + \left(1-\frac{1}{Y_{H,S}}\right)(mgCOD)O_2 + i_{NBM}(mgN)NH_3 \\ &\rightarrow 1(mgCOD)CH_aO_bN_c + \frac{1}{8\gamma_S}\left(\frac{1}{Y_{H,S}}-\frac{\gamma_S}{\gamma_X}\right)(mmol)CO_2 + (...)H_2O\end{aligned} \qquad \text{----- (Equation 5.2)}$$

$$\frac{1}{Y_{STO}}(mgCOD)CH_yO_z + \left(1-\frac{1}{Y_{STO}}\right)(mgCOD)O_2 \rightarrow 1(mgCOD)CH_pO_q + \frac{1}{8\gamma_S}\left(\frac{1}{Y_{STO}}-\frac{\gamma_S}{\gamma_{STO}}\right)(mmol)CO_2 + (...)H_2O \quad \text{----- (Equation 5.3)}$$

$$\frac{1}{Y_{H,STO}}(mgCOD)CH_pO_q + \left(1-\frac{1}{Y_{H,STO}}\right)(mgCOD)O_2 + i_{NBM}(mgN)NH_3 \rightarrow 1(mgCOD)CH_aO_bN_c + \frac{1}{8\gamma_{STO}}\left(\frac{1}{Y_{H,STO}}-\frac{\gamma_{STO}}{\gamma_X}\right)(mmol)CO_2 + (...)H_2O \quad \text{----- (Equation 5.4)}$$

where, $CH_aO_bN_c$, CH_yO_z and CH_pO_q represent the elemental composition of biomass, substrate (lauric acid) and storage products respectively. The yield coefficients for growth on substrate, storage on substrate and growth on storage products are expressed as $Y_{H,S}$, Y_{STO} and $Y_{H,STO}$ respectively. The degree of reduction of the substrate (γ_S), the storage products (γ_{STO}) and the biomass (γ_X) can be calculated as 4+y-2z, 4+p-2q and 4+a-2b-3c accordingly. The coefficient related to ammonia uptake (i_{NBM}) is expressed as gN per gCOD biomass unit basis that can be determined from the relation $14c/8\gamma_X$ (Sin, 2004).

According to the principles of SSAG model, part of the readily biodegradable compound, lauric acid, is considered to be uptaken for heterotrophic biomass growth while the rest of it is consumed for simultaneous storage formation. Proton production takes place as lauric acid leaves H^+ in the liquid medium before it is consumed by biomass cell that has been supplemented due to ammonia assimilation for biomass growth. In Table 5.1, the parameter "p" represents the fraction of NH_4^+ in the liquid phase which is derived as $1/(1+10^{pH-\ pK_{NH4}})$ by Gernaey et al. (2002a). During the aerobic growth on storage process, it is assumed that the biomass accumulates nitrogen too within the cell along with carbon source for their subsequent growth purpose (see the ammonium balance in Table 5.1), which is also assumed for acetate biodegradation modeling as described in Chapter 4.

Table 5.1: Process matrix involved in the proposed model for surfactant (SDS) biodegradation

Process	X_H (g COD)	X_{NHacc} (g N)	X_{STO} (g COD)	S_S (g COD)	X_{SDS} (g COD)	S_{HCO_3} (mol)	S_{CO_2} (mol)	S_{Hp} (mol)	S_{NH} (g N)	S_O (g O_2)	Kinetics
Hydrolysis	--	--	--	1	-1	--	--	$\frac{1}{C}$	--	--	$k_h.M_{X_{SDS}/X_H}.X_H$
S_{NH} accumulation	--	i_{NBM}	--	--	--	--	--	$\frac{i_{NBM}\,p}{14}$	$-i_{NBM}$	--	$(1-e^{-t/\tau}).k_{NHacc}.M_S.X_H$
Aerobic growth on S_S	1	--	--	$-\frac{1}{Y_{H,S}}$	--	--	$\frac{1}{8\gamma_S}\left(\frac{1}{Y_{H,S}}-\frac{\gamma_S}{\gamma_X}\right)$	$\frac{i_{NBM}\,p}{14}+\frac{3}{C}$	$-i_{NBM}$	$-\frac{1-Y_{H,S}}{Y_{H,S}}$	$(1-e^{-t/\tau}).\mu_{MAX,S}.M_S.X_H$
Formation of X_{STO}	--	--	1	$-\frac{1}{Y_{STO}}$	--	--	$\frac{1}{8\gamma_S}\left(\frac{1}{Y_{STO}}-\frac{\gamma_S}{\gamma_{STO}}\right)$	--	--	$-\frac{1-Y_{STO}}{Y_{STO}}$	$(1-e^{-t/\tau}).k_{STO}.M_S.X_H$
Aerobic growth on X_{STO}	1	$-i_{NBM}$	$-\frac{1}{Y_{H,STO}}$	--	--	--	$\frac{1}{8\gamma_{STO}}\left(\frac{1}{Y_{H,STO}}-\frac{\gamma_{STO}}{\gamma_X}\right)$	--	--	$-\frac{1-Y_{H,STO}}{Y_{H,STO}}$	$\mu_{MAX,STO}\left(\frac{(X_{STO}/X_H)^2}{K_2+K_1.(X_{STO}/X_H)}\right)\left(\frac{K_S}{S_S+K_S}\right)X_H$
Endogenous respiration	-1	--	--	--	--	--	$\frac{1-f_{XI}}{8\gamma_X}$	$-\frac{(i_{NBM}-f_{XI}i_{NXI})\,p}{14}$	$i_{NBM}-i_{NXI}f_{XI}$	$-(1-f_{XI})$	$b_H.X_H$
X_{STO} respiration	--	--	-1	--	--	--	$\frac{1}{8\gamma_{STO}}$	--	--	-1	$b_{STO}.X_{STO}$
Aqueous CO_2 equilibrum	--	--	--	--	--	1	-1	1	--	--	$k_1 S_{CO_2}-k_1 10^{pk_1-pH} S_{HCO_3}$
CO_2 stripping	--	--	--	--	--	--	1	--	--	--	$K_L a_{CO2}(S^*_{CO2}-S_{CO2})$

Assuming that ammonia required for the biomass growth during storage to growth process is taken from the internal source (cell) instead of the external environment

Moreover, the biological reactions during endogenous respiration as well as the respiration on storage lead to CO_2 production in the system thus influence the process titrimetry that can be estimated using the stoichiometric expression as mentioned in equation 5.5 and 5.6 accordingly. Table 5.1 presents the production of CO_2 for the respective oxygen uptake of (1-f_{XI}) gCOD (as derived by Sin and Vanrolleghem, 2007). The parameter γ_{STO} in equation 5.6 refers to the degree of reduction of the storage products.

$$1(mgCOD)CH_aO_bN_c + 1(mgCOD)O_2 \rightarrow \frac{1}{8\gamma_X}(mmol)CO_2 + (...)H_2O + i_{NBM}(mgN)NH_3 \quad \text{----- (Equation 5.5)}$$

$$1(mgCOD)CH_pO_q + 1(mgCOD)O_2 \rightarrow \frac{1}{8\gamma_{STO}}(mmol)CO_2 + (...)H_2O \quad \text{----- (Equation 5.6)}$$

The kinetics and stoichiometry corresponding to the processes of aqueous CO_2 equilibrium and CO_2 stripping are kept the same as those used for acetate biodegradation modeling (see section 4.4 in Chapter 4).

5.4 Model calibration and parameter estimation

5.4.1 Parameter estimation approach

The proposed model was calibrated with both the respirometric and titrimetric measurements where assays were conducted for SDS pulses of 50, 75 and 100 mg COD/L to the activated sludge. Three different calibration approaches were applied: using the respirometric measurements alone, the titrimetric measurements alone and combined respirometric-titrimetric measurements followed by model parameter estimation. The results were compared for validation of the proposed SSAG model. Non-linear technique was employed for the parameter estimation process using the MATLAB optimisation toolbox (R2007a). Minimization of the mean squared error (MSE) between the model and the experimental output was calculated as the main criterion for curve fitting.

The model parameters K_S, q_{MAX}, $Y_{H,S}$, Y_{STO}, $Y_{H,STO}$, K_1, K_2, k_h, K_X and τ were estimated along with calculation of 95% confidence intervals. A description of the model parameters is presented in Appendix A. Default values assigned in the ASM3 model for the parameter f_{XI} (0.2) were assumed for the current analysis. The values for the parameters b_H and b_{STO} were fixed at 0.00036 per min (0.52 day^{-1}) for better curve fitting, though it is higher than the ASM3 default one (0.2 day^{-1}). For successful model calibration Carvalho et al. (2001) and Beccari et al. (2002) assumed the parameter b_H in their study as 0.72 and 0.041 day^{-1} respectively. In the current study, a value of 0.2 day^{-1} was considered for the parameter $k_{NHacc.}$ at the beginning of the parameter estimation process, and was revised later for better curve fitting. The ASM3 prescribed values for the parameters i_{NXI} (0.02 gN/g COD X_I) and i_{NBM} (0.07 gN/g COD X_H) were fixed during the proposed model calibration. The parameter f_{STO} was fixed at 0.65 for successful model calibration. The maximum storage rate (k_{STO}) and the maximum growth rate of the biomass ($\mu_{MAX,S}$) were calculated from the estimates of the parameters q_{MAX} and f_{STO} based on the procedure explained in Sin et al. (2005) where the parameter $\mu_{MAX,STO}$ is assumed to be the same order of magnitude as $\mu_{MAX,S}$. The relationship $OUR_{end}(0) = (1-f_{XI}).b_H.X_H(0)$ was employed to calculate the initial concentration of the biomass, $X_H(0)$.

The parameter k_1 (1.0762 per min) was kept at the same value it was used for the acetate biodegradation study (see Chapter 4), and total inorganic carbon in the aqueous medium, $C_{T,init}$ was adjusted for different assays to fit the experimental profile with the "model one". The initial concentrations of CO_2 and HCO_3 in the reactor were calculated using their relationship with $C_{T,init}$ (Sin, 2004). During the model calibration, the value for $K_L a_{CO_2}$ was calculated as 0.055 min^{-1} from the oxygen transfer coefficient ($K_L a$) using the relationship between their diffusivity coefficients (Sperandio and Paul, 1997; Sin and Vanrolleghem, 2007), whereas the parameter pK_1 was taken as 6.39 (Sperandio and Paul, 1997). The default values suggested by Stumm and Morgan (1996) for the parameters pK_{NH4} (9.25) and $S^*_{CO_2}$ (0.017 mmol/L) were assumed during the parameter estimation process. Besides, the degree of reduction of the substrate (γ_S) and biomass (γ_X) were calculated as 5.67 and 4.2 using the elemental composition of lauric acid ($C_{12}H_{23}O_2$) and biomass ($CH_{1.8}O_{0.5}N_{0.2}$) respectively. The degree of reduction coefficient γ_{STO} was kept at 4.5

assuming polyhydroxybutyrate (PHB) types storage compounds formed in biomass cell to consume it later for their growth.

5.4.2 Results and discussions of model calibration

The proposed SSAG model was found to be satisfactory in explaining the experimental OUR and *Hp* measurements corresponding to SDS biodegradation in the activated sludge process. The proposed SSAG model was calibrated for the initial SDS concentrations of 100, 75 and 50 mg COD/L which are presented in Figure 5.7, Figure 5.8 and Figure 5.9 respectively. Table 5.2 shows the parameter estimation results using on-line respirometric measurements alone with their confidence interval for three different SDS concentration studies. Observation shows that the hydrolysis related kinetic parameters such as k_h and K_X increase with initial SDS concentrations. The parameter k_h is estimated as 26.2 and 31.1 day^{-1} for the SDS concentrations of 50 and 100 mg COD/L respectively. Besides, the parameter K_X shows a relatively higher value (0.44) for the higher SDS concentration (100 mg COD/L). There is little evidence reported in the literature about SDS biodegradation kinetics. Most of it refers to a first order or simple Monod model (Zhang et al., 1999; Chen et al., 2001) ignoring the hydrolysis phase though SDS was found to be hydrolyzed before it underwent the oxidation process (see sub-section 5.3.1). Moreover, they calibrated the model using off-line substrate depletion measurements that resulted in an inaccurate parameter estimation process due to the constraints involved in the collection of frequent bio-kinetic information from the system. In this study, model calibration was performed with on-line measurements where the parameter estimation process gives the hydrolysis rate relatively higher than ASM3 default values (3.4 day^{-1}). Information regarding the kinetics of SDS hydrolysis is very limited in the literature; however the hydrolysis rate was noticed to be significant (18.5 day^{-1}) by Lopez Zavala et al. (2004) when they investigated the biodegradation of faeces under aerobic conditions. In addition, Karahan et al. (2006) estimated the hydrolysis rate as high as 30 day^{-1} for soluble starch biodegradation using sequencing batch reactor in their experimental study. While Carucci et al. (2001) estimated the parameters k_h (22.9 h^{-1}) and K_X (12.3) very high for filtered wastewater biodegradation, opposing results were found by Beccari et al. (2002) who

observed the respective parameters as low as 0.0082 h^{-1} and 0.0001 using simultaneous storage and growth for model calibration.

Parameter estimation shows that the substrate affinity constant, K_S lies between 0.62 and 0.65 mg COD/L for all three initial SDS concentration studies indicating the affinity to be as strong as observed in the acetate biodegradation study (see Chapter 4). The calculated maximum biomass growth rate $\mu_{MAX,S}$ ranges from 3.97 to 4.19 day^{-1}, while a faster storage formation rate (9.7-10.3 day^{-1}) is observed from the model calibration and parameter estimation process. It is noteworthy that similar sludge behavior was observed during the acetate biodegradation study where the calculated parameter k_{STO} was found to be higher than that for the parameter $\mu_{MAX,S}$ (see section 4.5 in Chapter 4). However, the parameter $\mu_{MAX,S}$ was found to be less (0.67-2.01 day^{-1}) for the acetate biodegradation. Using SDS as a test substrate, Chen et al. (2001) identified a high biomass growth rate (8.88 day^{-1}), whereas Zhang et al. (1999) estimated the parameter $\mu_{MAX,S}$ as 2.76 day^{-1} applying Monod kinetics in their model. While Anderson et al. (1990) showed the estimated parameter for $\mu_{MAX,S}$ to range between 0.67 and 2.01 day^{-1}, the growth rate was observed by Marchesi et al. (1997) to be significantly higher (28.32 day^{-1}) when the exponential growth based model was calibrated with residual SDS measurements.

From the parameter estimation process, the yield coefficients $Y_{H,S}$, Y_{STO} and $Y_{H,STO}$ are found to be 0.64, 0.84 and 0.73 for all three SDS concentrations. The literature reports combined yield coefficient (Y) ranges from 0.34 (Chen et al., 2001) to 0.915 (Zhang et al., 1999) when a Monod kinetic based model was used for calibration. The current study also reveals the biomass yield for storage Y_{STO} higher when compared to other yield coefficients in the process. A similar observation was noted for the acetate biodegradation study where the yield coefficient Y_{STO} (0.88) was found to be greater than the yield coefficient $Y_{H,S}$ (0.71) (see section 4.5 in Chapter 4). It confirms the common sludge behavior showing remarkable storage formation approach during both the SDS and acetate biodegradation process. The reason is that, when the sludge was acclimatized, it was fed with the substrate twice a day, therefore having feast and famine period. During this acclimatisation, the sludge might have got increased capacity to store the substrate to consume for growth in the absence of an external source.

The proposed SSAG model was successfully calibrated with the titrimetric measurements for all three SDS concentrations study (Figure 5.7-5.9). The estimated model parameters are presented in tabular form along with their confidence intervals for checking the estimation accuracy (Table 5.3). The estimated model parameters k_H (23-30.5 day^{-1}), K_X (0.41 and 0.44 mg/mg), K_S (0.59-0.64 mg COD/L), k_{STO} (9.69 and 10.17 day^{-1}), $\mu_{MAX,S}$ (3.98 and 4.13 day^{-1}), $Y_{H,S}$ (0.64), Y_{STO} (0.84) and $Y_{H,STO}$ (0.73) were found to be very close to the results obtained using respirometric measurements alone (Table 5.2).

Figure 5.7c-5.9c show the model calibration outcome based on combined respirometric-titrimetic measurements. Observation shows that the model profiles for all three SDS concentrations are well fitted with both the experimental OUR and *Hp* data. The parameter estimation result is presented in Table 5.4. The estimated model parameters are consistent with the respective parameters that were estimated using either respirometric data alone or titrimetric data alone (see Table 5.2-5.4). The confidence intervals for all the estimated parameters are reasonable except that for K_2. A similar problem was noticed during the acetate biodegradation modeling where the SSAG model parameters K_1 and K_2 were identified as interdependent under the feast phase of the biodegradation process (Sin et al., 2005).

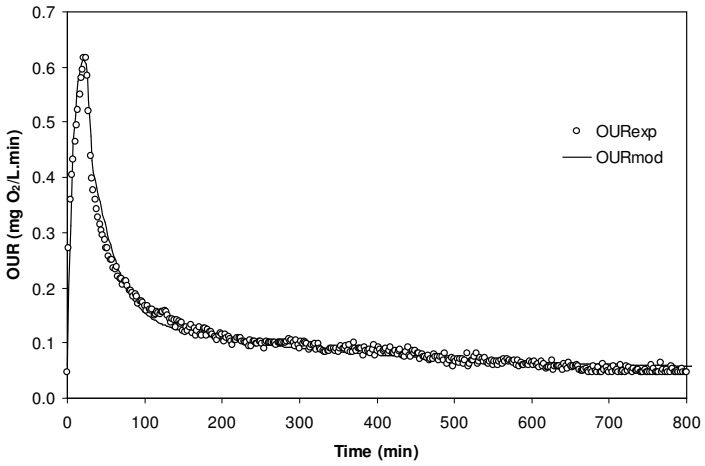

(a)

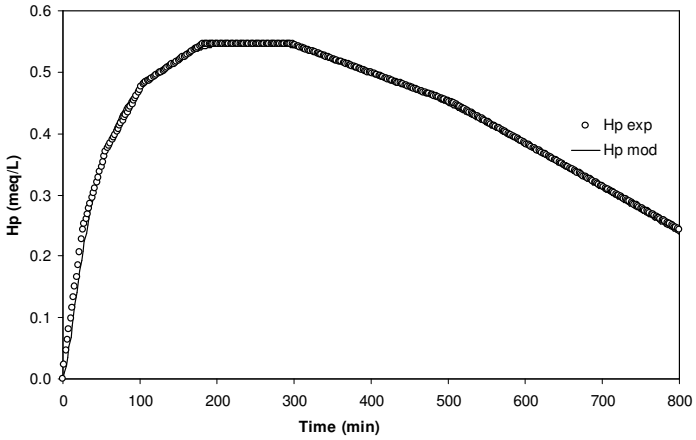

(b)

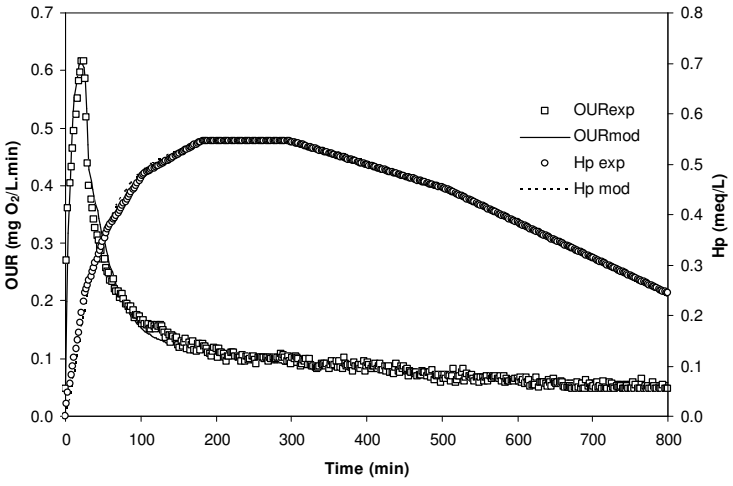

(c)

Figure 5.7: Model calibration using (a) respirometric data alone (b) titrimetric data alone and (c) combined respirometric-titrimetric data (SDS = 100 mg COD /L)

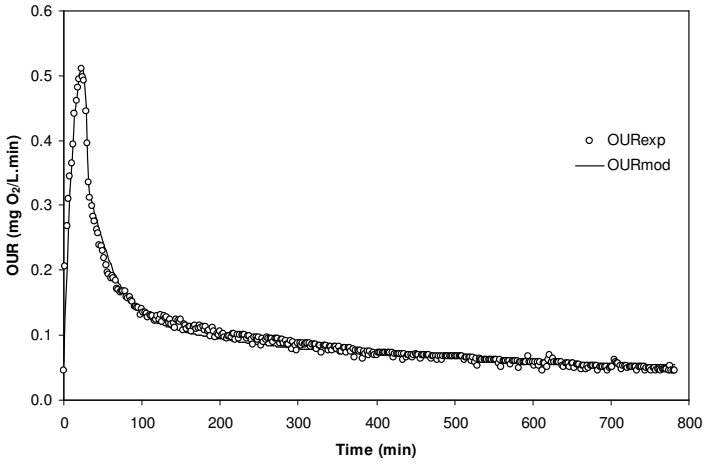

(a)

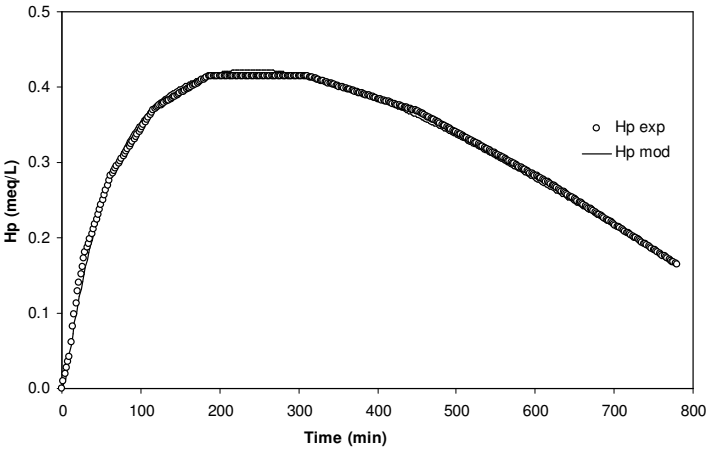

(b)

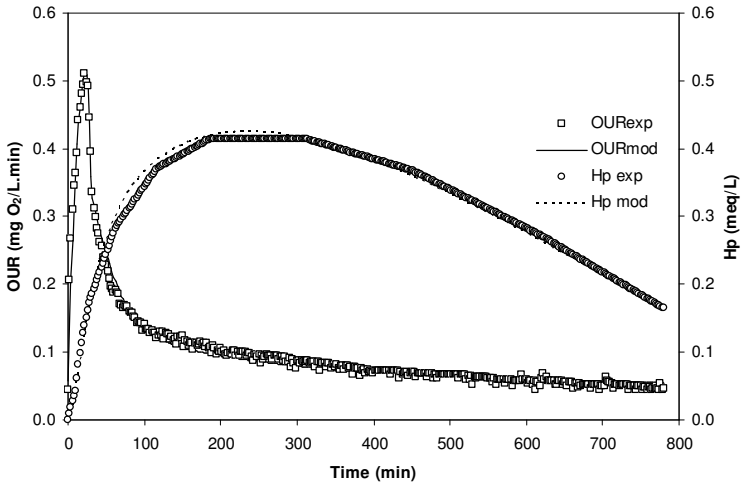

(c)

Figure 5.8: Model calibration using (a) respirometric data alone (b) titrimetric data alone and (c) combined respirometric-titrimetric data (SDS = 75 mg COD /L)

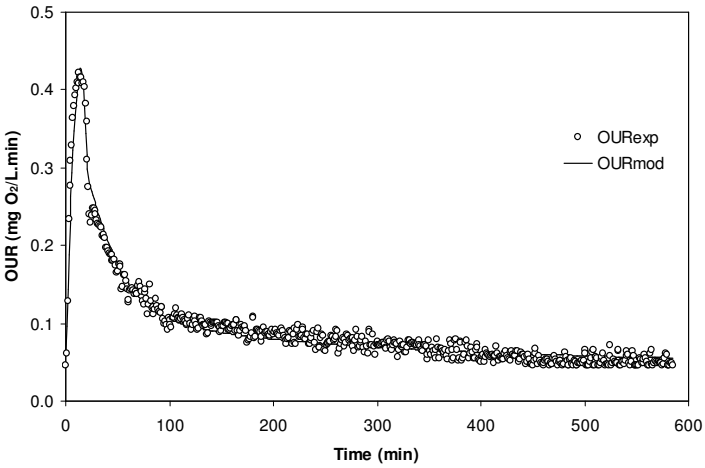

(a)

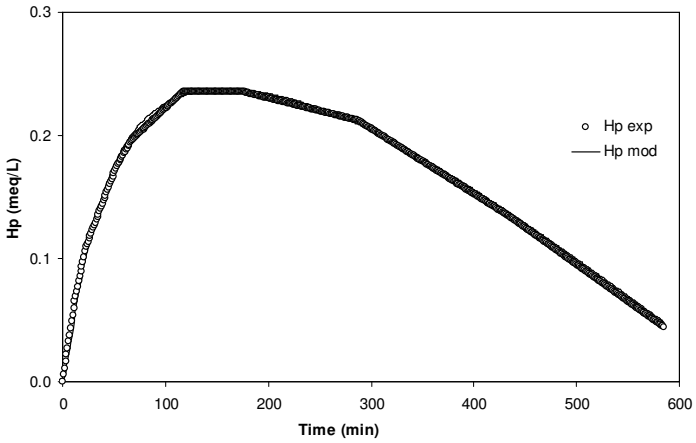

(b)

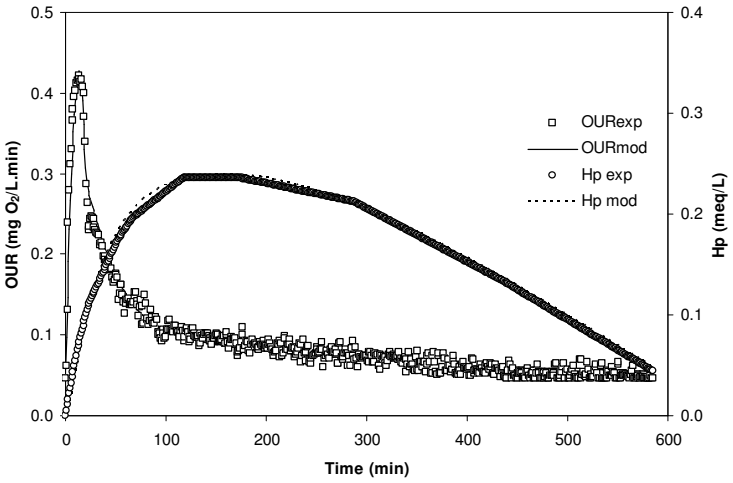

(c)

Figure 5.9: Model calibration using (a) respirometric data alone (b) titrimetric data alone and (c) combined respirometric-titrimetric data (SDS = 50 mg COD /L)

Table 5.2: Parameter estimation results using respirometric data alone for three different concentration studies (confidence intervals are shown in brackets as percentages)

Parameters	SDS 100 mg COD/L (Confidence interval, %)	SDS 75 mg COD/L (Confidence interval, %)	SDS 50 mg COD/L (Confidence interval, %)
Parameters Estimated:			
q_{MAX} (1/min)	$0.0131 \pm 6.1\times10^{-4}$ (4.65)	$0.0125 \pm 9.2\times10^{-4}$ (7.36)	$0.0123 \pm 2.6\times10^{-3}$ (21.13)
k_h (1/min)	$0.0216 \pm 1.1\times10^{-3}$ (5.09)	$0.0191 \pm 9.6\times10^{-4}$ (5.03)	$0.0182 \pm 2.0\times10^{-3}$ (10.98)
K_S (mgCOD/L)	0.63 ± 0.087 (13.8)	0.62 ± 0.061 (9.84)	0.65 ± 0.115 (17.69)
K_X (mgCOD X_S/mgCOD X_H)	0.44 ± 0.049 (11.14)	0.42 ± 0.045 (10.71)	0.39 ± 0.084 (21.54)
$Y_{H,S}$ (mgCOD X_H/mgCOD S_S)	0.64 ± 0.062 (9.69)	0.64 ± 0.087 (13.59)	0.64 ± 0.203 (31.71)
Y_{STO} (mgCOD X_{STO}/mgCOD S_S)	0.84 ± 0.33 (39.28)	0.84 ± 0.17 (20.2)	0.84 ± 0.218 (25.95)
$Y_{H,STO}$ (mgCOD X_H/mgCOD X_{STO})	0.73 ± 0.128 (17.53)	0.73 ± 0.144 (19.73)	0.73 ± 0.075 (10.27)
K_1 (mgCOD X_{STO}/mgCOD X_H)	0.83 ± 0.315 (37.95)	0.7 ± 0.106 (15.14)	0.63 ± 0.151 (23.97)
K_2 (mgCOD X_{STO}/mgCOD X_H)	$8.2\times10^{-5} \pm 1.5\times10^{-4}$ (182.9)	$8.1\times10^{-6} \pm 2.8\times10^{-5}$ (345.7)	$9.8\times10^{-7} \pm 2.08\times10^{-6}$ (212.2)
τ (min)	6.51 ± 0.46 (7.07)	11.72 ± 1.05 (8.96)	9.29 ± 1.28 (13.78)
Parameters Assumed:			
b_H (1/min)	0.00036	0.00036	0.00036
b_{STO} (1/min)	0.00036	0.00036	0.00036
k_{NHacc} (1/min)	0.000056	0.000056	0.000056
f_{STO}[b] (mgCOD X_{STO}/mgCOD S_S)	0.65	0.65	0.65
f_{XI} (mgCOD /mgCOD)	0.2	0.2	0.2
Parameters Calculated:			
k_{STO} (1/min)	0.007161	0.006857	0.006721
$\mu_{MAX,S}$ (1/min)	0.002911	0.002812	0.002755
$\mu_{MAX,STO}$ (1/min)	0.002911	0.002812	0.002755
X_H (mgCOD/L)	200	200	200
MSE[a]	2.05×10^{-4}	7.58×10^{-5}	1.15×10^{-4}

[a] MSE refers to the mean squared error which is calculated from sum of squared errors divided by number of observations

[b] Parameters were fixed by trials for the better fit of experimental profile with the model

Table 5.3: Parameter estimation results using titrimetric data alone for three different concentration studies (confidence intervals are shown in brackets as percentages)

Parameters	SDS 100 mg COD/L (Confidence interval, %)	SDS 75 mg COD/L (Confidence interval, %)	SDS 50 mg COD/L (Confidence interval, %)
Parameters Estimated:			
q_{MAX} (1/min)	$0.0129 \pm 8.3\times10^{-4}$ (6.43)	$0.0125 \pm 1.6\times10^{-3}$ (12.8)	$0.0123 \pm 1.08\times10^{-3}$ (8.78)
k_h (1/min)	$0.0212 \pm 3.0\times10^{-3}$ (14.15)	$0.016 \pm 8.6\times10^{-4}$ (5.38)	$0.0181 \pm 3.06\times10^{-3}$ (16.9)
K_S (mgCOD/L)	0.64 ± 0.037 (5.78)	0.59 ± 0.085 (14.4)	0.63 ± 0.117 (18.57)
K_X (mgCOD X_S/mgCOD X_H)	0.44 ± 0.096 (21.82)	0.42 ± 0.074 (17.62)	0.41 ± 0.055 (13.41)
$Y_{H,S}$ (mgCOD X_H/mgCOD S_S)	0.64 ± 0.168 (26.25)	0.64 ± 0.114 (17.8)	0.64 ± 0.079 (12.34)
Y_{STO} (mgCOD X_{STO}/mgCOD S_S)	0.84 ± 0.089 (10.6)	0.84 ± 0.085 (10.12)	0.84 ± 0.021 (2.5)
$Y_{H,STO}$ (mgCOD X_H/mgCOD X_{STO})	0.73 ± 0.194 (26.58)	0.73 ± 0.19 (26.02)	0.73 ± 0.046 (6.3)
K_1 (mgCOD X_{STO}/mgCOD X_H)	0.83 ± 0.212 (25.54)	0.7 ± 0.209 (29.86)	0.65 ± 0.059 (9.08)
K_2 (mgCOD X_{STO}/mgCOD X_H)	$8.14\times10^{-5} \pm 1.73\times10^{-4}$ (208.4)	$8.2\times10^{-6} \pm 1.1\times10^{-5}$ (134.2)	$9.85\times10^{-7} \pm 1.79\times10^{-6}$ (181.7)
τ (min)	5.01 ± 0.55 (10.98)	8.18 ± 0.68 (8.31)	6.54 ± 0.56 (8.56)
Parameters Assumed:			
b_H (1/min)	0.00036	0.00036	0.00036
b_{STO} (1/min)	0.00036	0.00036	0.00036
k_{NHacc} (1/min)	0.000056	0.000056	0.000056
f_{STO}[b] (mgCOD X_{STO}/mgCOD S_S)	0.65	0.65	0.65
f_{XI} (mgCOD /mgCOD)	0.2	0.2	0.2
k_I (1/min)	1.0762	1.0762	1.0762
$K_L a_{CO2}$ (1/min)	0.055	0.055	0.055
$C_{T,init}$[b] (mmol/L)	1.3	1.2	1.3
Parameters Calculated:			
HCO_3 (mmol/L)	1.2511	1.1549	1.2511
CO_2 (mmol/L)	0.0489	0.0451	0.0489
k_{STO} (1/min)	0.007064	0.006849	0.006729
$\mu_{MAX,S}$ (1/min)	0.002867	0.002809	0.002764
$\mu_{MAX,STO}$ (1/min)	0.002867	0.002809	0.002764
X_H (mgCOD/L)	200	200	200
MSE[a]	5.84×10^{-5}	3.98×10^{-5}	1.64×10^{-5}

[a] MSE refers to the mean squared error which is calculated from sum of squared errors divided by number of observations

[b] Parameters were fixed by trials for the better fit of experimental profile with the model

Table 5.4: Parameter estimation results using combined respirometric-titrimetric data for three different concentration studies (confidence intervals are shown in brackets as percentages)

Parameters	SDS 100 mg COD/L (Confidence interval, %)	SDS 75 mg COD/L (Confidence interval, %)	SDS 50 mg COD/L (Confidence interval, %)
Parameters Estimated:			
q_{MAX} (1/min)	$0.0131 \pm 2.86\times10^{-4}$ (2.18)	$0.0125 \pm 4.73\times10^{-4}$ (3.78)	$0.0123 \pm 8.78\times10^{-4}$ (7.14)
k_h (1/min)	$0.0216 \pm 9.8\times10^{-4}$ (4.54)	$0.0189 \pm 1.7\times10^{-3}$ (8.99)	$0.0182 \pm 2.35\times10^{-3}$ (12.91)
K_S (mgCOD/L)	0.63 ± 0.078 (12.38)	0.6 ± 0.087 (14.5)	0.63 ± 0.113 (17.94)
K_X (mgCOD X_S/mgCOD X_H)	0.44 ± 0.03 (6.82)	0.42 ± 0.046 (10.95)	0.39 ± 0.075 (19.23)
$Y_{H,S}$ (mgCOD X_H/mgCOD S_S)	0.64 ± 0.053 (8.28)	0.64 ± 0.075 (11.72)	0.64 ± 0.057 (8.9)
Y_{STO} (mgCOD X_{STO}/mgCOD S_S)	0.84 ± 0.018 (2.14)	0.84 ± 0.024 (2.86)	0.84 ± 0.019 (2.26)
$Y_{H,STO}$ (mgCOD X_H/mgCOD X_{STO})	0.73 ± 0.039 (5.34)	0.73 ± 0.052 (7.12)	0.73 ± 0.043 (5.89)
K_1 (mgCOD X_{STO}/mgCOD X_H)	0.83 ± 0.034 (4.09)	0.7 ± 0.047 (6.71)	0.63 ± 0.067 (10.64)
K_2 (mgCOD X_{STO}/mgCOD X_H)	$8.1\times10^{-5} \pm 3.2\times10^{-4}$ (395.1)	$8.2\times10^{-6} \pm 2.1\times10^{-5}$ (256.1)	$9.85\times10^{-7} \pm 1.73\times10^{-6}$ (175.6)
τ (min)	6.35 ± 0.17 (2.68)	11.7 ± 0.5 (4.27)	9.01 ± 0.66 (7.33)
Parameters Assumed:			
b_H (1/min)	0.00036	0.00036	0.00036
b_{STO} (1/min)	0.00036	0.00036	0.00036
k_{NHacc} (1/min)	0.000056	0.000056	0.000056
f_{STO}[b] (mgCOD X_{STO}/mgCOD S_S)	0.65	0.65	0.65
f_{XI} (mgCOD /mgCOD)	0.2	0.2	0.2
k_I (1/min)	1.0762	1.0762	1.0762
$K_L a_{CO2}$ (1/min)	0.055	0.055	0.055
$C_{T,init}$[b] (mmol/L)	1.3	1.2	1.3
Parameters Calculated:			
HCO_3 (mmol/L)	1.2511	1.1549	1.2511
CO_2 (mmol/L)	0.0489	0.0451	0.0489
k_{STO} (1/min)	0.007153	0.006849	0.00674
$\mu_{MAX,S}$ (1/min)	0.002911	0.002809	0.002768
$\mu_{MAX,STO}$ (1/min)	0.002911	0.002809	0.002768
X_H (mgCOD/L)	200	200	200
MSE[a]	8.68×10^{-5}	7.45×10^{-5}	8.32×10^{-5}

[a] MSE refers to the mean squared error which is calculated from sum of squared errors divided by number of observations

[b] Parameters were fixed by trials for the better fit of experimental profile with the model

5.4.3 Proposed model evaluation

The proposed SSAG model has been evaluated using three different initial surfactant (SDS) concentrations (50, 75 and 100 mg COD/L) in an activated sludge system. The model has also been validated by three different calibration approaches: using on-line respirometric measurements alone, titrimetric measurements alone and combined respirometric titrimetric measurements, illustrating satisfactory calibration results (Figure 5.7-5.9). The estimated parameters are shown in tabular form (Table 5.2-5.4) along with parameter estimation errors calculated for 95% confidence intervals and mean squared error (MSE). The estimated parameters using respirometry alone gives almost the same values as estimated from the titrimetric data alone, as well as from the combined approach, thereby confirming the accuracy of the proposed model. The calculated confidence intervals and mean squared error are acceptable from a statistical perspective. Along with on-line measurements, the proposed model was validated following off-line methods where the surfactant and ammonium in the liquid medium were monitored during the oxidation period. Figure 5.10 shows the time profile study with model simulation that also validates the proposed SSAG model.

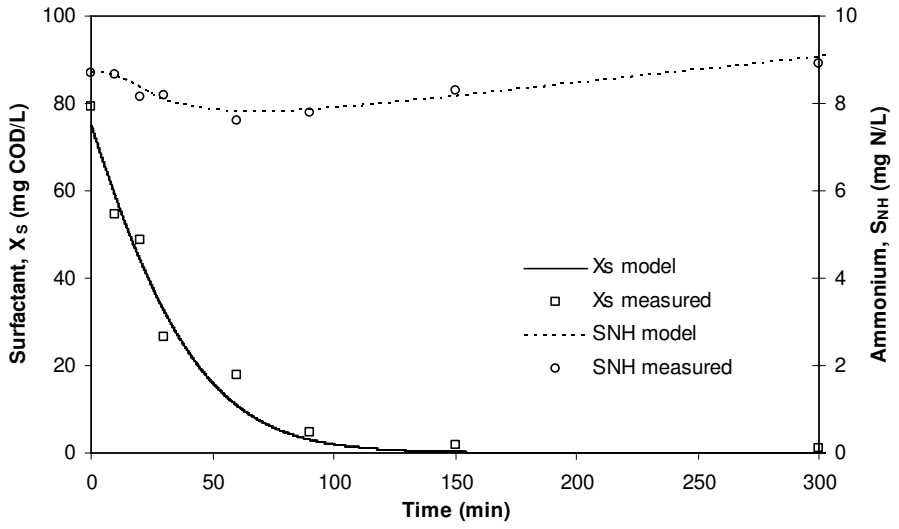

Figure 5.10: Model validation using off-line measurements for surfactant (SDS = 75 mg COD/L) biodegradation

The model consists of the kinetic parameter k_{NHacc} that was fixed to 0.08 day^{-1} for better model calibration. In the proposed SSAG model, polyhydroxybutyrate (PHB) was assumed to be stored in the biomass cell during the process. Contrary to several

reports in the literature that indicate the formation of PHB during acetate biodegradation, there was no strong result to show what kind of storage products are formed during SDS biodegradation. However the lauric acid synthesis generated acetyl group compound that was assumed to form PHB for storage in the biomass cell as observed in the acetate biodegradation process. The degree of reduction of storage products, γ_{STO} was calculated as 4.5 by considering the formula as $CH_{1.5}O_{0.5}$. The i_{NBM} content corresponding to the biomass composition $CH_{1.8}O_{0.5}N_{0.2}$ was calculated as 0.083 gN/g COD X_H which lies within the range of 7% to 8.6% reported by Henze et al. (2000) as typical value for the parameter i_{NBM}.

5.5 Applying the proposed model for different pH of sludge

The proposed model consists of titrimetric components related to SDS biodegradation including dynamic CO_2 transfer phenomena in an activated sludge system. Section 5.4 describes the proposed SSAG model that was successfully calibrated using both the respirometric and titrimetric measurements when pH was maintained at 7.8 ± 0.03. Since the model parameters related to the titrimetry are highly sensitive to sludge pH, the proposed model needed to be justified for different pH values. Hence the SDS biodegradation was investigated at different pH levels of 8.5 and 7, and the results were compared to those obtained in the pH 7.8 study. A constant SDS concentration of 75 mg COD/L was used for all three pH studies. Details of the model calibration and parameter estimation process are discussed in the following sub-sections.

5.5.1 Parameter estimation strategy

The proposed model was calibrated using three calibration approaches: calibration with the respirometric measurements alone, titrimetric data alone and using combined respirometric-titrimetric measurements. Different sludge pH levels (7 and 8.5) were maintained during the biodegradation process. The model parameters were then estimated and compared for validation purpose. While the parameters K_S, q_{MAX}, $Y_{H,S}$, Y_{STO}, $Y_{H,STO}$, K_1, K_2, k_h, K_X and τ were estimated along with the calculation of the errors at a 95% confidence interval, the parameters k_{STO} , $\mu_{MAX,S}$, $\mu_{MAX,STO}$, initial HCO_3 and CO_2 concentration in liquid phase were calculated following the same

procedure as described in sub-section 5.4.1. In the parameter estimation process, the rest of the model parameters were assumed to be the same as in the pH 7.8 study along with the same elemental composition of substrate, biomass and storage products for the titrimetric model calibration.

5.5.2 Results and discussions of model calibration

Figure 5.11 and Figure 5.12 illustrate the model calibration results for the SDS concentration of 75 mg COD/L when the sludge pH was maintained at 8.5 and 7 respectively. The proposed SSAG model was successfully calibrated with the experimental measurements where three different calibration methods were applied. Table 5.5-5.7 represent the comparison of estimated model parameters for pH 8.5, 7.8 and 7 studies respectively with their confidence intervals and MSE values.

The estimated model parameters using respirometric measurements alone are observed to be consistent with the respective parameters that were estimated using either titrimetric measurements alone or with combined respirometric-titrimetric measurements. The confidence intervals for the estimated model parameters are found to be reasonable (Table 5.5-5.7). Calculated MSE from the parameter estimation process shows satisfactory results that statistically confirm the accuracy of the proposed SSAG model. The parameters $C_{T,init}$ and f_{STO} were adjusted during the calibration process for better curve fitting. The proposed model was calibrated using a similar storage products formula ($CH_{1.5}O_{0.5}$) that was applied in the pH 7.8 study (see sub-section 5.4.3) The biomass composition was also kept as $CH_{1.8}O_{0.5}N_{0.2}$ that gives the i_{NBM} content 0.083 gN/g COD X_H. Comparison of the estimated model parameters for the three different pH studies is discussed in sub-section 5.5.3.

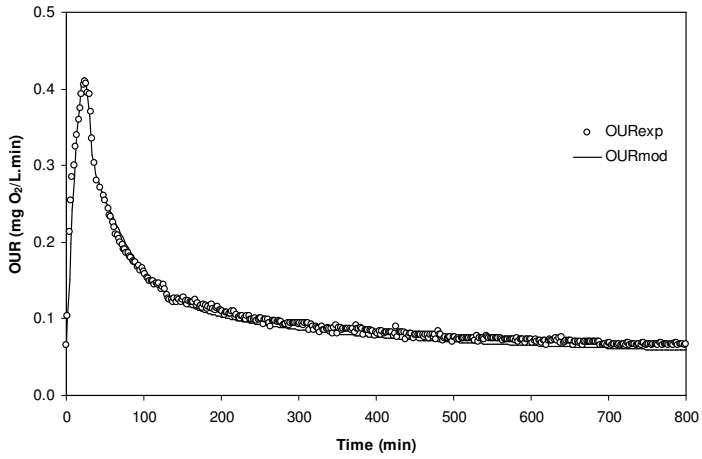

(a)

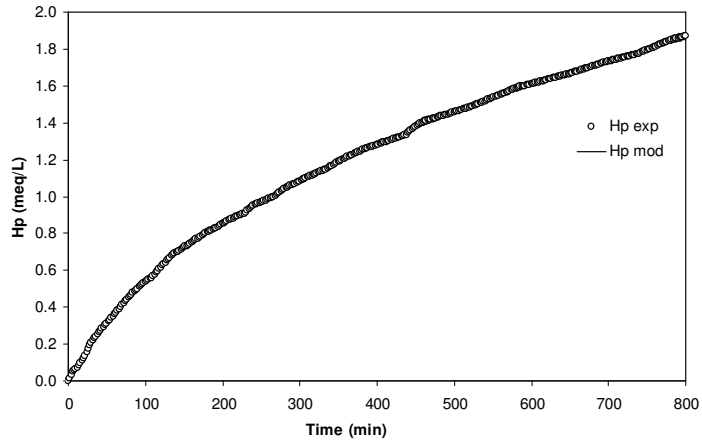

(b)

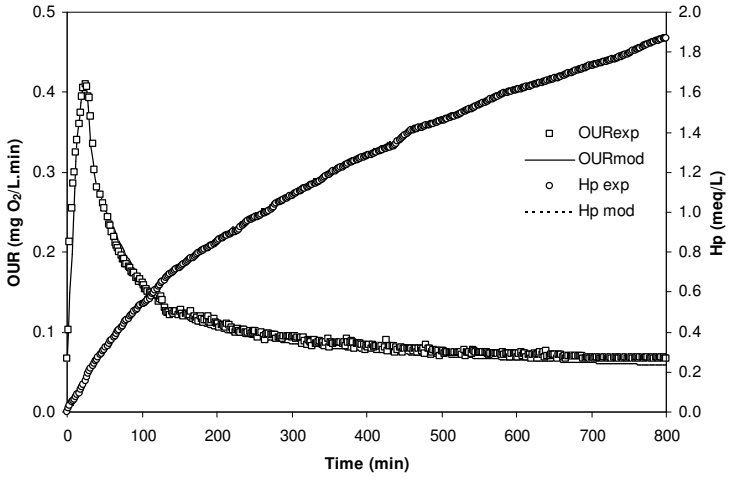

(c)

Figure 5.11: Model calibration using (a) respirometric data alone (b) titrimetric data alone and (c) combined respirometric-titrimetric data for the SDS pulse of 75 mg COD /L in activated sludge (pH = 8.5)

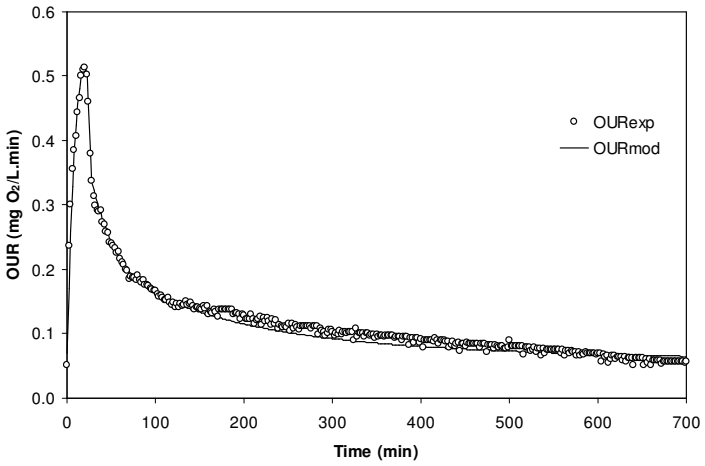

(a)

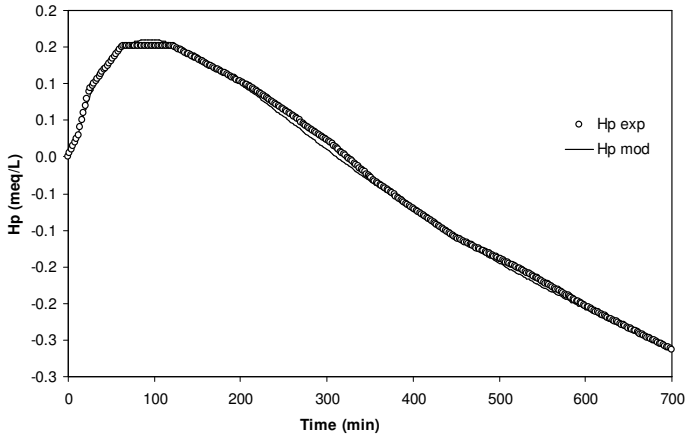

(b)

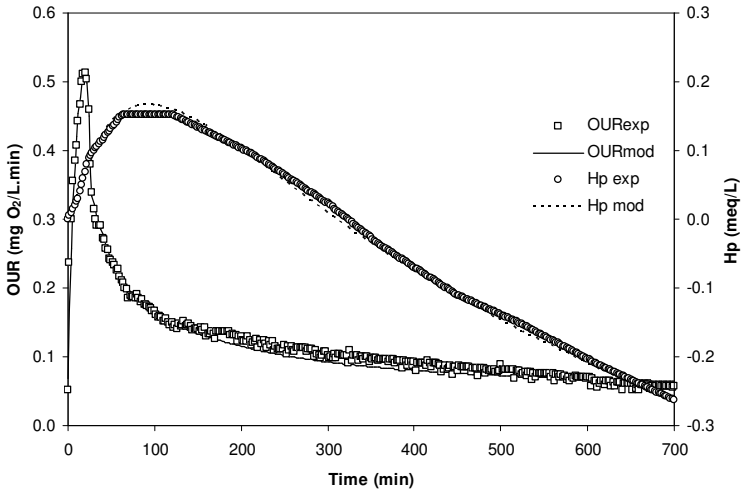

(c)

Figure 5.12: Model calibration using (a) respirometric data alone (b) titrimetric data alone and (c) combined respirometric-titrimetric data for the SDS pulse of 75 mg COD /L in activated sludge (pH = 7)

Table 5.5: Parameter estimation results using respirometric-titrimetric measurements for the pH of 8.5 (confidence intervals are shown in brackets as percentages)

Parameters	Respirometric data alone (Confidence interval, %)	Titrimetric data alone (Confidence interval, %)	Combined data (Confidence interval, %)
Parameters Estimated:			
q_{MAX} (1/min)	$0.0127 \pm 1.8\text{x}10^{-3}$ (14.17)	$0.0129 \pm 2.2\text{x}10^{-3}$ (17.05)	$0.0129 \pm 1.5\text{x}10^{-3}$ (11.63)
k_h (1/min)	$0.0125 \pm 9.6\text{x}10^{-4}$ (7.68)	$0.0125 \pm 2.6\text{x}10^{-3}$ (20.8)	$0.0125 \pm 2.1\text{x}10^{-3}$ (16.8)
K_S (mgCOD/L)	1.75 ± 0.37 (21.14)	1.93 ± 0. 34 (17.62)	1.89 ± 0.44 (23.28)
K_X (mgCOD X_S/mgCOD X_H)	0.4 ± 0.057 (14.25)	0.41 ± 0.088 (21.46)	0.41 ± 0.067 (16.34)
$Y_{H,S}$ (mgCOD X_H/mgCOD S_S)	0.62 ± 0.3 (48.3)	0.62 ± 0.117 (18.87)	0.62 ± 0.16 (25.8)
Y_{STO} (mgCOD X_{STO}/mgCOD S_S)	0.84 ± 0.171 (20.36)	0.84 ± 0.161 (19.17)	0.84 ± 0.058 (6.9)
$Y_{H,STO}$ (mgCOD X_H/mgCOD X_{STO})	0.74 ± 0.065 (8.78)	0.75 ± 0.16 (21.33)	0.74 ± 0.033 (4.46)
K_1 (mgCOD X_{STO}/mgCOD X_H)	0.732 ± 0.196 (26.78)	0.732 ± 0.062 (8.47)	0.731 ± 0.24 (32.8)
K_2 (mgCOD X_{STO}/mgCOD X_H)	$6.69\text{x}10^{-6} \pm 1.42\text{x}10^{-5}$ (212.3)	$1.0\text{x}10^{-5} \pm 1.95\text{x}10^{-5}$ (195)	$1.0\text{x}10^{-5} \pm 2.8\text{x}10^{-5}$ (280)
τ (min)	19.36 ± 2.4 (12.4)	21.97 ± 1.2 (5.46)	19.5 ± 1.7 (8.71)
Parameters Assumed:			
b_H (1/min)	0.00036	0.00036	0.00036
b_{STO} (1/min)	0.00036	0.00036	0.00036
k_{NHacc} (1/min)	0.000056	0.000056	0.000056
f_{STO}[b] (mgCOD X_{STO}/mgCOD S_S)	0.64	0.64	0.64
f_{XI} (mgCOD /mgCOD)	0.2	0.2	0.2
k_I (1/min)	--	1.0762	1.0762
$K_L a_{CO2}$ (1/min)	--	0.055	0.055
$C_{T,init}$[b] (mmol/L)	--	0.73	0.73
Parameters Calculated:			
HCO_3 (mmol/L)	--	0.7244	0.7244
CO_2 (mmol/L)	--	0.0056	0.0056
k_{STO} (1/min)	0.00686	0.006968	0.006968
$\mu_{MAX,S}$ (1/min)	0.002844	0.002889	0.002889
$\mu_{MAX,STO}$ (1/min)	0.002844	0.002889	0.002889
X_H (mgCOD/L)	220	220	220
MSE[a]	$1.64\text{x}10^{-4}$	$8.31\text{x}10^{-5}$	$1.1\text{x}10^{-4}$

[a] MSE refers to the mean squared error which is calculated from sum of squared errors divided by number of observations

[b] Parameters were fixed by trials for the better fit of experimental profile with the model

Table 5.6: Parameter estimation results using respirometric-titrimetric measurements for the pH of 7.8 (confidence intervals are shown in brackets as percentages)

Parameters	Respirometric data alone (Confidence interval, %)	Titrimetric data alone (Confidence interval, %)	Combined data (Confidence interval, %)
Parameters Estimated:			
q_{MAX} (1/min)	$0.0125 \pm 9.2\times10^{-4}$ (7.36)	$0.0125 \pm 1.6\times10^{-3}$ (12.8)	$0.0125 \pm 4.73\times10^{-4}$ (3.78)
k_h (1/min)	$0.0191 \pm 9.6\times10^{-4}$ (5.03)	$0.016 \pm 8.6\times10^{-4}$ (5.38)	$0.0189 \pm 1.7\times10^{-3}$ (8.99)
K_S (mgCOD/L)	0.62 ± 0.061 (9.84)	0.59 ± 0.085 (14.4)	0.6 ± 0.087 (14.5)
K_X (mgCOD X_S/mgCOD X_H)	0.42 ± 0.045 (10.71)	0.42 ± 0.074 (17.62)	0.42 ± 0.046 (10.95)
$Y_{H,S}$ (mgCOD X_H/mgCOD S_S)	0.64 ± 0.087 (13.59)	0.64 ± 0.114 (17.8)	0.64 ± 0.075 (11.72)
Y_{STO} (mgCOD X_{STO}/mgCOD S_S)	0.84 ± 0.17 (20.2)	0.84 ± 0.085 (10.12)	0.84 ± 0.024 (2.86)
$Y_{H,STO}$ (mgCOD X_H/mgCOD X_{STO})	0.73 ± 0.144 (19.73)	0.73 ± 0.19 (26.02)	0.73 ± 0.052 (7.12)
K_1 (mgCOD X_{STO}/mgCOD X_H)	0.7 ± 0.106 (15.14)	0.7 ± 0.209 (29.86)	0.7 ± 0.047 (6.71)
K_2 (mgCOD X_{STO}/mgCOD X_H)	$8.1\times10^{-6} \pm 2.8\times10^{-5}$ (345.7)	$8.2\times10^{-6} \pm 1.1\times10^{-5}$ (134.2)	$8.2\times10^{-6} \pm 2.1\times10^{-5}$ (256.1)
τ (min)	11.72 ± 1.05 (8.96)	8.18 ± 0.68 (8.31)	11.7 ± 0.5 (4.27)
Parameters Assumed:			
b_H (1/min)	0.00036	0.00036	0.00036
b_{STO} (1/min)	0.00036	0.00036	0.00036
k_{NHacc} (1/min)	0.000056	0.000056	0.000056
f_{STO} [b] (mgCOD X_{STO}/mgCOD S_S)	0.65	0.65	0.65
f_{XI} (mgCOD /mgCOD)	0.2	0.2	0.2
k_1 (1/min)	--	1.0762	1.0762
$K_L a_{CO2}$ (1/min)	--	0.055	0.055
$C_{T,init}$ [b] (mmol/L)	--	1.2	1.2
Parameters Calculated:			
HCO_3 (mmol/L)	--	1.1549	1.1549
CO_2 (mmol/L)	--	0.0451	0.0451
k_{STO} (1/min)	0.006857	0.006849	0.006849
$\mu_{MAX,S}$ (1/min)	0.002812	0.002809	0.002809
$\mu_{MAX,STO}$ (1/min)	0.002812	0.002809	0.002809
X_H (mgCOD/L)	200	200	200
MSE [a]	7.58×10^{-5}	3.98×10^{-5}	7.45×10^{-5}

[a] MSE refers to the mean squared error which is calculated from sum of squared errors divided by number of observations

[b] Parameters were fixed by trials for the better fit of experimental profile with the model

Table 5.7: Parameter estimation results using respirometric-titrimetric measurements for the pH of 7 (confidence intervals are shown in brackets as percentages)

Parameters	Respirometric data alone (Confidence interval, %)	Titrimetric data alone (Confidence interval, %)	Combined data (Confidence interval, %)
Parameters Estimated:			
q_{MAX} (1/min)	$0.0119 \pm 1.0\text{x}10^{-3}$ (8.4)	$0.0112 \pm 1.16\text{x}10^{-3}$ (10.35)	$0.0119 \pm 6.2\text{x}10^{-4}$ (5.21)
k_h (1/min)	$0.025 \pm 2.4\text{x}10^{-3}$ (9.6)	$0.024 \pm 4.61\text{x}10^{-3}$ (19.2)	$0.025 \pm 5.9\text{x}10^{-3}$ (23.6)
K_S (mgCOD/L)	0.6 ± 0.088 (14.67)	0.6 ± 0.17 (28.33)	0.6 ± 0.11 (18.33)
K_X (mgCOD X_S/mgCOD X_H)	0.45 ± 0.08 (17.78)	0.46 ± 0.13 (28.2)	0.46 ± 0.12 (26.08)
$Y_{H,S}$ (mgCOD X_H/mgCOD S_S)	0.68 ± 0.14 (20.58)	0.68 ± 0.036 (5.29)	0.68 ± 0.028 (4.12)
Y_{STO} (mgCOD X_{STO}/mgCOD S_S)	0.88 ± 0.094 (10.68)	0.88 ± 0.03 (3.41)	0.88 ± 0.008 (0.91)
$Y_{H,STO}$ (mgCOD X_H/mgCOD X_{STO})	0.64 ± 0.087 (13.59)	0.64 ± 0.055 (8.59)	0.64 ± 0.046 (7.19)
K_1 (mgCOD X_{STO}/mgCOD X_H)	0.55 ± 0.13 (23.64)	0.55 ± 0.18 (32.7)	0.55 ± 0.03 (5.45)
K_2 (mgCOD X_{STO}/mgCOD X_H)	$1.0\text{x}10^{-6} \pm 3.05\text{x}10^{-6}$ (305)	$1.0\text{x}10^{-6} \pm 3.07\text{x}10^{-6}$ (307)	$1.0\text{x}10^{-6} \pm 2.66\text{x}10^{-6}$ (266)
τ (min)	7.82 ± 0.86 (10.99)	7.81 ± 0.95 (12.16)	7.88 ± 0.3 (3.81)
Parameters Assumed:			
b_H (1/min)	0.00036	0.00036	0.00036
b_{STO} (1/min)	0.00036	0.00036	0.00036
k_{NHacc} (1/min)	0.000056	0.000056	0.000056
f_{STO}[b] (mgCOD X_{STO}/mgCOD S_S)	0.7	0.7	0.7
f_{XI} (mgCOD /mgCOD)	0.2	0.2	0.2
k_1 (1/min)	--	1.0762	1.0762
$K_L a_{CO2}$ (1/min)	--	0.055	0.055
$C_{T,init}$[b] (mmol/L)	--	0.55	0.55
Parameters Calculated:			
HCO_3 (mmol/L)	--	0.4412	0.4412
CO_2 (mmol/L)	--	0.1088	0.1088
k_{STO} (1/min)	0.007347	0.006915	0.007347
$\mu_{MAX,S}$ (1/min)	0.002428	0.002292	0.002435
$\mu_{MAX,STO}$ (1/min)	0.002428	0.002292	0.002435
X_H (mgCOD/L)	240	240	240
MSE[a]	$9.66\text{x}10^{-5}$	$3.9\text{x}10^{-5}$	$1.14\text{x}10^{-4}$

[a] MSE refers to the mean squared error which is calculated from sum of squared errors divided by number of observations

[b] Parameters were fixed by trials for the better fit of experimental profile with the model

5.5.3 Discussion on estimated parameters for three different pH

The estimated kinetic parameters $\mu_{MAX,S}$, k_{STO}, k_h, K_S and K_X from different pH studies with their standard deviations are compared in Figure 5.13. The estimated parameters $\mu_{MAX,S}$ and k_{STO} show no significant variation for the three pH levels. The mean value for the parameter $\mu_{MAX,S}$ varies from 0.172 to 0.143 h^{-1}, and the estimated parameter k_{STO} falls within the range 0.416-0.432 h^{-1} for the pH of 8.5 and 7 respectively. The effect of the parameter K_X with the varying pH levels is also found to be insignificant as the estimated parameter lies between 0.40 and 0.46 mg/mg for the pH of 8.5 and 7 respectively. However, both the kinetic parameters, hydrolysis rate (k_h) and substrate affinity constant (K_S), are found to be sensitive to the sludge

pH. The estimated parameters k_h and K_S show the optimum result at pH 7 compared to that for alkaline conditions (at pH 8.5).

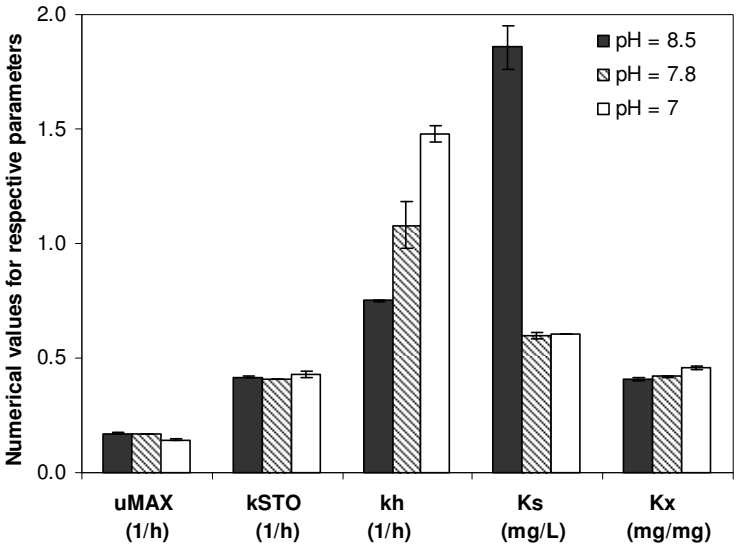

Figure 5.13: Comparison of kinetic parameters for three different pH levels of sludge (SDS = 75 mg COD/L)

Figure 5.14 demonstrates the relative stoichiometric parameters for three different pH levels (8.5, 7.8 and 7) with a constant SDS concentration of 75 mg COD/L in activated sludge. The yield coefficients $Y_{H,S}$ and Y_{STO} are observed to increase when the pH was maintained at 7. The parameter $Y_{H,S}$ lies between 0.62 and 0.68 for pH levels of 8.5 and 7 respectively. Besides, the yield coefficient Y_{STO} is higher than the yield coefficient $Y_{H,S}$ which is estimated as 0.84, 0.84 and 0.88 for the pH levels at 8.5, 7.8 and 7 respectively. Though the yield coefficient $Y_{H,STO}$ falls within a narrow range (0.73-0.74) when pH was kept at 7.8 and above, the parameter is found to have dropped to 0.64 in low pH study (7). No significant difference is observed for the estimated parameter f_{STO} (0.64-0.65) when pH was maintained at 8.5 or 7.8; however it jumps to 0.7 when the pH from 7.8 to 7 referring the storage formation prominent at pH 7. Parameter estimation showed similar trend in acetate biodegradation study where the f_{STO} was found to be higher at pH 7 compared to that at pH 7.8 (see section 4.6 in Chapter 4).

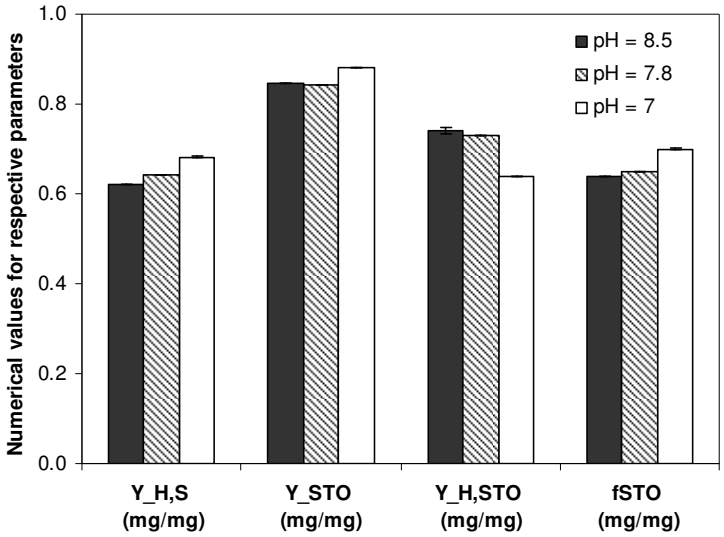

Figure 5.14: Comparison of stoichiometric parameters for three different pH levels of sludge (SDS = 75 mg COD/L)

5.6 Monod kinetic parameters for SDS biodegradation

Monod kinetic parameters for surfactant (SDS) biodegradation were estimated in this study and compared with those for acetate biodegradation. Figure 5.15 represents the estimated biomass growth rate against initial substrate concentration with calibrated Monod profile. Coefficient of determination (R^2) was calculated as 0.99 and 0.95 for the test substrate SDS and acetate respectively. Estimated parameters K_S and $\mu_{MAX,S}$ for SDS and acetate biodegradation are presented in Table 5.8. While the acetate biodegradation gives the maximum biomass growth rate on substrate ($\mu_{MAX,S}$) as 1.81 day^{-1}, high growth rate (4.15 day^{-1}) was observed when the SDS was used as test substrate elevating Monod profile for SDS degradation over the acetate case. Chen et al. (2001) noted a high biomass growth rate (8.88 day^{-1}) in their SDS biodegradation study, whereas Zhang et al. (1999) estimated the growth rate as 2.76 day^{-1} when using a Monod model for calibration. Besides, Anderson et al. (1990) estimated the parameter $\mu_{MAX,S}$ to range from 0.67 to 2.01 day^{-1} by calibrating the exponential growth based model with residual SDS measurements. In this current research, the substrate affinity constant K_S for SDS and acetate biodegradation were estimated to be 0.65 and 0.84 mg COD/L respectively. The observation reveals that the substrate SDS is biodegradable in nature as is acetate, although SDS has a relatively complex molecular structure compared to acetate. It is noteworthy that the sludge was

sufficiently acclimatized (for 15 days) with SDS before starting the main batch experiments to enhance the adaptation capacity of the biomass with SDS. It may have resulted in the biomass showing a high affinity to SDS during the biodegradation.

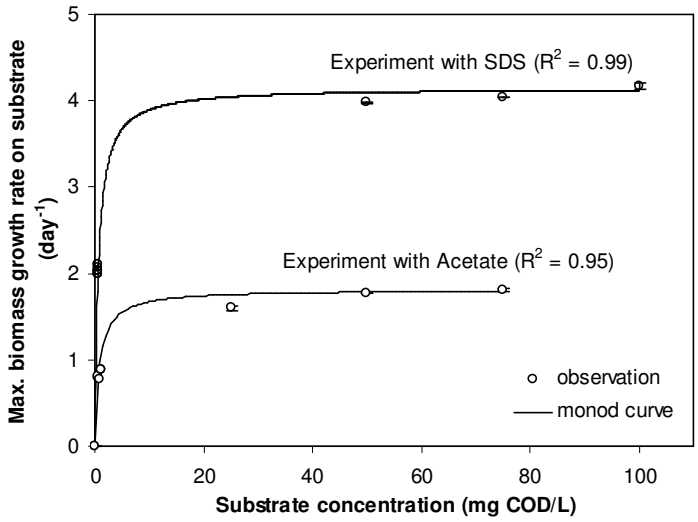

Figure 5.15: Monod profile for maximum biomass growth rate on substrate (SDS and acetate) at pH of 7.8

Table 5.8: Estimated Monod kinetics for SDS and acetate biodegradation at pH 7.8

Parameter	SDS	Acetate
K_S (mg COD/L)	$0.65 \pm 1.6 \times 10^{-4}$	$0.84 \pm 1.27 \times 10^{-3}$
$\mu_{MAX,S}$ (day^{-1})	$4.15 \pm 3.3 \times 10^{-6}$	$1.81 \pm 7.7 \times 10^{-4}$

5.7 Conclusions

The simultaneous storage and growth (SSAG) model was improved during this study by considering the SDS biodegradation pathway and calibrating the model using both the respirometric and titrimetric measurements in an activated sludge system. The proposed model introduced the hydrolysis process and considered the non-linear carbon dioxide transfer rate in the liquid medium. In addition to the respirometry all relevant stoichiometric parameters were considered to enable the proposed model to explain the titrimetric measurements of SDS biodegradation process. The proposed SSAG model was successfully calibrated for different initial SDS concentrations and

pH levels of the sludge. Parameter estimations from three different calibration approaches were found to be satisfactory and show very close results that validate the proposed model. Besides, off-line measurements of COD and ammonium concentration confirm the accuracy and validity of the model. Among the model parameters, the hydrolysis rate and substrate affinity constant are found to be sensitive to the pH. The biomass growth rate on substrate was noted as faster for SDS compared to that for acetate for a constant pH (7.8) in the activated sludge system. Moreover, the study reveals that the test surfactant SDS is readily biodegradable in nature and has a similar substrate affinity as acetate when the sludge is properly acclimatized with the respective substrate.

Chapter 6
Modeling of Nitrification Process

6.1 Introduction

This chapter investigates the nitrification kinetics of organic nitrogen in an activated sludge system using urea as a test substrate. It describes a proposed bio-kinetic model for urea nitrification. The model includes hydrolysis and dynamic carbon dioxide transfer in the liquid medium to explain both the experimental respirometric and titrimetric behavior. This chapter further discusses the model calibration and parameter estimation using three different calibration approaches for three different initial urea concentrations. The suitability of the proposed model for explaining inorganic nitrogen (ammonium) biodegradation in an activated sludge process is also described. The discussion also includes the model calibration and parameter estimation for nitrification using ammonium as a substrate. Model validation was performed in this current research project using off-line NH_4-N, NO_2-N and NO_3-N measurements. The chapter concludes with the estimation of Monod kinetic parameters for both the urea and ammonium nitrification processes.

6.2 Experimental observations during nitrification

6.2.1 Urea as a test substrate

In this experiment, nitrification in an activated sludge system was investigated using urea as an organic nitrogen source. A series of batch experiments with initial urea concentrations of 5, 10 and 20 mg N/L was conducted to observe the influence of urea on nitrification. The activated sludge, which was used in this research project, was fed with urea for 5 days prior to the commencement of the main experiments to allow the microorganisms to acclimatize with the test substrate so that they could perform the biodegradation to their maximum capacity. A constant pH at 7.8 ± 0.03 was maintained during the urea nitrification study.

Figure 6.1 represents the OUR and titrimetric profiles when three different initial urea concentrations were added to an activated system. The OUR profiles follow the same pattern in all concentration studies. The OUR increases to a maximum level due to the consumption of urea under the feast period. The peak of the OUR profile is found to increase proportionally with the increase of initial substrate concentration. The OUR then drops to a level producing a "tail" in the OUR profile which finally decreases gradually to an endogenous OUR level. This kind of "tail" in the nitrification process was also noted in the literature and explained as due to nitrite accumulation in the liquid medium (Brouwer et al., 1998). It was also confirmed through off-line measurements where significant nitrite accumulated during the nitrification process (Figure 6.10).

Urea nitrification initially causes acid addition to the reactor followed by a continuous base addition under feast conditions (Figure 6.1). Equation 6.1 also shows that urea hydrolysis results in proton consumption in the liquid medium. The current study reveals that urea is hydrolyzed to ammonium at a very fast rate (see the sub-section 6.4.2 for the detail). Hence, the substrate urea was often treated as a readily biodegradable compound like ammonium and hydrolysis was excluded in the nitrification modeling (Gernaey et al., 2001) to keep the model simple. However, this does not reflect the real life situation. Though the proton consumption (acid addition) during the urea nitrification is minor compared to the proton production (base addition) in the system, both the acid and base addition were found to increase proportionally with the increase in initial urea concentration as presented in Figure 6.1. After the end of the feast period, the CO_2 stripping leads the titrimetric process to drop the profile to the background proton consumption (acid addition) rate which was also observed before the addition of urea to the reactor when pH was maintained at 7.8.

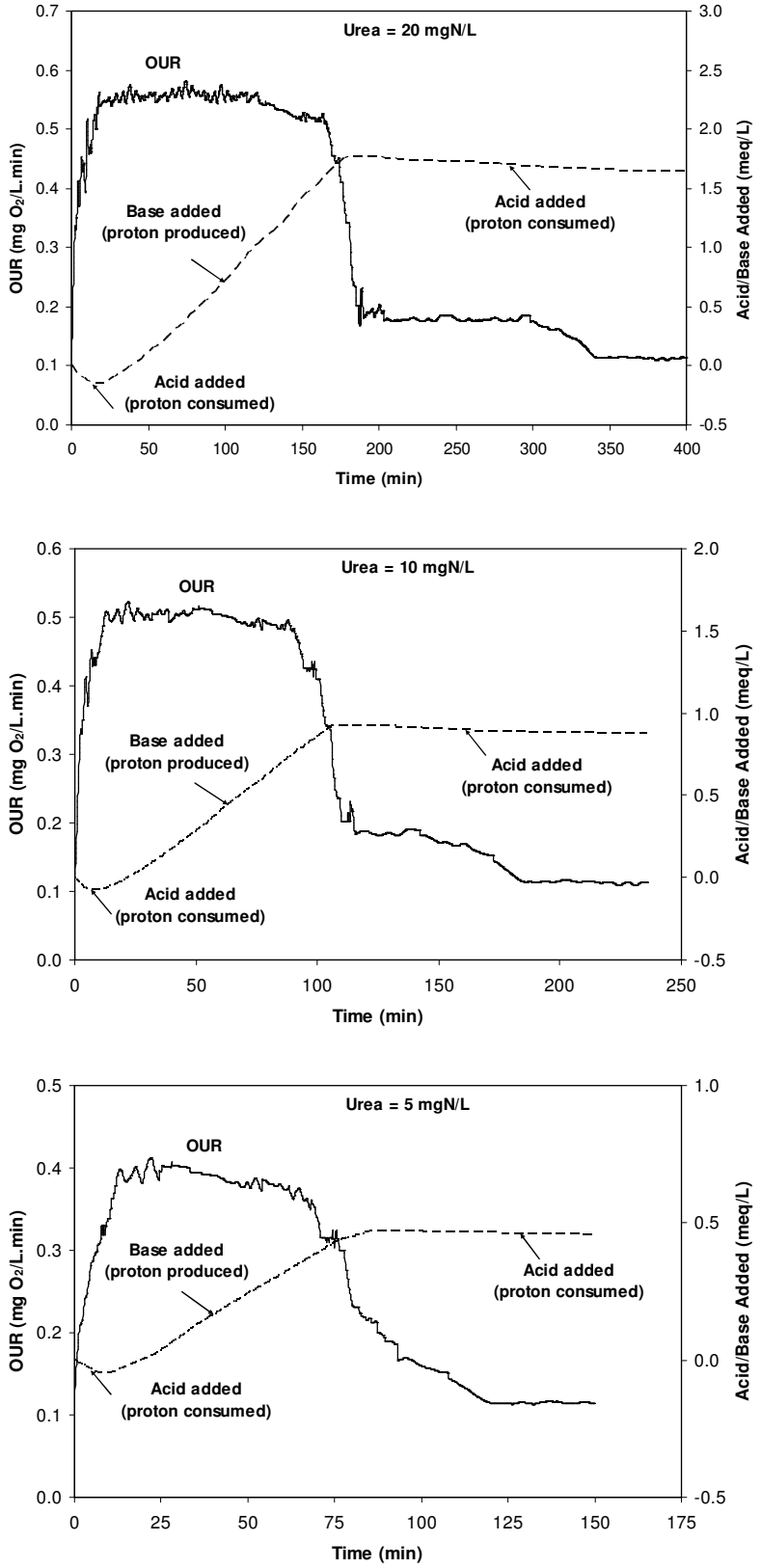

Figure 6.1: OUR with titrimetric profiles for three different urea concentrations in an activated sludge system

6.2.2 Ammonium as a test substrate

Inorganic nitrogen biodegradation was investigated using ammonium (synthetic NH_4Cl solution), which has a relatively simple chemical composition compared to that of urea, as a test substrate. The activated sludge was properly acclimatized with the substrate ammonium to enhance the metabolic functions during the aerobic biodegradation process (see sub-section 3.2.3 in Chapter 3). Three different initial ammonium concentrations (2.5, 6.5 and 11 mg N/L) were added to the reactor to investigate the effect of the concentration on the ammonium nitrification process by maintaining the same pH (7.8 ± 0.03) as used during the urea nitrification.

Figure 6.2 illustrates the OUR and titrimetric profiles for the three different initial ammonium concentrations in an activated system. The OUR pattern is found to be similar to that of the urea nitrification study (see Figure 6.1 and Figure 6.2). For each ammonium concentration, the OUR reaches a maximum level immediately after adding the substrate and is followed by a "tail" indicating nitrite accumulation in the liquid medium (Brouwer et al., 1998). Off-line NO_2-N measurements also confirmed nitrite accumulation in the system (see Figure 6.11). Similar to the urea study, the maximum oxygen rate increased with the increase in initial ammonium concentration.

In addition, Figure 6.2 shows the titrimetric profile of the ammonium nitrification process for three different initial substrate concentrations. This study reveals that base addition occurs only during the feast period of ammonium nitrification. A similar observation was noted in the literature where proton production took place during the ammonium consumption period in an activated sludge system (Gernaey et al., 1997, 2001; Petersen et al., 2001, Yuan and Bogaert, 2001). In this current study, the base addition was found to increase proportionally with the increase in initial ammonium concentration. Under the endogenous phase, the titrimetric profile reaches its background proton consumption (acid addition) rate as observed before adding ammonium to the reactor. This was also noticed during urea nitrification. Moreover, the background proton consumption was noted in the acetate and surfactant biodegradation study particularly when the pH was maintained at 7.8 as the

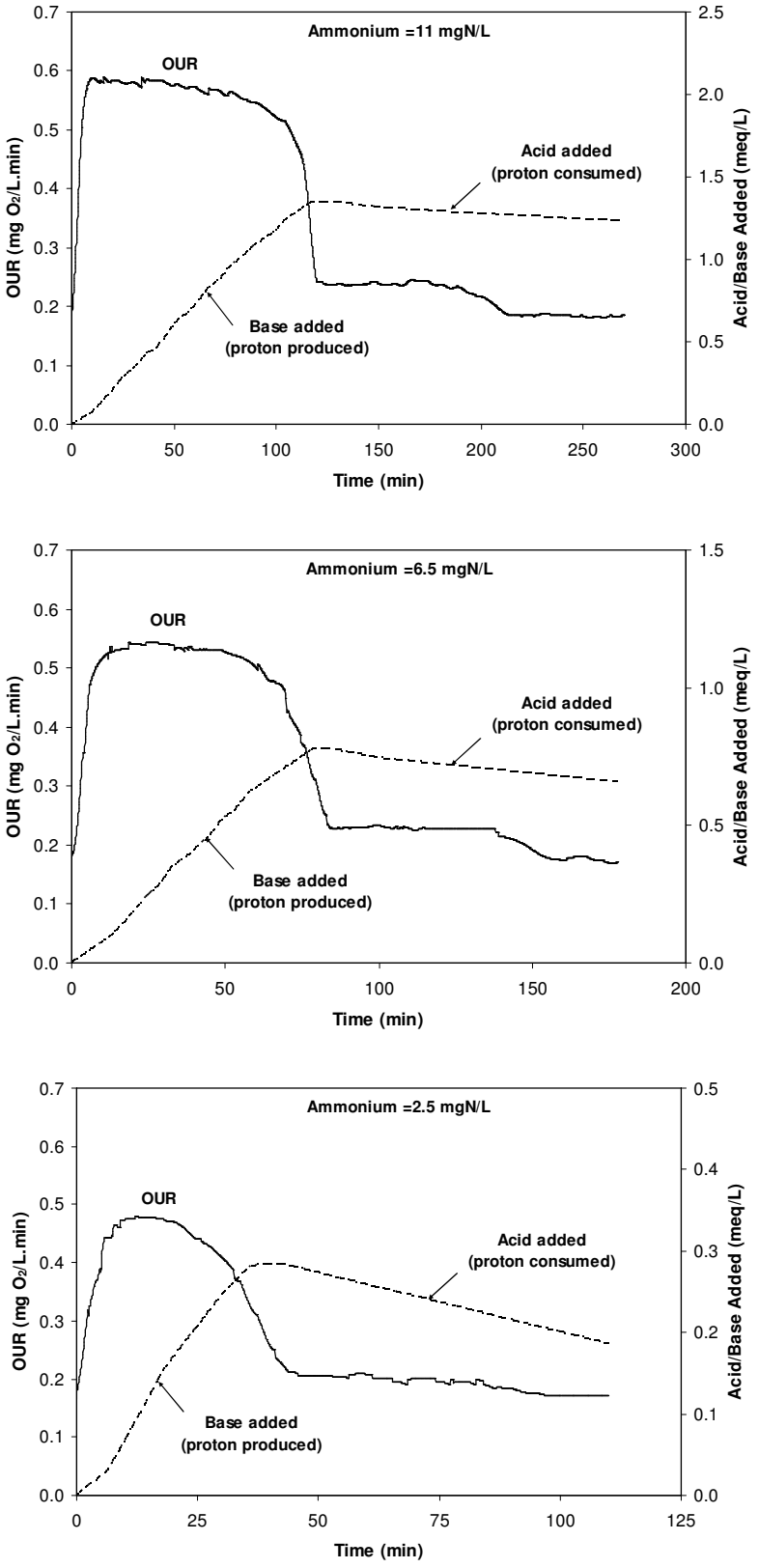

Figure 6.2: OUR with titrimetric profiles for three different ammonium concentrations in an activated sludge system

CO_2 stripping leads the titrimetric process during the endogenous period (Sin and Vanrolleghem, 2007) (see Chapter 4 and Chapter 5 for more information).

6.3 Proposed model for nitrification

Development of a biodegradation model for a simple organic nitrogen source such as urea has been demonstrated in the literature with a two-step nitrification model where a constant carbon dioxide transfer rate (CTR) was assumed during modeling (Gernaey et al., 2001). According to Pratt et al. (2003, 2004), a constant CTR may be applicable only when the system is controlled with a low CO_2 transfer coefficient at a pH higher than 8. Consequently, Sin and Vanrolleghem (2007) considered a non-linear CTR in the liquid phase and proposed a titrimetric model for acetate biodegradation. However, there is no reference in the literature depicting the titrimetric model for nitrification that pays due attention to the dynamic CTR process taking place in the liquid phase in an activated sludge system. In addition, Gernaey et al. (2001) determined the urea biodegradation kinetics without including the hydrolysis process in the model structure that does not reflect reality (see equation 6.1 for the process details).

Hence, in this dissertation, a nitrification model is proposed considering the hydrolysis process and the physical-chemical interactions of CO_2 in the liquid medium to enable a model-based interpretation of both the respirometric and titrimetric behavior in an activated sludge system. The major steps during the biodegradation process include ammonification, ammonium oxidation, nitrite oxidation, endogenous respiration, aqueous CO_2 equilibrium and stripping of CO_2 (see Table 6.1 for process matrix). The following sub-sections describe the basic theory corresponding to the proposed titrimetric model development.

6.3.1 Ammonification

Ammonification represents the hydrolysis of urea (NH_2CONH_2) to ammonium (NH_4^+) in the presence of the enzyme *urease* in the environment. Equation 6.1 shows the conversion of urea to ammonium where proton (H^+) is consumed and bicarbonate (HCO_3^-) is released in the environment (Havlin, Beaton, Tisdale and Nelson, 1999).

Sometimes, the proton consumption is expressed in terms of hydroxyl ion (OH^-) production in the system (Fujita et al., 2008), which, in turn, represents the same conversion process.

$$NH_2CONH_2 + H^+ + 2H_2O \rightarrow 2NH_4^+ + HCO_3^- \quad \text{----- (Equation 6.1)}$$

Based on the chemical conversion as shown in the above equation, the proton production during hydrolysis can be estimated using the model matrix (Table 6.1). The kinetic expression used by Spanjers and Vanrolleghem (1995) for ammonification (as hydrolysis) was applied in the proposed model based on the assumption that ammonification is not dependent on biomass concentration.

6.3.2 Ammonium oxidation (Nitrification step 1)

Ammonium is oxidized to nitrite by *Nitrosomonas* species during the first nitrification step by releasing proton in the liquid medium. Equation 6.2 represents the biochemical conversion of ammonium to nitrite assuming CO_2 as the carbon source required for autotrophic microorganisms biosynthesis (Gernaey et al., 1998). The equation is expressed in molar unit basis where elemental conservation and a balance of the degrees of reduction were used to determine the stoichiometric coefficient.

$$\left(\frac{1}{Y_{SA1}} + c\right)NH_4(mmol-N) + \frac{1}{2}\left(\frac{3}{Y_{SA1}} - \frac{\gamma_X}{2}\right)O_2(mmol) + CO_2(mmol-C) \quad \text{----- (Equation 6.2)}$$
$$\rightarrow 1CH_aO_bN_c(C-mmol) + \frac{1}{Y_{SA1}}NO_2(mmol-N) + (...)H_2O + \left(\frac{2}{Y_{SA1}} + c\right)H^+(mmol)$$

In the above equation, $CH_aO_bN_c$ represents the elemental composition of biomass and γ_X represents the degree of reduction of the biomass which is calculated as 4+a-2b-3c. Y_{SA1} is the autotrophic biomass yield of the first nitrification step (molar unit basis). Equation 6.3 is the stoichiometric expression that can be derived by converting the units from mol-N to g N and C-mol to g COD and dividing both sides of equation 6.2 with "$8\gamma_X$" where 8 gCOD is assumed as equivalent for each mol electron (Henze et al., 2000).

$$\left(\frac{1+Y_{A1}i_{NBM}}{Y_{A1}}\right)(mgN)NH_4+\left(\frac{3.43-Y_{A1}}{Y_{A1}}\right)(mgCOD)O_2+\frac{1}{8\gamma_X}(mmol)CO_2$$
$$\rightarrow 1(mgCOD)CH_aO_bN_c+\frac{1}{Y_{A1}}(mgN)NO_2+(...)H_2O+\left(\frac{2+Y_{A1}i_{NBM}}{14Y_{A1}}\right)(mmol)H^+ \quad \text{----- (Equation 6.3)}$$

Here, Y_{A1} refers to the autotrophic biomass yield of the first nitrification step (mgCOD/mgN) which is equal to $8Y_{SA1}.\gamma_X/14$. The coefficient related to CO_2 and proton (H^+) production/consumption are expressed in molar units that is more relevant to titrimetric analysis. In Table 6.1, the parameter "p" represents the fraction of NH_4^+ in the liquid phase which is derived as $1/(1+10^{pH-\ pK_{NH4}})$ by Gernaey et al. (2002a). A single component for biomass concentration (X_B) was used to keep the proposed model simple. A combined parameter $f_{BA}.X_B$ was used to express the growth kinetics, where the coefficient f_{BA} represents the fraction of autotrophs in the mixed culture (Table 6.1).

6.3.3 Nitrite oxidation (Nitrification step 2)

Second nitrification step represents the conversion of nitrite (NO_2) to nitrate (NO_3) by *Nitrobacter* species. In a similar way as stated above, the consumption of CO_2 due to the biomass growth on nitrite can be estimated by using the following C-mol basis expression (equation 6.4):

$$cNH_3(mmol-N)+\frac{1}{Y_{SA2}}NO_2(mmol-N)+\frac{1}{2}\left(\frac{1}{Y_{SA2}}-\frac{\gamma_X}{2}\right)O_2(mmol)+CO_2(mmol-C)$$
$$\rightarrow 1CH_aO_bN_c(C-mmol)+\frac{1}{Y_{SA2}}NO_3(mmol-N)+(...)H_2O \quad \text{----- (Equation 6.4)}$$

In equation 6.4, Y_{SA2} is the autotrophic biomass yield of the second nitrification step (molar unit basis). The same biomass composition was assumed for both the *Nitrosomonas* and *Nitrobacter* species to avoid complexity in the modeling. Equation 6.5 can be derived similarly as described in the above section where the growth yield, Y_{A2} is presented in terms of gCOD/gN that is equal to $8Y_{SA2}.\gamma_X/14$. The coefficient related to ammonia uptake (i_{NBM}) is expressed as gN per gCOD biomass unit basis and can be determined from the relation $14c/8\gamma_X$ (Sin, 2004).

$$i_{NBM}(mgN)NH_3 + \frac{1}{Y_{A2}}(mgN)NO_2 + \left(\frac{1.14 - Y_{A2}}{Y_{A2}}\right)(mgCOD)O_2 + \frac{1}{8\gamma_X}(mmol)CO_2 \rightarrow 1(mgCOD)CH_aO_bN_c + \frac{1}{Y_{A2}}(mgN)NO_3 + (...)H_2O$$ ----- (Equation 6.5)

In addition, the above equation demonstrates the stoichiometric components related to ammonia and oxygen uptake for a unit biomass growth (mg COD basis) during the second step nitrification process (see model matrix in Table 6.1).

6.3.4 Endogenous respiration

The biological reaction during endogenous respiration leads to CO_2 production that can be estimated using the stoichiometric expression as shown in equation 6.6.

$$1(mgCOD)CH_aO_bN_c + 1(mgCOD)O_2 \rightarrow \frac{1}{8\gamma_X}(mmol)CO_2 + (...)H_2O + i_{NBM}(mgN)NH_3$$ ----- (Equation 6.6)

Table 6.1 presents the production of CO_2 for the respective oxygen uptake of (1-f_{XI}) g COD (as derived by Sin and Vanrolleghem, 2007).

6.3.5 Aqueous CO_2 equilibrium

The kinetics and stoichiometry related to the process aqueous CO_2 equilibrium are kept the same as those used during the acetate and surfactant biodegradation modeling (see Chapter 4 and Chapter 5).

6.3.6 CO_2 stripping

Model components for CO_2 stripping are kept the same as those used during the acetate and surfactant biodegradation modeling (see Chapter 4 and Chapter 5).

Table 6.1: Process matrix involved in the proposed model for urea nitrification

Process	X_B (g COD)	X_N (g N)	S_{NH} (g N)	S_{NO_2} (g N)	S_{NO_3} (g N)	S_O (g O_2)	S_{HCO_3} (mol)	S_{CO_2} (mol)	S_{Hp} (mol)	Kinetics
Ammonification		-1	1				$\frac{1}{28}$		$-\frac{1}{28}$	$k_N.X_N$
S_{NH} Oxidation (Nitrification 1)	1		$-\frac{1}{Y_{A1}}-i_{NBM}$	$\frac{1}{Y_{A1}}$		$-\frac{3.43-Y_{A1}}{Y_{A1}}$	--	$-\frac{1}{8\gamma_X}$	$\frac{i_{NBM}\,p}{14}+\frac{1}{7Y_{A1}}$	$(1-e^{-t/\tau}).\mu_{MAX,A1}.\frac{S_{NH}}{K_{SA1}+S_{NH}}.f_{BA}.X_B$
S_{NO_2} Oxidation (Nitrification 2)	1		$-i_{NBM}$	$-\frac{1}{Y_{A2}}$	$\frac{1}{Y_{A2}}$	$-\frac{1.14-Y_{A2}}{Y_{A2}}$	--	$-\frac{1}{8\gamma_X}$	$\frac{i_{NBM}\,p}{14}$	$(1-e^{-t/\tau}).\mu_{MAX,A2}.\frac{S_{NO2}}{K_{SA2}+S_{NO2}}.f_{BA}.X_B$
Endogenous respiration	-1		$i_{NBM}-i_{NXI}f_{XI}$			$-(1-f_{XI})$	--	$\frac{1-f_{XI}}{8\gamma_X}$	$-((i_{NBM}-f_{XI}i_{NXI})/14)\,p$	$b\ .X_B$
Aqueous CO_2 equilibrium	--		--			--	1	-1	1	$k_1 S_{CO_2}-k_1 10^{pk_1-pH} S_{HCO_3}$
CO_2 stripping	--		--			--	--	1	--	$K_L a_{CO_2}(S^*_{CO_2}-S_{CO_2})$

The first order expression ($1-e^{-t/\tau}$) is used to explain the start-up phase in the batch experiment (Petersen, 2000)

6.4 Model calibration and parameter estimation

6.4.1 Parameter estimation approach

For both the urea and ammonium nitrification studies, the proposed model was calibrated using three different calibration approaches: using respirometric measurements alone, titrimetric measurements alone and combined respirometric-titrimetric measurements, followed by model parameter estimation. A non-linear technique employing the algorithms in the optimisation toolbox included in MATLAB (R2007a) was used during the parameter estimation process. Minimization of the mean squared error (MSE) between the model and the experimental output was calculated as the main criterion for curve fitting. For proper model evaluation, the proposed model was calibrated using varying initial substrate concentrations. In the urea nitrification study, the initial concentrations of 5, 10 and 20 mg N/L were added to the reactor for the experimental observations, whereas initial concentrations of 2.5, 6.5 and 11 mg N/L were used during the ammonium nitrification kinetics determination.

In the case of urea nitrification, the model parameters k_N, K_{SA1}, K_{SA2}, $\mu_{MAX,A1}$, $\mu_{MAX,A2}$, Y_{A1}, Y_{A2} and τ were estimated along with calculation of 95% confidence intervals, while the parameters K_{SA1}, K_{SA2}, $\mu_{MAX,A1}$, $\mu_{MAX,A2}$, Y_{A1}, Y_{A2} and τ were estimated during the ammonium nitrification study (the parameter k_N was excluded since hydrolysis is not relevant with ammonium nitrification). In this study, the parameter f_{BA} was assumed to be 0.3 based on the fact that the heterotrophic biomass outweighs autotrophic biomass in subtropical regions (Buck et al., 1996). Readers are referred to Appendix A for the description of model parameters.

The ASM default values for the parameters b (0.15 day^{-1}), f_{XI} (0.2) and i_{NXI} (0.02 gN/g COD X_I) were assumed here for the proposed model calibration and parameter estimation. The relationship OUR_{end} (0) = (1-f_{XI}).b.X_B(0) was employed to calculate the initial concentration of biomass, X_B(0). Total inorganic carbon in the aqueous medium, $C_{T,init}$ was adjusted reasonably for different assays to fit the experimental profile with the model one. The initial concentrations of CO_2 and HCO_3 in the reactor were calculated using their relationship with $C_{T,init}$ (Sin, 2004). The

parameter k_1 was adjusted to 1.5 min^{-1} for better curve fitting and lies within the range (0.15 to 1.8 min^{-1}) noted by Stumm and Morgan (1996). During the model calibration, the value for $K_L a_{CO_2}$ was calculated as 0.0728 min^{-1} from the oxygen transfer coefficient ($K_L a$) using the relationship between their diffusivity coefficients (Sperandio and Paul, 1997; Sin and Vanrolleghem, 2007). The parameter pK_1 was taken as 6.39 (Sperandio and Paul, 1997). The default values suggested by Stumm and Morgan (1996) for the parameters pK_{NH4} (9.25) and $S^*_{CO_2}$ (0.017 mmol/L) were assumed during the parameter estimation process. In addition, the degree of reduction of the biomass (γ_X) and the nitrogen content of the biomass (i_{NBM}) were calculated as 4.2 and 0.083 gN/g COD X_B respectively based on the biomass formula of $CH_{1.8}O_{0.5}N_{0.2}$ that was revised later for better curve fitting.

6.4.2 Results and discussions of model calibration for urea

The proposed model was calibrated with the experimental OUR and *Hp* measurements using three different initial urea concentrations of 20, 10 and 5 mg N/L which are presented in Figure 6.3, Figure 6.4 and Figure 6.5 respectively. The parameter estimation results are shown in Table 6.2 to 6.4 where the calibration approaches: using respirometric measurements alone, titrimetric measurements alone and combined respirometric-titrimetric measurements, were applied.

This study reveals that the parameter k_N varies from 0.034 to 0.081 min^{-1} as the urea concentration decreases from 20 to 5 mg N/L. There is little reported in the literature about urea ammonification (hydrolysis) kinetics to compare with current observations. However Spanjers and Vanrolleghem (1995) noted the organic nitrogen hydrolysis rate to be 0.04 min^{-1} when using raw wastewater as a test substrate. The autotrophic maximum growth rate for the first nitrification step ($\mu_{MAX,A1}$) is found to increase from 0.065 to 0.1 day^{-1} when the urea concentration changes from 5 to 20 mg N/L respectively. On the other hand, a very slow biomass growth rate was noticed during the second nitrification step (conversion of nitrite to nitrate) showing an average $\mu_{MAX,A2}$ value of 7.98×10^{-3} day^{-1} (Table 6.2-6.4). It results in nitrite accumulation in the liquid medium which was also confirmed by off-line NO_2-N measurement (Figure 6.10). Though for the overall nitrification process

ASM suggested an autotrophic maximum growth rate higher (0.8 day^{-1} in ASM1, 1.0 day^{-1} in ASM3) than the current observation, Gernaey et al. (2001) observed a maximum autotrophic biomass growth rate as slow as $4.7x10^{-3}$ day^{-1} during the first step of ammonium nitrification process. Parameter estimation results show that the calculated combined parameter $(3.43-Y_{A1})\mu_{MAX,A1}f_{BA}.X_B/Y_{A1}$ lies between 0.264-0.393. It is found to be consistent with the observation of Gernaey et al. (2001) who estimated the average value for the combined parameter as 0.319 for the first step of the urea nitrification process.

The estimated parameter K_{SA1} gives an average value of 0.29 mg N/L that leads to the combined parameter $(3.43-Y_{A1}).K_{SA1}$ as 0.936. However, Gernaey et al. (2001) recorded this combined parameter slightly higher (1.277) than the current observation when investigating urea nitrification kinetics in an activated sludge system. In this current study, the average value for the biomass yield coefficient Y_{A1} is found to be 0.2, whereas the estimated parameter Y_{A2} is found to vary from 0.023-0.029. Though Kim et al. (2009) revealed the yield coefficients Y_{A1} and Y_{A2} as 0.33 and 0.083 respectively; Marsili-Libelli and Tabani (2002) noted the combined autotrophic biomass yield ($Y_{A1} + Y_{A2}$) varied from 0.258 to 0.296. In addition, ASM prescribed the overall autotrophic biomass yield (Y_A) to be 0.24 which supports the current observation.

The titrimetry related component $C_{T,init}$ was adjusted to 1.5 mmol CO_2/L for all three urea concentration studies for the better fit of experimental profiles with the model one. For all three calibration approaches the model parameters are found to be consistent with reasonable confidence intervals (Table 6.2-6.4) which validates the accuracy of the model calibration and parameter estimation processes. In addition, the mean squared errors (MSEs), calculated from three different initial urea concentrations and calibration approaches, are acceptable and statistically confirm the soundness of the proposed model.

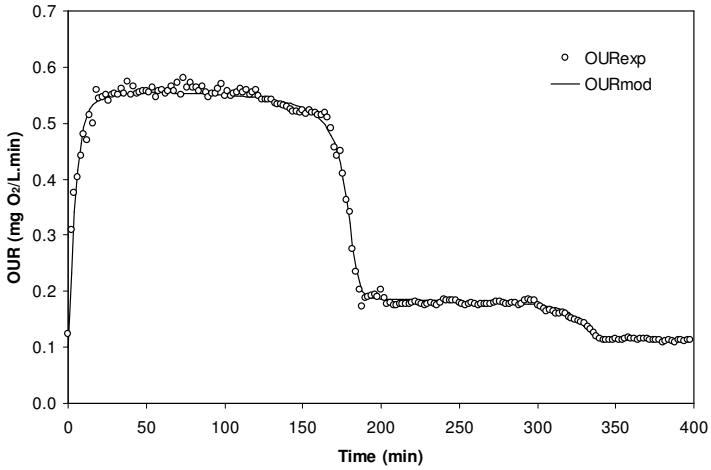

(a)

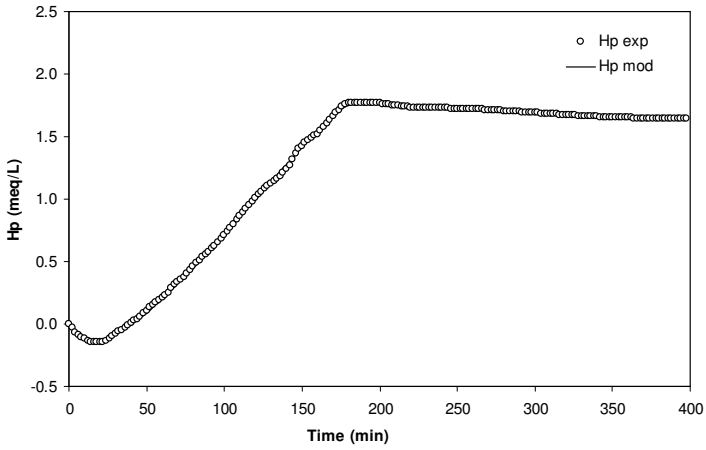

(b)

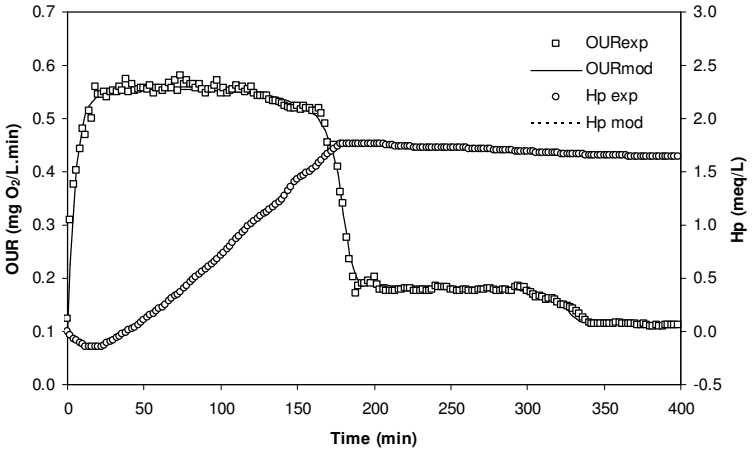

(c)

Figure 6.3: Model calibration using (a) respirometric data alone (b) titrimetric data alone and (c) combined respirometric-titrimetric data (Urea = 20 mg N /L)

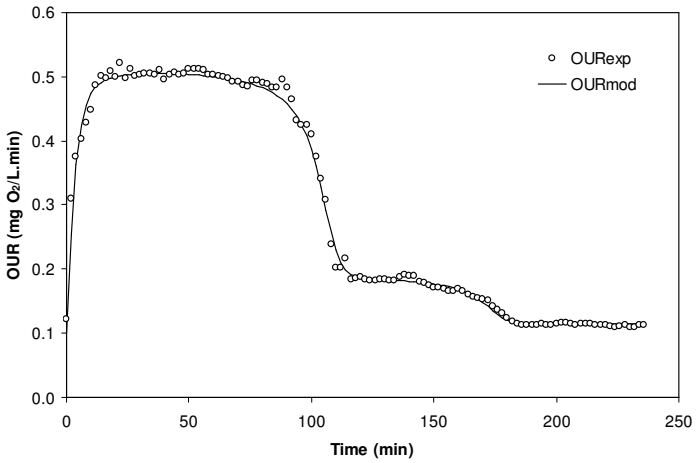

(a)

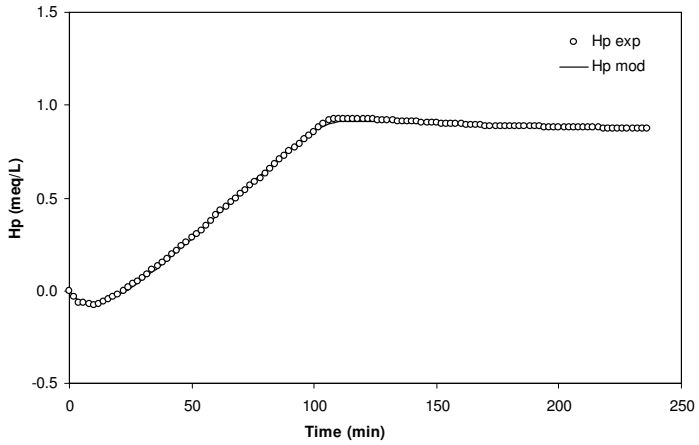

(b)

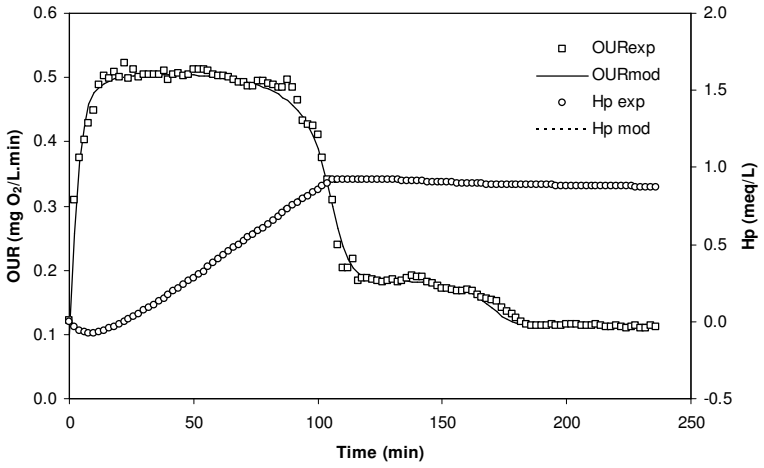

(c)

Figure 6.4: Model calibration using (a) respirometric data alone (b) titrimetric data alone and (c) combined respirometric-titrimetric data (Urea = 10 mg N /L)

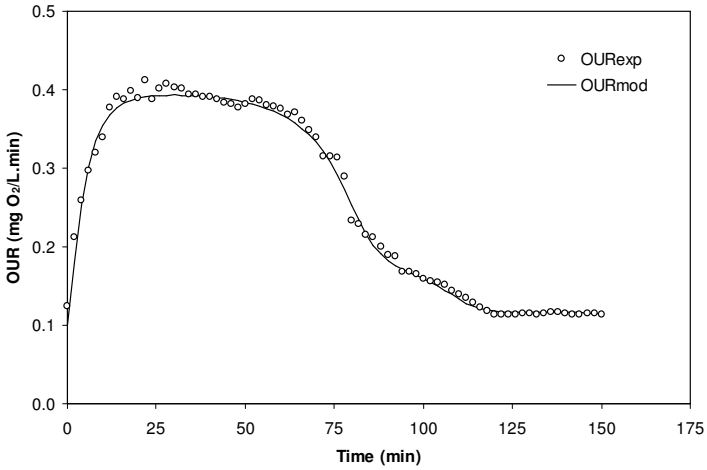

(a)

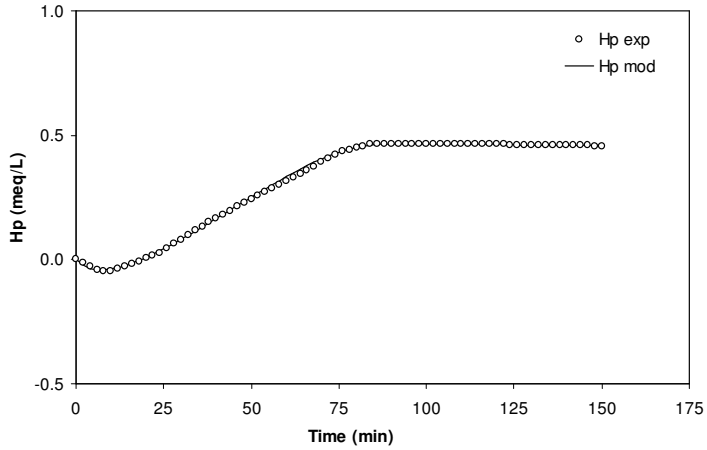

(b)

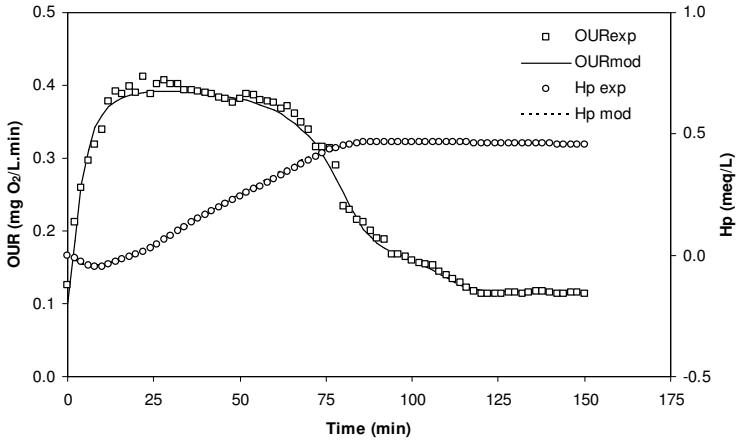

(c)

Figure 6.5: Model calibration using (a) respirometric data alone (b) titrimetric data alone and (c) combined respirometric-titrimetric data (Urea = 5 mg N /L)

Table 6.2: Parameter estimation results using respirometric data alone for three different concentration studies (confidence intervals are shown in brackets as percentages)

Parameters	Urea 20 mg N/L (Confidence interval, %)	Urea 10 mg N/L (Confidence interval, %)	Urea 5 mg N/L (Confidence interval, %)
Parameters Estimated:			
$\mu_{MAX,A1}$ (1/min)	$6.91\times10^{-5} \pm 4.11\times10^{-8}$ (0.06)	$6.22\times10^{-5} \pm 7.14\times10^{-8}$ (0.12)	$4.5\times10^{-5} \pm 4.53\times10^{-8}$ (0.1)
$\mu_{MAX,A2}$ (1/min)	$5.54\times10^{-6} \pm 1.87\times10^{-9}$ (0.03)	$4.86\times10^{-6} \pm 1.4\times10^{-9}$ (0.03)	$4.3\times10^{-6} \pm 2.42\times10^{-9}$ (0.06)
k_N (1/min)	$0.036 \pm 1.37\times10^{-5}$ (0.04)	$0.061 \pm 6.27\times10^{-5}$ (0.1)	$0.081 \pm 9.9\times10^{-4}$ (1.22)
K_{SA1} (mgN/L)	$0.278 \pm 5.56\times10^{-4}$ (0.2)	$0.273 \pm 8.9\times10^{-4}$ (0.33)	$0.271 \pm 2.59\times10^{-4}$ (0.33)
K_{SA2} (mgN/L)	$0.202 \pm 1.82\times10^{-3}$ (0.9)	$0.2 \pm 2.22\times10^{-3}$ (1.1)	0.198 ± 0.011 (5.56)
Y_{A1} (mgCOD X_B/mgN S_{NH})	$0.204 \pm 3.62\times10^{-5}$ (0.02)	$0.204 \pm 7.81\times10^{-5}$ (0.04)	$0.2 \pm 9.23\times10^{-4}$ (0.46)
Y_{A2} (mgCOD X_B/mgN S_{NO2})	$0.029 \pm 6.37\times10^{-6}$ (0.02)	$0.025 \pm 4.27\times10^{-5}$ (0.17)	$0.024 \pm 8.42\times10^{-4}$ (3.51)
Parameters Assumed:			
b (1/min)	0.0001042	0.0001042	0.0001042
f_{XI} (mgCOD /mgCOD)	0.2	0.2	0.2
Parameters Calculated:			
X_B (mgCOD/L)	1200	1200	1200
MSE [a]	1.25×10^{-4}	1.01×10^{-4}	9.6×10^{-5}

[a] MSE refers to the mean squared error which is calculated from sum of squared errors divided by number of observations

Table 6.3: Parameter estimation results using titrimetric data alone for three different concentration studies (confidence intervals are shown in brackets as percentages)

Parameters	Urea 20 mg N/L (Confidence interval, %)	Urea 10 mg N/L (Confidence interval, %)	Urea 5 mg N/L (Confidence interval, %)
Parameters Estimated:			
$\mu_{MAX,A1}$ (1/min)	$6.91\times10^{-5} \pm 7.51\times10^{-8}$ (0.11)	$6.22\times10^{-5} \pm 8.72\times10^{-8}$ (0.14)	$4.51\times10^{-5} \pm 6.83\times10^{-8}$ (0.15)
$\mu_{MAX,A2}$ (1/min)	$5.52\times10^{-6} \pm 1.51\times10^{-9}$ (0.03)	$4.83\times10^{-6} \pm 2.98\times10^{-9}$ (0.06)	$4.3\times10^{-6} \pm 1.15\times10^{-9}$ (0.03)
k_N (1/min)	$0.034 \pm 2.12\times10^{-5}$ (0.06)	$0.059 \pm 1.82\times10^{-5}$ (0.03)	$0.078 \pm 1.04\times10^{-4}$ (0.13)
K_{SA1} (mgN/L)	$0.289 \pm 2.77\times10^{-4}$ (0.1)	$0.3 \pm 3.5\times10^{-4}$ (0.12)	$0.297 \pm 2.55\times10^{-3}$ (0.86)
K_{SA2} (mgN/L)	0.202 ± 0.043 (21.29)	0.2 ± 0.059 (29.5)	0.186 ± 0.092 (49.46)
Y_{A1} (mgCOD X_B/mgN S_{NH})	$0.202 \pm 6.79\times10^{-5}$ (0.03)	$0.204 \pm 1.8\times10^{-5}$ (0.01)	0.198 ± 0.014 (7.07)
Y_{A2} (mgCOD X_B/mgN S_{NO2})	$0.029 \pm 7.24\times10^{-5}$ (0.25)	$0.026 \pm 4.39\times10^{-5}$ (0.17)	0.023 ± 0.013 (56.52)
Parameters Assumed:			
b (1/min)	0.0001042	0.0001042	0.0001042
f_{XI} (mgCOD /mgCOD)	0.2	0.2	0.2
k_l [b] (1/min)	1.5	1.5	1.5
K_La_{CO2} (1/min)	0.0728	0.0728	0.0728
$C_{T,init}$ [b] (mmol/L)	1.5	1.5	1.5
Parameters Calculated:			
HCO_3 (mmol/L)	1.4447	1.4447	1.4447
CO_2 (mmol/L)	0.0553	0.0553	0.0553
X_B (mgCOD/L)	1200	1200	1200
MSE [a]	1.09×10^{-4}	4.77×10^{-5}	4.42×10^{-5}

[a] MSE refers to the mean squared error which is calculated from sum of squared errors divided by number of observations

[b] Parameters were fixed by trials for the better fit of experimental profile with the model

Table 6.4: Parameter estimation results using combined respirometric-titrimetric data for three different concentration studies (confidence intervals are shown in brackets as percentages)

Parameters	Urea 20 mg N/L (Confidence interval, %)	Urea 10 mg N/L (Confidence interval, %)	Urea 5 mg N/L (Confidence interval, %)
Parameters Estimated:			
$\mu_{MAX,A1}$ (1/min)	$6.91\times10^{-5} \pm 7.7\times10^{-8}$ (0.11)	$6.22\times10^{-5} \pm 1.07\times10^{-8}$ (0.02)	$4.5\times10^{-5} \pm 2.45\times10^{-8}$ (0.05)
$\mu_{MAX,A2}$ (1/min)	$5.57\times10^{-6} \pm 2.25\times10^{-9}$ (0.04)	$4.86\times10^{-6} \pm 2.7\times10^{-9}$ (0.06)	$4.3\times10^{-6} \pm 9.96\times10^{-9}$ (0.23)
k_N (1/min)	$0.034 \pm 1.15\times10^{-5}$ (0.03)	$0.059 \pm 1.95\times10^{-5}$ (0.03)	$0.08 \pm 8.93\times10^{-4}$ (1.11)
K_{SA1} (mgN/L)	$0.287 \pm 8.88\times10^{-4}$ (0.31)	$0.289 \pm 9.52\times10^{-4}$ (0.33)	$0.28 \pm 2.42\times10^{-4}$ (0.09)
K_{SA2} (mgN/L)	0.202 ± 0.003 (1.49)	0.2 ± 0.005 (2.5)	0.2 ± 0.047 (23.5)
Y_{A1} (mgCOD X_B/mgN S_{NH})	$0.203 \pm 7.23\times10^{-5}$ (0.04)	$0.204 \pm 1.22\times10^{-4}$ (0.06)	$0.2 \pm 4.9\times10^{-3}$ (2.45)
Y_{A2} (mgCOD X_B/mgN S_{NO2})	$0.029 \pm 7.64\times10^{-5}$ (0.26)	$0.025 \pm 8.21\times10^{-5}$ (0.33)	$0.024 \pm 3.61\times10^{-3}$ (15.04)
Parameters Assumed:			
b (1/min)	0.0001042	0.0001042	0.0001042
f_{XI} (mgCOD /mgCOD)	0.2	0.2	0.2
k_I [b] (1/min)	1.5	1.5	1.5
K_La_{CO2} (1/min)	0.0728	0.0728	0.0728
$C_{T,init}$ [b] (mmol/L)	1.5	1.5	1.5
Parameters Calculated:			
HCO_3 (mmol/L)	1.4447	1.4447	1.4447
CO_2 (mmol/L)	0.0553	0.0553	0.0553
X_B (mgCOD/L)	1200	1200	1200
MSE [a]	1.33×10^{-4}	6.13×10^{-5}	5.66×10^{-5}

[a] MSE refers to the mean squared error which is calculated from sum of squared errors divided by number of observations

[b] Parameters were fixed by trials for the better fit of experimental profile with the model

6.4.3 Results and discussions of model calibration for ammonium

A bio-kinetic model was proposed particularly for urea nitrification. This model resembles the ammonium nitrification model when the ammonification process is excluded from the model structure. Considering this fact, the proposed model was justified for ammonium nitrification by conducting separate sets of experimental observations in an activated sludge system.

The proposed model was successfully calibrated for three different initial ammonium concentrations of 11, 6.5 and 2.5 mg N/L which are presented in Figure 6.6, Figure 6.7 and Figure 6.8 respectively. In addition, the parameter estimation results from three different calibration approaches: using on-line respirometric measurements alone, titrimetric alone and combined respirometric-titrimetric measurements are shown in Table 6.5, Table 6.6 and Table 6.7 respectively. They also include the calculated 95% confidence intervals for the estimated parameters and the mean squared errors (MSEs) to evaluate the model calibration and parameter estimation

process from a statistical aspect. The estimated model parameters are found to be consistent for all three calibration approaches thereby confirming the soundness of the proposed model (see Table 6.5-6.7).

The parameter estimation shows that the maximum growth rate for *Nitrosomonas* ($\mu_{MAX,A1}$) varies from 0.035 to 0.038 day^{-1} for the initial ammonium concentration of 2.5 and 11 mg N/L respectively. Baquerizo et al. (2005) estimated the parameter $\mu_{MAX,A1}$ as 0.82 day^{-1} which is significantly higher than the current observation. However, Gernaey et al. (2001) observed a maximum autotrophic biomass growth rate as slow as $4.7x10^{-3}$ day^{-1} during the first step of ammonium nitrification process. In this current study, the maximum growth rate for *Nitrobacter* ($\mu_{MAX,A2}$) is found within the range $5.76x10^{-3}$ to $9.2x10^{-3}$ day^{-1} which shows a very slow growth rate compared to the growth rate for the first step nitrification process. Nitrite accumulation generally occurs in the liquid medium when the biomass growth rate for the second nitrification step is slower than that for the first step nitrification process (Brouwer et al., 1998). This was also confirmed here through off-line NO_2-N measurement which is shown in Figure 6.11. The substrate affinity constant for the first nitrification step, K_{SA1} lies between 0.22 to 0.29 mg N/L which is consistent with the study by Gernaey et al. (2001). They noted the parameter K_{SA1} within the range 0.25-0.3 mg N/L when using ammonium as a test substrate. A similar K_{SA1} value (0.29 mg N/L) was noted during the urea nitrification study (see sub-section 6.4.2) where the same activated sludge was used for the experiments.

The average values for the biomass yield coefficients Y_{A1} and Y_{A2} were estimated as 0.13 (mg COD/mg N) and 0.05 (mg COD/mg N) respectively. Kim et al. (2009) noted the yield coefficients Y_{A1} and Y_{A2} as 0.33 and 0.083 respectively; however Pambrun et al. (2006) used lower value for the parameters Y_{A1} (0.21) and Y_{A2} (0.03) during ammonium nitrification based model calibration. Gapes et al. (2003) used the yield coefficients Y_{A1} and Y_{A2} as 0.082 (mg VSS/mg-N) and 0.04 (mg VSS/mg-N) respectively when examining nitrification process in wastewater treatment. They chose these values in accordance with the guideline established by the EPA (EPA, 1993). After the unit conversion from “mg COD” to “mg VSS” the estimated parameters Y_{A1} and Y_{A2} from current observations are

found to be 0.091 (mg VSS/mg-N) and 0.035 (mg VSS/mg-N) respectively. These are consistent with the literature (Gapes et al., 2003).

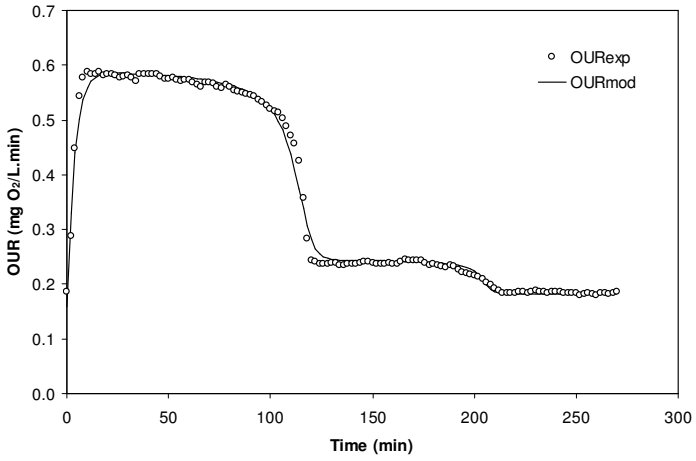

(a)

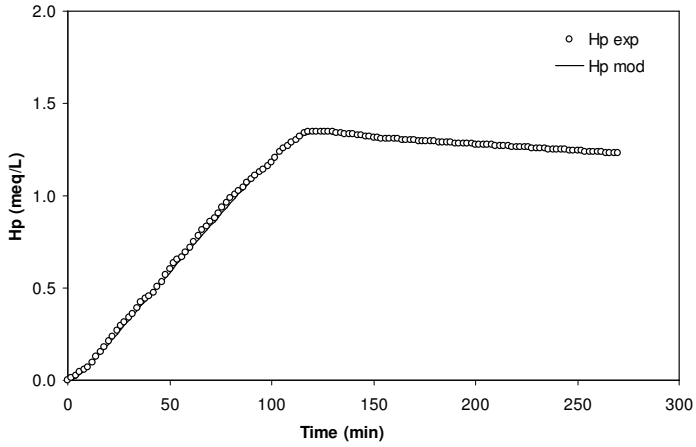

(b)

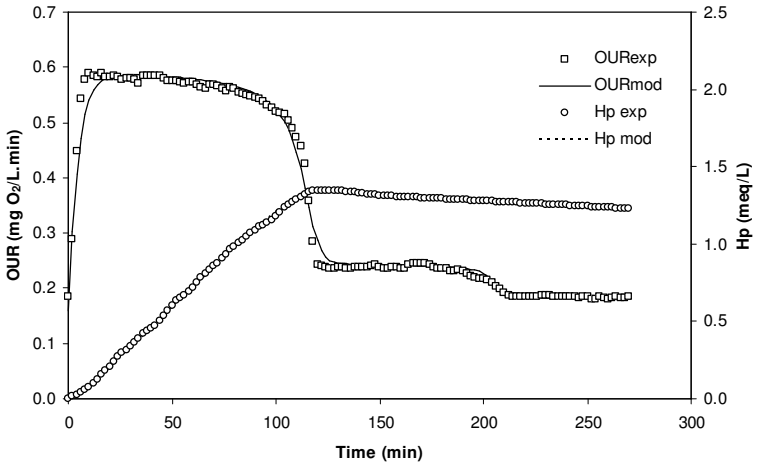

(c)

Figure 6.6: Model calibration using (a) respirometric data alone (b) titrimetric data alone and (c) combined respirometric-titrimetric data (Ammonium = 11 mg N /L)

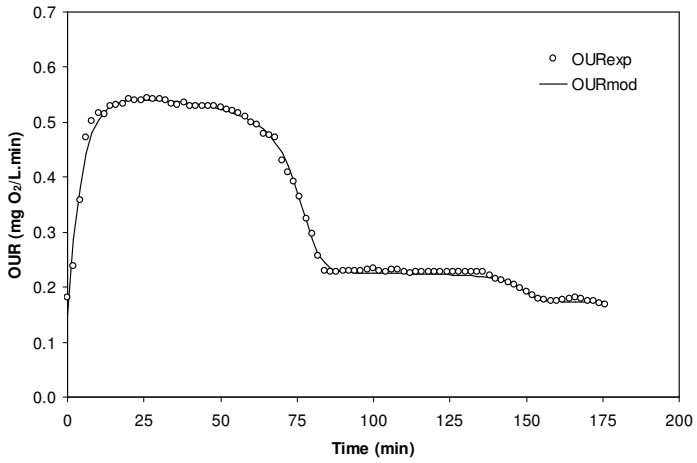

(a)

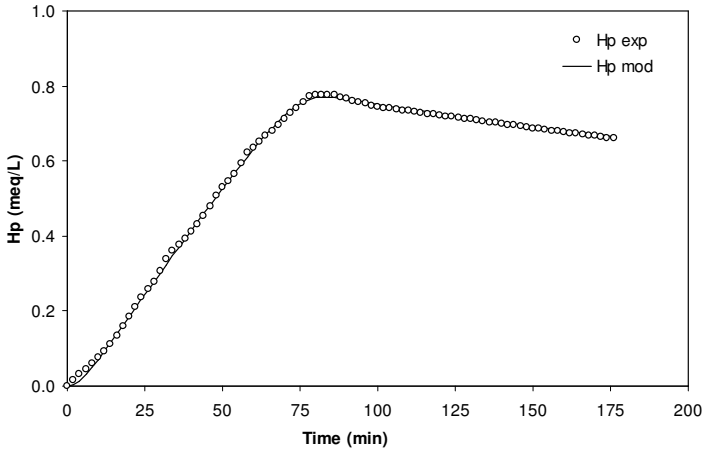

(b)

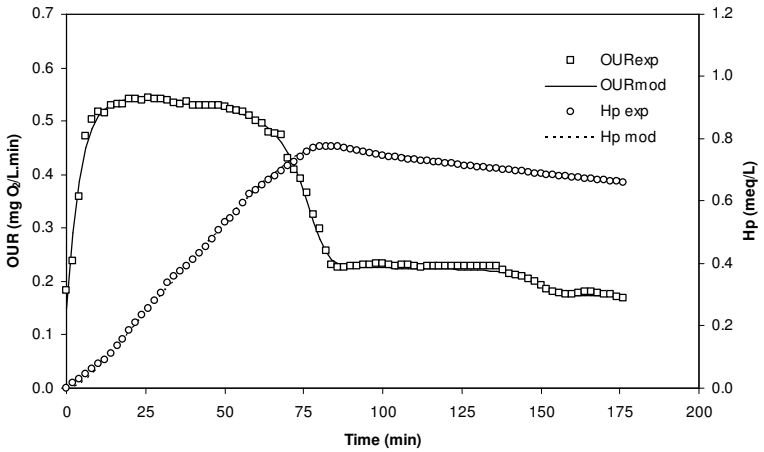

(c)

Figure 6.7: Model calibration using (a) respirometric data alone (b) titrimetric data alone and (c) combined respirometric-titrimetric data (Ammonium = 6.5 mg N /L)

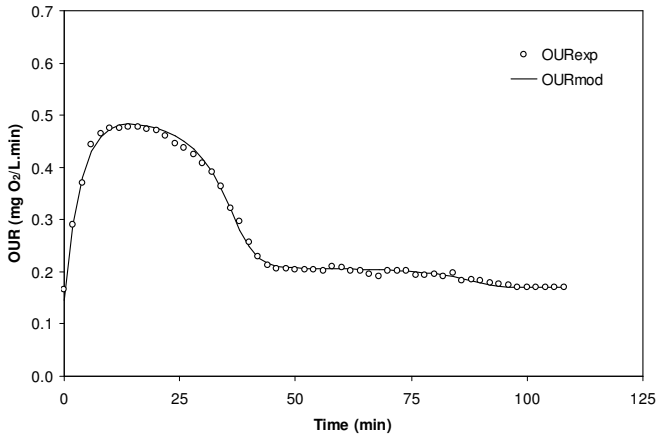

(a)

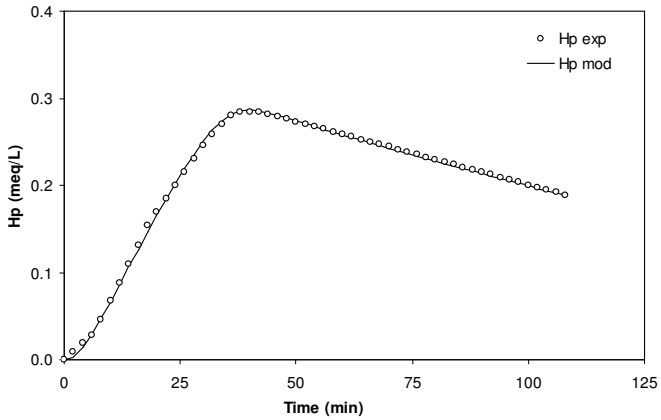

(b)

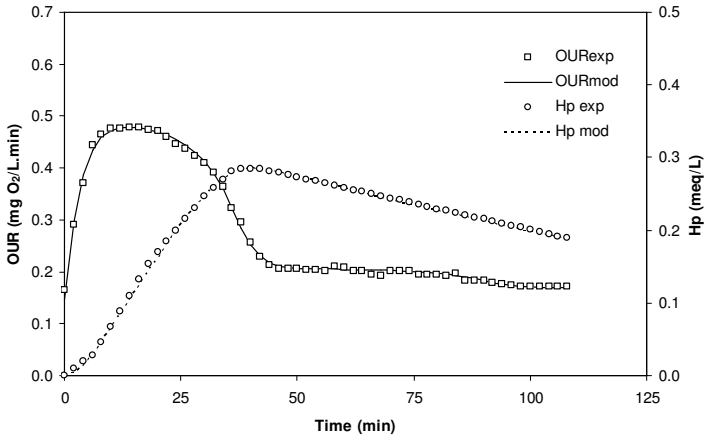

(c)

Figure 6.8: Model calibration using (a) respirometric data alone (b) titrimetric data alone and (c) combined respirometric-titrimetric data (Ammonium = 2.5 mg N /L)

Table 6.5: Parameter estimation results using respirometric data alone for three different concentration studies (confidence intervals are shown in brackets as percentages)

Parameters	Ammonium 11 mg N/L (Confidence interval, %)	Ammonium 6.5 mg N/L (Confidence interval, %)	Ammonium 2.5 mg N/L (Confidence interval, %)
Parameters Estimated:			
$\mu_{MAX,A1}$ (1/min)	$2.62\text{x}10^{-5} \pm 1.49\text{x}10^{-6}$ (5.69)	$2.53\text{x}10^{-5} \pm 1.49\text{x}10^{-6}$ (5.89)	$2.48\text{x}10^{-5} \pm 2.21\text{x}10^{-6}$ (8.91)
$\mu_{MAX,A2}$ (1/min)	$6.39\text{x}10^{-6} \pm 5.41\text{x}10^{-7}$ (8.47)	$5.21\text{x}10^{-6} \pm 6.21\text{x}10^{-7}$ (11.92)	$4.0\text{x}10^{-6} \pm 1.02\text{x}10^{-6}$ (25.5)
K_{SA1} (mgN/L)	$0.294 \pm 9.39\text{x}10^{-3}$ (3.19)	$0.251 \pm 6.68\text{x}10^{-3}$ (2.66)	$0.215 \pm 6.5\text{x}10^{-3}$ (3.02)
K_{SA2} (mgN/L)	0.084 ± 0.029 (34.52)	0.08 ± 0.023 (28.75)	0.079 ± 0.02 (25.32)
Y_{A1} (mgCOD X_B/mgN S_{NH})	$0.131 \pm 7.5\text{x}10^{-3}$ (5.73)	$0.127 \pm 7.57\text{x}10^{-3}$ (5.96)	0.126 ± 0.011 (8.73)
Y_{A2} (mgCOD X_B/mgN S_{NO2})	$0.057 \pm 5.52\text{x}10^{-3}$ (9.68)	$0.051 \pm 6.78\text{x}10^{-3}$ (13.29)	0.05 ± 0.014 (28)
Parameters Assumed:			
b (1/min)	0.0001042	0.0001042	0.0001042
f_{XI} (mgCOD /mgCOD)	0.2	0.2	0.2
Parameters Calculated:			
X_B (mgCOD/L)	1900	1800	1750
MSE [a]	$1.53\text{x}10^{-4}$	$6.54\text{x}10^{-5}$	$2.81\text{x}10^{-5}$

[a] MSE refers to the mean squared error which is calculated from sum of squared errors divided by number of observations

Table 6.6: Parameter estimation results using titrimetric data alone for three different concentration studies (confidence intervals are shown in brackets as percentages)

Parameters	Ammonium 11 mg N/L (Confidence interval, %)	Ammonium 6.5 mg N/L (Confidence interval, %)	Ammonium 2.5 mg N/L (Confidence interval, %)
Parameters Estimated:			
$\mu_{MAX,A1}$ (1/min)	$2.53\text{x}10^{-5} \pm 9.65\text{x}10^{-7}$ (3.81)	$2.5\text{x}10^{-5} \pm 7.11\text{x}10^{-7}$ (2.84)	$2.47\text{x}10^{-5} \pm 2.15\text{x}10^{-6}$ (8.7)
$\mu_{MAX,A2}$ (1/min)	$6.76\text{x}10^{-6} \pm 2.54\text{x}10^{-7}$ (3.76)	$5.3\text{x}10^{-6} \pm 2.38\text{x}10^{-7}$ (4.49)	$4.01\text{x}10^{-6} \pm 1.23\text{x}10^{-6}$ (30.67)
K_{SA1} (mgN/L)	0.282 ± 0.014 (4.96)	0.262 ± 0.013 (4.96)	0.221 ± 0.014 (6.34)
K_{SA2} (mgN/L)	0.084 ± 0.019 (22.62)	0.081 ± 0.017 (20.98)	0.079 ± 0.01 (12.66)
Y_{A1} (mgCOD X_B/mgN S_{NH})	$0.128 \pm 4.92\text{x}10^{-3}$ (3.84)	$0.127 \pm 3.69\text{x}10^{-3}$ (2.91)	0.125 ± 0.011 (8.8)
Y_{A2} (mgCOD X_B/mgN S_{NO2})	$0.049 \pm 4.1\text{x}10^{-3}$ (8.37)	$0.045 \pm 2.38\text{x}10^{-3}$ (5.29)	0.037 ± 0.011 (29.73)
Parameters Assumed:			
b (1/min)	0.0001042	0.0001042	0.0001042
f_{XI} (mgCOD /mgCOD)	0.2	0.2	0.2
k_l [b] (1/min)	1.5	1.5	1.5
K_La_{CO2} (1/min)	0.0728	0.0728	0.0728
$C_{T,init}$ [b] (mmol/L)	2.8	2.8	2.8
Parameters Calculated:			
HCO_3 (mmol/L)	2.6968	2.6968	2.6968
CO_2 (mmol/L)	0.1032	0.1032	0.1032
X_B (mgCOD/L)	1900	1800	1750
MSE [a]	$8.45\text{x}10^{-5}$	$3.38\text{x}10^{-5}$	$6.26\text{x}10^{-6}$

[a] MSE refers to the mean squared error which is calculated from sum of squared errors divided by number of observations

[b] Parameters were fixed by trials for the better fit of experimental profile with the model

Table 6.7: Parameter estimation results using combined respirometric-titrimetric data for three different concentration studies (confidence intervals are shown in brackets as percentages)

Parameters	Ammonium 11 mg N/L (Confidence interval, %)	Ammonium 6.5 mg N/L (Confidence interval, %)	Ammonium 2.5 mg N/L (Confidence interval, %)
Parameters Estimated:			
$\mu_{MAX,A1}$ (1/min)	$2.6\text{x}10^{-5} \pm 9.66\text{x}10^{-7}$ (3.72)	$2.52\text{x}10^{-5} \pm 1.81\text{x}10^{-6}$ (7.18)	$2.43\text{x}10^{-5} \pm 2.88\text{x}10^{-6}$ (11.85)
$\mu_{MAX,A2}$ (1/min)	$6.4\text{x}10^{-6} \pm 3.8\text{x}10^{-7}$ (5.94)	$5.21\text{x}10^{-6} \pm 8.07\text{x}10^{-7}$ (15.49)	$3.88\text{x}10^{-6} \pm 1.15\text{x}10^{-6}$ (29.64)
K_{SA1} (mgN/L)	0.292 ± 0.01 (3.43)	0.25 ± 0.007 (2.8)	0.222 ± 0.006 (2.7)
K_{SA2} (mgN/L)	0.084 ± 0.027 (32.14)	0.083 ± 0.031 (37.35)	0.08 ± 0.023 (28.75)
Y_{A1} (mgCOD X_B/mgN S_{NH})	$0.129 \pm 4.89\text{x}10^{-3}$ (3.79)	$0.126 \pm 9.23\text{x}10^{-3}$ (7.33)	0.125 ± 0.015 (12)
Y_{A2} (mgCOD X_B/mgN S_{NO2})	$0.057 \pm 3.92\text{x}10^{-3}$ (6.88)	$0.051 \pm 8.92\text{x}10^{-3}$ (17.49)	0.05 ± 0.016 (32)
Parameters Assumed:			
b (1/min)	0.0001042	0.0001042	0.0001042
f_{XI} (mgCOD /mgCOD)	0.2	0.2	0.2
k_1 [b] (1/min)	1.5	1.5	1.5
$K_L a_{CO2}$ (1/min)	0.0728	0.0728	0.0728
$C_{T,init}$ [b] (mmol/L)	2.8	2.8	2.8
Parameters Calculated:			
HCO_3 (mmol/L)	2.6968	2.6968	2.6968
CO_2 (mmol/L)	0.1032	0.1032	0.1032
X_B (mgCOD/L)	1900	1800	1750
MSE [a]	$1.25\text{x}10^{-4}$	$4.56\text{x}10^{-5}$	$1.26\text{x}10^{-5}$

[a] MSE refers to the mean squared error which is calculated from sum of squared errors divided by number of observations

[b] Parameters were fixed by trials for the better fit of experimental profile with the model

6.4.4 Model evaluation

Three different initial concentrations were considered during both the urea and ammonium nitrification studies for proper model evaluation. The proposed model explains well both the experimental respirometric and titrimetric measurements as evident by the good fit of the model profiles with the experimental observations. In addition, the estimated model parameters show consistent results for all three calibration approaches (i.e. calibration with respirometric measurements alone, titrimetric measurements alone and combined respirometric titrimetric measurements). Moreover, the parameter estimation errors (calculated for 95% confidence intervals) as well as the mean squared errors (MSEs) for all three calibration approaches were reasonable and confirm the statistical soundness of the proposed model.

In the proposed nitrification model, the biomass formula was assumed to be $CH_{1.5}O_{0.2}N_{0.1}$ (for both the urea and ammonium nitrification studies) to achieve a good fit between the model and experimental profiles for all three calibration

approaches. Based on the assumed biomass formula the calculated degree of reduction of biomass, γ_x was fixed at 4.8 during calibration where the i_{NBM} content was calculated as 0.036 g N/g COD X_B, though the typical value for the nitrogen content of biomass was reported between the range 7% to 8.6% (Henze et al., 2000). Conversely, Sin and Vanrolleghem (2007) estimated the i_{NBM} content within the range 2.4% to 5.7% which supports the current observation. Gernaey et al. (2002b) also reported the parameter i_{NBM} as low as 3.8% during their organic carbon biodegradation study.

Gernaey et al. (2001) verified the respirometric method of their proposed model by investigating the linearity between BOD_{st} values and NH_4-N concentrations added to the activated sludge. With this in mind, an attempt was made in this current study to determine the relationship between BOD_{st} and substrate concentration (as pressed mg N/L). This is presented in Figure 6.9.

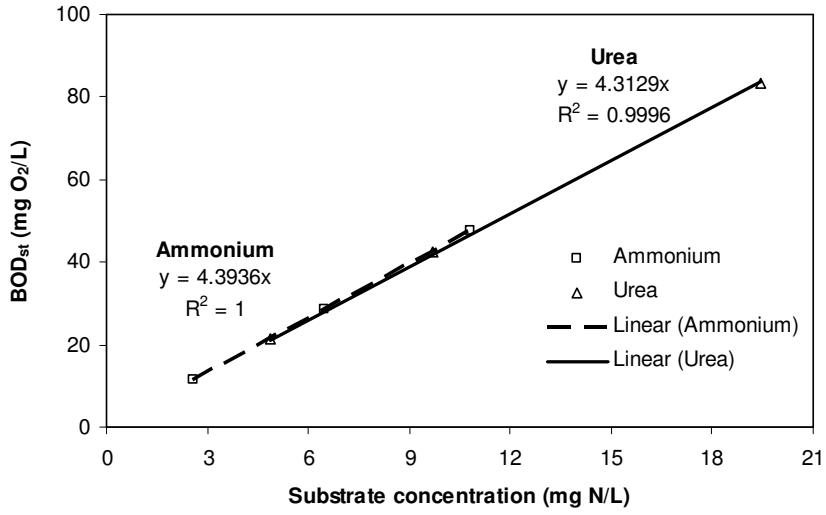

Figure 6.9: BOD_{st} as a function of the initial substrate concentration (expressed as mg N/L)

The area under the OUR profiles were considered to calculate the BOD_{st} for respective substrate concentration study. Readers are referred to Figure 6.1 and Figure 6.2 for OUR profiles associated with urea and ammonium nitrification respectively. The slope (4.57-Y_A) of the BOD_{st} vs NH_4-N concentration curve is typically expected to be 4.33 g O_2/g NH_4-N (Henze et al., 1987). From the Figure 6.9 the slopes of the curves are found to be 4.31 g O_2/g NH_4-N and 4.39 g O_2/g NH_4-N for urea and ammonium nitrification respectively. Though the slope for

ammonium nitrification study is slightly higher than expected, the current observations are reasonable when compared to the study by Gernaey et al.(2001) who found the slope as high as 4.44 g O_2/g NH_4-N for urea nitrification.

In addition to on-line respirometric and titrimetric methods, the proposed model was validated using off-line NH_4-N, NO_2-N and NO_3-N measurements during both the urea and ammonium nitrification studies. The results are presented in Figure 6.10 and Figure 6.11 respectively.

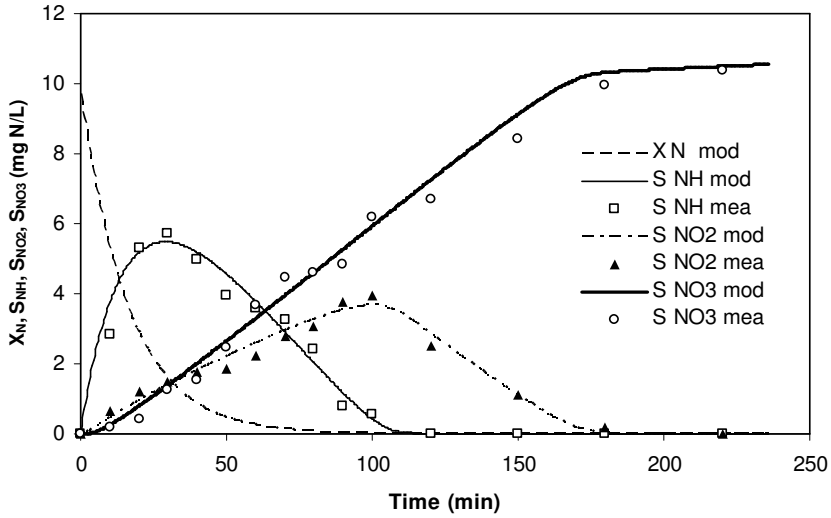

Figure 6.10: Model validation using off-line ammonium, nitrite and nitrate measurements during urea (10 mg N/L) nitrification

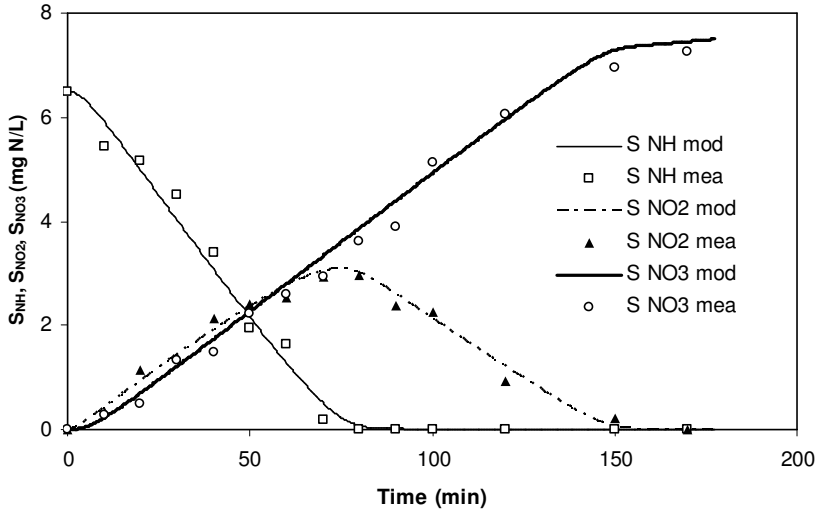

Figure 6.11: Model validation using off-line ammonium, nitrite and nitrate measurements during ammonium (6.5 mg N/L) nitrification

For both case studies (urea and ammonium nitrification), the model-simulated profiles present reasonably the off-line experimental observations confirming the precision of the proposed model. In addition, the nitrite accumulation is noted significant during both the urea and ammonium nitrification studies. It was supported by the parameter estimation results where the maximum growth rate of *Nitrobacter* species ($\mu_{MAX,A2}$) was observed to be significantly slower compared to that of *Nitrosomonas* species ($\mu_{MAX,A1}$).

6.5 Monod kinetic parameters for the nitrification study

In this current study, nitrification kinetics for both the urea and ammonium were investigated with varying initial substrate concentrations. An attempt was made to determine the Monod parameters for urea and ammonium nitrification based on the observation of different initial substrate concentrations. Figure 6.12 represents the estimated biomass growth rate against the initial substrate concentration along with the calibrated Monod profile. The coefficient of determination (R^2) for the test substrates urea and ammonium were calculated as 0.93 and 0.99 respectively. Table 6.8 shows a comparison of the estimated Monod parameters (K_{A1} and $\mu_{MAX,A!}$) corresponding to the urea and ammonium nitrification processes.

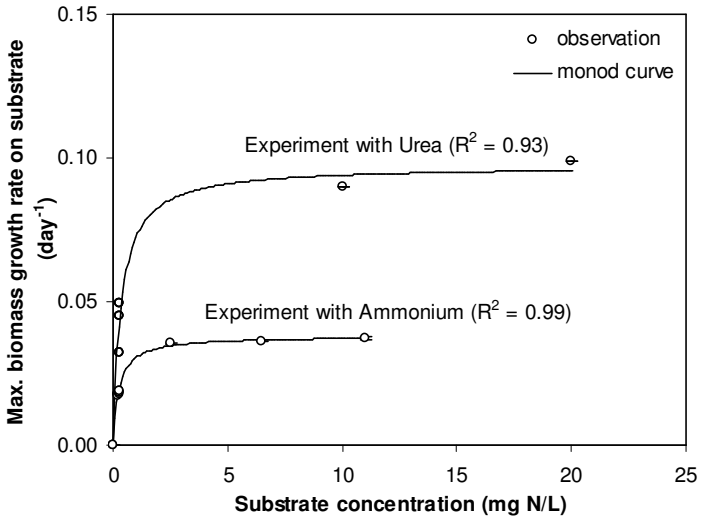

Figure 6.12: Monod profile for maximum biomass growth rate on urea and ammonium at pH of 7.8

During urea nitrification the maximum autotrophic biomass growth rate ($\mu_{MAX,A1}$) and the substrate affinity constant (K_{A1}) were found to be relatively higher than those parameters estimated from the ammonium oxidation process as shown in Table 6.8. The affinity coefficient indicates that the autotrophic bacteria has a higher affinity to ammonium than urea. The autotrophic biomass is capable of consuming ammonium directly when ammonium itself is used as a test substrate, however in the case of urea the autotrophic biomass needs urea to hydrolyze and produce ammonium for biomass consumption. However, this can not be generalized, since there are several parameters that may affect the process kinetics including the sludge composition and operation system of treatment plants from where sludge is collected for study (Hoque et al., 2009b). The sludge for these experimental studies, using urea and ammonium as substrates, was collected from the plant during different seasons. This could have affected the results as well.

Table 6.8: Estimated Monod kinetics for urea and ammonium nitrification at pH 7.8

Parameter	Urea	Ammonium
K_{SA1} (mg N/L)	0.34 ± 0.002	$0.25 \pm 1.87 \times 10^{-4}$
$\mu_{MAX,A1}$ (day^{-1})	$0.097 \pm 2.45 \times 10^{-5}$	$0.038 \pm 4.9 \times 10^{-7}$

6.6 Conclusions

A nitrification model was proposed to interpret urea biodegradation by paying due attention to the urea biodegradation pathway and dynamic CO_2 transfer in the liquid medium. The proposed model was then justified for ammonium nitrification with varying initial substrate concentrations. For both cases (urea and ammonium), the proposed model successfully explained both the respirometric and titrimetric measurements. In addition, the estimated model parameters were found to be consistent for all three calibration approaches thereby validating the proposed model. Moreover, the estimated model parameters compared favorably with values recorded in the literature. In addition to on-line methods, the model was validated with off-line NH_4-N, NO_2-N and NO_3-N measurements for both the urea and ammonium nitrification processes which confirms the precision of the proposed model.

Chapter 7
Modeling of Glutamic Acid Biodegradation

7.1 Introduction

Glutamic acid is a typical organic nitrogen compound that releases organic carbon and nitrogen molecules during the initial hydrolysis process, both of which are subjected to oxidation to produce carbon dioxide and nitrate respectively under aerobic conditions. This chapter discusses the development of a kinetic model that is capable of explaining respirometric and titrimetric behaviour during the biodegradation of a typical organic nitrogen compound such as glutamic acid. Initially, it focuses on the calibration of model parameters using respirometric and titrimetric measurements where the nitrification process was inhibited during the experiment and consequently the sole organic carbon oxidation of glutamic acid occurred during the biodegradation process. Once the model was calibrated for organic carbon oxidation, the next phase investigated the biodegradation of glutamic acid kinetics without nitrification inhibition where combined organic carbon oxidation and nitrification took place in the activated sludge process. Furthermore, this chapter focuses on the proposed model calibration and parameter estimation with discussion enhanced by statistical analysis. The proposed model evaluation and determination of Monod kinetic parameters are presented at the end of this chapter.

7.2 Experimental observations on glutamic acid biodegradation

Activated sludge was fed with glutamic acid for 12 days prior to the commencement of the main experiments to allow the microorganisms to acclimatize with the test substrate so that they could perform the biodegradation at their maximum capacity (see sub-section 3.2.3 in Chapter 3). Batch studies were performed using on-line respirometric and titrimetric measurement techniques where initial glutamic acid concentrations of 50, 100 and 150 mg COD/L were added to investigate the combined effect of carbon oxidation and nitrification in the activated sludge process. In addition, a separate study was conducted to observe sole carbon oxidation kinetics

in glutamic acid biodegradation process where allylthiourea (ATU) was added to inhibit nitrification. The pH was maintained at 7.8 ± 0.03 in every case study.

Figure 7.1 shows the experimental oxygen uptake rate (OUR) and titrimetric profile corresponding to glutamic acid biodegradation (100 mg COD/L) for the nitrification inhibition study. The OUR increases to its maximum rate under the feast phase, then drops to a level higher than the endogenous OUR followed by a gradual declination until it reaches the endogenous state as observed for the acetate study (Guisasola et al., 2005; Sin et al., 2005) and the surfactant biodegradation study (see Chapter 5). Furthermore, a continuous base addition was observed during the feast conditions indicating proton production taking place in the liquid medium whereas acid was added for the period of endogenous respiration. Acid addition (proton consumption) under endogenous conditions was also observed in the previous experimental studies (see Chapter 4, Chapter 5 and Chapter 6) particularly when the pH was maintained at 7.8.

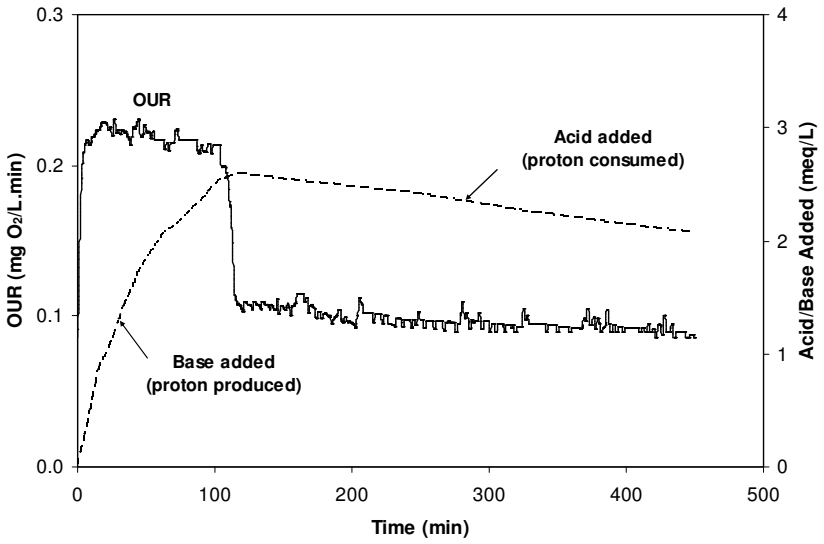

Figure 7.1: OUR with titrimetric profile for the nitrification inhibition study (Glutamic acid = 100 mg COD/L)

The OUR and titrimetric profiles for glutamic acid concentrations of 50, 100 and 150 mg COD/L when pH was maintained at 7.8 are presented in Figure 7.2 where both organic carbon oxidation and nitrification occurred in the activated sludge system. The OUR profiles for the studies, with nitrification inhibition and without inhibition (Figure 7.1 and Figure 7.2), are distinctive, especially during the feast period. The OUR drops from its maximum peak to a second peak due to the oxygen consumption of the nitrification process.

The glutamic acid biodegradation process results in proton production in the system. This is the net result of glutamic acid hydrolysis, alfa-ketoglutarate (intermediate products) uptake, nitrification, endogenous respiration and the CO_2 production as described in section 7.3. With nitrification inhibition, the conversion of ammonium to nitrite is completely restricted. As a result, the net proton production rate during the feast period is less than that observed when nitrification is not inhibited (Figure 7.1 and Figure 7.2). In addition, the cumulative pulse of base addition to the reactor increases proportionally with the initial glutamic acid concentration. This is illustrated in Figure 7.2.

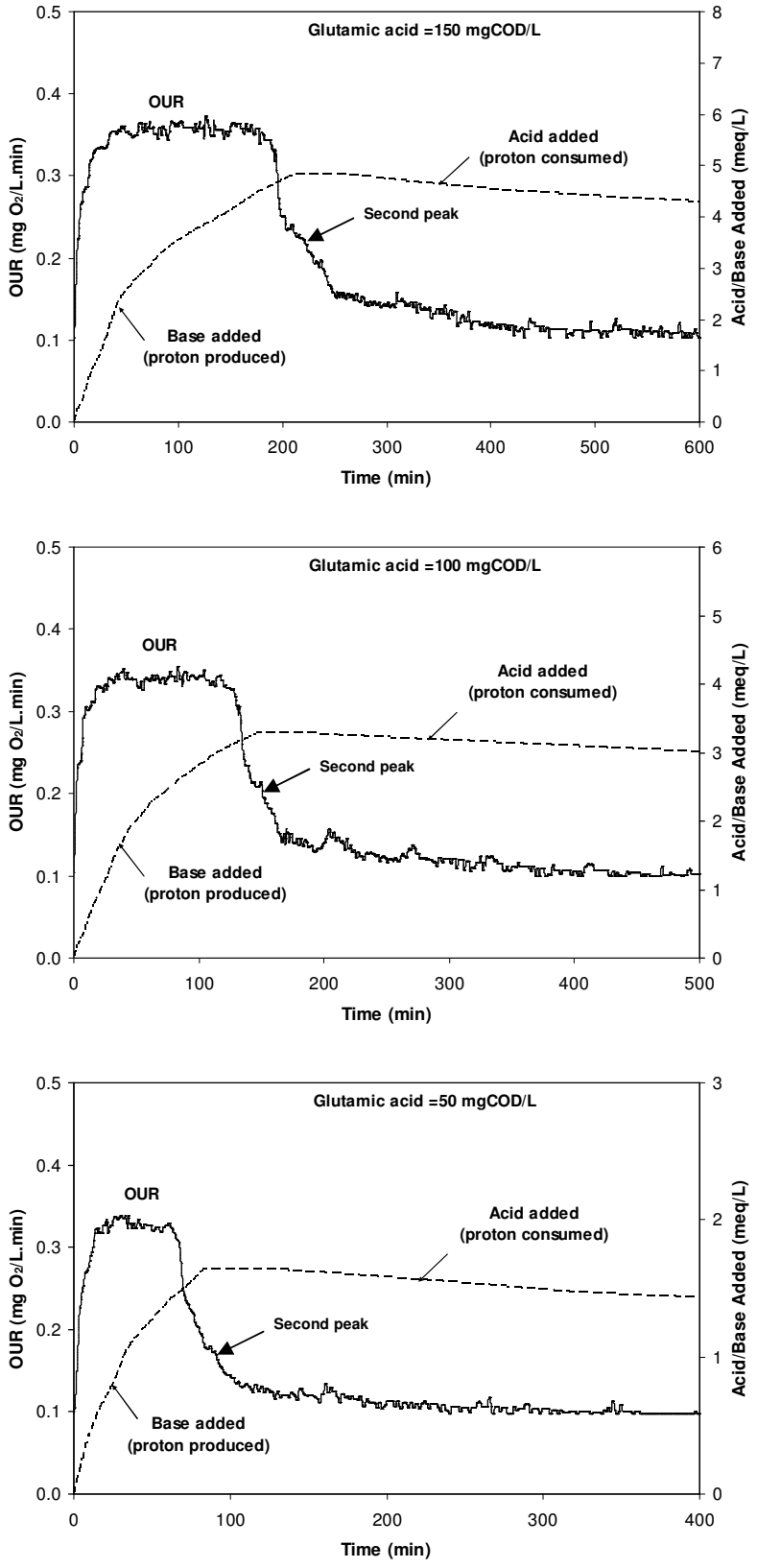

Figure 7.2: OUR with titrimetric profiles for three different glutamic acid concentrations in an activated sludge system (without nitrification inhibition)

7.3 Proposed model for glutamic acid biodegradation

The glutamic acid biodegradation process in a mixed culture generally includes organic carbon oxidation and nitrification processes that are governed by heterotrophic and autotrophic microorganisms respectively. There is some evidence of the modeling of glutamic acid biodegradation where respirometric measurements were used for model calibration (Beccari et al. 2002). However model calibration with titrimetric measurements could not be found in the literature although both pH changes (as reflected in titrimetry) and oxygen consumption (as derived in respirometry) occur concurrently in an activated sludge system. In this study, a bio-kinetic model is proposed to describe both the respirometric and titrimetric behavior of glutamic acid biodegradation in activated sludge. The proposed model was developed by paying due attention to the biodegradation pathway of glutamic acid, since an in-depth understanding of the biochemical conversion of respective substrate is essential, particularly for titrimetric model development.

Glutamic acid ($C_5H_9NO_4$) is converted to Alfa-ketoglutarate ($C_5H_4O_5$) and ammonium (NH_4^+) through hydrolysis in the presence of *glutamate dehydrogenase* enzyme where H^+ is released in the liquid medium (Stryer, 1988) (see equation 7.1). In the proposed model alfa-ketoglutarate was considered to be a readily biodegradable substrate (S_S) which is subjected to biochemical oxidation by the heterotrophic biomass to produce CO_2 in the system. At the same time, the ammonium produced from glutamic acid hydrolysis undergoes a nitrification process releasing nitrate (NO_3^-) as the end product.

$$C_5H_9O_4N + H_2O \rightarrow C_5H_4O_5 + NH_4^+ + 3H^+ \qquad \text{----- (Equation 7.1)}$$

Table 7.1 represents the proposed model for glutamic acid biodegradation in a matrix format. While a two-step nitrification process was adopted in the proposed model to describe ammonium nitrification, the extended simultaneous storage and growth (SSAG) model used during the surfactant biodegradation study (see Chapter 5) was applied here to explain the organic carbon oxidation in an activated sludge process. The proposed model introduces the stoichiometric parameters related to titrimetry at

each step of the growth and storage phases along with consideration of the non-linear carbon dioxide transfer rate in the liquid medium.

Based on the chemical conversion as shown in equation 7.1, the proton production during hydrolysis can be estimated using the model matrix (Table 7.1) where the parameters M and M' represent the molecular weight of glutamic acid (208 gCOD/mol) and alfa-ketoglutarate (112 gCOD/mol) respectively. Relevant stoichiometric components for proton production are obtained from the biochemical conversion (equations 7.2 and 7.3) of nitrification processes assuming CO_2 as the carbon source that is required for autotrophic microorganisms biosynthesis (Gernaey et al., 1998). Readers are referred to Chapter 6 for the derivation of equations 7.2 and 7.3.

In addition, CO_2 production during heterotrophic biomass growth on the substrate, the formation of storage products and the growth on storage products can easily be determined by using equations 7.4, 7.5 and 7.6 respectively (see Chapter 4 for the derivation). Ammonia assimilation takes place during the consumption of substrate (alfa-ketoglutarate) by the heterotrophic biomass that results in proton production in the liquid medium (Table 7.1). The parameter "p" presented in the model matrix refers to the fraction of NH_4^+ in the liquid phase which is derived as $1/(1+10^{pH-\ pK_{NH4}})$ by Gernaey et al. (2002a). Under the aerobic growth on storage process, it is assumed that the biomass also accumulates nitrogen within the cell along with carbon as a source for subsequent growth purposes (see the ammonium balance in Table 7.1). This was also assumed for the acetate and surfactant biodegradation modeling (see Chapter 4 and Chapter 5).

Conversion by autotrophic biomass:

$$\left(\frac{1+Y_{A1}i_{NBM}}{Y_{A1}}\right)(mgN)NH_4+\left(\frac{3.43-Y_{A1}}{Y_{A1}}\right)(mgCOD)O_2+\frac{1}{8\gamma_X}(mmol)CO_2 \quad \text{----- (Equation 7.2)}$$
$$\rightarrow 1(mgCOD)CH_aO_bN_c+\frac{1}{Y_{A1}}(mgN)NO_2+(...)H_2O+\left(\frac{2+Y_{A1}i_{NBM}}{14Y_{A1}}\right)(mmol)H^+$$

$$i_{NBM}(mgN)NH_3+\frac{1}{Y_{A2}}(mgN)NO_2+\left(\frac{1.14-Y_{A2}}{Y_{A2}}\right)(mgCOD)O_2+\frac{1}{8\gamma_X}(mmol)CO_2 \quad \text{----- (Equation 7.3)}$$
$$\rightarrow 1(mgCOD)CH_aO_bN_c+\frac{1}{Y_{A2}}(mgN)NO_3+(...)H_2O$$

Conversion by heterotrophic biomass:

$$\frac{1}{Y_{H,S}}(mgCOD)CH_yO_z + \left(1-\frac{1}{Y_{H,S}}\right)(mgCOD)O_2 + i_{NBM}(mgN)NH_3 \rightarrow 1(mgCOD)CH_aO_bN_c + \frac{1}{8\gamma_S}\left(\frac{1}{Y_{H,S}} - \frac{\gamma_S}{\gamma_X}\right)(mmol)CO_2 + (...)H_2O \quad \text{----- (Equation 7.4)}$$

$$\frac{1}{Y_{STO}}(mgCOD)CH_yO_z + \left(1-\frac{1}{Y_{STO}}\right)(mgCOD)O_2 \rightarrow 1(mgCOD)CH_pO_q + \frac{1}{8\gamma_S}\left(\frac{1}{Y_{STO}} - \frac{\gamma_S}{\gamma_{STO}}\right)(mmol)CO_2 + (...)H_2O \quad \text{----- (Equation 7.5)}$$

$$\frac{1}{Y_{H,STO}}(mgCOD)CH_pO_q + \left(1-\frac{1}{Y_{H,STO}}\right)(mgCOD)O_2 + i_{NBM}(mgN)NH_3 \rightarrow 1(mgCOD)CH_aO_bN_c + \frac{1}{8\gamma_{STO}}\left(\frac{1}{Y_{H,STO}} - \frac{\gamma_{STO}}{\gamma_X}\right)(mmol)CO_2 + (...)H_2O \quad \text{----- (Equation 7.6)}$$

In the above equations, the elemental composition of biomass, substrate (alfa-ketoglutarate) and storage products are expressed as $CH_aO_bN_c$, CH_yO_z and CH_pO_q respectively. The parameters Y_{A1}, Y_{A2}, $Y_{H,S}$, Y_{STO} and $Y_{H,STO}$ represent the yield coefficients for aerobic growth on ammonium, growth on nitrite, growth on substrate, storage on substrate and growth on storage products respectively. The degree of reduction of the substrate (γ_S), the storage products (γ_{STO}) and the biomass (γ_X) can be calculated as 4+y-2z, 4+p-2q and 4+a-2b-3c accordingly. The coefficient related to ammonia uptake (i_{NBM}) is expressed as g N per g COD biomass unit basis that can be determined from the relation $14c/8\gamma_X$ (Sin, 2004).

Although mixed liquor contains both autotrophic and heterotrophic biomass constituents, a single component for biomass concentration (X_B) was used to keep the proposed model simple. Combined parameters $f_{BA}.X_B$ and $f_{BH}.X_B$ were used in growth the kinetics expression, where the coefficients f_{BA} and f_{BH} represent respectively the proportion of autotrophs and heterotrophs in the mixed culture (Table 7.1). The stoichiometry and kinetics for the processes of endogenous respiration, respiration on storage, aqueous CO_2 equilibrium and CO_2 stripping were kept the same as those used during the acetate and surfactant biodegradation modeling (see Chapter 4 and Chapter 5).

Table 7.1: Process matrix involved in the proposed model for glutamic acid biodegradation

Process	X_B (g COD)	X_{NHacc} (g N)	X_{STO} (g COD)	S_S (g COD)	X_S (g COD)	S_{HCO_3} (mol)	S_{CO_2} (mol)	S_{Hp} (mol)	S_{NH} (g N)	S_{NO_2} (g N)	S_{NO_3} (g N)	S_O (g O_2)	Kinetics
Hydrolysis	--	--	--	1	$-\frac{M}{M'}$	--	--	$\frac{3}{M'}$	$\frac{14}{M'}$	--	--	--	$k_h.M_{X_S/X_H}.X_B$
S_{NH} accumulation	--	i_{NBM}	--	--	--	--	--	$\frac{i_{NBM}\,p}{14}$	$-i_{NBM}$	--	--	--	$(1-e^{-t/\tau}).k_{NHacc}.M_S.X_B$
Aerobic growth on S_S	1	--	--	$-\frac{1}{Y_{H,S}}$	--	--	$\frac{1}{8\gamma_S}\left(\frac{1}{Y_{H,S}}-\frac{\gamma_S}{\gamma_X}\right)$	$\frac{i_{NBM}\,p}{14}$	$-i_{NBM}$	--	--	$-\frac{1-Y_{H,S}}{Y_{H,S}}$	$(1-e^{-t/\tau}).\mu_{MAX,S}.M_S.f_{BH}.X_B$
Formation of X_{STO}	--	--	1	$-\frac{1}{Y_{STO}}$	--	--	$\frac{1}{8\gamma_S}\left(\frac{1}{Y_{STO}}-\frac{\gamma_S}{\gamma_{STO}}\right)$	--	--	--	--	$-\frac{1-Y_{STO}}{Y_{STO}}$	$(1-e^{-t/\tau}).k_{STO}.M_S.f_{BH}.X_B$
Aerobic growth on X_{STO}	1	$-i_{NBM}$	$-\frac{1}{Y_{H,STO}}$	--	--	--	$\frac{1}{8\gamma_{STO}}\left(\frac{1}{Y_{H,STO}}-\frac{\gamma_{STO}}{\gamma_X}\right)$	--	--	--	--	$-\frac{1-Y_{H,STO}}{Y_{H,STO}}$	$\mu_{MAX,STO}\left(\frac{(X_{STO}/X_H)^2}{K_2+K_1.(X_{STO}/X_H)}\right)\left(\frac{K_S}{S_S+K_S}\right).f_{BH}.X_B$
S_{NH} Oxidation	1	--	--	--	--	--	$-\frac{1}{8\gamma_X}$	$\frac{i_{NBM}\,p}{14}+\frac{1}{7Y_{A1}}$	$-\frac{1}{Y_{A1}}-i_{NBM}$	$\frac{1}{Y_{A1}}$		$-\frac{3.43-Y_{A1}}{Y_{A1}}$	$(1-e^{-t/\tau}).\mu_{MAX,A1}.\frac{S_{NH}}{K_{SA1}+S_{NH}}.f_{BA}.X_B$
S_{NO_2} Oxidation	1	--	--	--	--	--	$-\frac{1}{8\gamma_X}$	$\frac{i_{NBM}\,p}{14}$	$-i_{NBM}$	$-\frac{1}{Y_{A2}}$	$\frac{1}{Y_{A2}}$	$-\frac{1.14-Y_{A2}}{Y_{A2}}$	$(1-e^{-t/\tau}).\mu_{MAX,A2}.\frac{S_{NO2}}{K_{SA2}+S_{NO2}}.f_{BA}.X_B$
Endogenous respiration	-1	--	--	--	--	--	$\frac{1-f_{XI}}{8\gamma_X}$	$-\frac{(i_{NBM}-f_{XI}i_{NXI})\,p}{14}$	$i_{NBM}-i_{NXI}f_{XI}$	--	--	$-(1-f_{XI})$	$b.X_B$
X_{STO} respiration	--	--	-1	--	--	--	$\frac{1}{8\gamma_{STO}}$	--	--	--	--	-1	$b_{STO}.X_{STO}$
Aqueous CO_2 equilibrum	--	--	--	--	--	1	-1	1	--	--	--	--	$k_1 S_{CO_2}-k_1 10^{pk_1-pH} S_{HCO_3}$
CO_2 stripping	--	--	--	--	--	--	1	--	--	--	--	--	$K_L a_{CO2}(S^*_{CO2}-S_{CO2})$

The ammonia required for the biomass growth during storage to growth process is assumed to be taken from the internal source (cell) instead of the external environment.

7.4 Model calibration and parameter estimation

7.4.1 Parameter estimation approach

The proposed model was calibrated and model parameters were estimated for the glutamic acid biodegradation study by utilizing a non-linear parameter estimation technique using MATLAB optimisation toolbox (R2007a). Both the cases with nitrification inhibition and without inhibition conditions were taken into account. Three different calibration approaches: using respirometric measurements alone, using titrimetric measurements alone and using combined respirometric-titrimetric measurements were applied during the study. Minimization of the mean squared error (MSE) between the model and the experimental output was calculated as the main criterion for curve fitting. Estimated parameters were finally compared for validation of the proposed model.

In the nitrification inhibition study, the proposed model was calibrated with the experimental respirometric and titrimetric measurements corresponding to an initial glutamic acid concentration of 100 mg COD/L in activated sludge. The model parameters K_S, q_{MAX}, $Y_{H,S}$, Y_{STO}, $Y_{H,STO}$, K_1, K_2, k_h, K_X and τ were estimated along with the calculation of 95% confidence intervals (Table 7.2). The description of model parameters is presented in Appendix A. In the study conducted without inhibition, model calibration was done for three different glutamic acid concentrations (50, 100 and 150 mg COD/L) where sixteen model parameters (K_S, q_{MAX}, $Y_{H,S}$, Y_{STO}, $Y_{H,STO}$, K_1, K_2, k_h, K_X, K_{SA1}, K_{SA2}, $\mu_{MAX,A1}$, $\mu_{MAX,A2}$, Y_{A1}, Y_{A2} and τ) were considered for estimation along with their 95% confidence interval calculations (Table 7.3-7.5).

Default values assigned in the ASM3 model for the parameters f_{XI} (0.2), b (0.2 day^{-1}) and b_{STO} (0.2 day^{-1}) were assumed here for model calibration and parameter estimation. A similar value (0.2 day^{-1}) was considered for the parameter k_{NHacc} at the beginning of the parameter estimation process, and was revised later for better curve fitting. Besides, the ASM3 prescribed value for the parameters i_{NXI} (0.02 gN/g COD X_I) and i_{NBM} (0.07 gN/g COD X_B) were fixed during the proposed model calibration. The parameter f_{STO} was fixed at 0.65 to assist with successful model calibration. The maximum storage rate (k_{STO}) and the maximum growth rate of biomass ($\mu_{MAX,S}$) were

calculated from the estimates of the parameters q_{MAX} and f_{STO} based on the procedure explained in Sin et al. (2005) where they assumed the parameter $\mu_{MAX,STO}$ to be the same order of magnitude as $\mu_{MAX,S}$. The relationship $OUR_{end}(0) = (1-f_{XI}).b.X_B(0)$ was employed to calculate the initial concentration of biomass, $X_B(0)$. In this study, the proportion of f_{BA} to f_{BH} was assumed to be 0.35:0.65 due to the fact that the heterotrophic biomass outweighs autotrophic biomass in subtropical regions (Buck et al., 1996).

Total inorganic carbon in the aqueous medium, $C_{T,init}$ was adjusted for different assays to fit the experimental profile with the model one. The initial concentrations of CO_2 and HCO_3 in the reactor were calculated using their relationship with $C_{T,init}$ (Sin, 2004). The parameter k_1 (1.0762 per min) was kept the same as that used for the acetate and surfactant biodegradation studies (see Chapter 4 and Chapter 5). During the model calibration, the value for $K_L a_{CO_2}$ was calculated as 0.0555 min^{-1} from the oxygen transfer coefficient ($K_L a$) using the relationship between their diffusivity coefficients (Sperandio and Paul, 1997; Sin and Vanrolleghem, 2007). The parameter pK_1 was taken as 6.39 (Sperandio and Paul, 1997). The default values suggested by Stumm and Morgan (1996) for the parameters pK_{NH4} (9.25) and $S^*_{CO_2}$ (0.017 mmol/L) were assumed during the parameter estimation process. In addition, the degree of reduction of the substrate (γ_S) and biomass (γ_X) were calculated as 2.8 and 4.2 using the elemental composition of alfa-ketoglutarate ($C_5H_4O_5$) and biomass ($CH_{1.8}O_{0.5}N_{0.2}$) respectively. The degree of reduction coefficient γ_{STO} was kept at 4.5 assuming polyhydroxybutyrate (PHB) type storage compounds were formed in the biomass cell to be consumed it later for growth.

7.4.2 Results and discussions of model calibration (with inhibition)

Nitrification inhibition during the glutamic acid biodegradation process allows sole carbon oxidation since ammonium conversion to nitrite is completely inhibited in the system. Without the nitrification components, the proposed model which explains both the respirometric and titrimetric measurements of the glutamic acid biodegradation process would be similar to the SSAG model developed for the surfactant biodegradation study (see Chapter 5). Figure 7.3 represents the calibration

results for glutamic acid biodegradation (100 mg COD/L) with nitrification inhibition where the simulated model profiles fit well with the experimental OUR and *Hp* measurements. The estimated model parameters for three different calibration approaches are presented in a tabular form along with their confidence intervals for checking the parameter estimation accuracy (Table 7.2).

Parameter estimation results gained from three calibration approaches show the hydrolysis rate k_h to vary from 12.82 to 12.96 day^{-1} which is higher than ASM3 default value prescribed for wastewater (3 day^{-1}). Even though Beccari et al. (2002) performed model based data interpretation for glutamic acid biodegradation, they ignored the hydrolysis process during modeling. Due to the lack of information in the literature, it was not possible to verify the results of the hydrolysis kinetics relating to the glutamic acid biodegradation process. However, the hydrolysis rate was reported as high as 18.5 day^{-1} by Lopez Zavala et al. (2004) when they investigated the biodegradation of faeces under aerobic conditions. In addition to the hydrolysis rate, this current study reveals that the saturation coefficient for hydrolysis (K_X) lies within the range 0.29-0.3 showing a lower value to that suggested in ASM3 (1.0). The same activated sludge was used in the surfactant biodegradation study where the estimated parameter K_X was found to vary from 0.39 to 0.44 (Chapter 5). Conversely, the parameter K_X was noted to be very low (0.025-0.1) when Yildiz et al. (2008) conducted their study using the organic compounds generated from polyamide-based carpet manufacturing.

In the current study, the estimated maximum heterotrophic biomass growth rate $\mu_{MAX,S}$ ranges from 0.31 to 0.32 day^{-1} which is lower than the ASM3 prescribed value (2 day^{-1}). Beccari et al. (2002) also found the maximum biomass growth rate to be slow (0.11 day^{-1}) during investigation of glutamic acid biodegradation. In addition, the estimated parameters K_S (0.63-0.631 mg COD/L), k_{STO} (0.73 and 0.75 day^{-1}), $Y_{H,S}$ (0.63), Y_{STO} (0.79-0.8) and $Y_{H,STO}$ (0.87) are found to be consistent for all three different calibration approaches. This confirms the validity of the model calibration and parameter estimation process (see Table 7.2).

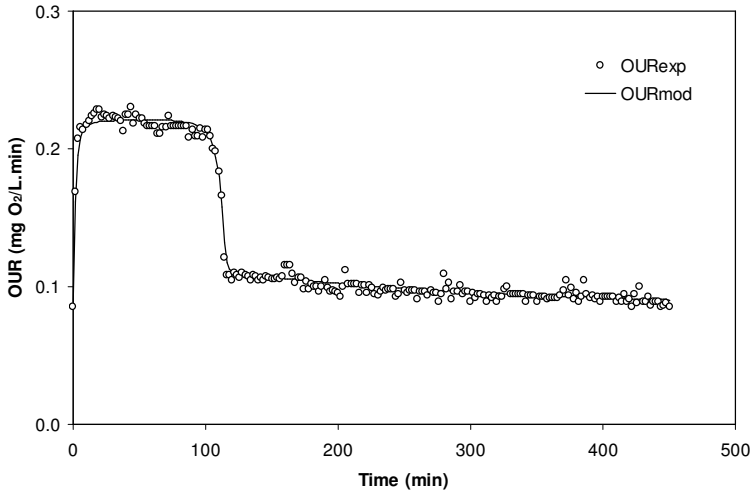

(a)

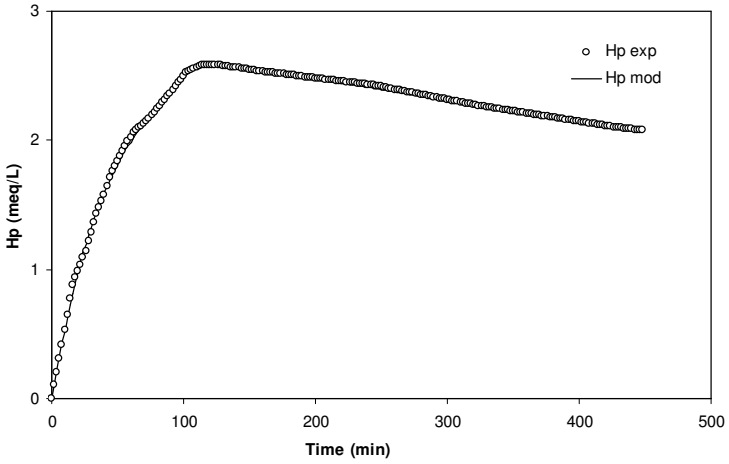

(b)

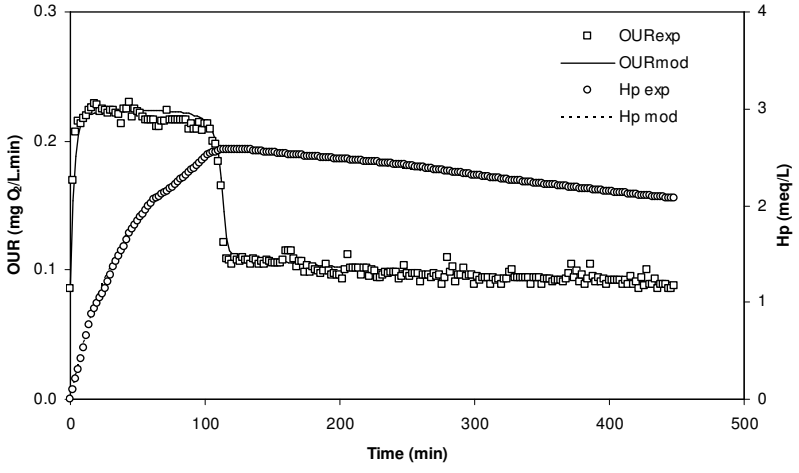

(c)

Figure 7.3: Model calibration using (a) respirometric data alone (b) titrimetric data alone and (c) combined respirometric-titrimetric data (Glu = 100 mg COD/L with nitrification inhibition)

Table 7.2: Parameter estimation results obtained from glutamic acid biodegradation with nitrification inhibition (confidence intervals are shown in brackets as percentages)

Parameters	Respirometric data alone (Confidence interval, %)	Titrimetric data alone (Confidence interval, %)	Combined data (Confidence interval, %)
Parameters Estimated:			
q_{MAX} (1/min)	$9.95\text{x}10^{-4} \pm 1.4\text{x}10^{-7}$ (0.01)	$9.9\text{x}10^{-4} \pm 2\text{x}10^{-7}$ (0.02)	$9.9\text{x}10^{-4} \pm 1.2\text{x}10^{-7}$ (0.01)
k_h (1/min)	$9.0\text{x}10^{-3} \pm 3.8\text{x}10^{-4}$ (4.22)	$8.9\text{x}10^{-3} \pm 5.1\text{x}10^{-6}$ (0.06)	$8.9\text{x}10^{-3} \pm 1.5\text{x}10^{-6}$ (0.02)
K_S (mgCOD/L)	0.63 ± 0.003 (0.48)	0.631 ± 0.059 (9.35)	0.631 ± 0.015 (2.38)
K_X (mgCOD X_S/mgCOD X_B)	0.29 ± 0.005 (1.72)	0.3 ± 0.007 (2.33)	0.3 ± 0.003 (1.0)
$Y_{H,S}$ (mgCOD X_B/mgCOD S_S)	0.63 ± 0.083 (13.17)	0.63 ± 0.022 (3.49)	0.63 ± 0.025 (3.97)
Y_{STO} (mgCOD X_{STO}/mgCOD S_S)	0.8 ± 0.243 (30.4)	0.79 ± 0.421 (53.3)	0.79 ± 0.053 (6.7)
$Y_{H,STO}$ (mgCOD X_B/mgCOD X_{STO})	0.87 ± 0.008 (0.92)	0.87 ± 0.079 (9.08)	0.87 ± 0.022 (2.53)
K_1 (mgCOD X_{STO}/mgCOD X_B)	0.03 ± 0.002 (6.67)	0.029 ± 0.003 (10.35)	0.029 ± 0.005 (17.24)
K_2 (mgCOD X_{STO}/mgCOD X_B)	$5.0\text{x}10^{-5} \pm 1.5\text{x}10^{-7}$ (0.3)	$4.9\text{x}10^{-5} \pm 1.8\text{x}10^{-5}$ (36.7)	$4.9\text{x}10^{-5} \pm 8.4\text{x}10^{-6}$ (17.14)
Parameters Assumed:			
b (1/min)	0.0001389	0.0001389	0.0001389
b_{STO} (1/min)	0.0001389	0.0001389	0.0001389
k_{NHacc} (1/min)	0.000056	0.000056	0.000056
f_{STO}[b] (mgCOD X_{STO}/mgCOD S_S)	0.65	0.65	0.65
f_{XI} (mgCOD /mgCOD)	0.2	0.2	0.2
k_1 (1/min)	--	1.0762	1.0762
$K_L a_{CO2}$ (1/min)	--	0.0555	0.0555
$C_{T,init}$[b] (mmol/L)	--	1.3	1.3
Parameters Calculated:			
HCO_3 (mmol/L)	--	1.251	1.251
CO_2 (mmol/L)	--	0.049	0.049
k_{STO} (1/min)	0.000518	0.000508	0.00051
$\mu_{MAX,S}$ (1/min)	0.00022	0.000218	0.000219
$\mu_{MAX,STO}$ (1/min)	0.00022	0.000218	0.000219
X_B (mgCOD/L)	800	800	800
MSE[a]	$1.96\text{x}10^{-5}$	$5.87\text{x}10^{-4}$	$3.0\text{x}10^{-4}$

[a] MSE refers to the mean squared error which is calculated from sum of squared errors divided by number of observations

[b] Parameters were fixed by trials for the better fit of experimental profile with the model

7.4.3 Results and discussions of model calibration (without inhibition)

The proposed model was found to explain both the carbon oxidation and nitrification behavior of the glutamic acid biodegradation process very well. The model was successfully calibrated with experimental OURs and *Hp* measurements for all three glutamic acid concentration studies (Figure 7.4-7.6).

Table 7.3 represents the parameter estimation results obtained from the three initial glutamic acid concentration studies where the proposed model was calibrated using OUR measurements alone. Observation shows that the hydrolysis related kinetic parameters such as k_h and K_X increase with the initial concentration. This was also noticed in the surfactant (SDS) biodegradation study (see Chapter 5). The hydrolysis rate (k_h) is found to vary from 12.1 to 13.68 day^{-1}, while the estimated parameter K_X lies between 0.26 and 0.37 for the glutamic acid concentration of 50 mg COD/L and 150 mg COD/L respectively. Details of glutamic acid biodegradation kinetics for comparison with this present study could not be found in the literature, as in most cases researchers limited their observations to characterizing and/or investigating glutamic acid biodegradation behavior (Pickartz et al., 1996; Dionisi et al. 2004; Chang et al., 2009). Even though Beccari et al. (2002) evaluated three different bio-kinetic models using glutamic acid as one of the test substrates, they ignored the glutamic acid hydrolysis kinetics during the parameter estimation process. However, the estimated parameters k_h and K_X here are found to be consistent with the parameter estimation results that were obtained from the glutamic acid biodegradation with nitrification inhibition study (Table 7.2 and Table 7.3).

This study reveals that the maximum growth rate of heterotrophic biomass on substrate $\mu_{MAX,S}$ (0.3 to 0.33 day^{-1}) is relatively slower than the storage formation rate k_{STO} (0.73-0.77 day^{-1}) (Table 7.3). ASM3 also prescribed a higher value (5 day^{-1}) for the parameter k_{STO} than for the parameter $\mu_{MAX,S}$ (2 day^{-1}), however both the default parameters are significantly higher than the current observation. Beccari et al. (2002) also noted slow rates for storage formation (0.11 day^{-1}) as well as for maximum biomass growth (0.007 day^{-1}) when they investigated glutamic acid biodegradation kinetics using a simultaneous storage and growth model for the calibration. They used the default ASM3 value (2 mg COD/L) for the parameter K_S during model

calibration, while in this study the parameter is found to lie within the range 0.58-0.63 mg COD /L indicating a strong biomass affinity to the substrate (glutamic acid). Activated sludge was sufficiently acclimatized with glutamic acid (see sub-section 3.2.3 in Chapter 3) prior to commencement of the main experiments to enhance the adaptation capacity of microorganisms. This seems to be the possible reason for such a strong biomass affinity to the glutamic acid during its biodegradation period. In addition, the estimated yield coefficient $Y_{H,S}$ from three different initial glutamic acid concentrations study lies within the range 0.61-0.63. In order to avoid complexity, Beccari et al. (2002) fixed the parameter $Y_{H,S}$ *to* 0.85 in their kinetic estimation studies using acetate, ethanol, glutamic acid and wastewater as substrates.

In fact, nitrification has little influence on carbon oxidation kinetics since two different types of biomass species, autotrophs and heterotrophs, are responsible for nitrification and carbon oxidation respectively, even though nitrifiers and heterotrophic bacteria compete with each other for the common substrate oxygen. In the presence of sufficient oxygen, the competition between the two different bacteria is minimized, even though heterotrophic bacteria generally outgrow the nitrifiers and consume the oxygen faster than the nitrifiers. Hence, the estimated model parameters that represent carbon oxidation (i.e. K_S, q_{MAX}, $Y_{H,S}$, Y_{STO}, $Y_{H,STO}$, K_1 and K_2) should be consistent for a particular substrate when the same activated sludge is used regardless of whether or not nitrification is allowed during the experiment. This fact was also reflected in the glutamic acid biodegradation modeling where the carbon oxidation related parameters estimated from the nitrification inhibition study were consistent with those estimated from the study without nitrification inhibition (Table 7.2 and Table 7.3).

The autotrophic maximum growth rate for the first step nitrification process ($\mu_{MAX,A1}$) is found to vary from 0.057 to 0.066 day^{-1} (Table 7.3). Even though for the overall nitrification process ASM suggested an autotrophic maximum growth rate (0.8 day^{-1} in ASM1, 1.0 day^{-1} in ASM3) higher than the current observation, Gernaey et al. (2001) observed a maximum autotrophic biomass growth rate as slow as 0.0047 day^{-1} during the first step of ammonium nitrification process (i.e. during the conversion of ammonium to nitrite). The parameter estimation results show that the maximum autotrophic biomass growth rate for the second nitrification step ($\mu_{MAX,A2}$) is

significantly slower than that for the first nitrification step, which consequently causes nitrite accumulation in the liquid medium (Brouwer et al., 1998). It was also confirmed by off-line nitrite nitrogen measurements where nitrite accumulation was clearly evident (Figure 7.9). Moreover, the estimated parameter K_{SA1} ranges between 0.26 to 0.31 mgN/L which is consistent with Gernaey et al. (2001). While the biomass yield coefficient Y_{A1} lies between 0.19-0.22, the parameter Y_{A2} is found within 0.032-0.036. Though Kim et al. (2009) revealed the yield coefficients Y_{A1} and Y_{A2} as 0.33 and 0.083 respectively; ASM prescribed the combined autotrophic biomass yield (Y_{A1} + Y_{A2}) to be 0.24 which supports the current observation. In addition, the estimated nitrification related model parameters are consistent with those for the urea and ammonium nitrification study, described in Chapter 6, where the same activated sludge and pH was used.

Table 7.4 shows the parameter estimation results with their confidence intervals where titrimetric measurement alone was used during model calibration. Parameter estimation results obtained from combined respirometric-titrimetric measurements are presented in Table 7.5. The titrimetry related component $C_{T,init}$ was adjusted to 1.6, 1.55 and 1.83 mmol CO_2/L for the glutamic acid concentrations of 150, 100 and 50 mg COD/L respectively for the better fit of experimental profiles with the model one. It should be noted that the experiment with the 50 mg COD/L glutamic acid concentration was performed after finishing the run for 100 and 150 mg COD/L concentrations. As a result inorganic carbon accumulation may have taken place in the reactor and resulted in a higher $C_{T,init}$ value. The model parameter estimation results for all three calibration approaches are found to be consistent thereby validating the proposed model. In addition, the confidence intervals for all estimated parameters are found to be reasonable except that for K_2. A similar problem was noted by Sin et al. (2005) where the parameters K_1 and K_2 were identified as interdependent under the feast phase of the biodegradation process. However, in the current study the calculated mean squared errors (MSEs) for all three calibration approaches (Table 7.3-Table 7.5) are found to be acceptable which statistically confirms the soundness of the proposed model.

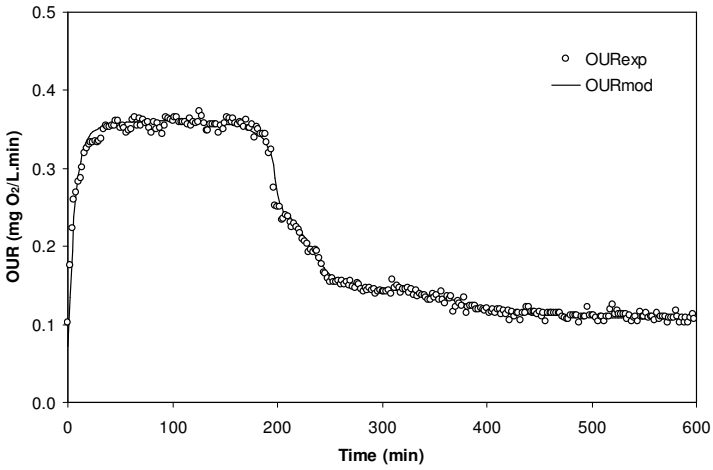

(a)

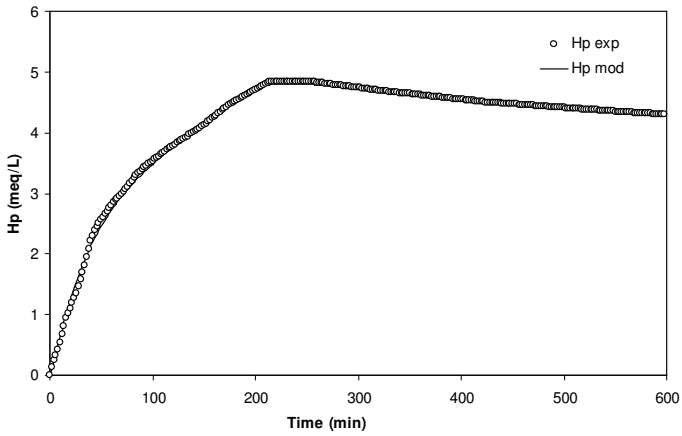

(b)

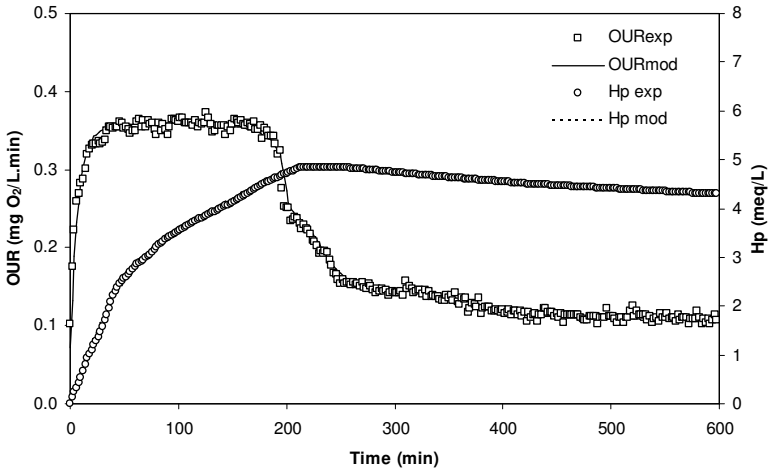

(c)

Figure 7.4: Model calibration using (a) respirometric data alone (b) titrimetric data alone and (c) combined respirometric-titrimetric data (Glu = 150 mg COD/L without nitrification inhibition)

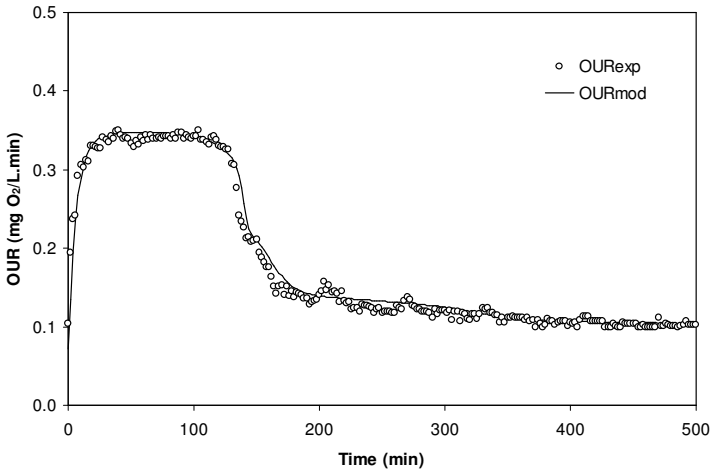

(a)

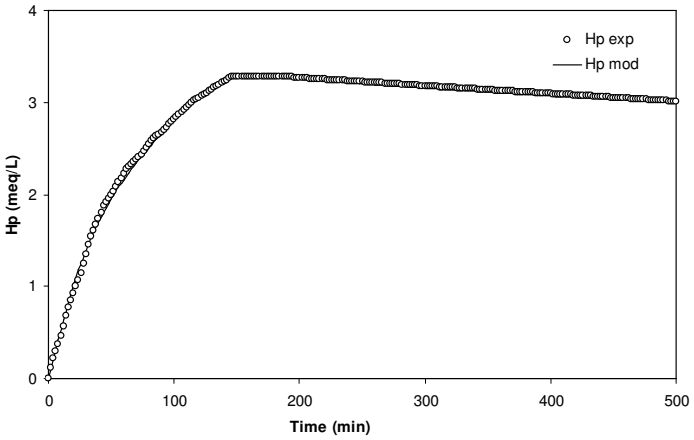

(b)

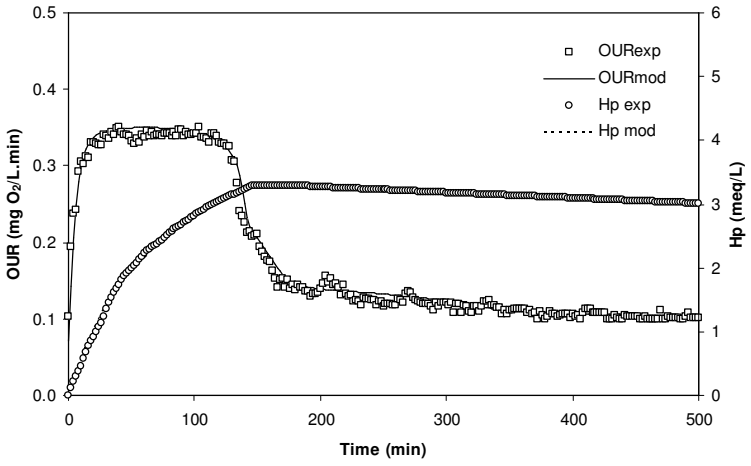

(c)

Figure 7.5: Model calibration using (a) respirometric data alone (b) titrimetric data alone and (c) combined respirometric-titrimetric data (Glu = 100 mg COD/L without nitrification inhibition)

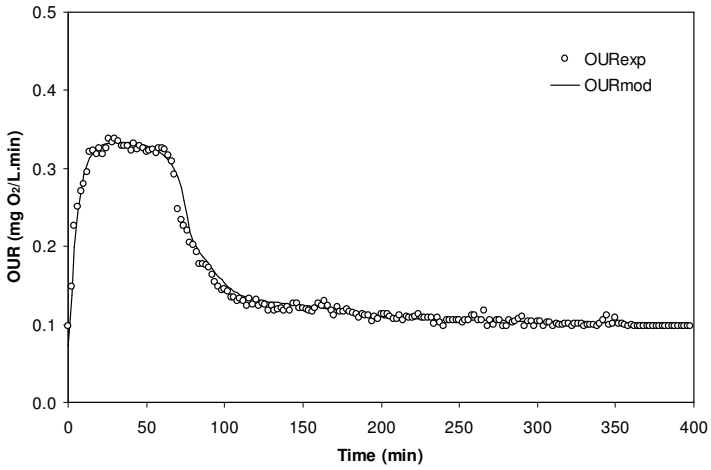

(a)

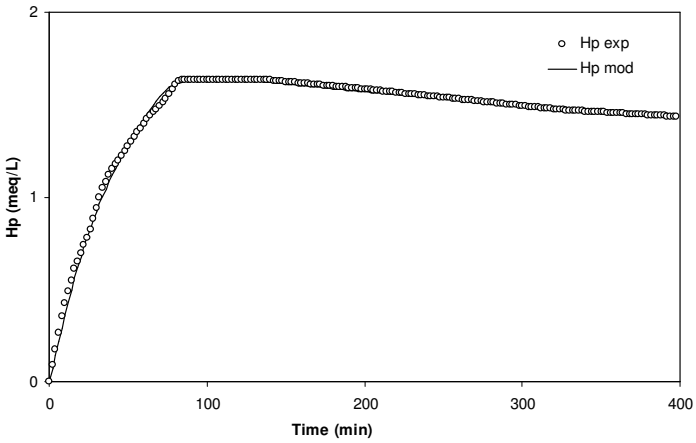

(b)

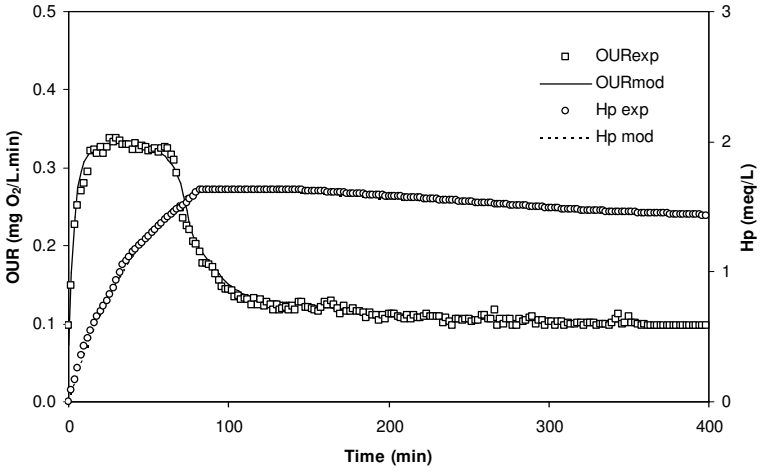

(c)

Figure 7.6: Model calibration using (a) respirometric data alone (b) titrimetric data alone and (c) combined respirometric-titrimetric data (Glu = 50 mg COD/L without nitrification inhibition)

Table 7.3: Parameter estimation results using respirometric data alone for three different concentration studies without nitrification inhibition (confidence intervals are shown in brackets as percentages)

Parameters	Glu 150 mg COD/L (Confidence interval, %)	Glu 100 mg COD/L (Confidence interval, %)	Glu 50 mg COD/L (Confidence interval, %)
Parameters Estimated:			
k_h (1/min)	$9.5\times10^{-3} \pm 1.2\times10^{-3}$ (12.63)	$9.02\times10^{-3} \pm 4.36\times10^{-4}$ (4.83)	$8.4\times10^{-3} \pm 7.61\times10^{-4}$ (9.06)
q_{MAX} (1/min)	$1.03\times10^{-3} \pm 1.72\times10^{-7}$ (0.02)	$1.0\times10^{-3} \pm 6.81\times10^{-7}$ (0.07)	$9.8\times10^{-4} \pm 3.35\times10^{-7}$ (0.03)
$\mu_{MAX,A1}$ (1/min)	$4.55\times10^{-5} \pm 1.01\times10^{-8}$ (0.02)	$4.52\times10^{-5} \pm 5.92\times10^{-8}$ (0.13)	$3.95\times10^{-5} \pm 1.79\times10^{-7}$ (0.45)
$\mu_{MAX,A2}$ (1/min)	$5.18\times10^{-6} \pm 9.71\times10^{-9}$ (0.19)	$4.28\times10^{-6} \pm 3.39\times10^{-9}$ (0.08)	$3.87\times10^{-6} \pm 1.13\times10^{-9}$ (0.03)
K_X (mgCOD X_S/mgCOD X_B)	0.37 ± 0.04 (10.81)	0.29 ± 0.075 (25.86)	0.26 ± 0.113 (43.46)
K_S (mgCOD/L)	0.63 ± 0.01 (1.59)	0.629 ± 0.032 (5.09)	0.58 ± 0.059 (10.17)
K_1 (mgCOD X_{STO}/mgCOD X_B)	$0.033 \pm 2.2\times10^{-4}$ (0.67)	$0.03 \pm 6.57\times10^{-4}$ (27.58)	0.028 ± 0.003 (10.71)
K_2 (mgCOD X_{STO}/mgCOD X_B)	$7.08\times10^{-5} \pm 4.63\times10^{-6}$ (6.54)	$5.1\times10^{-5} \pm 2.57\times10^{-5}$ (50.39)	$4.8\times10^{-5} \pm 1.73\times10^{-5}$ (36.04)
K_{SA1} (mgN/L)	0.311 ± 0.001 (0.32)	0.29 ± 0.003 (1.03)	0.258 ± 0.03 (11.63)
K_{SA2} (mgN/L)	0.219± 0.018 (8.22)	0.191 ± 0.053 (27.75)	0.17 ± 0.072 (42.35)
$Y_{H,S}$ (mgCOD X_B/mgCOD S_S)	0.63 ± 0.33 (52.38)	0.63 ± 0.15 (23.81)	0.61 ± 0.55 (90.16)
Y_{STO} (mgCOD X_{STO}/mgCOD S_S)	0.8 ± 0.09 (11.25)	0.8 ± 0.36 (45)	0.8 ± 0.14 (17.5)
$Y_{H,STO}$ (mgCOD X_B/mgCOD X_{STO})	0.87 ± 0.02 (2.3)	0.87 ± 0.24 (2.19)	0.87 ± 0.12 (13.79)
Y_{A1} (mgCOD X_B/mgN S_{NH})	0.221 ± 0.091 (41.18)	0.219 ± 0.129 (58.9)	0.19 ± 0.038 (20)
Y_{A2} (mgCOD X_B/mgN S_{NO2})	$0.036 \pm 5.81\times10^{-4}$ (1.61)	0.036 ± 0.003 (8.33)	0.032 ± 0.008 (25)
Parameters Assumed:			
b (1/min)	0.0001389	0.0001389	0.0001389
b_{STO} (1/min)	0.0001389	0.0001389	0.0001389
k_{NHacc} (1/min)	0.000056	0.000056	0.000056
f_{STO} [b] (mgCOD X_{STO}/mgCOD S_S)	0.65	0.65	0.65
f_{XI} (mgCOD /mgCOD)	0.2	0.2	0.2
Parameters Calculated:			
k_{STO} (1/min)	0.000536	0.00052	0.00051
$\mu_{MAX,S}$ (1/min)	0.000227	0.00022	0.00021
$\mu_{MAX,STO}$ (1/min)	0.000227	0.00022	0.00021
X_B (mgCOD/L)	650	650	650
MSE [a]	5.33×10^{-5}	1.15×10^{-4}	5.69×10^{-5}

[a] MSE refers to the mean squared error which is calculated from sum of squared errors divided by number of observations

[b] Parameters were fixed by trials for the better fit of experimental profile with the model

Table 7.4: Parameter estimation results using titrimetric data alone for three different concentration studies without nitrification inhibition (confidence intervals are shown in brackets as percentages)

Parameters	Glu 150 mg COD/L (Confidence interval, %)	Glu 100 mg COD/L (Confidence interval, %)	Glu 50 mg COD/L (Confidence interval, %)
Parameters Estimated:			
k_h (1/min)	$9.4\times10^{-3} \pm 1.05\times10^{-6}$ (0.01)	$8.8\times10^{-3} \pm 5.03\times10^{-6}$ (0.06)	$8.31\times10^{-3} \pm 2.14\times10^{-5}$ (0.26)
q_{MAX} (1/min)	$1.03\times10^{-3} \pm 4.05\times10^{-7}$ (0.04)	$1.01\times10^{-3} \pm 2.44\times10^{-7}$ (0.02)	$9.75\times10^{-4} \pm 1.33\times10^{-7}$ (0.01)
$\mu_{MAX,A1}$ (1/min)	$4.56\times10^{-5} \pm 2.6\times10^{-7}$ (0.57)	$4.55\times10^{-5} \pm 2.89\times10^{-7}$ (0.64)	$3.94\times10^{-5} \pm 5.72\times10^{-7}$ (1.45)
$\mu_{MAX,A2}$ (1/min)	$5.18\times10^{-6} \pm 7.69\times10^{-8}$ (1.49)	$4.28\times10^{-6} \pm 6.06\times10^{-8}$ (1.42)	$3.81\times10^{-6} \pm 4.39\times10^{-7}$ (11.52)
K_X (mgCOD X_S/mgCOD X_B)	0.38 ± 0.003 (0.79)	0.31 ± 0.007 (2.26)	0.24 ± 0.025 (10.42)
K_S (mgCOD/L)	0.64 ± 0.38 (59.38)	0.622 ± 0.228 (36.66)	0.61 ± 0.59 (96.72)
K_1 (mgCOD X_{STO}/mgCOD X_B)	0.033 ± 0.005 (15.15)	0.029 ± 0.008 (27.58)	0.027 ± 0.023 (85.19)
K_2 (mgCOD X_{STO}/mgCOD X_B)	$9.1\times10^{-5} \pm 3.3\times10^{-4}$ (362.6)	$5.2\times10^{-5} \pm 1.02\times10^{-4}$ (196.2)	$4.7\times10^{-5} \pm 1.19\times10^{-4}$ (253.2)
K_{SA1} (mgN/L)	0.316 ± 0.03 (9.49)	0.28 ± 0.15 (53.57)	0.26 ± 0.057 (21.92)
K_{SA2} (mgN/L)	0.246 ± 0.064 (26.02)	0.2 ± 0.026 (13)	0.17 ± 0.081 (47.65)
$Y_{H,S}$ (mgCOD X_B/mgCOD S_S)	0.63 ± 0.58 (92.06)	0.63 ± 0.06 (9.52)	0.61 ± 0.086 (14.1)
Y_{STO} (mgCOD X_{STO}/mgCOD S_S)	0.8 ± 0.22 (27.5)	0.8 ± 0.21 (26.25)	0.77 ± 0.58 (75.32)
$Y_{H,STO}$ (mgCOD X_B/mgCOD X_{STO})	0.87 ± 0.43 (49.43)	0.87 ± 0.41 (47.13)	0.87 ± 0.126 (14.48)
Y_{A1} (mgCOD X_B/mgN S_{NH})	0.23 ± 0.061 (26.52)	0.22 ± 0.065 (29.55)	0.2 ± 0.157 (78.5)
Y_{A2} (mgCOD X_B/mgN S_{NO2})	0.038 ± 0.03 (78.95)	0.034 ± 0.027 (79.41)	0.032 ± 0.022 (68.75)
Parameters Assumed:			
b (1/min)	0.0001389	0.0001389	0.0001389
b_{STO} (1/min)	0.0001389	0.0001389	0.0001389
k_{NHacc} (1/min)	0.000056	0.000056	0.000056
f_{STO}[b] (mgCOD X_{STO}/mgCOD S_S)	0.65	0.65	0.65
f_{XI} (mgCOD /mgCOD)	0.2	0.2	0.2
k_1 (1/min)	1.0762	1.0762	1.0762
$K_L a_{CO2}$ (1/min)	0.055	0.055	0.055
$C_{T,init}$[b] (mmol/L)	1.6	1.55	1.83
Parameters Calculated:			
HCO_3 (mmol/L)	1.5398	1.4917	1.7612
CO_2 (mmol/L)	0.0602	0.0583	0.0688
k_{STO} (1/min)	0.000536	0.000525	0.000484
$\mu_{MAX,S}$ (1/min)	0.000227	0.000223	0.000208
$\mu_{MAX,STO}$ (1/min)	0.000227	0.000223	0.000208
X_B (mgCOD/L)	650	650	650
MSE[a]	2.04×10^{-3}	8.35×10^{-4}	3.17×10^{-4}

[a] MSE refers to the mean squared error which is calculated from sum of squared errors divided by number of observations

[b] Parameters were fixed by trials for the better fit of experimental profile with the model

Table 7.5: Parameter estimation results using combined respirometric-titrimetric data for three different concentration studies without nitrification inhibition (confidence intervals are shown in brackets as percentages)

Parameters	Glu 150 mg COD/L (Confidence interval, %)	Glu 100 mg COD/L (Confidence interval, %)	Glu 50 mg COD/L (Confidence interval, %)
Parameters Estimated:			
k_h (1/min)	$9.5\times10^{-3} \pm 1.43\times10^{-6}$ (0.02)	$9.0\times10^{-3} \pm 5.97\times10^{-6}$ (0.81)	$8.3\times10^{-3} \pm 6.76\times10^{-5}$ (0.81)
q_{MAX} (1/min)	$1.03\times10^{-3} \pm 2.24\times10^{-6}$ (0.22)	$1.0\times10^{-3} \pm 1.52\times10^{-6}$ (0.15)	$9.75\times10^{-4} \pm 1.94\times10^{-7}$ (0.02)
$\mu_{MAX,A1}$ (1/min)	$4.55\times10^{-5} \pm 2.25\times10^{-8}$ (0.05)	$4.55\times10^{-5} \pm 1.41\times10^{-7}$ (0.31)	$3.95\times10^{-5} \pm 6.51\times10^{-9}$ (0.02)
$\mu_{MAX,A2}$ (1/min)	$5.2\times10^{-6} \pm 7.3\times10^{-10}$ (0.01)	$4.2\times10^{-6} \pm 7.9\times10^{-10}$ (0.02)	$3.8\times10^{-6} \pm 1.31\times10^{-9}$ (0.03)
K_X (mgCOD X_S/mgCOD X_B)	0.38 ± 0.004 (1.05)	0.3 ± 0.011 (3.67)	0.26 ± 0.097 (37.3)
K_S (mgCOD/L)	0.633 ± 0.157 (24.8)	0.63 ± 0.145 (23.01)	0.58 ± 0.113 (19.48)
K_1 (mgCOD X_{STO}/mgCOD X_B)	0.032 ± 0.009 (23.08)	0.03 ± 0.013 (23.08)	0.026 ± 0.006 (23.08)
K_2 (mgCOD X_{STO}/mgCOD X_B)	$7.1\times10^{-5} \pm 1.94\times10^{-4}$ (273.2)	$5.0\times10^{-5} \pm 9.85\times10^{-5}$ (197)	$4.5\times10^{-5} \pm 8.66\times10^{-5}$ (192.4)
K_{SA1} (mgN/L)	0.32 ± 0.028 (8.75)	0.27 ± 0.019 (7.04)	0.26 ± 0.058 (22.3)
K_{SA2} (mgN/L)	0.22 ± 0.083 (37.73)	0.22 ± 0.099 (45)	0.17 ± 0.047 (27.6)
$Y_{H,S}$ (mgCOD X_B/mgCOD S_S)	0.63 ± 0.13 (20.64)	0.63 ± 0.435 (69.05)	0.61 ± 0.185 (30.33)
Y_{STO} (mgCOD X_{STO}/mgCOD S_S)	0.8 ± 0.061 (7.63)	0.8 ± 0.116 (14.5)	0.8 ± 0.738 (92.25)
$Y_{H,STO}$ (mgCOD X_B/mgCOD X_{STO})	0.87 ± 0.151 (17.36)	0.87 ± 0.178 (20.46)	0.87 ± 0.705 (81.03)
Y_{A1} (mgCOD X_B/mgN S_{NH})	0.22 ± 0.005 (2.27)	0.22 ± 0.096 (43.64)	0.19 ± 0.097 (51.05)
Y_{A2} (mgCOD X_B/mgN S_{NO2})	0.037 ± 0.023 (62.16)	0.034 ± 0.022 (64.71)	0.03 ± 0.01 (33.33)
Parameters Assumed:			
b (1/min)	0.0001389	0.0001389	0.0001389
b_{STO} (1/min)	0.0001389	0.0001389	0.0001389
k_{NHacc} (1/min)	0.000056	0.000056	0.000056
f_{STO}[b] (mgCOD X_{STO}/mgCOD S_S)	0.65	0.65	0.65
f_{XI} (mgCOD /mgCOD)	0.2	0.2	0.2
k_1 (1/min)	1.0762	1.0762	1.0762
K_La_{CO2} (1/min)	0.0555	0.055	0.055
$C_{T,init}$[b] (mmol/L)	1.6	1.55	1.83
Parameters Calculated:			
HCO_3 (mmol/L)	1.5398	1.4917	1.7612
CO_2 (mmol/L)	0.0602	0.0583	0.0688
k_{STO} (1/min)	0.000536	0.000521	0.000507
$\mu_{MAX,S}$ (1/min)	0.000227	0.000221	0.000208
$\mu_{MAX,STO}$ (1/min)	0.000227	0.000221	0.000208
X_B (mgCOD/L)	650	650	650
MSE[a]	1.11×10^{-3}	4.86×10^{-4}	2.11×10^{-4}

[a] MSE refers to the mean squared error which is calculated from sum of squared errors divided by number of observations

[b] Parameters were fixed by trials for the better fit of experimental profile with the model

7.4.4 Model evaluation

To ensure the accuracy of the model, calibration and parameter estimation were performed using three different calibration approaches: using respirometric measurements alone, titrimetric measurements alone and combined respirometric titrimetric measurements. Figure 7.3 shows the calibration results for a glutamic acid concentration of 100 mg COD/L with nitrification inhibition where the proposed model explains the experimental behavior very well. Furthermore, the estimated model parameters from the three different calibration approaches provide consistent results with reasonable confidence intervals and mean squared errors (Table 7.2) thereby validating the proposed model.

In the nitrification inhibition study, the proposed model was validated using off-line ammonium nitrogen measurements in the liquid medium as well and was found to fit the model simulated profile (Figure 7.7). It was not possible to measure the glutamic acid concentration in the liquid medium. However an attempt was made to measure the total COD (Figure 7.7) using off-line measurement technique to provide an understanding of the net chemical oxygen demand corresponding to glutamic acid, alfa-ketoglutarate and ammonium oxidation processes.

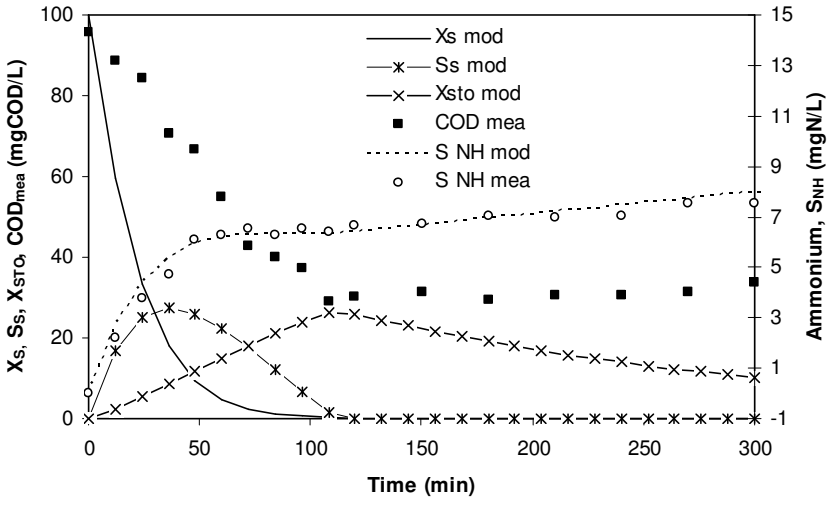

Figure 7.7: Model validation using off-line COD and ammonium measurements during glutamic acid (100 mg COD/L) biodegradation with nitrification inhibition

In the study without nitrification inhibition, the model was calibrated for three different initial glutamic acid concentrations (50, 100 and 150 mg COD/L) to justify the precision of the model calibration and parameter estimation processes. The proposed model was found to fit well with on-line respirometric and titrimetric measurements for all three concentrations (Figure 7.4-7.6). In addition, the estimated parameters were found to lie within a narrow range providing reasonable confidence intervals and mean squared errors (Table 7.3-7.5) thereby confirming the accuracy of the proposed model.

Though it was not possible to measure the glutamic acid concentration in the liquid medium, off-line COD measurement was performed (Figure 7.8) which show, in the case without nitrification inhibition, the net chemical oxygen demand for glutamic acid, alfa-ketoglutarate, ammonium and nitrite oxidation. Figure 7.9 illustrates the model validation using off-line ammonium, nitrite and nitrate nitrogen measurements during glutamic acid biodegradation (100 mg COD/L) where both carbon oxidation and nitrification take place. The model simulated profiles for the respective state variables (ammonium, nitrite and nitrate concentrations) are found to be a reasonable match with the measured data and validate the proposed model.

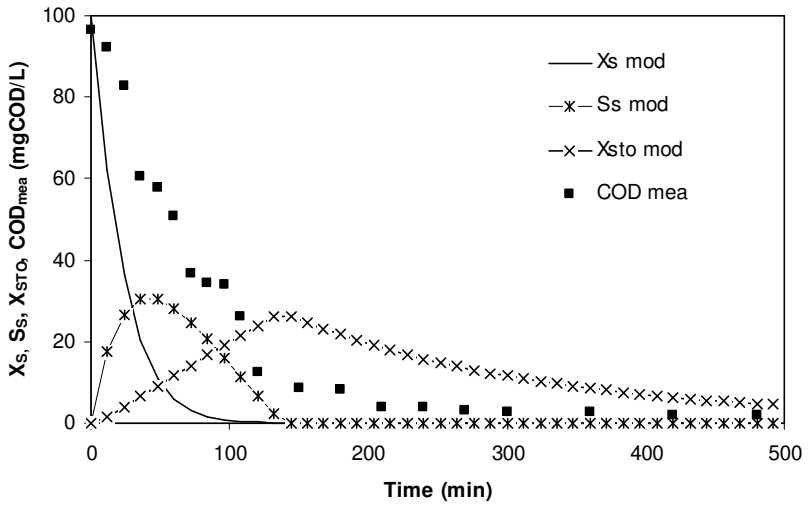

Figure 7.8: Off-line COD measurements during glutamic acid (100 mg COD/L) biodegradation without nitrification inhibition

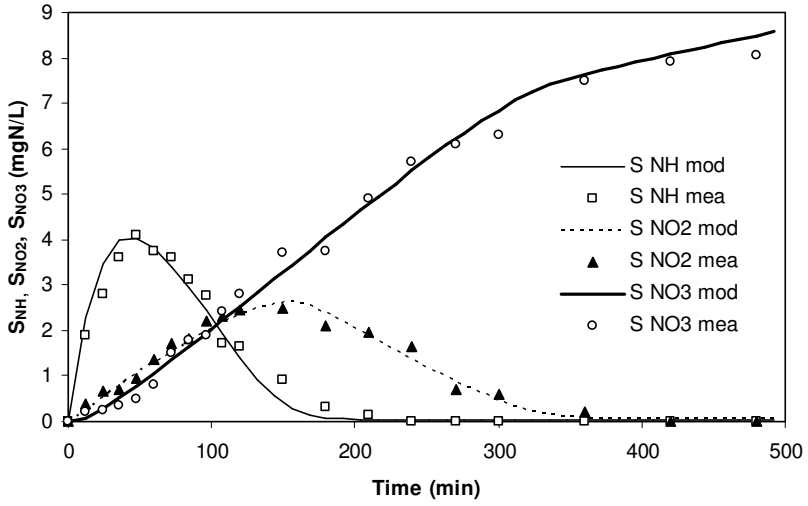

Figure 7.9: Model validation using off-line ammonium, nitrite and nitrate measurements during glutamic acid (100 mg COD/L) biodegradation without nitrification inhibition

In the proposed model, the i_{NBM} content corresponding to the biomass composition $CH_{1.8}O_{0.5}N_{0.2}$ was calculated as 0.083 gN/g COD X_B which lies within the typical range of range 7% to 8.6% for the nitrogen content of biomass as reported by Henze et al. (2000). The model includes the kinetic parameter k_{NHacc} that was fixed to 0.08 day^{-1} for better model calibration. Though there is no strong evidence on what kind of storage products are formed during glutamic acid biodegradation, the contribution of acetyl-CoA during glutamic acid biodegradation is noted. Based on the above explanation, it was assumed that polyhydroxybutyrate (PHB), which is usually observed in the acetate biodegradation process (Dircks et al. 2001), is formed as storage products in the biomass cell. The degree of reduction of storage products, γ_{STO} was calculated as 4.5 by considering the formula as $CH_{1.5}O_{0.5}$ (Van Aalst-van Leeuwen et al., 1997).

7.5 Monod kinetic parameters for glutamic acid biodegradation

Based on three different initial glutamic acid concentration studies (without nitrification inhibition), Monod kinetic parameters, K_S and $\mu_{MAX,S}$, were estimated and are shown in Table 7.6. The table also includes the calculation of 95% confidence intervals for the respective kinetic parameters estimates. Figure 7.10 represents the estimated maximum biomass growth rate against initial substrate

(glutamic acid) concentrations with a calibrated Monod profile. In this study, the parameter $\mu_{MAX,S}$ was estimated as 0.326 day^{-1} which is lower than the typical ASM3 value (2 day^{-1}) indicating a relatively slow biomass growth rate on glutamic acid. Beccari et al. (2002) also observed a slow biomass growth rate where the parameter $\mu_{MAX,S}$ was estimated to be 0.11 day^{-1} using a simultaneous storage and growth model to explain glutamic acid biodegradation behavior. The substrate affinity constant K_S for glutamic acid biodegradation was estimated in this study as 0.65 mg COD/L whereas Beccari et al. (2002) used the default ASM3 value (2 mg COD/L) for model calibration. It is noteworthy that the sludge was sufficiently acclimatized (for 12 days) with glutamic acid before starting the main batch experiments to enhance the adaptation capacity of the biomass with glutamic acid. It may cause a strong affinity to glutamic acid in the biodegradation process.

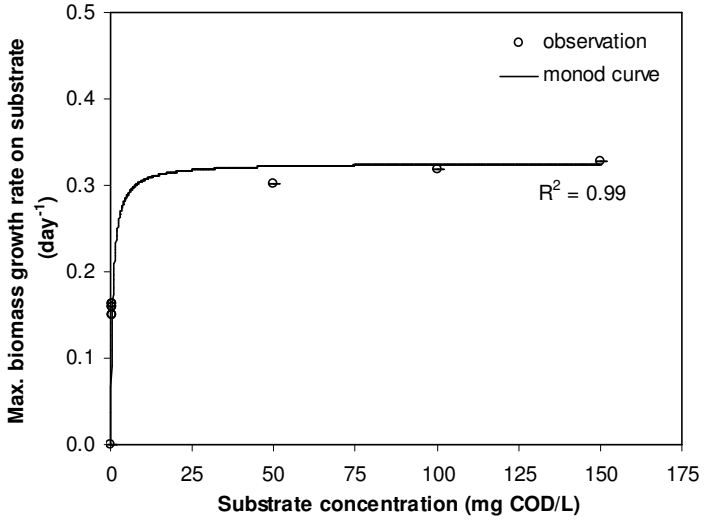

Figure 7.10: Monod profile for maximum biomass growth rate on glutamic acid at pH of 7.8

Table 7.6: Estimated Monod kinetics for glutamic acid biodegradation at pH 7.8

Parameter	Glutamic acid
K_S (mg COD/L)	$0.65 \pm 4.9 \times 10^{-4}$
$\mu_{MAX,S}$ (day^{-1})	$0.326 \pm 1.36 \times 10^{-5}$

7.6 Conclusions

An improved bio-kinetic model was proposed in the current study to explain both the organic carbon oxidation and nitrification in an activated sludge system where glutamic acid was used as the test compound. The proposed model included the hydrolysis process along with the consideration of a non-linear carbon dioxide transfer rate in the liquid medium. In addition to the respirometry, all relevant stoichiometric parameters were taken into account to demonstrate the titrimetric measurements of the glutamic acid biodegradation process. The proposed model was successfully calibrated with the experimental observations relating to glutamic acid biodegradation both with and without nitrification inhibition. Model parameters were estimated using three different calibration approaches and compared to justify the proposed model. The estimated model parameters were found to be very close for all three calibration approaches and confirm the precision of the parameter estimation process. More importantly, the common model parameters (related to carbon oxidation) that were estimated from the assays for glutamic acid biodegradation with and without nitrification inhibition were found to be identical. Validation of the proposed model was also performed using off-line ammonium, nitrite and nitrate nitrogen measurements where the model explained reasonably well the glutamic acid biodegradation process both with and without nitrification inhibition.

Chapter 8
Conclusions and Recommendations

The overall objective of this project was to develop and calibrate activated sludge models for organic carbon and nitrogen oxidation using on-line respirometric and titrimetric measurements in the liquid phase.

To achieve this objective, acetate and surfactant (SDS) were used to investigate sole carbon oxidation (see Chapter 4 and Chapter 5 respectively); while ammonium and urea were selected to observe nitrification (see Chapter 6). The effect of the combined carbon and nitrogen components on the aerobic biodegradation process was investigated using glutamic acid (see Chapter 7). An improved model was developed to include oxygen and proton balances for each of these substrates. The model was then successfully calibrated using simultaneous respirometric and titrimetric measurements. The following subsections outline the conclusions based on experimental observations, model development, model calibration and model parameter estimation followed by some recommendations for future research work.

8.1 Summary and Conclusions

8.1.1 Experimental observations

In this study, the investigation of the aerobic biodegradation of five different substrates namely acetate, surfactant (SDS), urea, ammonium and glutamic acid were conducted by monitoring the respirometric and titrimetric measurements in an activated sludge system using batch experiments. The activated sludge, which was used in this research project, was properly acclimatized with the respective test substrate prior to the commencement of the main experiments to allow the microorganisms to perform at their optimum capacity. The substrate-based experimental outcomes of the aerobic biodegradation studies are summarized below.

Acetate biodegradation

- Acetate is a well-established easily-biodegradable carbon compound that degrades quickly as evidenced by this current research project where the biodegradation behavior was monitored using dissolved oxygen and pH change measurements.

- The oxygen uptake rate (OUR) increased to the maximum level during the feast period of the biodegradation process. It dropped to a level higher than the endogenous respiration rate when acetate was completely removed followed by a gradual decrease to the endogenous OUR level producing a "tail" in the profile. This kind of "tail" is described in the literature and attributed to the accumulation of storage products in the biomass cell to be used for growth during the absence of external substrate in the liquid medium.

- Acid addition was noted during acetate biodegradation indicating proton consumption in the system. Both the oxygen and proton consumption rates were observed to increase with the initial acetate concentration. In addition, both rates dropped at the same time indicating that all the acetate in the liquid phase was used up by the activated sludge.

- The change in pH from 7.8 to 7 did not have any significant effect on the titrimetric process of acetate biodegradation.

- Under endogenous conditions, the titrimetric profile dropped to the background proton consumption rate that was observed before adding acetate into the reactor when pH was maintained at 7.8. The CO_2 stripping leads the titrimetric process during this period.

Surfactant (SDS) biodegradation

- Although SDS has a relatively complex chemical structure compared to that of acetate, the oxygen consumption rate in SDS biodegradation was observed to increase drastically as was observed in acetate biodegradation. It must be noted that the sludge used for the SDS biodegradation study was acclimatized with SDS (until consistant OUR profiles were obtained for successive SDS

pulses) before commencing the main experiments. This may have led the SDS to degrade readily.

- Similar to acetate biodegradation, SDS biodegradation caused a dramatic increase in the OUR immediately after the addition of the substrate to the reactor. The OUR profile, however, showed a longer "tail" than that observed during acetate biodegradation indicating a significant contribution of storage products to the SDS biodegradation process during the famine phase.

- SDS biodegradation caused base addition to the reactor (i.e. proton production) under feast conditions as opposed to the observations made in the acetate study where proton consumption took place. Both the oxygen and proton consumption rates were observed to increase with the initial SDS concentration.

- The change in pH (from 8.5 to 7) had a significant influence on the titrimetric process. Base addition occurred throughout the exogenous and endogenous states of the SDS biodegradation when the pH was maintained at 8.5 indicating proton production in the liquid medium. However, base addition was observed under the exogenous state followed by acid addition indicating proton consumption in the liquid medium during the endogenous state when the pH was maintained at 7 and 7.8. The net proton production was found to decrease significantly when the pH of the reactor dropped from 7.8 to 7.

- Under endogenous conditions, when pH was maintained at 7.8 the titrimetric profile dropped (due to CO_2 stripping) to the background proton consumption rate that was observed before adding SDS into the reactor.

Urea and Ammonium nitrification

- Respirometric observations showed a double peak in the OUR profile indicating two different nitrification steps for substrates of urea and ammonium. It indicates a slower autotrophic biomass growth rate for the second nitrification step (conversion of nitrite to nitrate) than for the first nitrification step (conversion of ammonium to nitrite) and results in nitrite accumulation in the system. This nitrite accumulation was also confirmed using off-line nitrite measurements.

- Urea nitrification initially caused acid addition (i.e. proton consumption) to the reactor followed by a continuous base addition under feast conditions. Ammonium nitrification, however, resulted only in base addition to the reactor representing proton production during the feast period.

- Both the oxygen uptake rate and proton consumption/production rate were observed to increase proportionally with the initial substrate (urea or ammonium) concentration.

- The titrimetric profile dropped to the background proton consumption rate under endogenous conditions (at pH 7.8), during which the CO_2 stripping leads the titrimetric process.

Glutamic Acid biodegradation

- The OUR profiles for the studies with and without nitrification inhibition were found to be distinctive, especially during the feast period of the glutamic acid biodegradation process. The OUR dropped from its maximum peak to a second peak during the nitrification process without inhibition. However, that pattern was not exhibited in the case of nitrification inhibition.

- Nitrite accumulation during the biodegradation process contributed to the formation of a prominent "tail" in the OUR profile. Off-line nitrite measurements also confirmed the nitrite accumulation in the system.

- A continuous base addition was observed during feast conditions representing proton production during glutamic acid biodegradation. Both the maximum oxygen uptake rate and the proton production rate were found to increase with the initial glutamic acid concentration.

- Acid was added during the period of endogenous respiration when the pH was maintained at 7.8. This was also noted during the acetate, surfactant, urea and ammonium biodegradation studies.

8.1.2 Development of bio-kinetic models

The following substrate-based modeling summary reflects the major contributions of this dissertation to bio-kinetic model development.

Acetate biodegradation

Activated sludge models evolved from single growth to simultaneous storage and growth models and were normally calibrated using experimental respirometric measurements. A recently developed simultaneous storage and growth (SSAG) model addressed all the shortcomings of previously developed models, and proposed an improved kinetic expression for the degradation of storage products under famine conditions. This model was well-calibrated using respirometric experimental measurements. However, this model required further modification to enable it to interpret the titrimetric behavior of the substrate biodegradation process as both dissolved oxygen and pH dynamics occur simultaneously in a bio-reactor. Hence, in this current study an extended SSAG model was proposed by:

- introducing stoichiometric parameters involving titrimetry in each step of the growth and storage phases; and,
- considering a non-linear carbon dioxide transfer rate in the liquid medium.

Surfactant (SDS) biodegradation

The extended SSAG model, which was used for acetate biodegradation, was applied with necessary modifications to interpret both the respirometric and titrimetric behavior of the SDS biodegradation process. The main features of the SDS biodegradation modeling are as follows.

- The hydrolysis process was included in the proposed SSAG model.
- In addition to respirometry, all relevant stoichiometric parameters were considered during modeling to interpret the titrimetric measurements of the SDS biodegradation process. The SDS biodegradation pathway was taken into account during the titrimetric model development.

Urea and Ammonium nitrification

A two-step nitrification model was proposed to interpret both the urea and ammonium nitrification processes. The main features of the SDS biodegradation modeling are as follows.

- The hydrolysis process was included in the proposed model since urea is initially hydrolyzed to ammonium which then undergoes a nitrification process.
- The stoichiometric parameters related to both the respirometric and titrimetric components were introduced in the proposed model following the urea biodegradation pathway. These parameters were derived directly from the biochemical conversion of urea under aerobic conditions.
- The titrimetric model included the dynamic (non-linear) CO_2 transfer process.

Glutamic Acid biodegradation

An improved bio-kinetic model was proposed to explain both the organic carbon oxidation and the nitrification of the glutamic acid biodegradation process. The proposed model included:

- the hydrolysis process that leads to the formation of ammonium and carbon-based compound (alfa-ketoglutarate);
- a two-step nitrification model (as described in the above) for ammonium nitrification;
- the extended SSAG model as used during SDS biodegradation modeling to interpret the carbon-based compound (alfa-ketoglutarate) biodegradation;
- all relevant stoichiometric parameters relating to both the respirometric and titrimetric components where the glutamic acid biodegradation pathway and dynamic CO_2 transfer process were taken into account.

8.1.3 Model calibration, parameter estimation and validation

In each test substrate biodegradation study, the proposed model was successfully calibrated with experimental respirometric and titrimetric measurements. Model calibration was undertaken using varying initial substrate concentrations and pH

levels (where applicable) for proper model evaluation. In addition, three different calibration approaches: using respirometric measurements alone, using titrimetric measurements alone and using combined respirometric-titrimetric measurements, were applied during the study. In every case study, the estimated model parameters showed consistent results for all three calibration approaches thereby confirming the precision of the proposed model. Moreover, estimated model parameters were found to be comparable to values in the literature. The parameter estimation errors calculated for 95% confidence intervals and the mean squared errors (MSEs) for the different calibration approaches were reasonable and confirm the statistical soundness of the proposed model. In addition, the proposed model was validated during each test substrate biodegradation study using off-line measurements. The model-simulated profiles were found to represent reasonably the off-line experimental observations as discussed below.

- The proposed model was validated using off-line COD and NH_4-N measurements during both the acetate and surfactant (SDS) biodegradation studies.
- The proposed nitrification model was validated using off-line NH_4-N, NO_2-N and NO_3-N measurements during both the urea and ammonium nitrification studies.
- The proposed model was validated using off-line NH_4-N, NO_2-N and NO_3-N measurements during the glutamic acid biodegradation without nitrification inhibition study. In the case of glutamic acid biodegradation with nitrification inhibition the model was validated using off-line NH_4-N measurements only.

8.1.4 Comparison of model parameters

The estimated model parameters obtained from the acetate, surfactant (SDS), urea, ammonium and glutamic acid aerobic biodegradation studies were critically evaluated and discussed in previous chapters (see Chapter 4 – 7). A comparison of some of these model parameters for different substrate biodegradation processes is presented in Table C1 in Appendix C. Following is a brief outline of this comparison.

- The average hydrolysis rate (k_h) was notably faster (27.65 day^{-1}) for surfactant (SDS) than the rate (12.82 day^{-1}) for glutamic acid. In addition, during hydrolysis the saturation coefficient (K_X) was higher for SDS than for glutamic acid.

- For all carbon-based substrate biodegradation studies, the storage rate was comparably greater than the heterotrophic biomass growth rate. Moreover, the comparison study showed both the maximum storage rate (k_{STO}) and the maximum growth rate of the heterotrophic biomass ($\mu_{MAX,S}$) were fastest for the SDS biodegradation, followed by the rates obtained from the acetate and the glutamic acid biodegradation studies (Table C1 in Appendix C).

- The growth of the autotrophic biomass is inherently slower than that of the heterotrophic biomass. It was evident in this study. While the maximum growth rate of the heterotrophic biomass during glutamic acid biodegradation was 0.326 day^{-1}, the autotrophic biomass growth rate for the first nitrification step ($\mu_{MAX,A1}$) was as low as 0.063 day^{-1}. In addition, the biomass growth rate for the first nitrification step was fastest for the urea study followed by the glutamic acid and the ammonium studies. More importantly, a very slow rate for autotrophic biomass growth ($\mu_{MAX,A2}$) was observed for the second nitrification step compared to that for the first nitrification step regardless of whether the substrate was ammonium, urea or glutamic acid. This resulted in nitrite accumulation in the system which was confirmed via off-line nitrite measurements.

- Though SDS and glutamic acid have relatively complex chemical compositions compared to that of acetate, the heterotrophic biomass showed a high affinity for both these substrates (SDS or glutamic acid) as observed during the biodegradation of an easily biodegradable compound like acetate biodegradation. It is noteworthy that the sludge was sufficiently acclimatized using test substrates before commencing the main batch experiments to enhance the adaptation capacity of the biomass. It may have resulted in the biomass showing such a high affinity.

- The average yield coefficient of direct heterotrophic growth on substrate ($Y_{H,S}$) was higher (0.71) for the acetate biodegradation than that for the SDS and the glutamic acid biodegradation processes. From the three different yield coefficients (i.e. $Y_{H,S}$, Y_{STO}, $Y_{H,STO}$), the yield coefficient of storage (Y_{STO}) was found to be significant for all three carbon-based compound (i.e. acetate, SDS and glutamic acid) biodegradation studies. In addition, the average yield coefficient of heterotrophic growth on internal storage products ($Y_{H,STO}$) was notable (0.87) when using glutamic acid as a test substrate. The oxygen consumption rate of biomass during the famine period, which is greatly affected by this yield coefficient, tends to decrease with the increase in $Y_{H,STO}$ value (Hoque et al., 2009b). This results in reducing the "tail" of the OUR profile of the carbon-based substrate biodegradation process under investigation.

- The average values for the autotrophic biomass yield for nitrification was lower than that for the heterotrophic biomass regardless of whether the substrate was ammonium, urea or glutamic acid. In addition, the autotrophic biomass yield for the first nitrification step (Y_{A1}) was higher than that for the second nitrification step (Y_{A2}) with each of the test substrates; ammonium, urea and glutamic acid biodegradation.

8.2 Recommendations for future work

The proposed bio-kinetic models were successfully calibrated and validated using on-line as well as off-line measurements from organic carbon and nitrogen biodegradation processes. However, the aerobic studies in this research project were limited to the investigation of biodegradation process using synthetic chemical compounds that have known chemical formulae. This facilitated the determination of the stoichiometric coefficients used for titrimetric calibration. Based on research outcomes and conclusions the following points are recommended for possible future research as a continuation of this work.

- The profiles of simulated intermediate and storage products, related to carbon-based compound biodegradation process, were not validated using analytical measurements due to resource constraints. Though

polyhydroxybutyrate (PHB) was observed to be stored in the biomass cell when acetate was used as a substrate, Beccari et al. (2002) concluded there may be storage compounds in a form other than PHB that need to be investigated for different substrates. Since it was not possible within the scope of this research project to identify these storage compounds, it is recommended that they be investigated and measured for different substrate biodegradation processes using appropriate analytical measurement techniques for proper model validation.

- While activated sludge contains both autotrophic and heterotrophic microorganisms, a single elemental composition for the biomass was used during modeling to keep the proposed model simple. Therefore it is suggested that the proposed model be refined using two different biomass components for two different biomass species to reflect better the real-life situation. In addition, the biomass composition, which was assumed in this study, should be examined experimentally for more accurate modeling purposes.

- The model parameter estimation could be improved by conducting a practical identifiability analysis of the model parameters. It determines the parameter combination to be taken into account for better accuracy of the parameter estimation process.

- In this current study, experiments were conducted while maintaining a constant temperature (20^0C). In addition, a constant pH of 7.8 was maintained most of the time while investigating different substrate aerobic biodegradation processes. However, both the autotrophic and heterotrophic biomass in activated sludge are temperature and pH sensitive. Since a change in temperature and pH which affect microbial activities are very common in wastewater treatment plants, it is recommended that the models be validated using varying temperatures and pH levels.

- The proposed models were developed in this study using synthetic organic carbon and nitrogen compounds in an activated sludge system. Real wastewater, which is a mixture of organic carbon, nitrogen and other nutrients, needs to be investigated for biodegradation modeling purposes. Advanced analytical chemistry could be used to determine the elemental

composition of real wastewater to improve the model using titrimetric components. This current research work could thereby be extended for real wastewater biodegradation modeling using combined respirometric-titrimetric measurements for model calibration and parameter estimation.

References

Anderson, D. J., Day, M. J., Russell, N. J., and White, G. F. (1990). "Die-away kinetic analysis of the capacity of epilithic and planktonic bacteria from clean and polluted river water to biodegrade sodium dodecyl sulfate." *Applied and Environmental Microbiology*, 56(3), 758-763.

APHA. (1995). "Standard methods for the examination of water and wastewater, 19th Edition." American Public Health Association, Washington, DC.

ASCE. (1996). "Standard Guidelines for In-Process Oxygen Transfer Testing." ASCE-18-96.

Baquerizo, G., Maestre, J. P., Sakuma, T., Deshusses, M. A., Gamisans, X., Gabriel, D., and Lafuente, J. (2005). "A detailed model of a biofilter for ammonia removal: Model parameters analysis and model validation." *Chemical Engineering Journal*, 113, 205-214.

Beccari, M., Dionisi, D., Giuliani, A., Majone, M., and Ramadori, R. (2002). "Effect of different carbon sources on aerobic storage by activated sludge." *Water Science and Technology*, 45(6), 157-168.

Benes, O., Spanjers, H., and Holba, M. (2002). "Respirometry techniques and activated sludge models." *Water Science and Technology*, 46(4-5), 1-6.

Beun, J. J., Dircks, K., Van Loosdrecht, M. C. M., and Heijnen, J. J. (2002). "Poly-β-hydroxybutyrate metabolism in dynamically fed mixed microbial cultures." *Water Research*, 36(5), 1167-1180.

Beun, J. J., Paletta, F., VanLoosdrecht, M. C. M., and Heijnen, J. J. (2000). "Stoichiometry and kinetics of Poly-β-Hydroxybutyrate metabolism in aerobic, slow growing, activated sludge cultures." *Biotechnology & Bioengineering*, 67(4), 379-389.

Boursier, H., Beline, F., and Paul, E. (2004). "Activated Sludge Model No. 1 calibration for piggery wastewater treatment using respirometry." *Water Science and Technology*, 49(5-6), 389-396.

Brouwer, H., Klapwijk, A., and Keesman, K. J. (1998). "Identification of activated sludge and wastewater characteristics using respirometric batch-experiments." *Water Research*, 32(4), 1240-1254.

Brun, R., Kühni, M., Siegrist, H., Gujer, W., and Reichert, P. (2002). "Practical identifiability of ASM2d parameters--systematic selection and tuning of parameter subsets." *Water Research*, 36(16), 4113-4127.

Buck, K. R., Chavez, F. P., and Campbell, L. (1996). "Basin-wide distributions of living carbon components and the inverted trophic pyramid of the central gyre of the North Atlantic Ocean, summer 1993." *Aquatic Microbial Ecology*, 10, 283-298.

Carucci, A., Dionisi, D., Majone, M., Rolle, E., and Smurra, P. (2001). "Aerobic storage by activated sludge on real wastewater." *Water Research*, 35(16), 3833-3844.

Carucci, A., Rolle, E., and Smurra, P. (1999). "Management optimisation of a large wastewater treatment plant." *Water Science and Technology*, 39(4), 129-136.

Carvalho, G., Nopens, I., Novais, J. M., Vanrolleghem, P. A., and Pinheiro, H. M. (2001). "Modelling of activated sludge acclimisation to a non-ionic surfactant." *Water Science and Technology*, 43(7), 9-17.

Chang, K.-Y., Cheng, L.-W., Ho, G.-H., Huang, Y.-P., and Lee, Y.-D. (2009). "Fabrication and characterization of poly (gamma-glutamic acid)-graft-chondroitin sulfate/polycaprolactone porous scaffolds for cartilage tissue engineering." *Acta Biomaterialia*, 5(6), 1937-1947.

Chen, G., Strevett, K. A., and Vanegas, B. A. (2001). "Naphthalene, phenanthrene and surfactant biodegradation." *Biodegradation*, 12, 433-442.

Colt, J. (1984). *Computation of Dissolved Gas Concentrations in Water as Functions of Temperature and Salinity and Pressure*, American Fisheries Society Spec. Pub. 14, Bethesda, MD.

Corominas, L., Sin, G., Puig, S., Traore, A., Balaguer, M., Colprim, J., and Vanrolleghem, P. A. (2006). "Model-based evaluation of an on-line control

strategy for SBRs based on OUR and ORP measurements." *Water Science and Technology*, 53(4-5), 161-169.

Costa, C., Rodriguez, J., and Marquez, M. C. (2009). "A simplified dynamic model for the activated sludge process with high strength wastewaters." *Environmental Modeling and Assessment*, 14, 739-747.

Damayanti, A., Ujang, Z., Salim, M. R., Olsson, G., and Sulaiman, A. Z. (2010). "Respirometric analysis of activated sludge models from palm oil mill effluent." *Bioresource Technology*, 101, 144-149.

Davison, J., Brunel, F., Phanopoulos, A., Prozzi, D., and Terpstra, P. (1992). "Cloning and sequencing of Pseudomonas genes determining sodium dodecyl sulfate biodegradation." *Gene*, 114(1), 19-24.

De Pauw, D. J. W., Sin, G., Insel, G., Van Hulle, S., Vandenberghe, V., and Vanrolleghem, P. A. (2004). "Discussion of "Assessing Parameter Identifiability of Activated Sludge Model Number 1" by Pedro Afonso and Maria da Conceic¸a¨o Cunha." *Journal of Environmental Engineering*, 130(1), 110-112.

Dionisi, D., Majone, M., Tandoi, V., and Beccari, M. (2001). "Sequencing Batch Reactor: Influence of Periodic Operation on Performance of Activated Sludges in Biological Wastewater Treatment." *Ind. Eng. Chem. Res.*, 40(23), 5110-5119.

Dionisi, D., Renzi, V., Majone, M., Beccari, M., and Ramadori, R. (2004). "Storage of substrate mixtures by activated sludges under dynamic conditions in anoxic or aerobic environments." *Water Research*, 38, 2196-2206.

Dircks, K., Henze, M., van Loosdrecht, M. C. M., Mosbæk, H., and Aspegren, H. (2001). "Storage and degradation of poly-[beta]-hydroxybutyrate in activated sludge under aerobic conditions." *Water Research*, 35(9), 2277-2285.

Dizdaroglu-Risvanoglu, G., Karahan, O., Cokgor, E. U., Orhon, D., and van Loosdrecht, M. C. M. (2007). "Substrate storage concepts in modeling activated sludge systems for tannery wastewaters." *Journal of Environmental Science and Health Part a-Toxic/Hazardous Substances & Environmental Engineering*, 42(14), 2159-2166.

Dochain, D., and Vanrolleghem, P. A. (2001). *Dynamical modelling and estimation in wastewater treatment processes*, IWA Publishing, London, UK.

Dold, P. (1980). "A general model for the activated sludge process." *Prog. Wat. Tech.*, 12(6), 47-77.

EPA. (1993). "Process chemistry and kinetics of biological nitrification." Manual: Nitrogen control (Chapter 3), EPA, Ohio, US.

Fujita, Y., Taylor, J. L., Gresham, T. L. T., Delwiche, M. E., Colwell, F. S., Mcling, T. L., Petzke, L. M., and Smith, R. W. (2008). "Stimulation of microbial urea hydrolysis in groundwater to enhance calcite precipitation." *Environmental Science and Technology*, 42, 3025-3032.

Gapes, D., Pratt, S., Yuan, Z., and Keller, J. (2003). "Online titrimetric and off-gas analysis for examining nitrification processes in wastewater treatment." *Water Research*, 37(11), 2678-2690.

Gernaey, A. K., Petersen, B., Ottoy, J. P., and Vanrolleghem, P. (2001). "Activated sludge monitoring with combined respirometric-titrimetric measurements." *Water Research*, 35(5), 1280-1294.

Gernaey, K., Bogaert, H., Massone, A., Vanrolleghem, P., and Verstraete, W. (1997). "On-line nitrification monitoring in activated sludge with a titrimetric sensor." *Environmental Science & Technology*, 31(8), 2350-2355.

Gernaey, K., Petersen, B., Dochain, D., and Vanrolleghem, P. A. (2002b). "Modeling aerobic carbon source degradation processes using titrimetric data and combined respirometric-titrimetric data: Structural and practical identifiability." *Biotechnology and Bioengineering*, 79(7), 754-767.

Gernaey, K., Petersen, B., Nopens, I., Comeau, Y., and Vanrolleghem, P. A. (2002a). "Modeling aerobic carbon source degradation processes using titrimetric data and combined respirometric-titrimetric data: Experimental data and model structure." *Biotechnology and Bioengineering*, 79(7), 741-753.

Gernaey, K., Vanrolleghem, P., and Verstraete, W. (1998). "On-line estimation of Nitrosomonas kinetic parameters in activated sludge samples using titration in-sensor-experiments." *Water Research*, 32(1), 71-80.

Guisasola, A., Sin, G., Baeza, J. A., Carrera, J., and Vanrolleghem, P. A. (2005). "Limitations of ASM1 and ASM3: a comparison based on batch oxygen uptake rate profiles from different full-scale wastewater treatment plants." *Water Science and Technology*, 52(10), 69-77.

Gujer, W., Henze, M., Mino, T., and Loosdrecht, M. v. (1999). "Activated Sludge Model No. 3." *Water Science and Technology*, 39(1), 183-193.

Havlin, J. L., Beaton, J. D., Tisdale, S. L., and Nelson, W. L. (1999). *Soil Fertility and Fertilizers: An Introduction to Nutrient Management*, Prentice Hall, New York.

Henze, M., Grady, C. J., Gujer, W., Marais, G., and Matsuo, T. (1987). "Activated Sludge Model No. 1." *IAWPRC Scientific and Technical Report No. 1*, IAWPRC, London, UK.

Henze, M., Gujer, W., Mino, T., Matsuo, T., Wentzel, M. C., Marais, G. v. R., and van Loosdrecht, M. C. M. (1999). "Activated Sludge Model No.2d, ASM2D." *Water Science and Technology*, 39(1), 165-182.

Henze, M., Gujer, W., Mino, T., Matsuo, T., Wentzel, M. C. M., and Marais, G. v. R. (1995). "Activated Sludge Model No. 2." *IAWQ Scientific and Technical Report No. 3*, IAWQ, London, UK.

Henze, M., Gujer, W., Mino, T., and van Loosdrecht, M. C. M. (2000). "Activated Sludge Models ASM1, ASM2, ASM2d and ASM3." *IWA Scientific and Technical Report No. 9*, IWA, London, UK.

Hoque, M. A., Aravinthan, V., and Pradhan, N. M. (2009a). "Assessment on activated sludge models for acetate biodegradation under aerobic conditions." *Water Science and Technology*, 60(4), 983-994.

Hoque, M. A., Aravinthan, V., and Pradhan, N. M. (2009b). "Can we decode the messages of activated sludge through the respirograms ?" *Water, Air, and Soil Pollution: Focus*, 9(5-6), 449-459.

Hoque, M. A., Aravinthan, V., and Pradhan, N. M. (2010). "Calibration of biokinetic model for acetate biodegradation using combined respirometric and titrimetric measurements." *Bioresource Technology*, 101(5), 1426-1434.

Iacopozzi, I., Innocenti, V., Marsili-Libelli, S., and Giusti, E. (2007). "A modified Activated Sludge Model No. 3 (ASM3) with two-step nitrification - denitrification." *Environmental Modelling and Software*, 22(6), 847-861.

Insel, G., Karahan-Gul, O., Orhon, D., Vanrolleghem, P. A., and M., H. (2002). "Important limitations in the modeling of activated sludge: biased calibration of the hydrolysis process." *Water Science and Technology*, 45(12), 23-36.

Jeppsson, U. (1996). "Modelling aspects of wastewater treatment processes," PhD thesis: Department of Industrial Electrical Engineering and Automation, Lund Institute of Technology, Sweden.

Karahan, O., Orhon, D., and Van Loosdrecht, M. C. M. (2008). "Simultaneous storage and utilization of polyhydroxyalkanoates and glycogen under aerobic conditions." *Water Science and Technology*, 58(4), 945-951.

Karahan, O., Van Loosdrecht, M. C. M., and Orhon, D. (2006). "Modeling the utilization of starch by activated sludge for simultaneous substrate storage and microbial growth." *Biotechnology and Bioengineering*, 94(1), 43-53.

Karahan-Gul, O., Artan, N., Orhon, D., Henze, M., and van Loosdrecht, M. C. M. (2002). "Respirometric assessment of storage yield for different substrates." *Water Science and Technology*, 46(1-2), 345-352.

Karahan-Gul, O., Van Loosdrecht, M. C. M., and Orhon, D. (2003). "Modification of Activated Sludge Model no. 3 considering direct growth on primary substrate." *Water Science and Technology*, 47(11), 219-225.

Kim, J.-H., Guo, X., Behera, S. K., and Park, H.-S. (2009). "A unified model of ammonium oxidation rate at various initial ammonium strength and active ammonium oxidizer concentrations." *Bioresource Technology*, 100(7), 2118-2123.

Koch, G., Kuhni, M., Gujer, W., and Siegrist, H. (2000). "Calibration and validation of activated sludge model no. 3 for Swiss municipal wastewater." *Water Research*, 34(14), 3580-3590.

Kok, M., Oldenhuis, R., van der Linden, M. P., Meulenberg, C. H., Kingma, J., and Witholt, B. (1989). "The Pseudomonas oleovorans alkBAC operon encodes

two structurally related rubredoxins and an aldehyde dehydrogenase." *The Journal of Biological Chemistry*, 264(10), 5442-5451.

Krishna, C., and Van Loosdrecht, M. C. M. (1999). "Substrate flux into storage and growth in relation to activated sludge modeling." *Water Research*, 33(14), 3149-3161.

Levstek, M., Plazl, I., and Koloini, T. (2006). "Modelling of a pilot wastewater treatment plant operated with variable inflows." *Chemical and Biochemical Engineering Quarterly*, 20(1), 85-91.

Lopez Zavala, M. A., Funamizu, N., and Takakuwa, T. (2004). "Modeling of aerobic biodegradation of feces using sawdust as a matrix." *Water Research*, 38(5), 1327-1339.

Majone, M., Dircks, K., and Beun, J. J. (1999). "Aerobic storage under dynamic conditions in activated sludge processes. The state of the art." *Water Science and Technology*, 39(1), 61-73.

Marchesi, J. R., White, G. F., Russell, N. J., and House, W. A. (1997). "Effect of river sediment on the biodegradation kinetics of surfactant and non-surfactant compounds." *FEMS Microbiology Ecology*, 23, 55-63.

Marsili-Libelli, S., and Tabani, F. (2002). "Accuracy analysis of a respirometer for activated sludge dynamic modelling." *Water Research*, 36(5), 1181-1192.

Moussa, M. S., Hooijmans, C. M., Lubberding, H. J., Gijzen, H. J., and van Loosdrecht, M. C. M. (2005). "Modelling nitrification, heterotrophic growth and predation in activated sludge." *Water Research*, 39, 5080-5098.

Munz, G., Gori, R., Cammilli, L., and Lubello, C. (2008). "Characterization of tannery wastewater and biomass in a membrane bioreactor using respirometric analysis." *Bioresource Technology*, 99, 8612-8618.

Ni, B.-J., Yu, H.-Q., and Sun, Y.-J. (2008). "Modeling simultaneous autotrophic and heterotrophic growth in aerobic granules." *Water Research*, 42(6-7), 1583-1594.

Okutman, D., Ovez, S., and Orhon, D. (2001). "Hydrolysis of settleable substrate in domestic sewage." *Biotechnology Letters*, 23, 1907-1914.

Orhon, D., Cokgor, E. U., and Sozen, S. (1999). "Experimental basis for the hydrolysis of slowly biodegradable substrate in different wastewaters." *Water Science and Technology*, 39(1), 87-95.

Pambrun, V., Paul, E., and Sperandio, M. (2006). "Modeling the partial nitrification in squencing batch reactor for biomass adapted to high ammonia concentraions." *Biotechnology and Bioengineering*, 95(1), 120-131.

Petersen, B. (2000). "Calibration, identifiability and optimal experimental design of activated sludge models," PhD thesis: Faculty of Agricultural and Applied Biological Science, Ghent University, Belgium.

Petersen, B., Gernaey, K., Devisscher, M., Dochain, D., and Vanrolleghem, P. A. (2003). "A simplified method to assess structurally identifiable parameters in Monod-based activated sludge models." *Water Research*, 37(12), 2893-2904.

Petersen, B., Gernaey, K., M., H., and Vanrolleghem, P. A. (2002). "Evaluation of an ASM1 model calibration procedure on a municipal-industrial wastewater treatment plant." *Journal of Hydroinformatics*, 4(1), 15-38.

Petersen, B., Gernaey, K., and Vanrolleghem, P. A. (2001). "Practical identifiability of model parameters by combined respirometric-titrimetric measurements." *Water Science Technology*, 43(7), 347-356.

Pickartz, S., Oppermann, F. B., and Steinbuchel, A. (1996). "Biodegradation of poly-gamma-glutamic acid." In: *Biodeterioration and Biodegradation*, W. Sand, ed., 655-662.

Pratt, S., Yuan, Z., Gapes, D., Dorigo, M., Zeng, R., and Keller, J. (2003). "Development of a novel titration and off-gas analysis (TOGA) sensor for study of biological processes in wastewater treatment systems." *Biotechnology and Bioengineering*, 81(4), 482-495.

Pratt, S., Yuan, Z., and Keller, J. (2004). "Modelling aerobic carbon oxidation and storage by integrating respirometric, titrimetric, and off-gas CO_2 measurements." *Biotechnology & Bioengineering*, 88(2), 135-147.

Schreiner, A., Asmussen, C., Wiesmann, U., and Stan, H.-J. (1999). "Investigation of Aerobic Degradation Kinetics of Surfactants Using Respirometric Batch Experiments." *Acta Biotechnol.*, 19(4), 293-304.

Shahriari, H., Eskicioglu, C., and Droste, R. L. (2006). "Simulating activated sludge system by simple-to-advanced models." *Journal of Environmental Engineering*, 132(1), 42-50.

Sin, G. (2004). "Systematic calibration of activated sludge models," PhD thesis: Faculty of Agricultural and Applied Biological Science, Ghent University Belgium.

Sin, G., Guisasola, A., DePauw, D. J. W., Juan, A. B., Carrera, J., and Vanrolleghem, P. A. (2005). "A new approach for modelling simultaneous storage and growth processes for activated sludge systems under aerobic conditions." *Biotechnology & Bioengineering*, 92(5), 600-613.

Sin, G., Malisse, K., and Vanrolleghem, P. A. (2003). "An integrated sensor for the monitoring of aerobic and anoxic activated sludge activities in biological nitrogen removal plants." *Water Science and Technology*, 47(2), 141-148.

Sin, G., and Vanrolleghem, P. A. (2007). "Extensions to modeling aerobic carbon degradation using combined respirometric-titrimetric measurements in view of activated sludge model calibration." *Water Research*, 41(15), 3345-3358.

Spanjers, H. (1993). "Respirometry in activated sludge," PhD thesis, Landbouwuniversiteit Wageningen, the Netherlands.

Spanjers, H., and Vanrolleghem, P. (1995). "Respirometry as a tool for rapid characterization of wastewater and activated sludge." *Water Science and Technology*, 31(2), 105-114.

Spanjers, H., Vanrolleghem, P., Olsson, G., and Dold, P. (1998). "Respirometry in control of the activated sludge process: Principles." *IAWQ Scientific and Technical Report No. 7*, International Association on Water Quality, London, UK.

Sperandio, M., and Paul, E. (1997). "Determination of carbon dioxide evolution rate using on-line gas analysis during dynamic biodegradation experiments." *Biotechnology and Bioengineering*, 53(3), 243-252.

Stricker, A. E., and Racault, Y. (2005). "Application of Activated Sludge Model No. 1 to biological treatment of pure winery effluents: case studies." *Water Science and Technology*, 51(1), 121-127.

Stryer, L. (1988). *Biochemistry*, 3rd Ed., W.H. Freeman and Company, New York.

Stumm, W., and Morgan, J. J. (1996). *Aquatic Chemistry: chemical equilibria and rates in natural waters*, 3rd Ed., John Wiley and Sons, Inc.

Swisher, R. D. (1987). *Surfactant biodegradation*, 2nd Ed., Marcel Dekker Inc., New York.

Van Aalst-van Leeuwen, M. A., Pot, M. A., Van Loosdrecht, M. C. M., and Heijnen, J. J. (1997). "Kinetic modelling of poly (β-hydroxybutyrate) production and consumption by *Paracoccus pantotrophus* under dynamic substrate supply." *Biotechnology & Bioengineering*, 55(5), 773-782.

Van Beilen, J. B., Eggink, G., Enequist, H., Bos, R., and Witholt, B. (1992). "DNA sequence determination and functional characterization of the OCT-plasmid-encoded alkJKL genes of Pseudomonas oleovorans." *Molecular Microbiology*, 6(21), 3121-3136.

Van Loosdrecht, M. C. M., and Heijnen, J. J. (2002). "Modelling of activated sludge processes with structured biomass." *Water Science and Technology*, 45(6), 12-23.

Van Loosdrecht, M. C. M., and Henze, M. (1999). "Maintenance, endogenous respiration, lysis, decay and starvation." *Water Science and Technology*, 39(1), 107-117.

Van Loosdrecht, M. C. M., Pot, M. A., and Heijnen, J. J. (1997). "Importance of bacterial storage polymers in bioprocesses." *Water Science and Technology*, 35(1), 41-47.

Vanrolleghem, P. A., Sin, G., and Geraney, K. V. (2004). "Transient Response of Aerobic and Anoxic Activated Sludge Activities to Sudden Substrate Concentration Changes." *Biotechnology & Bioengineering*, 86(3), 277-290.

Vanrolleghem, P. A., and Spanjers, H. (1994). "Comparison of two respirometric principles for the determination of short-term biochemical oxygen demand." *Proc. 49th Purdue Industrial Waste Conference*, Lewis Publ., Chelsea, Michigan, 177-188.

Vanrolleghem, P. A., Spanjers, H., Petersen, B., Ginestet, P., and Takacs, I. (1999). "Estimating (combinations of) Activated Sludge Model No. 1 parameters and components by respirometry." *Water Science and Technology*, 39(1), 195-214.

Wanner, O., Kappeler, J., and Gujer, W. (1992). "Calibration of an activated sludge model based on human expertise and on a mathematical optimization technique - A comparison." *Water Science and Technology*, 25(6), 141-148.

Weijers, S. R., and Vanrolleghem, P. A. (1997). "A procedure for selecting best identifiable parameters in calibrating activated sludge model no. 1 to full scale plant data." *Water Science and Technology*, 36(5), 69-79.

Yao, G. (2006). "Dodecyl Sulfate Pathway Map." *University of Minnesota,* viewed 28 November 2007, <http://umbbd.msi.umn.edu/dds/dds_map.html>.

Yildiz, G., Insel, G., Cokgor, E. U., and Orhon, D. (2008). "Biodegradation kinetics of the soluble slowly biodegradable substrate in polyamide carpet finishing wastewater." *Journal of Chemical Technology and Biotechnology*, 83(1), 34-40.

Yuan, Z., and Bogaert, H. (2001). "A titrimetric respirometer measuring the nitrifiable nitrogen in wastewater using in-sensor-experiment." *Water Research*, 35(1), 180-188.

Zhang, C. L., Valsaraj, K. T., Constant, W. D., and Roy, D. (1999). "Aerobic biodegradation kinetics of four anionic and nonionic surfactants at sub- and supra-critical micelle concentrations (CMCs)." *Water Research*, 33(1), 115-124.

Appendix A
Abbreviations and Notations

Abbreviations

AEO	Alcohol Ethoxylate
APHA	American Public Health Association
ASCE	American Society of Civil Engineers
ASM	Activated Sludge Model
ASM1	Activated Sludge Model No. 1
ASM2	Activated Sludge Model No. 2
ASM2d	Activated Sludge Model No. 2d
ASM3	Activated Sludge Model No. 3
ATP	Adenosine Triphosphate
ATU	Allylthiourea
BOD	Biochemical Oxygen Demand
COD	Chemical Oxygen Demand
CSTR	Continuous Stirred Tank Reactor
CTR	Carbon dioxide Transfer Rate
DO	Dissolved Oxygen
EBPR	Enhanced Biological Phosphorus Removal
EPA	Environmental Protection Agency
FoES	Faculty of Engineering and Surveying
Glu	Glutamic Acid
ICS	Ion Chromatography System
IWA	International Water Association
IAWPRC	International Association on Water Pollution Research and Control
IAWQ	International Association on Water Quality
LPM	Liter Per Minute
MBR	Membrane Bioreactor
MLSS	Mixed Liquor Suspended Solids
MLVSS	Mixed Liquor Volatile Suspended Solids

MSE	Mean Squared Error
OUR	Oxygen Uptake Rate
PHA	Polyhydroxyalkanoates
PHB	Polyhydroxybutyrate
SBR	Sequencing Batch Reactor
SDS	Sodium Dodecyl Sulfate
SRT	High sludge retention time
SSAG	Simultaneous Storage and Growth
SSE	Sum of Squared Errors
TOGA	Titration and Off-Gas Analysis
USQ	University of Southern Queensland
VSS	Volatile Suspended Solids
WWTP	Wastewater Treatment Plant

Notations

δ	Efficiency of the oxidative phosphorylation (mol/mol)
τ	First order time constant (day)
γ_S	Degree of reduction of substrate (mol electron/C-mol)
γ_{STO}	Degree of reduction of storage products (mol electron/C-mol)
γ_X	Degree of reduction of biomass (mol electron/C-mol)
$\mu_{MAX,A!}$	Maximum autotrophic biomass growth rate for the first nitrification step (day^{-1})
$\mu_{MAX,A2}$	Maximum autotrophic biomass growth rate for the second nitrification step (day^{-1})
$\mu_{MAX,S}$	Maximum growth rate of heterotrophic biomass on substrate (day^{-1})
$\mu_{MAX,STO}$	Maximum growth rate of heterotrophic biomass on storage products (day^{-1})
b	Endogenous decay coefficient of biomass (day^{-1})
b_H	Endogenous decay coefficient of heterotrophic biomass (day^{-1})
b_{STO}	Endogenous decay of storage products (day^{-1})
BOD_5	5-day biochemical oxygen demand (mg/L)
BOD_{st}	Short-term biochemical oxygen demand (mg/L)
$CH_aO_bN_c$	Elemental composition of biomass (C-mol)
CH_pO_q	Elemental composition of a storage polymer/product (C-mol)
CH_yO_z	Elemental composition of a substrate (C-mol)
$C_{T,init}$	Initial concentration of total inorganic carbon (mmol/L)
f_{BA}	Fraction of autotrophic biomass in the mixed culture (mg COD/mg COD)
f_{BH}	Fraction of heterotrophic biomass in the mixed culture (mg COD/mg COD)
$f_{max,acc}$	Maximum amount of accumulated compound (mgCOD X_{ACC}/mgCOD X_H)
f_{STO}	Fraction of substrate used for storage (mg COD X_{STO}/mg COD S_S)
f_{XI}	Inert fraction of biomass (mg COD/mg COD)
Hp	Proton concentration in liquid phase (meq/L)
i_{NBM}	Nitrogen content of biomass (mg N/mg COD)

i_{NXI}	Nitrogen content of the inert fraction of biomass (mg N/mg COD)
i_{XB}	Nitrogen content of biomass (mg N/mg COD)
K_1	Regulation constant of biomass controlling degradation rate of X_{STO} (mg COD X_{STO}/mg COD X_H)
K_2	A lumped parameter related to the affinity of biomass to storage fraction of biomass (mg COD X_{STO}/mg COD X_H)
k_1	Forward reaction rate for aqueous CO_2 equilibrium (day^{-1})
k_{ACC}	Maximum accumulation rate of biomass (day^{-1})
k_h	Hydrolysis rate (day^{-1})
K_H	Henry coefficient for CO_2 (mol/atm.L)
$K_{H,ACC}$	Affinity constant of biomass to accumulated compound (mgCOD X_{ACC}/mgCOD X_H)
$K_{H,STO}$	Affinity constant of biomass to storage products (mgCOD X_{STO}/mgCOD X_H)
k_N	Ammonification (hydrolysis) rate
k_{NHacc}	Nitrogen accumulation rate of biomass (day^{-1})
$K_L a_{CO_2}$	Carbon dioxide mass transfer coefficient (day^{-1})
$K_L a$	Oxygen mass transfer coefficient (day^{-1})
K_{NH}	Affinity constant for ammonium (mg N/L)
K_S	Substrate affinity constant (mg COD/L)
K_{SA1}	Substrate affinity constant for the first nitrification step (mg N/L)
K_{SA2}	Substrate affinity constant for the second nitrification step (mg N/L)
k_{STO}	Maximum storage rate of biomass (day^{-1})
$K_{STO,ACC}$	Fraction of storage products to accumulated compound (mgCOD X_{STO}/mgCOD X_{ACC})
K_X	Hydrolysis saturation constant (mg COD/mg COD)
m	Mole of H^+ consumed per mole of acetate taken up for growth
M_S	Monod function for substrate, S_S (i.e. $S_S/(K_S+S_S)$)
OUR_{end}	Endogenous oxygen uptake rate (mg O_2/L.d)
OUR_{exo}	Exogenous oxygen uptake rate (mg O_2/L.d)
P_{CO_2}	Partial pressure of CO_2 in air (atm)
p	Mole of H^+ released per mole of NH_4^+ taken up for growth
pK_1	Negative logarithm of the first acidity constant in the CO_2 equilibrium

pK_a	Negative logarithm of the first acidity constant in the CO_2 equilibrium
pK_{NH4}	Negative logarithm of the equilibrium constant for NH_4^+ dissociation
q_{MAX}	Maximum substrate uptake rate (day^{-1})
S_{CO_2}	CO_2 concentration in liquid phase (mmol/L)
$S^*_{CO_2}$	CO_2 saturation concentration at 1 atm (mmol/L)
S_{eq}	Equilibrium concentration of dissolved oxygen in liquid phase (mg/L)
S_{HCO_3}	Bicarbonate concentration in liquid phase (mmol/L)
S_I	Inert suspended solids (mg COD/L)
S_N	Initial concentration of nitrogenous compound (mg N/L)
S_{ND}	Biodegradable soluble organic nitrogen (mg N/L)
S_{NH}	Ammonium concentration (mg N/L)
S_{N2}	Nitrogen gas (mg N/L)
S_O	Dissolved oxygen concentration in liquid phase (mg/L)
S^*_O	Oxygen saturation concentration (mg/L)
S_S	Readily biodegradable substrate concentration (mg COD/L)
X_A	Autotrophic biomass concentration (mg COD/L)
X_{ACC}	Concentration of accumulated compound (mg COD/L)
X_B	Biomass concentration (mg COD/L)
$X_B(0)$	Initial biomass concentration (mg COD/L)
$X_{B,A}$	Autotrophic biomass concentration (mg COD/L)
$X_{B,H}$	Heterotrophic biomass concentration (mg COD/L)
X_H	Heterotrophic biomass concentration (mg COD/L)
$X_H(0)$	Initial heterotrophic biomass concentration (mg COD/L)
X_I	Inert particulate COD (mg COD/L)
X_{ND}	Particulate degradable organic nitrogen (mg N/L)
X_{NHacc}	Nitrogen accumulation (mg N/L)
X_S	Slowly degradable particulate COD (mg COD/L)
X_{STO}	storage products concentration (mg COD/L)
Y_A	Autotrophic yield coefficient (mg COD /mg N)
Y_{A1}	Autotrophic biomass yield of the first nitrification step (mg COD/mg N)
Y_{A2}	Autotrophic biomass yield of the second nitrification step (mg COD/mg N)

Y_{ACC}	Yield coefficient for accumulated compound on substrate (mgCOD X_{ACC}/mgCOD S_S)
Y_H	Heterotrophic yield coefficient (mg COD/mg COD)
$Y_{H,ACC}$	Yield coefficient for growth on accumulated compound (mgCOD X_H/mgCOD X_{ACC})
$Y_{H,S}$	Yield coefficient for growth on substrate (mg COD X_H/mg COD S_S)
$Y_{H,STO}$	Yield coefficient for growth on storage products (mg COD X_H/mg COD X_{STO})
Y_{STO}	Yield coefficient for storage on substrate (mg COD X_{STO}/mg COD S_S)
$Y_{STO,ACC}$	Yield coefficient for storage on accumulated compound (mgCOD X_{STO} /mgCOD X_{ACC})
Y_{SA1}	Autotrophic biomass yield of the first nitrification step (molar unit basis)
Y_{SA2}	Autotrophic biomass yield of the second nitrification step (molar unit basis)
Y_{SSTO}	Yield coefficient for storage formation (C-mol basis)
Y_{STOX}	Yield coefficient for growth on storage products (C-mol basis)
Y_{SX}	Yield coefficient for growth on substrate (C-mol basis)

Appendix B

Charts for DO correction

Table B1: Interpolated values for saturated DO at different temperature (at 760 mm Hg or 1013 hPa)

Temperature (^{0}C)	Saturated DO (mg/L)	Temperature (^{0}C)	Saturated DO (mg/L)
15	**10.05**	19.6	9.132
15.1	10.028	19.7	9.114
15.2	10.006	19.8	9.096
15.3	9.984	19.9	9.078
15.4	9.962	**20**	**9.06**
15.5	9.94	20.1	9.042
15.6	9.918	20.2	9.024
15.7	9.896	20.3	9.006
15.8	9.874	20.4	8.988
15.9	9.852	20.5	8.97
16	**9.83**	20.6	8.952
16.1	9.81	20.7	8.934
16.2	9.79	20.8	8.916
16.3	9.77	20.9	8.898
16.4	9.75	**21**	**8.88**
16.5	9.73	21.1	8.863
16.6	9.71	21.2	8.846
16.7	9.69	21.3	8.829
16.8	9.67	21.4	8.812
16.9	9.65	21.5	8.795
17	**9.63**	21.6	8.778
17.1	9.61	21.7	8.761
17.2	9.59	21.8	8.744
17.3	9.57	21.9	8.727
17.4	9.55	**22**	**8.71**
17.5	9.53	22.1	8.694
17.6	9.51	22.2	8.678
17.7	9.49	22.3	8.662
17.8	9.47	22.4	8.646
17.9	9.45	22.5	8.63
18	**9.43**	22.6	8.614
18.1	9.411	22.7	8.598
18.2	9.392	22.8	8.582
18.3	9.373	22.9	8.566
18.4	9.354	**23**	**8.55**
18.5	9.335	23.1	8.534
18.6	9.316	23.2	8.518
18.7	9.297	23.3	8.502
18.8	9.278	23.4	8.486
18.9	9.259	23.5	8.47
19	**9.24**	23.6	8.454
19.1	9.222	23.7	8.438
19.2	9.204	23.8	8.422
19.3	9.186	23.9	8.406
19.4	9.168	**24**	**8.39**
19.5	9.15		

DO values adopted from the chart supplied with the DO meter (TPS 90-D) are given in bold

Table B2: Interpolated values for vapor pressure of water at different temperature

Temperature (^{0}C)	Vapor pressure (mm Hg)	Temperature (^{0}C)	Vapor pressure (mm Hg)
15	**12.79**	19.6	17.116
15.1	12.875	19.7	17.222
15.2	12.96	19.8	17.328
15.3	13.045	19.9	17.434
15.4	13.13	**20**	**17.54**
15.5	13.215	20.1	17.652
15.6	13.3	20.2	17.764
15.7	13.385	20.3	17.876
15.8	13.47	20.4	17.988
15.9	13.555	20.5	18.1
16	**13.64**	20.6	18.212
16.1	13.729	20.7	18.324
16.2	13.818	20.8	18.436
16.3	13.907	20.9	18.548
16.4	13.996	**21**	**18.66**
16.5	14.085	21.1	18.777
16.6	14.174	21.2	18.894
16.7	14.263	21.3	19.011
16.8	14.352	21.4	19.128
16.9	14.441	21.5	19.245
17	**14.53**	21.6	19.362
17.1	14.625	21.7	19.479
17.2	14.72	21.8	19.596
17.3	14.815	21.9	19.713
17.4	14.91	**22**	**19.83**
17.5	15.005	22.1	19.955
17.6	15.1	22.2	20.08
17.7	15.195	22.3	20.205
17.8	15.29	22.4	20.33
17.9	15.385	22.5	20.455
18	**15.48**	22.6	20.58
18.1	15.58	22.7	20.705
18.2	15.68	22.8	20.83
18.3	15.78	22.9	20.955
18.4	15.88	**23**	**21.08**
18.5	15.98	23.1	21.211
18.6	16.08	23.2	21.342
18.7	16.18	23.3	21.473
18.8	16.28	23.4	21.604
18.9	16.38	23.5	21.735
19	**16.48**	23.6	21.866
19.1	16.586	23.7	21.997
19.2	16.692	23.8	22.128
19.3	16.798	23.9	22.259
19.4	16.904	**24**	**22.39**
19.5	17.01		

Values adopted from Colt, 1984 are given in bold

Appendix C
Comparison of model parameters

Table C1: Comparison of model parameters (average values) relating to different substrates biodegradation in an aerobic activated sludge system (pH = 7.8)

Parameters	Acetate	SDS	Ammonium	Urea	Glutamic acid
k_h (1/min)	--	0.0192	--	0.058**	0.0089
K_X (mgCOD X_S/mgCOD X_B)	--	0.42	--	--	0.31
k_{STO} (1/min)	2.1×10^{-3}	6.9×10^{-3}	--	--	5.19×10^{-4}
$\mu_{MAX,S}$ (1/min)	1.26×10^{-3}*	2.88×10^{-3}*	--	--	2.26×10^{-4}*
K_S (mg COD/L)	0.84*	0.65*	--	--	0.65*
$Y_{H,S}$ (mgCOD X_B/mgCOD S_S)	0.71	0.64	--	--	0.62
$Y_{H,STO}$ (mgCOD X_B/mgCOD X_{STO})	0.78	0.73	--	--	0.87
Y_{STO} (mgCOD X_{STO}/mgCOD S_S)	0.88	0.84	--	--	0.8
$\mu_{MAX,A1}$ (1/min)	--	--	2.64×10^{-5}*	6.74×10^{-5}*	4.35×10^{-5}
$\mu_{MAX,A2}$ (1/min)	--	--	5.24×10^{-6}	4.9×10^{-6}	4.42×10^{-6}
K_{SA1} (mgN/L)	--	--	0.25*	0.34*	0.29
K_{SA2} (mgN/L)	--	--	0.08	0.2	0.2
Y_{A1} (mgCOD X_B/mgN S_{NH})	--	--	0.13	0.2	0.21
Y_{A2} (mgCOD X_B/mgN S_{NO2})	--	--	0.05	0.026	0.034

* Parameters were taken from Monod parameter estimation process

** The parameter represents the ammonification rate (i.e. hydrolysis rate) of urea which is expressed as k_N

Appendix D
Sample MATLAB program

```
function glu_kinetics
%Modeling for Glutamic acid (Glu) kinetics allowing nitrification
inhibition
%Estimation of parameters using combined respirometric and
titrimetric measurements
%History
%Basic script for acetate biodegradation modeling was developed by
Vasantha Aravinthan on 3rd Dec, 2007,
%Model was improved for glutamic acid biodegradation and revised
script was written by Muhammad Azizul Hoque on 21 March, 2010
%Close all; clear all
%Input
%Data from Respirometric and Titrimetric experiments
%time (minutes), OUR (mg/L/min), Hp (meq/L)

combined=xlsread('Glu_100.xls','input');
t=combined(:,1);
h=combined(:,2);
r=combined(:,3);

%Interpolate the data in desired time interval
tf=t(end);
tf=t(end);
ti=0.4;
tspan = [0:ti:tf]';
th=interp1(t,h,tspan);
tour=interp1(t,r,tspan);
tu=[tspan th tour];
disp('Enter to contines with Model'); disp(' '); pause

%default values
pk1=6.392023261;
pH=7.8;
Ct_in=1.3;

%Parameters calculated using these default values
S_HCO3_0=Ct_in*(1/(1+10^(pk1-pH)));
S_CO2_0=Ct_in*(1/(1+10^(pH-pk1)));

%Input the guesses for initial model parameters
Ks=0.63;
qmax=0.001;
Yh_s=0.63;
Y_sto=0.8;
Yh_sto=0.87;
K1=0.03;
K2=0.00005;
kh=0.009;
Kx=0.3;
Tr=3;% Tr represents first order time constant

%Initial guesses for state variables
x0=[100 0 0 800 S_HCO3_0 S_CO2_0 0];
%X1 = Xs; X2 = Ss; X3 = Xsto; X4 = Xbh; X5 = S_HCO3; X6 = S_CO2; X7
= S_HP;
p_init=[Ks, qmax, Yh_s, Y_sto, Yh_sto, K1, K2, kh, Kx, Tr];

%Fixed model parameters
k1=1.0762;
KLaCO2=0.0555;
```

```
bh=0.00013889;
b_sto=0.00013889;
fxi=0.2;
f_sto=0.65;

p_fix=[k1 KLaCO2 bh b_sto fxi f_sto x0(1) x0(2) x0(3) x0(4) x0(5)
x0(6) x0(7)];
lb=[0.55;0.0009;0.6;0.75;0.85;0.025;0.00004;0.007;0.2;2];
ub=[0.65;0.0015;0.65;0.8;0.9;0.03;0.00006;0.009;0.4;6];
%lb refers to lower bound
%ub refers to upper bound

options = optimset('Display','iter','TolFun', 1e-4,...%default; 1e-4
'TolX',1e-5,...%defaul; 1e-4
'LevenbergMarquardt','on',...%default; on
'LargeScale','on') %default: on

%LSQNONLIN: objective function should return the model error
[p_est,resnorm,RESIDUAL,exitflag,OUTPUT,LAMBDA,Jacobian] = ...
lsqnonlin(@obj_fn,p_init,lb,ub,options...
,p_fix,tspan,tu); disp(' ')
disp(' step5')

%Accuracy:
%lsqnonlin returns the Jacobian as a sparse matrix
varp = resnorm*inv(Jacobian'*Jacobian)/length(tspan);
stdp = sqrt(diag(varp)); %The standard deviation is the square root
of the variance

p=[p_est(1),p_est(2),p_est(3),p_est(4),p_est(5),p_est(6),p_est(7)
...,p_est(8),p_est(9),p_est(10),p_fix(1),p_fix(2),p_fix(3),p_fix(4),
p_fix(5)...,p_fix(6)];

x0=[p_fix(7),p_fix(8),p_fix(9),p_fix(10),p_fix(11),p_fix(12)
...,p_fix(13)];

%Calculated model kinetics
ksto=p_fix(6).*p_est(2).*p_est(4);
umaxs=(1-p_fix(6))*p_est(2).*p_est(3);
umax_sto=umaxs;

CI(1)=stdp(1)^2;
CI(2)=stdp(2)^2;
CI(3)=stdp(3)^2;
CI(4)=stdp(4)^2;
CI(5)=stdp(5)^2;
CI(6)=stdp(6)^2;
CI(7)=stdp(7)^2;
CI(8)=stdp(8)^2;
CI(9)=stdp(9)^2;
CI(10)=stdp(10)^2;

disp('Parameters:')
disp(['Ks = ', num2str(p_est(1)), '+/-', num2str(CI(1))])
disp(['qmax= ', num2str(p_est(2)), '+/-', num2str(CI(2))])
disp(['Yh_s = ', num2str(p_est(3)), '+/-', num2str(CI(3))])
disp(['Y_sto = ', num2str(p_est(4)), '+/-', num2str(CI(4))])
disp(['Yh_sto = ', num2str(p_est(5)), '+/-', num2str(CI(5))])
disp(['K1 = ', num2str(p_est(6)), '+/-', num2str(CI(6))])
disp(['K2 = ', num2str(p_est(7)), '+/-', num2str(CI(7))])
```

```
disp(['kh = ', num2str(p_est(8)), '+/-', num2str(CI(8))])
disp(['Kx = ', num2str(p_est(9)), '+/-', num2str(CI(9))])
disp(['Tr = ', num2str(p_est(10)), '+/-', num2str(CI(10))])
disp(['k1 = ', num2str(p_fix(1))])
disp(['KLaCO2= ', num2str(p_fix(2))])
disp(['bh = ', num2str(p_fix(3))])
disp(['b_sto = ', num2str(p_fix(4))])
disp(['fxi = ', num2str(p_fix(5))])
disp(['f_sto = ', num2str(p_fix(6))])
disp(['slow = ', num2str(p_fix(7))])
disp(['sub = ', num2str(p_fix(8))])
disp(['sto = ', num2str(p_fix(9))])
disp(['bio = ', num2str(p_fix(10))])
disp(['Ct_in= ', num2str(Ct_in)])
disp(['S_HCO3 = ', num2str(p_fix(11))])
disp(['S_CO2 = ', num2str(p_fix(12))])
disp(['S_HP = ', num2str(p_fix(13))])
disp(['ksto = ', num2str(ksto)])
disp(['umaxs = ', num2str(umaxs)])
disp(['umax_sto = ', num2str(umax_sto)])

%Modeling output
glu = glu_sim(tspan,x0,tu,p);
slow=glu(:,1);
sub=glu(:,2);
sto=glu(:,3);
bio=glu(:,4);
HCO3=glu(:,5);
CO2=glu(:,6);
HP=glu(:,7);
hmod=glu(:,8);
rmod=glu(:,9);
h=tu(:,2);

%Mean squared error determination
e1 = hmod-h;
r = tu(:,3);
e2 =rmod-r;
n=2*(((tf-0)/ti)+1);%here two is multiplied because of two data sets
i.e. respirometric and titrimetric data
e=e1+e2;
E=e.*e;
MSE=sum(E)/n

%Output data interpolation
T=[0:2:tf]';
H=interp1(tspan,th,T);
OUR=interp1(tspan,tour,T);
hmod1=interp1(tspan,hmod,T);
rmod1=interp1(tspan,rmod,T);

%For writing the output in Excel file
output=[tspan sub h hmod r rmod];
output1={'Ks',p_est(1);'qmax',p_est(2);'Yh_s',p_est(3);'Y_sto',
p_est(4);'Yh_sto',p_est(5);'K1',p_est(6)...;'K2',p_est(7);'kh',p_est
(8);'Kx',p_est(9);'Tr',p_est(10);'k1',p_fix(1);'KLaCO2',p_fix(2);'bh
',p_fix(3)...;'b_sto',p_fix(4);'fxi',p_fix(5);'f_sto',p_fix(6);'slow
',p_fix(7);'sub',p_fix(8);'sto',p_fix(9)...;'bio',p_fix(10);'S_HCO3'
,p_fix(11);'S_CO2',p_fix(12);'S_HP',p_fix(13);'Ct_in',Ct_in;'ksto',k
sto...;'umaxs',umaxs;'umax_sto',umax_sto};
output2=[T H OUR];
```

```
output3=[T hmod1 rmod1];
output4=[tspan HCO3 CO2];
output5={'Ks',CI(1);'qmax',CI(2);'Yh_s',CI(3);'Y_sto',CI(4);
'Yh_sto',CI(5)...;'K1',CI(6);'K2',CI(7);'kh',CI(8);'Kx',CI(9);'Tr',C
I(10);'MSE',MSE};

[stat mmsg] = xlswrite('Glu_100.xls',output, 'OURmod', 'B8');
[stat mmsg] = xlswrite('Excel_sim.xls',output1,'MATLAB_est', 'N8');
[stat mmsg] = xlswrite('Glu_100.xls',output2, 'model', 'g6');
[stat mmsg] = xlswrite('Glu_100.xls',output3, 'model', 'j6');
[stat mmsg] = xlswrite('Glu_100.xls',output4, 'model', 'm6');
[stat mmsg] = xlswrite('Excel_sim.xls',output5,'MATLAB_est', 'N38');

figure (2);
plot(tspan,hmod,'--r',T,H,'og',tspan,rmod,'--
b',T,OUR,'or','Linewidth',1); hold on;
legend('H_m_o_d','H_e_x_p','OURmodel','OURexp');
ylabel('Hp(meq/L),OUR(mg/L/min)');xlabel('time(min)');
hold off;

%%%%%%%%%%%%%%%%%%%%%%%%%%%%%%%%%%%%%%%%%%%%%%%%%%%%%%%%%%%%%%%%%%%%%%%
%%%%%%%%%%%%%%%%%%%%%%%%%%%%%%%%%%%%%%%%%%%%%%%%%%%%%%%%%%%%%%%%%%%%%%%
function e = obj_fn(p_var,p_fix,tspan,tu)
%10 unknown model parameters & 6 fix model parameters:
p=[p_var(1),p_var(2),p_var(3),p_var(4),p_var(5),p_var(6),p_var(7),p_
var(8)...,p_var(9),p_var(10),p_fix(1),p_fix(2),p_fix(3),p_fix(4),p_f
ix(5),p_fix(6)];

%7 state variable taken as fixed:
x0=[p_fix(7),p_fix(8),p_fix(9),p_fix(10),p_fix(11),p_fix(12),p_fix(1
3)];
glu = glu_sim(tspan,x0,tu,p);
disp(' step3')

%LSQNONLIN: objective function should return the model error
h = tu(:,2);
hmod=glu(:,8);
e1 =hmod-h;
r = tu(:,3);
rmod=glu(:,9);
e2 =rmod-r;
e=e1+e2;

%%%%%%%%%%%%%%%%%%%%%%%%%%%%%%%%%%%%%%%%%%%%%%%%%%%%%%%%%%%%%%%%%%%%%%%
function glu = glu_sim(tspan,x0,tu,p)
%Simulation of glutamic acid biodegradation using the model.
ode_options = [];
%ode_options = odeset('RelTol',1e-4,'AbsTol',[1e-4 1e-4 1e-5]);
[t,X]=ode45(@d_out,tspan,x0,ode_options,p);
slow =X(:,1);
sub =X(:,2);
sto = X(:,3);
bio = X(:,4);
HCO3 =X(:,5);
CO2 = X(:,6);
HP = X(:,7);
hmod=HP;
ksto =p(16).*p(2).*p(4);
umaxs =(1-p(16)).*p(2).*p(3);
umax_sto=umaxs;
```

```
fbh=0.65; %the fraction of heterotrophic biomass (assumed value)
lag=(1-exp(-1*t./p(10)));
ds0=sub.*bio./(p(1)+sub);%ds0=Ss*Xh/(Ks+Ss)
ds1=lag.*ds0;%ds1=(1-exp(-1*t./Tr))*Ss*Xh/(Ks+Ss)
ds2=p(1).*bio./(p(1)+sub);%ds2=Ks*Xh/(Ks+Ss)
ds3=sto./bio;%ds3=Xsto/Xh
ds4=p(7)+(ds3*p(6));%ds4=K2+(Xsto/Xh)*K1
ds5=ds3.*ds3./ds4;%ds5=[(Xsto/Xh)^2]/[K2+(Xsto/Xh)*K1]
ds6=fbh*ksto.*ds1.*(1-p(4))./p(4);
%ds6=fbh*ksto.*(1-exp(-1*t./Tr))*Ss*Xh/(Ks+Ss).*((1-Y_sto)./Y_sto)
ds7=fbh*umaxs.*ds1.*(1-p(3))./p(3);
%ds7=fbh*umaxs.*(1-exp(-1*t./Tr))*Ss*Xh/(Ks+Ss).*((1-Yh_s)./Yh_s)
ds8=fbh*umax_sto.*ds5.*ds2.*(1-p(5))./p(5);
%ds8=fbh*umax_sto.*[(Xsto/Xh)^2]/[K2+(Xsto/Xh)*K1].*Ks*Xh/(Ks+Ss).*(
(1-Yh_sto)./Yh_sto)
ds9=(1-p(15))*p(13)*bio;%ds9=(1-fxi)*bh*Xh
rmod=(ds6+ds7+ds8+ds9+(p(14)*sto));
disp(' step2')
glu = [slow sub sto bio HCO3 CO2 HP hmod rmod];


%%%%%%%%%%%%%%%%%%%%%%%%%%%%%%%%%%%%%%%%%%%%%%%%%%%%%%%%%%%%%%%%%%%%%%%%%%%%
%%%%%%%%%%%%%%%%%%%%%%%%%%%%%%%%%%%%%%%%%%%%%%%%%%%%%%%%%%%%%%%%%%%%%%%%%%%%
function dx_dt=d_out(t,xin,p)
%For current glutamic acid biodegradation model (written on 21
March, 2010): p = [Ks, qmax, Yh_s, Y_sto, Yh_sto, K1, K2, kh, Kx,
Tr, k1, KLaCO2, bh, b_sto, fxi, f_sto ];
%xin(1)= Xs; xin(2) = Ss; xin(3) = Xsto; xin(4) = Xbh; xin(5) =
S_HCO3; xin(6) = S_CO2; xin(7) = S_HP;

Ks=p(1);
qmax=p(2);
Yh_s=p(3);
Y_sto=p(4);
Yh_sto=p(5);
K1=p(6);
K2=p(7);
kh=p(8);
Kx=p(9);
Tr=p(10);
k1=p(11);
KLaCO2=p(12);
bh=p(13);
b_sto=p(14);
fxi=p(15);
f_sto=p(16);

%Other fixed parameters
i_NBM=  0.0833333;
i_NXI=0.02;
M=208;
M_=112;
fbh=0.65;
kNHacc=0.000056;
pk1=6.392023261;
pH=7.8;
gs=2.8;
gx=4.2;
gsto=4.5;
phi=0.97;
SatCO2=0.017;
```

```
ksto =f_sto*qmax*Y_sto;
umaxs =(1-f_sto)*qmax*Yh_s;
umax_sto=umaxs;

lag=(1-exp(-1*t./Tr));
ds0=xin(2).*xin(4)./(Ks+xin(2));
ds1=lag.*ds0;
ds2=Ks.*xin(4)./(Ks+xin(2));
ds3=xin(3)./xin(4);
ds4=K2+(ds3*K1);
ds5=ds3.*ds3./ds4;
ds6=(-1)*fbh*umaxs.*ds1./Yh_s;
ds7=(-1)*fbh*ksto.*ds1./Y_sto;
ds7_0=kNHacc.*ds1;
ds8=(-1)*fbh*umax_sto.*ds5.*ds2./Yh_sto;
ds9=((gx-Yh_s*gs)/(8*gs*Yh_s*gx))*(-ds6*Yh_s);
ds9_1=((gsto-Y_sto*gs)/(8*gs*Y_sto*gsto))*(-ds7*Y_sto);
ds9_2=((gx-Yh_sto*gsto)/(8*gx*Yh_sto*gsto))*(-ds8*Yh_sto);
ds10=((1-fxi)/(8*gx)).*bh.*xin(4);
ds11=k1*xin(6)-k1*xin(5)*10^(pk1-pH);
ds12=KLaCO2.*(SatCO2-xin(6));
ds16=(1/(8*gsto)).*(b_sto.*xin(3));
ds18=xin(1)./xin(4);
ds19=Kx+ds18;
ds20=ds18./ds19;
ds21=kh.*ds20.*xin(4);

ds22=(3/M_).*ds21;
ds23=(i_NBM*phi/14)*ds7_0;
ds24=(i_NBM*phi/14).*(-ds6*Yh_s);
ds25=-((i_NBM-fxi*i_NXI)/14)*phi*bh.*xin(4);

dslow=(-M/M_)*ds21;
dsub=ds21+ds6+ds7;
dsto=(fbh*ksto.*ds1)+ds8-(b_sto*xin(3));
dbio=(fbh*umaxs.*ds1)+(fbh*umax_sto.*ds5.*ds2)-(bh.*xin(4));
dHCO3=ds11;
dCO2=ds9+ds9_1+ds9_2+ds10-ds11+ds12+ds16;
dHP=ds22+ds23+ds24+ds25+ds11;

dx_dt=[dslow dsub dsto dbio dHCO3 dCO2 dHP]';
return
```